NUREG/CR-0303
TREE-1232

EXPERIMENT DATA REPORT FOR PBF-LOCA TESTS LOC-11B AND 11C

RUSSELL J. BUCKLAND CHERYL E. COPPIN
CHRISTINE E. WHITE

October 1978

EG&G Idaho, Inc.

IDAHO NATIONAL ENGINEERING LABORATORY

DEPARTMENT OF ENERGY

IDAHO OPERATIONS OFFICE UNDER CONTRACT EY-76-C-07-1570

Available from
National Technical Information Service
Springfield, Virginia 22161
Price: Printed Copy A10; Microfiche $3.00

The price of this document for requesters outside the North American continent can be obtained from the National Technical Information Service.

NUREG/CR-0303
TREE-1232
R3

EXPERIMENT DATA REPORT FOR

PBF-LOCA TESTS LOC-11B AND 11C

Russell J. Buckland
Cheryl E. Coppin
Christine E. White

Date Published: October 1978

Idaho National Engineering Laboratory
Idaho Falls, Idaho
Operated by
EG&G Idaho, Inc.,
for the
U.S. Department of Energy
Idaho Operations Office

PREPARED FOR THE
U.S. NUCLEAR REGULATORY COMMISSION
UNDER CONTRACT NO. EY-76-C-07-1570

ABSTRACT

Recorded test data are presented for Tests LOC-11B and 11C of the Thermal Fuels Behavior Program Loss-of-Coolant Accident Test Series. These tests, the first in a series of LOCA experiments conducted at the Power Burst Facility, investigated the behavior of the cladding of nuclear fuel rods exposed to temperatures similar to those expected in a pressurized water reactor during the blowdown and heatup phases of a 200% double-ended cold leg break. Tests LOC-11B and 11C were conducted at axial peak powers of 46 and 68 kW/m, respectively, which resulted in respective peak cladding temperatures of 880 K and 1030 K. This report makes available the uninterpreted data for future analysis and test reporting activities. The data, presented in the form of graphs in engineering units, have been analyzed only to the extent necessary to ensure they are reasonable and consistent.

SUMMARY

Tests LOC-11B and 11C were performed as part of the Thermal Fuels Behavior Program conducted by EG&G Idaho, Inc., for the U.S. Nuclear Regulatory Commission. These tests were the first in the Loss-of-Coolant Accident (LOCA) Test Series designed to provide experimental information on fuel survival characteristics under off-normal or accident conditions. The test objective specific to LOC-11B and 11C was one of subjecting the cladding of four nuclear fuel rods of pressurized water reactor (PWR) design to temperatures similar to those experienced by the highest powered PWR fuel rod during the blowdown and heat-up phases of a 200% double-ended cold leg break.

The Power Burst Facility was designed to provide the neutron and coolant environment required to simulate conditions in a light water reactor during postulated accident events. The test facility consists primarily of:

(1) A reactor vessel and driver core region to provide the neutron environment

(2) An in-pile tube in the center of the driver core for containing the test rods

(3) A pressurized water flow loop to provide the coolant environment in the in-pile tube

(4) A blowdown system to simulate a blowdown accident.

The test experiment consisted of four separately shrouded unirradiated PWR-type fuel rods which were positioned in the in-pile tube at driver core level.

Each test consisted of the following phases:

(1) Heat-up – establishment of initial test coolant conditions

(2) Power calibration – calibration of experiment power with reactor power

(3) Preconditioning – period which allowed fuel cracking, restructuring, and fuel relocation

(4) Decay heat buildup – achievement of sufficient decay heat prior to blowdown

(5) Blowdown and quench – sequential shutdown of the reactor, blowdown of the in-pile tube, and cold water injection

(6) Cooldown – continuous cooling flow maintained to prevent rod damage from decay heat.

Three separate nuclear blowdown tests were performed on the same LOC-11 test train fuel and hardware. The first test, LOC-11A, was not conducted as planned due to spurious cycling of system valves which resulted in a delay in the onset of critical heat flux and low peak cladding temperatures. Test LOC-11B was next performed with the system operating properly but at an axial peak test rod power of almost 46 kW/m which resulted in low peak cladding temperatures of about 880 K. Although no significant fuel rod degradation occurred during the first two tests, Test LOC-11B was considered successful and provided important data. A third test, Test LOC-11C was subsequently performed with the same test rods but with increased rod powers and a reduction in time from reactor shutdown to blowdown initiation. Peak test rod cladding temperatures of approximately 1030 K resulted during the blowdown transient and satisfied test objectives.

The PBF-LOCA instrumentation system was designed to measure and record the important events that occurred prior to and during a LOCA test. Each test rod and its shroud cooling environment was fully instrumented. The blowdown piping variables were further characterized through use of instrumented spool pieces. The instrumentation on these spool pieces provided fluid temperature, pressure, velocity, and density information during the blowdown transient.

The data obtained from these tests have been subjected to a thorough review and subsequently divided into verified, restrained, trend, or failed data. The time span selected for the bulk of the data extends from 5 s prior to reactor shutdown for blowdown initiation, to 30 s following shutdown. Additional data plots with other time spans are included on microfiche attached to the back cover of this report.

CONTENTS

FIGURES

MICROFICHE ADDRESSES FOR TEST LOC-11B

C1 Plenum temperature in fuel Rod 1 (TE-3-1) (Sheet No. 1)

D1 Plenum temperature in fuel Rod 2 (TE-3-2) (Sheet No. 1)

E1 Plenum temperature in fuel Rod 3 (TE-3-3) (Sheet No. 1)

F1 Cladding temperature Rod 1, 0.53 m above fuel stack bottom (TE-5-1) (Sheet No.1)

G1 Cladding temperature Rod 2, 0.53 m above fuel stack bottom (TE-5-2) (Sheet No. 1)

H1 Cladding temperature Rod 3, 0.53 m above fuel stack bottom (TE-5-3) (Sheet No. 1)

I1 Cladding temperature Rod 4, 0.53 m above fuel stack bottom (TE-5-4) (Sheet No. 1)

J1 Cladding temperature Rod 1, 0.61 m above fuel stack bottom (TE-8-1) (Sheet No. 1)

K1 Cladding temperature Rod 2, 0.61 m above fuel stack bottom (TE-8-2) (Sheet No. 1)

L1 Cladding temperature Rod 3, 0.61 m above fuel stack bottom (TE-8-3) (Sheet No. 1)

M1 Cladding temperature Rod 4, 0.61 m above fuel stack bottom (TE-8-4) (Sheet No. 1)

N1 Cladding temperature Rod 1, 0.53 m above fuel stack bottom (TE-10-1) (Sheet No. 1)

O1 Cladding temperature Rod 2, 0.53 m above fuel stack bottom (TE-10-2) (Sheet No. 1)

P1 Cladding temperature Rod 3, 0.53 m above fuel stack bottom (TE-10-3) (Sheet No. 1)

B2 Cladding temperature Rod 4, 0.53 m above fuel stack bottom (TE-10-4) (Sheet No. 1)

C2 Cladding temperature Rod 1, 0.61 m above fuel stack bottom (TE-22-1) (Sheet No. 1)

D2 Cladding temperature Rod 2, 0.61 m above fuel stack bottom (TE-22-2) (Sheet No. 1)

E2 Cladding temperature Rod 3, 0.61 m above fuel stack bottom (TE-22-3) (Sheet No. 1)

F2 Cladding temperature Rod 4, 0.61 m above fuel stack bottom (TE-22-4) (Sheet No. 1)

G2 Fuel temperature Rod 1, 0.53 m above fuel stack bottom (TE-11-1) (Sheet No. 1)

H2 Fuel temperature Rod 2, 0.53 m above fuel stack bottom (TE-11-2) (Sheet No. 1)

I2 Fuel temperature Rod 3, 0.53 m above fuel stack bottom (TE-11-3) (Sheet No. 1)

J2 Fuel temperature Rod 4, 0.53 m above fuel stack bottom (TE-11-4) (Sheet No. 1)

K2 Fluid temperature in lower upper plenum (TE-1) (Sheet No. 1)

L2 Fluid temperature Rod 1 coolant outlet (TE-2-1) (Sheet No. 1)

M2 Fluid temperature Rod 2 coolant outlet (TE-2-2) (Sheet No. 1)

N2 Fluid temperature Rod 4 coolant outlet (TE-2-4) (Sheet No. 1)

O2 Fluid temperature Rod 1, 0.61 m above fuel stack bottom (TE-6-1) (Sheet No. 1)

P2 Fluid temperature Rod 3, 0.61 m above fuel stack bottom (TE-6-3) (Sheet No. 1)

B3 Fluid temperature Rod 4, 0.61 m fuel above stack bottom (TE-6-4) (Sheet No. 1)

C3 Fluid temperature Rod 1, 0.46 m above fuel stack bottom (TE-9-1) (Sheet No. 1)

D3 Fluid temperature Rod 2, 0.46 m above fuel stack bottom (TE-9-2) (Sheet No. 1)

E3 Fluid temperature Rod 3, 0.46 m above fuel stack bottom (TE-9-3) (Sheet No. 1)

F3 Fluid temperature Rod 4, 0.46 m above fuel stack bottom (TE-9-4) (Sheet No. 1)

G3 Fluid temperature Rod 1, 0.30 m above fuel stack bottom (TE-13-1) (Sheet No. 1)

H3 Fluid temperature Rod 2, 0.30 m above fuel stack bottom (TE-13-2) (Sheet No. 1)

I3 Fluid temperature Rod 4, 0.30 m above fuel stack bottom (TE-13-4) (Sheet No. 1)

J3 Fluid temperature of fuel Rod 1 inlet coolant (TE-14-1) (Sheet No. 1)

K3 Fluid temperature of fuel Rod 3 inlet coolant (TE-14-3) (Sheet No. 1)

L3 Fluid temperature of fuel Rod 4 inlet coolant (TE-14-4) (Sheet No. 1)

M3 Fluid temperature in test train lower particle screen (TE-15) (Sheet No. 1)

N3 Fluid temperature in test train lower particle screen (TE-16) (Sheet No. 1)

O3 Fluid temperature in test train bypass flow (TE-17) (Sheet No. 1)

P3 Fluid temperature in upper plenum exit (TE-18) (Sheet No. 1)

B4 Fluid temperature in upper plenum (TE-19) (Sheet No. 1)

C4 Fluid temperature in inlet spool (TE-20) (Sheet No. 1)

D4 Fluid temperature in inlet spool (TE-21) (Sheet No. 1)

E4 Fluid temperature in cold leg blowdown spool (TE-23) (Sheet No. 1)

F4 Fluid temperature in cold leg blowdown spool (TE-24) (Sheet No. 1)

G4 Fluid temperature in hot leg blowdown spool (TE-26) (Sheet No. 1)

H4 Fluid temperature in hot leg blowdown spool (TE-25) (Sheet No. 1)

I4 Differential temperature at fuel inlet and outlet Rod 1 (ΔT-1-1) (Sheet No. 1)

J4 Differential temperature at fuel inlet and outlet Rod 2 (ΔT-1-2) (Sheet No. 1)

K4 Differential temperature at fuel inlet and outlet Rod 3 (ΔT-1-3) (Sheet No. 1)

L4 Differential temperature at fuel inlet and outlet Rod 4 (ΔT-1-4) (Sheet No. 1)

M4 Material temperature Rod 1, 0.61 m above fuel stack bottom (TE-4-1) (Sheet No. 1)

N4 Material temperature Rod 2, 0.61 m above fuel stack bottom (TE-4-2) (Sheet No. 1)

O4 Material temperature Rod 3, 0.61 m above fuel stack bottom (TE-4-3) (Sheet No. 1)

P4 Material temperature Rod 4, 0.61 m above fuel stack bottom (TE-4-4) (Sheet No. 1)

B5 Material temperature Rod 1, 0.46 m above fuel stack bottom (TE-7-1) (Sheet No. 1)

C5 Material temperature Rod 2, 0.46 m above fuel stack bottom (TE-7-2) (Sheet No. 1)

D5 Material temperature Rod 3, 0.46 m above fuel stack bottom (TE-7-3) (Sheet No. 1)

E5 Material temperature Rod 4, 0.46 m above fuel stack bottom (TE-7-4) (Sheet No. 1)

F5 Material temperature Rod 1, 0.30 m above fuel stack bottom (TE-12-1) (Sheet No. 1)

G5 Material temperature Rod 2, 0.30 m above fuel stack bottom (TE-12-2) (Sheet No. 1)

H5 Material temperature Rod 3, 0.30 m above fuel stack bottom (TE-12-3) (Sheet No. 1)

I5 Material temperature Rod 4, 0.30 m above fuel stack bottom (TE-12-4) (Sheet No. 1)

J5 Absolute pressure in upper test train (PE-1) (Sheet No. 1)

K5 Absolute pressure in upper test train (PE-3) (Sheet No. 1)

L5 Absolute pressure below test train fuel rod (PE-6) (Sheet No. 1)

M5 Absolute pressure in inlet spool (PE-9) (Sheet No. 1)

N5 Absolute pressure in cold leg blowdown spool (PE-10) (Sheet No. 1)

O5 Absolute pressure in cold leg blowdown spool (PE-11) (Sheet No. 1)

P5 Absolute pressure in hot leg blowdown spool (PE-12) (Sheet No. 1)

B6 Absolute pressure in hot leg blowdown spool (PE-13) (Sheet No. 1)

C6 Differential pressure in cold leg blowdown spool (ΔPE-5) (Sheet No. 1)

D6 Volumetric flow rate in fuel Rod 1 upper shroud (FE-1-1) (Sheet No. 1)

E6 Volumetric flow rate in fuel Rod 2 upper shroud (FE-1-2) (Sheet No. 1)

F6 Volumetric flow rate in fuel Rod 3 upper shroud (FE-1-3) (Sheet No. 1)

G6 Volumetric flow rate in fuel Rod 4 upper shroud (FE-1-4) (Sheet No. 1)

H6 Volumetric flow rate in fuel Rod 1 lower shroud (FE-2-1) (Sheet No. 1)

I6 Volumetric flow rate in fuel Rod 2 lower shroud (FE-2-2) (Sheet No. 1)

J6 Volumetric flow rate in fuel Rod 3 lower shroud (FE-2-3) (Sheet No. 1)

K6 Volumetric flow rate in fuel Rod 4 lower shroud (FE-2-4) (Sheet No. 1)

L6 Volumetric flow rate from flowmeter in inlet spool (FE-5) (Sheet No. 1)

M6 Volumetric flow rate in cold leg blowdown spool (FE-6) (Sheet No. 1)

N6 Volumetric flow rate in hot leg blowdown spool (FE-9) (Sheet No. 1)

O6 Momentum flux in cold leg blowdown spool (FE-7) (Sheet No. 1)

P6 Momentum flux in hot leg blowdown spool (FE-8) (Sheet No. 1)

B7 Chordal density of upper gamma beam in cold leg (DEN-1-U) (Sheet No. 1)

C7 Chordal density of lower gamma beam in cold leg (DEN-1-L) (Sheet No. 1)

D7 Chordal density in hot leg blowdown spool, upper beam (DEN-2-U) (Sheet No. 1)

E7 Chordal density in hot leg blowdown spool, center beam (DEN-2-C) (Sheet No. 1)

F7 Chordal density in hot leg blowdown spool, lower beam (DEN-2-L) (Sheet No. 1)

G7 Average density of hot leg blowdown spool (DEN-2-AVE) (Sheet No. 1)

H7 Cladding displacement of Rod 1 (LVDT-1) (Sheet No. 1)

I7 Cladding displacement of Rod 2 (LVDT-2) (Sheet No. 1)

J7 Cladding displacement of Rod 3 (LVDT-3) (Sheet No. 1)

K7 Cladding displacement of Rod 4 (LVDT-4) (Sheet No. 1)

L7 Reactor power from plant protective system (PPS-1) (Sheet No. 1)

M7 SPND power trend 0.76 m above fuel stack bottom (SPND-1) (Sheet No. 1)

N7 SPND power trend 0.61 m above fuel stack bottom (SPND-2) (Sheet No. 1)

O7 SPND power trend 0.46 m above fuel stack bottom (SPND-3) (Sheet No. 1)

P7 SPND power trend 0.30 m above fuel stack bottom (SPND-4) (Sheet No. 1)

B8 SPND power trend 0.15 m above fuel stack bottom (SPND-5) (Sheet No. 1)

C8 Absolute pressure in upper test train (PE-3) (Sheet No. 1)

D8 Absolute pressure below test train fuel rod (PE-6) (Sheet No. 1)

E8 Absolute pressure in cold leg blowdown spool (PE-10) (Sheet No. 1)

F8 Absolute pressure in hot leg blowdown spool (PE-12) (Sheet No. 1)

MICROFICHE ADDRESSES FOR TEST LOC-11C

C1 Plenum temperature in fuel Rod 1 (TE-3-1) (Sheet No. 2)

D1 Plenum temperature in fuel Rod 2 (TE-3-2) (Sheet No. 2)

E1 Plenum temperature in fuel Rod 3 (TE-3-3) (Sheet No. 2)

F1 Cladding temperature Rod 1, 0.53 m above fuel stack bottom (TE-5-1) (Sheet No. 2)

G1 Cladding temperature Rod 2, 0.53 m above fuel stack bottom (TE-5-2) (Sheeet No. 2)

H1 Cladding temperature Rod 3, 0.53 m above fuel stack bottom (TE-5-3) (Sheet No. 2)

I1 Cladding temperature Rod 4, 0.53 m above fuel stack bottom (TE-5-4) (Sheet No. 2)

J1 Cladding temperature Rod 1, 0.61 m above fuel stack bottom (TE-8-1) (Sheet No. 2)

K1 Cladding temperature Rod 2, 0.61 m above fuel stack bottom (TE-8-2) (Sheet No. 2)

L1 Cladding temperature Rod 3, 0.61 m above fuel stack bottom (TE-8-3) (Sheet No. 2)

M1 Cladding temperature Rod 4, 0.61 m above fuel stack bottom (TE-8-4) (Sheet No. 2)

N1 Cladding temperature Rod 1, 0.53 m above fuel stack bottom (TE-10-1) (Sheet No. 2)

O1 Cladding temperature Rod 2, 0.53 m above fuel stack bottom (TE-10-2) (Sheet No. 2)

P1 Cladding temperature Rod 3, 0.53 m above fuel stack bottom (TE-10-3) (Sheet No. 2)

B2 Cladding temperature Rod 4, 0.53 m above fuel stack bottom (TE-10-4) (Sheet No. 2)

C2 Cladding temperature Rod 1, 0.61 m above fuel stack bottom (TE-22-1) (Sheet No. 2)

D2 Cladding temperature Rod 2, 0.61 m above fuel stack bottom (TE-22-2) (Sheet No. 2)

E2 Cladding temperature Rod 3, 0.61 m above fuel stack bottom (TE-22-3) (Sheet No. 2)

F2 Cladding temperature Rod 4, 0.61 m above fuel stack bottom (TE-22-4) (Sheet No. 2)

G2 Fuel temperature Rod 1, 0.53 m above fuel stack bottom (TE-11-1) (Sheet No. 2)

H2 Fuel temperature Rod 2, 0.53 m above fuel stack bottom (TE-11-2) (Sheet No. 2)

I2 Fuel temperature Rod 3, 0.53 m above fuel stack bottom (TE-11-3) (Sheet No. 2)

J2 Fuel temperature Rod 4, 0.53 m above fuel stack bottom (TE-11-4) (Sheet No. 2)

K2 Fluid temperature in lower upper plenum (TE-1) (Sheet No. 2)

L2 Fluid temperature of Rod 1 coolant outlet (TE-2-1) (Sheet No. 2)

M2 Fluid temperature of Rod 2 coolant outlet (TE-2-2) (Sheet No. 2)

N2 Fluid temperature of Rod 4 coolant outlet (TE-2-4) (Sheet No. 2)

O2 Fluid temperature Rod 1, 0.61 m above fuel stack bottom (TE-6-1) (Sheet No. 2)

P2 Fluid temperature Rod 3, 0.61 m above fuel stack bottom (TE-6-3) (Sheet No. 2)

B3 Fluid temperature Rod 4, 0.61 m above fuel stack bottom (TE-6-4) (Sheet No. 2)

C3 Fluid temperature Rod 1, 0.46 m above fuel stack bottom (TE-9-1) (Sheet No. 2)

D3 Fluid temperature Rod 2, 0.46 m above fuel stack bottom (TE-9-2) (Sheet No. 2)

E3 Fluid temperature Rod 3, 0.46 m above fuel stack bottom (TE-9-3) (Sheet No. 2)

F3 Fluid temperature Rod 4, 0.46 m above fuel stack bottom (TE-9-4) (Sheet No. 2)

G3 Fluid temperature Rod 1, 0.30 m above fuel stack bottom (TE-13-1) (Sheet No. 2)

H3 Fluid temperature Rod 2, 0.30 m above fuel stack bottom (TE-13-2) (Sheet No. 2)

I3 Fluid temperature Rod 4, 0.30 m above fuel stack bottom (TE-13-4) (Sheet No. 2)

J3 Fluid temperature of Rod 1 inlet coolant (TE-14-1) (Sheet No. 2)

K3 Fluid temperature of Rod 3 inlet coolant (TE-14-3) (Sheet No. 2)

L3 Fluid temperature in fuel Rod 4 inlet coolant (TE-14-4) (Sheet No. 2)

M3 Fluid temperature in test train lower particle screen (TE-15) (Sheet No. 2)

N3 Fluid temperature in test train lower particle screen (TE-16) (Sheet No. 2)

O3 Fluid temperature in test train bypass flow (TE-17) (Sheet No. 2)

P3 Fluid temperature in upper plenum exit (TE-18) (Sheet No. 2)

B4 Fluid temperature in upper plenum (TE-19) (Sheet No. 2)

C4 Fluid temperature in inlet spool (TE-20) (Sheet No. 2)

D4 Fluid temperature in inlet spool (TE-21) (Sheet No. 2)

E4 Fluid temperature in cold leg blowdown spool (TE-23) (Sheet No.2)

F4 Fluid temperature in cold leg blowdown spool (TE-24) (Sheet No. 2)

G4 Fluid temperature in hot leg blowdown spool (TE-26) (Sheet No. 2)

H4 Differential temperature at fuel inlet and outlet Rod 1 (ΔT-1-1) (Sheet No. 2)

I4 Differential temperature at fuel inlet and outlet Rod 2 (ΔT-1-2) (Sheet No. 2)

J4 Differential temperature at fuel inlet and outlet Rod 3 (ΔT-1-3) (Sheet No. 2)

K4 Differential temperature at fuel inlet and outlet Rod 4 (ΔT-1-4) (Sheet No. 2)

L4 Material temperature Rod 1, 0.61 m above fuel stack bottom (TE-4-1) (Sheet No. 2)

M4 Material temperature Rod 2, 0.61 m above fuel stack bottom (TE-4-2) (Sheet No. 2)

N4 Material temperature Rod 3, 0.61 m above fuel stack bottom (TE-4-3) (Sheet No. 2)

O4 Material temperature Rod 4, 0.61 m above fuel stack bottom (TE-4-4) (Sheet No. 2)

P4 Material temperature Rod 1, 0.46 m above fuel stack bottom (TE-7-1) (Sheet No. 2)

B5 Material temperature Rod 2, 0.46 m above fuel stack bottom (TE-7-2) (Sheet No. 2)

C5 Material temperature Rod 3, 0.46 m above fuel stack bottom (TE-7-3) (Sheet No. 2)

D5 Material temperature Rod 4, 0.46 m above fuel stack bottom (TE-7-4) (Sheet No. 2)

E5 Material temperature Rod 1, 0.30 m above fuel stack bottom (TE-12-1) (Sheet No. 2)

F5 Material temperature Rod 2, 0.30 m above fuel stack bottom (TE-12-2) (Sheet No. 2)

G5 Material temperature Rod 3, 0.30 m above fuel stack bottom (TE-12-3) (Sheet No. 2)

H5 Material temperature Rod 4, 0.30 m above fuel stack bottom (TE-12-4) (Sheet No. 2)

I5 Absolute pressure in upper test train (PE-1) (Sheet No. 2)

J5 Absolute pressure in upper test train (PE-3) (Sheet No. 2)

K5 Absolute pressure below test train fuel rod (PE-6) (Sheet No. 2)

L5 Absolute pressure in inlet spool (PE-9) (Sheet No. 2)

M5 Absolute pressure in cold leg blowdown spool (PE-10) (Sheet No. 2)

N5 Absolute pressure in cold leg blowdown spool (PE-11) (Sheet No. 2)

O5 Absolute pressure in hot leg blowdown spool (PE-12) (Sheet No. 2)

P5 Absolute pressure in hot leg blowdown spool (PE-13) (Sheet No. 2)

B6 Differential pressure in cold leg blowdown spool (ΔPE-5) (Sheet No. 2)

C6 Volumetric flow rate in fuel Rod 1 upper shroud (FE-1-1) (Sheet No. 2)

D6 Volumetric flow rate in fuel Rod 2 upper shroud (FE-1-2) (Sheet No. 2)

E6 Volumetric flow rate in fuel Rod 3 upper shroud (FE-1-3) (Sheet No. 2)

F6 Volumetric flow rate in fuel Rod 4 upper shroud (FE-1-4) (Sheet No. 2)

G6 Volumetric flow rate in fuel Rod 1 lower shroud (FE-2-1) (Sheet No. 2)

H6 Volumetric flow rate in fuel Rod 2 lower shroud (FE-2-2) (Sheet No. 2)

I6 Volumetric flow rate in fuel Rod 3 lower shroud (FE-2-3) (Sheet No. 2)

J6 Volumetric flow rate in fuel Rod 4 lower shroud (FE-2-4) (Sheet No. 2)

K6 Volumetric flow rate from flowmeter in inlet spool (FE-5) (Sheet No. 2)

L6 Volumetric flow rate in cold leg blowdown spool (FE-6) (Sheet No. 2)

M6 Momentum flux in cold leg blowdown spool (FE-7) (Sheet No. 2)

N6 Momentum flux in hot leg blowdown spool (FE-8) (Sheet No. 2)

O6 Volumetric flow rate in hot leg blowdown spool (FE-9) (Sheet No. 2)

P6 Chordal density of upper gamma beam in cold leg (DEN-1-U) (Sheet No. 2)

B7 Chordal density in hot leg blowdown spool, upper beam (DEN-2-U) (Sheet No. 2)

C7 Chordal density in hot leg blowdown spool, center beam (DEN-2-C) (Sheet No. 2)

D7 Chordal density in hot leg blowdown spool, lower beam (DEN-2-L) (Sheet No. 2)

E7 Average density of hot leg blowdown spool (DEN-2-AVE) (Sheet No. 2)

F7 Cladding displacement of Rod 1 (LVDT-1) (Sheet No. 2)

G7 Cladding displacement of Rod 2 (LVDT-2) (Sheet No. 2)

H7 Cladding displacement of Rod 3 (LVDT-3) (Sheet No. 2)

I7 Cladding displacement of Rod 4 (LVDT-4) (Sheet No. 2)

J7 Reactor power from plant protective system (PPS-1) (Sheet No. 2)

K7 SPND power trend 0.76 m above fuel stack bottom (SPND-1) (Sheet No. 2)

L7 SPND power trend 0.61 m above fuel stack bottom (SPND-2) (Sheet No. 2)

M7 SPND power trend 0.30 m above fuel stack bottom (SPND-4) (Sheet No. 2)

N7 SPND power trend 0.15 m above fuel stack bottom (SPND-5) (Sheet No. 2)

O7 Absolute pressure in upper test train (PE-3) (Sheet No. 2)

P7 Absolute pressure below test train fuel rod (PE-6) (Sheet No. 2)

B8 Absolute pressure below test train fuel rod (PE-12) (Sheet No. 2)

TABLES

EXPERIMENT DATA REPORT FOR

PBF-LOCA TESTS LOC-11B AND 11C

I. INTRODUCTION

The Thermal Fuels Behavior Program, one of several water reactor research test programs conducted by EG&G Idaho, Inc., for the U.S. Nuclear Regulatory Commission, produces data which will contribute to an improved understanding of the behavior of nuclear fuel rods operated under normal, off-normal, and accident conditions. The main objective of the Thermal Fuels Behavior Program is to develop an integral analytical and experimental effort which is accomplished by using experimental data to evaluate the completeness and accuracy of the analytical models.

The Loss-of-Coolant Accident (LOCA) Test Series, conducted as part of this program, is specifically designed to provide data over the range of conditions that could exist during the blowdown and heatup phases of a LOCA in a pressurized water reactor (PWR). The coolant conditions are characterized by a rapid system depressurization and extreme changes in both mass flow and quality with departure from nucleate boiling occurring within a few seconds of transient initiation.

The LOCA tests are conducted in the in-pile tube (IPT), the test space located vertically in the center of the Power Burst Facility (PBF) reactor core. The PBF loop coolant and blowdown systems allow PWR coolant conditions to be simulated in the IPT and provide the subsequent blowdown capability. The test train, an experiment support apparatus, positions the fuel in the core region of the IPT and provides support for the test instrumentation. The fuel rod dimensional characteristics are typical of those of a PWR except for the length and plenum volume, which are scaled proportionally to the active fuel length of a PWR rod. The 0.914-m rods are to be tested in both single and multirod arrays with temperature, pressure, and deformation measurements specified and used for model evaluation. Additional dynamic, pretest, and posttest measurements are specified to provide checks on individual models and to determine boundary conditions.

Test LOC-11, the first test planned in the LOCA test series had the overall objective of subjecting the cladding of PWR-type nuclear fuel rods to temperatures similar to those experienced by the highest power PWR fuel rod during the blowdown and heatup phases of a 200% double-ended cold leg break. A second objective was to compare the thermal response and cladding deformation of pressurized and unpressurized fuel rods during a LOCA. In the first LOCA test, Test LOC-11A, spurious cycling of the isolation valves caused coolant to enter the test train after the blowdown system had been isolated from the loop. Consequently, critical heat flux was delayed and intended peak cladding temperatures were not achieved. As a result of low temperatures, the pressurized fuel rods did not experience cladding ballooning, and cladding collapse did not occur on the unpressurized fuel rods. Test LOC-11B, the second test, was conducted using the LOC-11A configuration with the

blowdown and isolation valves operating properly. However, Test LOC-11B was conducted at an axial peak power of about 46 kW/m which resulted in relatively low peak cladding temperatures of about 880 K. Although no significant fuel rod degradation occurred during the first two tests, Test LOC-11B was considered a successful test and did provide important data. A third test, Test LOC-11C was subsequently performed with the same experiment test rods but with increased rod powers and a reduction in time from reactor shutdown to blowdown initiation. This test resulted in peak cladding temperatures of about 1030 K and satisfied test objectives.

The preblowdown nuclear phases of Test LOC-11 were: (1) the power calibration phase, which calibrates test rod power with reactor power, (2) the preconditioning phase, which promotes fuel pellet cracking and restructuring, and (3) the decay heat buildup phase which provides decay heat during the blowdown phase.

This report presents the data from Tests LOC-11B and LOC-11C in an uninterpreted but readily usable form for use by the nuclear community in advance of detailed analysis and interpretation. The data have been subjected to a thorough review and subsequently divided into verified, restrained, trend, or failed data. The time span selected for the bulk of the data extend from 5 s prior to reactor shutdown for blowdown initiation, to 30 s following shutdown. Additional data plots with other time spans are included in microfiche attached to the back cover of this report.

Section II of this report presents the system configuration, procedures, initial test conditions, and events that are applicable to Tests LOC-11B and LOC-11C; Section III provides brief descriptions of test instrumentation; and Section IV presents the data graphs and provides comments and supporting information necessary for data interpretation. Appendix A provides a complete history of all thermal and nuclear cycles experienced by the test train and test rod fuel; Appendix B describes the methods used in applying posttest corrective adjustments to the data and subsequent verification; and Appendix C presents a guide to the uncertainty associated with the data measurements.

II. SYSTEM AND EVENTS FOR TESTS LOC-11B AND LOC-11C

The following system configuration, procedures, and events are specific to Tests LOC-11B and 11C.

1. SYSTEM CONFIGURATION

The Power Burst Facility consists primarily of an open tank reactor vessel and driver core region with an active length of 0.91 m; a flux trap region in the center of the driver core contains an in-pile tube (IPT) in which the test fuel is located; and a pressurized water flow loop that permits control of the test fuel rod coolant flow rate, temperature, and pressure within typical PWR levels. Through the use of high-speed valves, the in-pile tube portion of the loop can be rapidly depressurized in a manner similar to that which would occur in a PWR during a postulated loss-of-coolant accident. The PBF system major components are shown in Figure 1.

The PBF core is approximately a right-circular annulus 1.3 m in diameter and 0.91 m in length, enclosing the centrally located vertical test space which is 0.21 m in diameter. The PBF core cross section is shown in Figure 2.

Any conceivable failure of the test fuel during a test (such as cladding failure, gross fuel melting, fuel-coolant interactions, fuel failure propagation, fission product release, or metal-water reactions) can be safely contained by the PBF in-pile tube without damage to the driver core.

A schematic of the pressurized water loop and associated blowdown hardware is shown in Figure 3. The loop pump, heaters and heat exchangers, and pressurizer provide the desired flow rates, temperatures, and pressures to simulate coolant conditions of a PWR in the IPT.

Thermal swell accumulators and acoustic filters are placed at the IPT inlet and outlet to reduce the magnitude of the pressure surges extending down the loop pipe. The isolation and bypass valves are actuated immediately prior to blowdown initiation so the loop can continue to operate at normal conditions through the bypass valve.

The IPT is a thick-walled, Inconel 718, high strength pressure tube designed to contain the steady-state operating pressure and the pressure surges that may result from test fuel rod failure. A flow tube with a central section (through the reactor core) of zircaloy-2 is positioned within the IPT to direct the IPT flow. Flow enters the IPT above the reactor core and flows down the annulus between the IPT wall and the flow tube. Flow reverses at the bottom, flows up through the central region of the flow tube, past the test fuel rods and exits the IPT above the reactor core. A nitrogen gas annulus is provided between the IPT

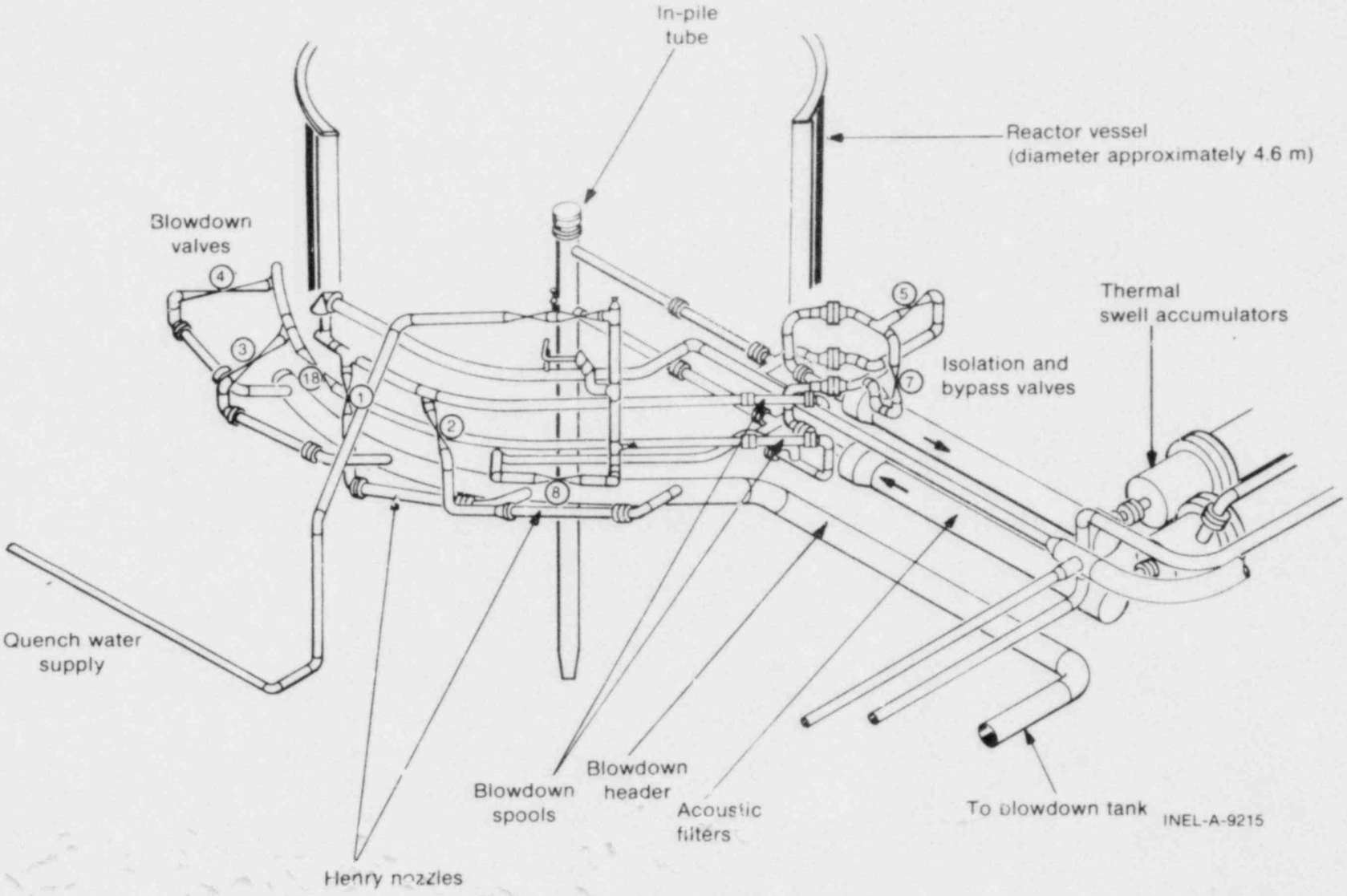

Fig. 1 PBF LOCA system – isometric.

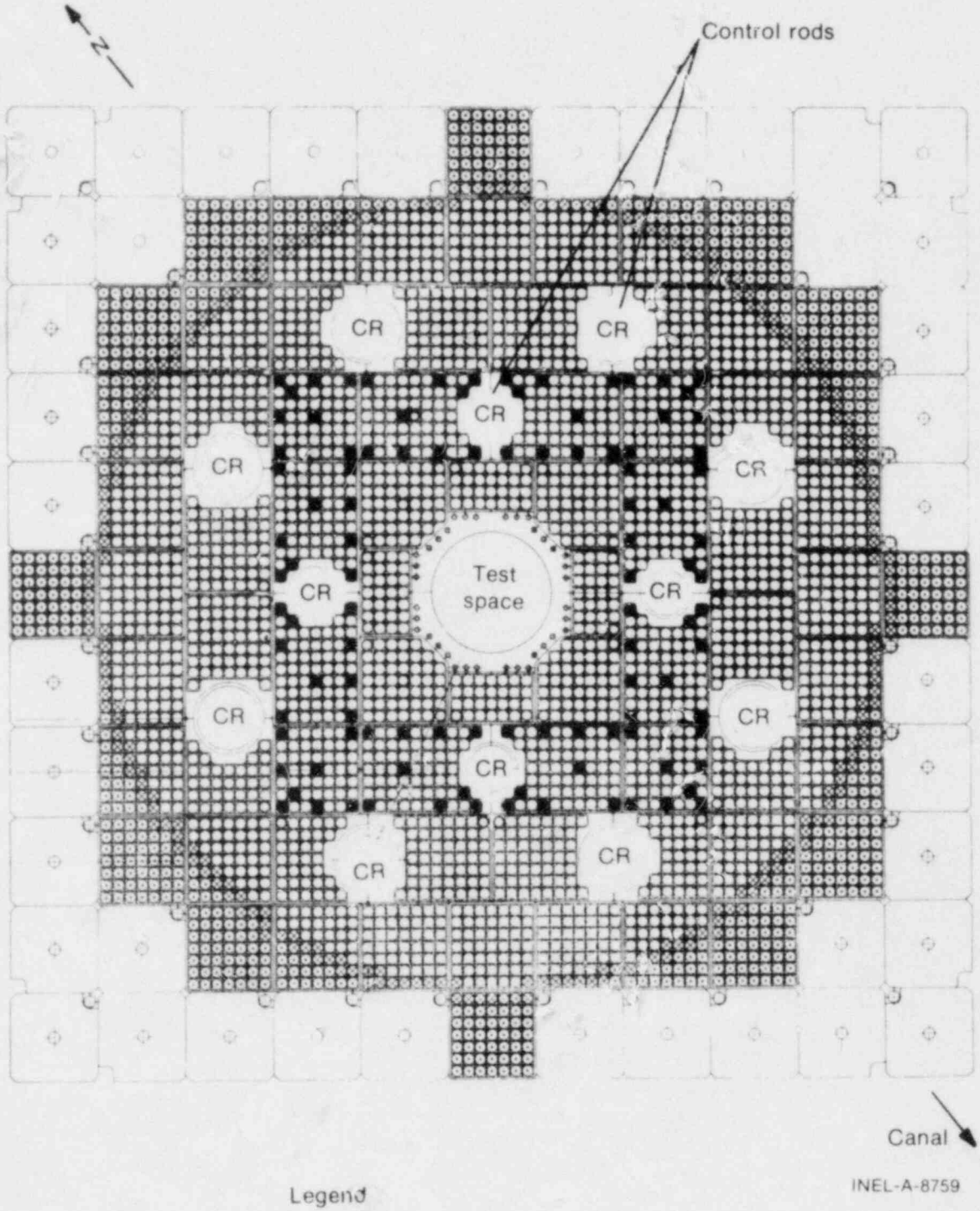

Fig. 2 Cross section of the PBF core.

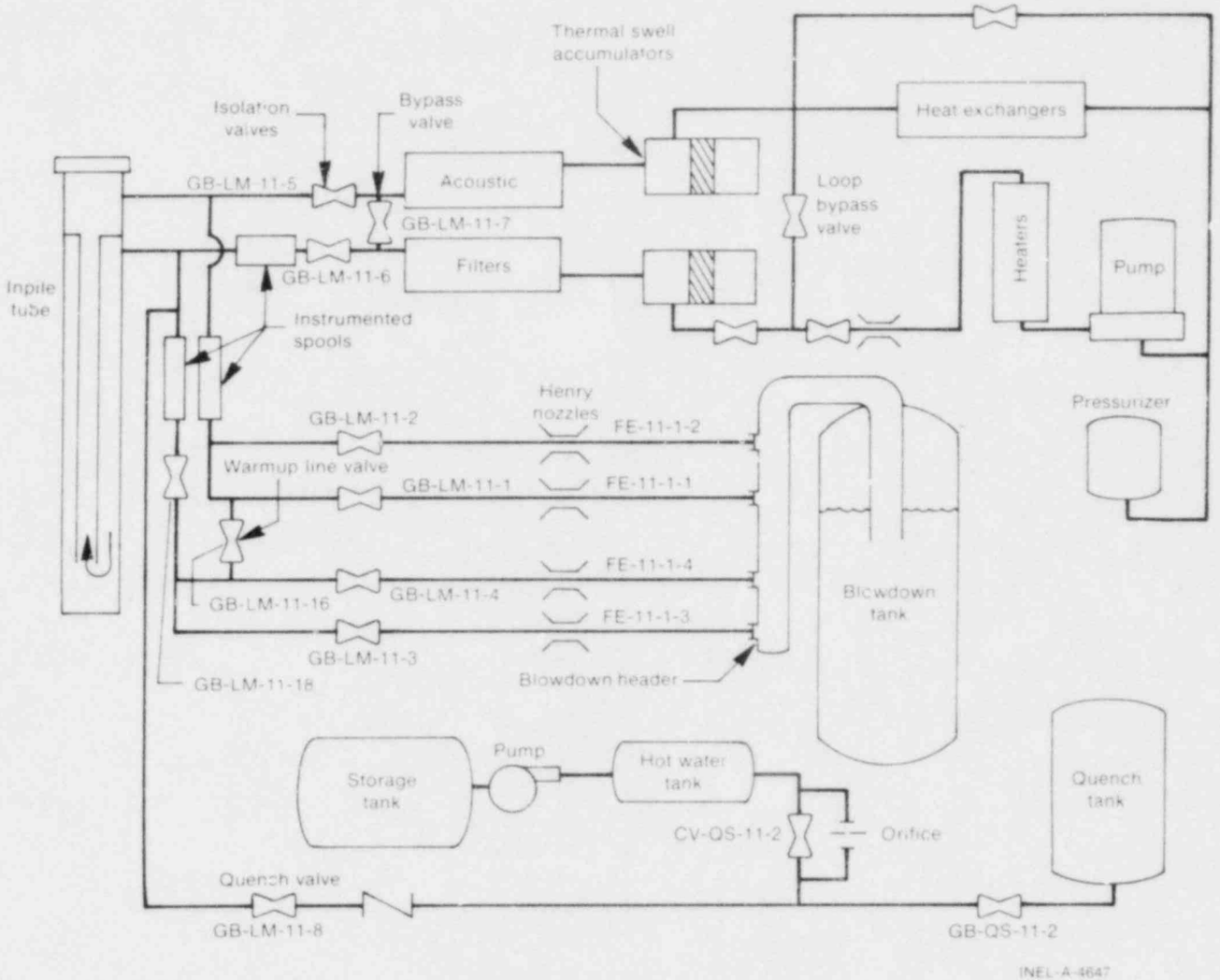

Fig. 3 PBF-LOCA modification system – schematic.

wall and aluminum core filler piece because of the temperature gradient between the two. A radial cross section of the IPT in the reactor core area is provided by Figure 4.

Blowdown capability is provided by two blowdown lines tied into the IPT inlet and outlet lines (cold leg-IPT inlet and hot leg-IPT outlet). Each line contains a measurement spool, two quick opening and closing (< 100 ms) blowdown valves, and two Henry nozzles which provide the break plane and control the break flow rate and depressurization rate.

The Henry nozzles, used in both Tests LOC-11B and 11C, are venturi type restrictors with throat diameters as tabulated in Table I.

The blowdown header and tank collect and contain the coolant ejected from the IPT and piping during blowdown and subsequent quench cooling.

Posttest quench cooling is accomplished by opening the quench valve, GB-LM-11-8, and closing GB-LM-11-18 (as shown in Figure 3) and the cold leg blowdown valves to permit coolant from the quench tank (pressurized by a nitrogen gas system) to enter the IPT. After the quench tank is emptied (about 60 s) coolant is pumped from the storage tank for up to four hours to provide cooling.

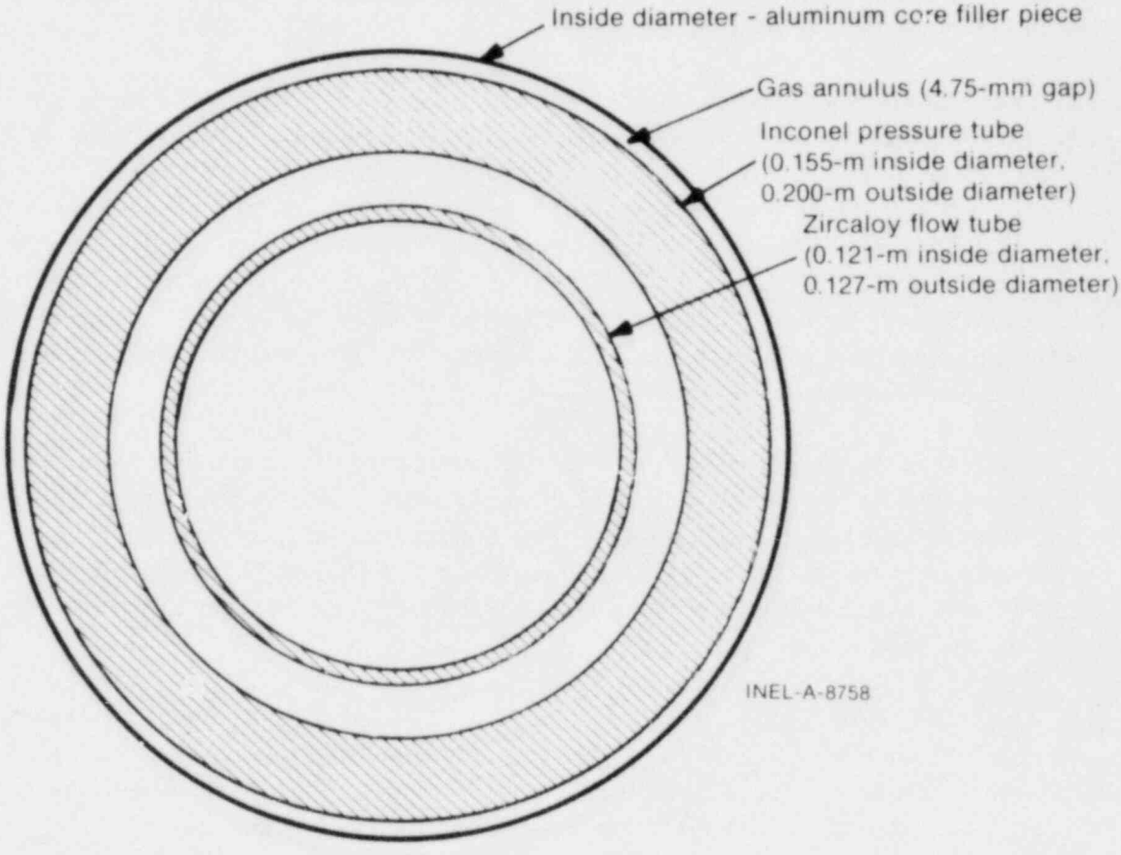

Fig. 4 Radial cross section of the PBF in-pile tube.

TABLE I

NOZZLE LOCATIONS AND DIAMETERS FOR TESTS LOC-11B AND 11C

Nozzle Designation	Location	Throat Diameter (mm)
FE-11-1-1	Hot leg	13.56
FE-11-1-2	Hot leg	14.22
FE-11-1-3	Cold leg	14.22
FE-11-1-4	Cold leg	13.56

A small warm-up line and valve connect the hot and cold blowdown piping legs and provide a small flow rate to keep the piping legs at system temperature prior to blowdown.

The sequencing of the valve operation during blowdown is controlled by a time-sequential programmer in the PBF programming and monitoring system. Signals for cladding temperature and elapsed time are also input into this system and determine the time of posttest quench cooling initiation.

The test experiment consisted of four separately shrouded unirradiated PWR-type fuel rods. The fuel rod characteristics are shown in Table II and the assembly configuration is shown in Figure 5. The fuel rod dimensional characteristics are typical of PWRs except for the length and plenum volume. The plenum volume is scaled proportionally to the active fuel length of a PWR. The helium prepressurization was selected so that two rods are pressurized to a value for the first LOFT core (0.1 MPa). The higher pressures shown in Table I for the remaining two rods correspond to cold values typical of the beginning-of-life and the end-of-life in a PWR. The enrichment is higher than that found in a PWR to obtain the desired peak linear heat rating in the PBF.

A fluted shroud design was selected for the fuel rod shrouds to minimize the chances of complete blockage of the flow channel in the event the uniform ballooning occurs as expected around the fuel rod circumference. The shroud is formed from a nominal 25.4-mm outside diameter zircaloy-2 tube with a wall thickness of 1.24 mm. The coolant flow area for each fuel rod contained within its shroud is 225.7 mm^2. The orientation of the fuel rods within the IPT is shown in Figure 6.

The LOC-11 test train is shown in Figure 7. During preblowdown steady-state conditions, the coolant flow enters the PBF reactor IPT inlet and passes downward outside the IPT flow tube to the vicinity of the lower particle screen. (The particle screens prevent fuel particles from being carried out of the IPT through the flow path.)

The coolant flow reverses at the IPT bottom and passes through the lower stainless steel particle screen and up the center of the IPT flow tube. The flow then enters one of

TABLE II

NOMINAL FUEL ROD CHARACTERISTICS FOR TESTS LOC-11B AND 11C

U_{235} enrichment	9.5%
UO_2 density	10.41 g/cm^3
Pellet diameter	9.30 mm
Cladding material	zircaloy-4
Cladding outside diameter	10.72 mm
Cladding inside diameter	9.50 mm
Cladding thickness	0.61 mm
Cladding finish	Pickled and rinsed
Diametral gap	0.20 mm
Pellet length	15.24 mm
Pellet dishing	Depth 0.33 mm
	Radius 3.30 mm
Plenum spring	Soiled carbon steel, 9.35 mm diameter
Insulating pellet length	15.24 mm
Active fuel stack length	914.4 mm maximum
Cladding overall length	1003.3 mm
Rod overall length	1205 mm
Helium prepressurization -	2 rods at 0.103 MPa (Rods 611-1 and 611-4)
	1 rod at 2.41 MPa (Rod 611-3)
	1 rod at 4.82 MPa (Rod 611-2)
Plenum volume	3.29 cm^3

means of turbine flowmeters. The orifice (located at the top and bottom of the fuel rod flow channel) also minimizes the effect of minor variations in hydraulic resistance on coolant mass flow rates between the four channels and aids in obtaining coolant flow stagnation in the fuel assembly during blowdown.

The coolant flow than passes through the annulus between the fluted shroud and the fuel rod, exits to the common upper plenum region, then passes through the upper particle screen and out the IPT exit. A filler block is located above the IPT exit to reduce the coolant volume in the upper plenum.

Table III provides a list of hydrualic volumes and flow areas for the PBF-LOCA system piping.

TABLE III

PBF-LOCA SYSTEM HYDRAULIC VOLUMES AND FLOW AREAS

Volume Location Description	Volume (ℓ)	Flow Area (m^2)
Piping from isolation valve (GB-LM-11-6) to inlet spool	1.962	0.002 29
Inlet spool	2.089	0.003 05
Piping from inlet spool to cold leg blowdown piping	0.901	0.002 29
Cold leg blowdown piping from IPT to blowdown spool	8.645	0.002 29
IPT downcomer	19.715	0.005 80
IPT lower plenum below particle screen	1.787	0.005 85
IPT lower plenum above particle screen	1.727	0.005 49
Lower turbine meter volume	0.428	0.000 81
Test fuel rod shroud volume	0.826	0.000 90
Upper turbine meter volume	0.583	0.000 87
IPT upper plenum below particle screen	12.724	0.009 87
IPT upper plenum above particle screen	5.118	0.016 79
Hot leg blowdown piping from IPT to blowdown spool	8.615	0.002 29

TABLE III (continued)

Volume Location Description	Volume (ℓ)	Flow Area (m^2)
Piping from hot leg to isolation valve (GB-LM-11-5)	6.117	0.002 29
Hot leg spool	2.553	0.003 05
Hot leg blowdown piping to blowdown valves	12.524	0.002 29
Cold leg blowdown piping to blowdown valves	16.156	0.002 29
Cold leg spool	2.553	0.003 05
Test fuel rod shroud bypass volume	17.86	0.008 21
Downcomer to hot leg leakage flow path	0.427	0.000 76
Hot leg blowdown piping from blowdown valve to Henry nozzle FE-11-1-1	2.673	0.002 29
Hot leg blowdown piping from blowdown valve to Henry nozzle FE-11-1-2	2.673	0.002 29
Cold leg blowdown piping from blowdown valve to Henry nozzle FE-11-1-3	2.673	0.002 29
Cold leg blowdown piping from blowdown valve to Henry nozzle FE-11-1-4	2.673	0.002 29
Quench line piping from GB-LM-11-8 to cold leg blowdown piping	9.008	0.002 29

2. EXPERIMENT CONDUCT

The LOC-11 experiment test train was installed in the PBF-IPT on November 11, 1977. Prior to the LOC-11B and 11C tests, several thermal cycles and blowdowns were performed on the IPT system with the test train installed. A complete history of all temperature, nuclear, and blowdown cycles experienced by the LOC-11 test train is provided in Appendix A.

Each test consisted of six phases which have been designated:

(1) Heat-up

(2) Power calibration

(3) Preconditioning

(4) Decay heat buildup

(5) Blowdown and quench

(6) Cooldown.

Nuclear operation began with the power calibration phase and terminated immediately prior to the blowdown and quench phases. Figures 8 and 9 provide operating sequence plots of representative system parameters for the duration of nuclear operation of both the LOC-11B and 11C tests.

2.1 Heat-Up Phase

Prior to nuclear operation, the IPT system coolant conditions were established at 15.2 MPa pressure, 1.01 ℓ/s flow rate through each test rod shroud, and an inlet temperature of between 575 K and 600 K (600 K was desired but not attainable until after the start of nuclear operation when additional nuclear heat was generated by the test fuel).

Loop coolant chemistry requirements were established during loop heatup and adjusted within the following limits:

pH range	5.7 to 10.2
Specific conductivity	1.4 to 48 μs/cm
Dissolved oxygen	Less than 0.1 ppm
Chlorides	Less than 0.15 ppm
Total suspended solids	Less than 1.0 ppm

2.2 Power Calibration

The power calibration provided a means for calibrating the thermal-hydraulically determined experiment power with reactor power and the self-powered neutron detectors (SPNDs) mounted on the test train. The power calibrations were performed at the PBF core power levels ranging from 2.0 to 14.9 MW for LOC-11B and from 2.0 to 25.1 MW for LOC-11C.

Rod power was calculated from a thermal balance using measurements of individual rod flow and coolant temperature rise along with shroud inlet temperature and pressure. To help verify the calculations that were made, data from the SPNDs, the reactor power instrumentation, and the centerline thermocouple as a function of rod power were compared with similar data from previous tests performed in the PBF.

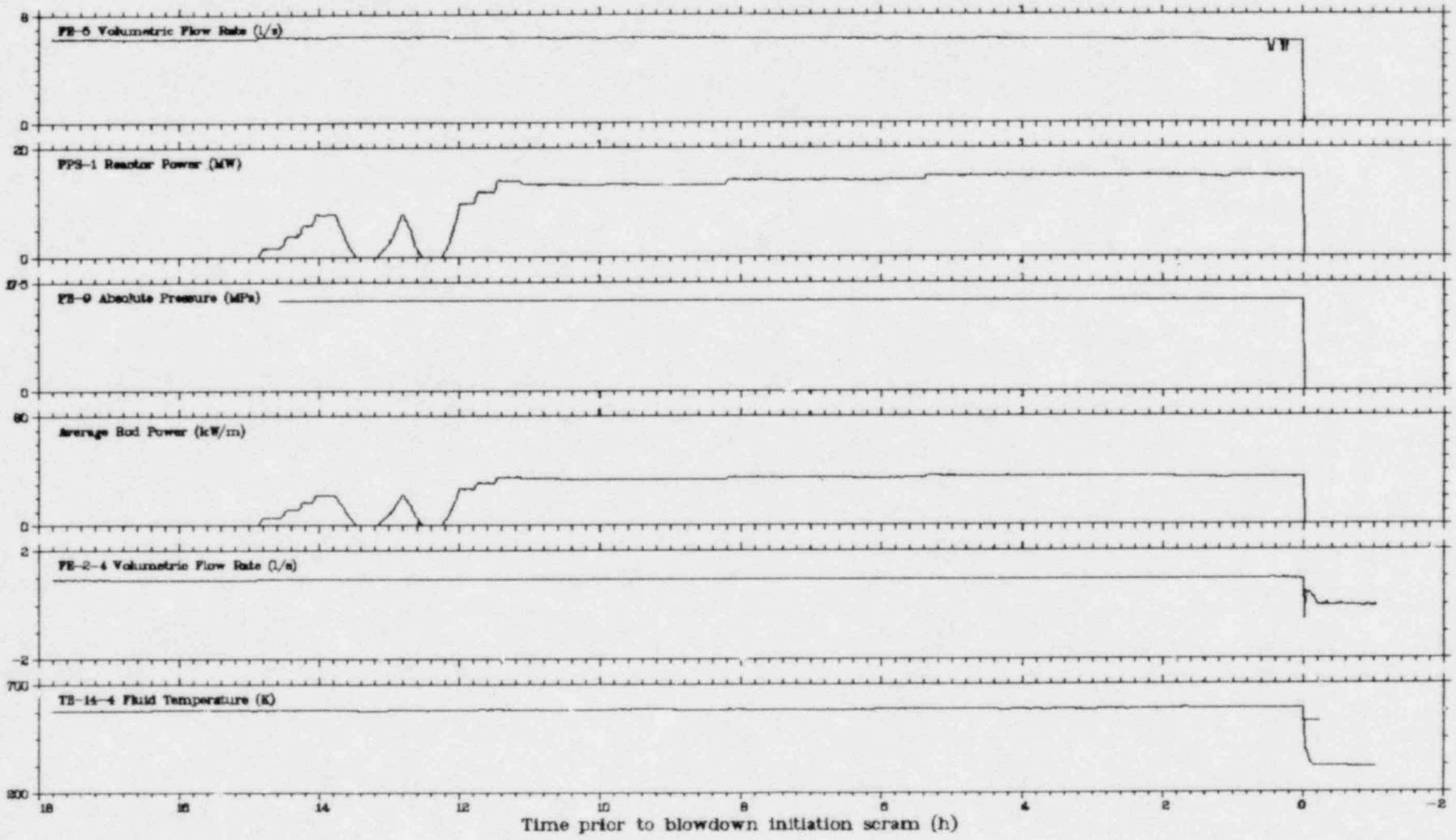

Fig. 8 Operating sequence of nuclear operation for Test LOC-11B.

(2) Power calibration

(3) Preconditioning

(4) Decay heat buildup

(5) Blowdown and quench

(6) Cooldown.

Nuclear operation began with the power calibration phase and terminated immediately prior to the blowdown and quench phases. Figures 8 and 9 provide operating sequence plots of representative system parameters for the duration of nuclear operation of both the LOC-11B and 11C tests.

2.1 Heat-Up Phase

Prior to nuclear operation, the IPT system coolant conditions were established at 15.2 MPa pressure, 1.01 ℓ/s flow rate through each test rod shroud, and an inlet temperature of between 575 K and 600 K (600 K was desired but not attainable until after the start of nuclear operation when additional nuclear heat was generated by the test fuel).

Loop coolant chemistry requirements were established during loop heatup and adjusted within the following limits:

pH range	5.7 to 10.2
Specific conductivity	1.4 to 48 μs/cm
Dissolved oxygen	Less than 0.1 ppm
Chlorides	Less than 0.15 ppm
Total suspended solids	Less than 1.0 ppm

2.2 Power Calibration

The power calibration provided a means for calibrating the thermal-hydraulically determined experiment power with reactor power and the self-powered neutron detectors (SPNDs) mounted on the test train. The power calibrations were performed at the PBF core power levels ranging from 2.0 to 14.9 MW for LOC-11B and from 2.0 to 25.1 MW for LOC-11C.

Rod power was calculated from a thermal balance using measurements of individual rod flow and coolant temperature rise along with shroud inlet temperature and pressure. To help verify the calculations that were made, data from the SPNDs, the reactor power instrumentation, and the centerline thermocouple as a function of rod power were compared with similar data from previous tests performed in the PBF.

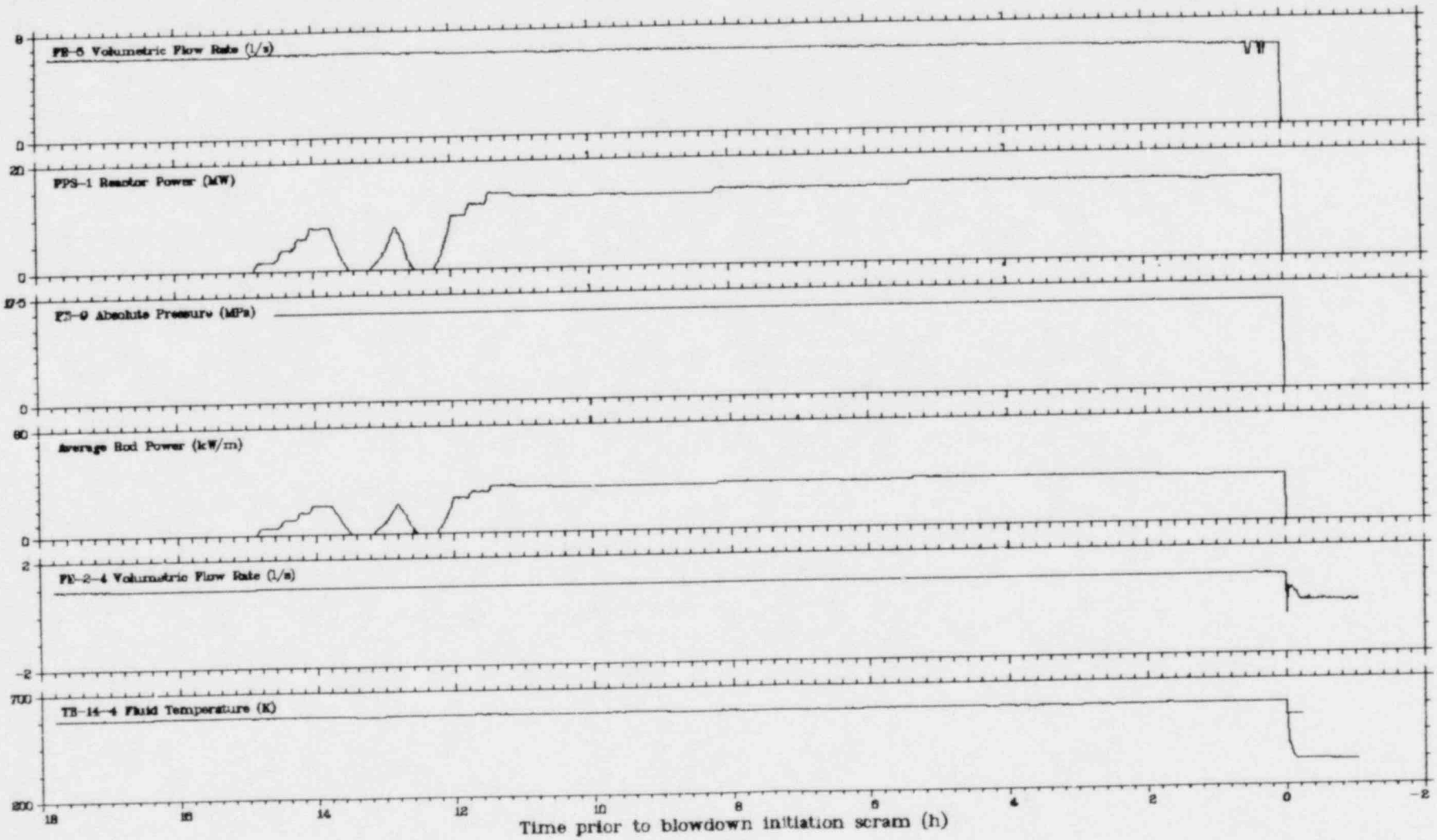

Fig. 8 Operating sequence of nuclear operation for Test LOC-11B.

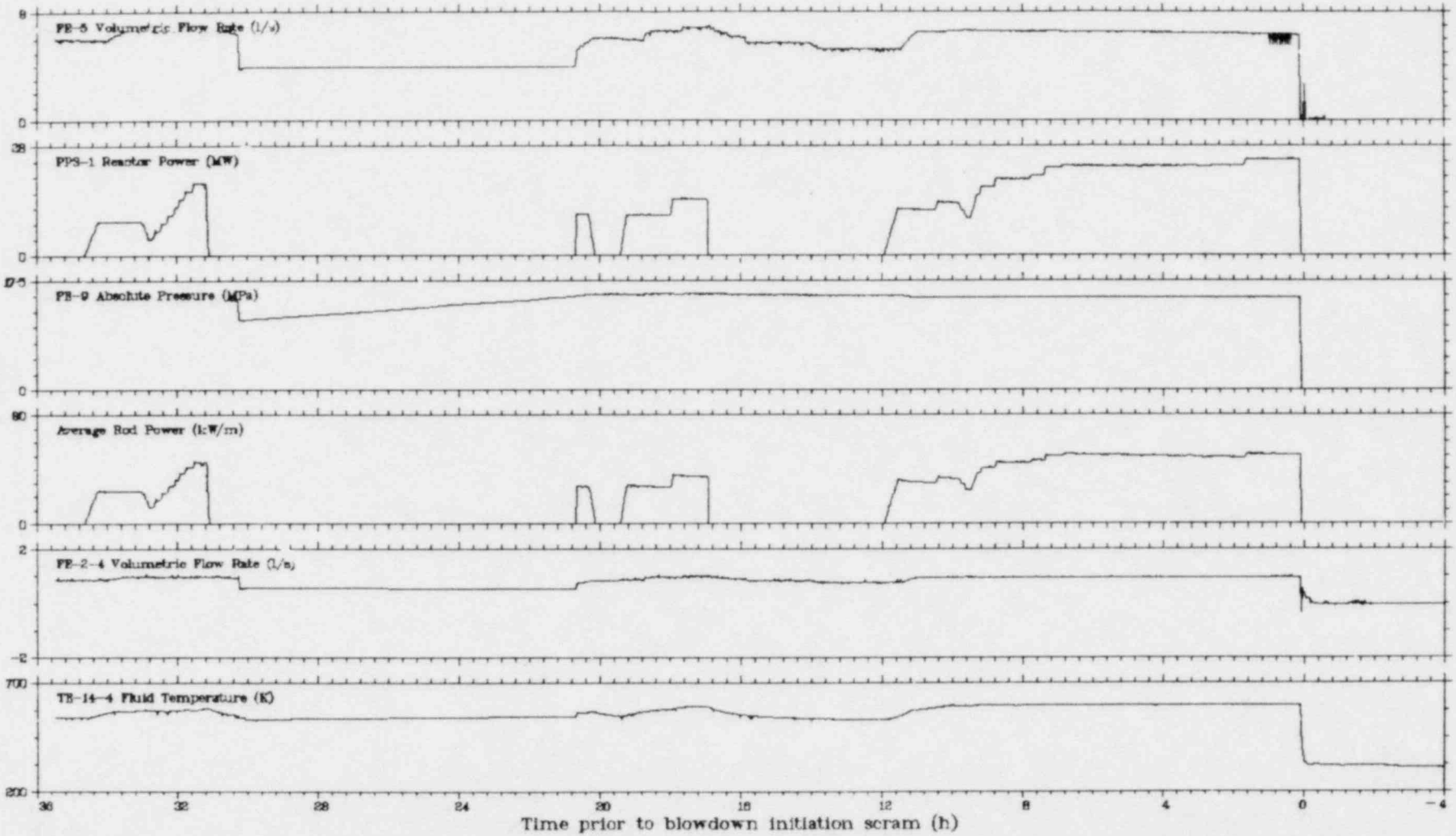

Fig. 9 Operating sequence of nuclear operation for Test LOC-11C.

Data required for the test rod average power are the coolant inlet temperature, pressure, flow rate, and the coolant temperature increase. Data taken for power calculations are average values from the most reliable instrumentation. The calculated rod power is most influenced by variations in the coolant inlet temperatures when the coolant is only a few degrees subcooled. A 2 σ analysis (95% confidence) for these inlet temperatures resulted in a ± 3 K and ± 2 K range for LOC-11B and LOC-11C, respectively. On the basis of these preblowdown temperatures, the minimum and maximum powers were determined. Table IV presents the calculated rod average and peak powers for both tests at blowdown initiation.

TABLE IV

TESTS LOC-11B AND 11C ROD POWERS

Test	Inlet Temperature (K)	Rod Peak Power (kW/m)	Rod Average Power (kW/m)
LOC-11B	Minimum 588	45.44	32.46
	Average 591	46.20	33.00
	Maximum 594	47.16	33.69
LOC-11C	Minimum 596	67.10	47.93
	Average 598	68.10	48.82
	Maximum 600	69.70	49.79

The axial power distribution was determined from the five axially distributed SPNDs and showed a peak-to-average ratio of 1.403 (± 1%, 95% confidence) at an elevation of 0.413 m (± 4%) measured from the bottom of the fuel stack.

2.3 Preconditioning

Preconditioning of the four test rods is accomplished by several cycles of power changes including the power calibration cycle. The power cycles promote fuel pellet cracking and restructuring and allow the initiation of pellet-cladding mechanical interaction to stablize.

Preconditioning cycles were performed in all three nuclear tests (LOC-11A, 11B, and 11C) and exact times and powers are tabulated in Appendix A.

2.4 Decay Heat Buildup

An uninterrupted period of nuclear operation at the approximate desired test rod power for blowdown was performed up to the time of blowdown initiation of both tests. A minimum desired time of ten hours at power was achieved for each test. This period was necessary to build up approximately 85% of the maximum possible decay heat in the rods. Exact times and powers are tabulated in Appendix A.

Prior to the blowdown initiation of LOC-11B and 11C, flow of approximately 6.5 ℓ/s had been established through the inlet spool piece. Approximately 1.0 ℓ/s of this value passed from the cold leg to the hot leg through the warm-up line. Approximately 4 ℓ/s passed through the four test rod shrouds. The piston ring seals at the lower support plate in the test train were designed to reduce the leakage flow around the lower support plate to approximately 0.1 ℓ/s. These three flow paths account for approximately 5.1 ℓ/s of the 6.5 ℓ/s flow measured at the inlet spool, implying that over 1.0 ℓ/s was bypassing the four test rod shrouds. Table V provides leakage flow data from both tests with no warm-up flow (GB-LM-11-18 closed).

TABLE V

LEAKAGE FLOW FOR TESTS LOC-11B AND 11C

Transducer	LOC-11B Time 01:16 1 February 1978	LOC-11C Time 00:09 15 February 1978
FE-2-1	1.02 ℓ/s	1.02 ℓ/s
FE-2-2	1.04 ℓ/s	1.07 ℓ/s
FE-2-3	1.04 ℓ/s	1.05 ℓ/s
FE-2-4	1.07 ℓ/s	1.07 ℓ/s
FE-5	5.41 ℓ/s	5.69 ℓ/s
Leakage	1.24 ℓ/s	1.48 ℓ/s
Percent leakage	30%	35%

Inspection of specified test train tolerances revealed some possibility of additional leakage paths through the flow tube metal transition locations and through the primary seal located at the top of the flow tube between the downcomer flow and the hot leg. These paths would bypass the test rod shroud area.

Since the location of the leakage path could not be determined with any certainty the amount of flow passing up through the test train outside the rod shrouds is unknown. It may be as much as 1.48 ℓ/s or as little as 0.1 ℓ/s. In addition, comparison of steady-state measurements taken from all three tests indicate that the magnitude of the leakage flow could vary significantly under supposedly similar hydraulic conditions. Possible explanations for this observed behavior are that the leakage flow is dependent upon thermal expansion effects of the IPT and IPT flow tube due to temperature gradients across the IPT wall and upon mechanical interaction effects of the cold leg flow with the IPT flow tube. If the leakage flow rate is dependent upon the effects mentioned above, then the flow resistance of the leakage flow rate will vary during the transient.

2.5 Blowdown and Quench

The LOC-11B blowdown sequence was initiated at 01:46:28 on February 1, 1978, and at 00:24:32 on February 15, 1978 for LOC-11C. The reactor scram occurred 30 s after blowdown initiation and the blowdown system valving sequenced as shown in Table VI. Shutdown of the reactor, reactor scram, was performed by rapid insertion of the control rods to their seat, or in core position. The time from scram initiation to rods seated was approximately 100 ms.

As noted in the valve sequencing table the stagnation time following isolation until blowdown initiation was reduced from 0.8 s in LOC-11B to 0.15 s in LOC-11C. This shorter stagnation period was achieved in conjunction with higher test rod powers to produce higher peak cladding temperatures during blowdown. The LOC-11B test was performed through the use of blowdown valves GB-LM-11-1 and -3 with Henry nozzle throat diameters of 13.56 and 14.22 mm, respectively. Test LOC-11C was performed through use of valves GB-LM-11-2 and -3, both of which were connected to Henry nozzles with a throat diameter of 14.22 mm.

The blowdown transient of both tests lasted about 30 s and was followed by a 20-s delay period prior to the quench initiation. The blowdown tank absolute pressure was 0.12 MPa prior to blowdown and remained essentially at that value throughout the transient.

Quench initiation was initiated approximately 50 s following reactor scram as indicated by the opening of the quench valve GB-LM-11-8 and the closing of the cold leg blowdown and shutoff valves. After injection of the 365 K quench tank water, cooling was maintained by continued flow from the hot water and storage tanks. The hot water tank prevents system thermal shock by providing an initial supply of heated water which gradually decreases to the ambient temperature of the storage tank supply.

2.6 Cooldown

Coolant was pumped from the storage tank for several hours at a maximum rate of 3.2 ℓ/s and a minimum rate of 0.15 ℓ/s. This rate was adjusted to ensure the cladding surface temperatures did not exceed 610 K.

No fuel rod cladding failure or fission product release to the system coolant was evident during or following any of the nuclear tests. Following Test LOC-11C, the experiment test train was removed from the PBF IPT for disassembly and inspection in the hot cell.

TABLE VI

VALVE SEQUENCING FOR TESTS LOC-11B AND 11C

	Test LOC-11B (s)[a]	Test LOC-11C (s)[a]
Reactor Scram	0.1150	0.0943
Bypass (GB-LM-11-7)	0.1150 begins to open 0.1619 open	0.0943 begins to open 0.1405 open
Cold leg isolation (GB-LM-11-6)	0.1314 begins to close 0.1862 closed	0.1150 begins to close 0.1703 closed
Hot leg isolation (GB-LM-11-5)	0.1418 begins to close 0.1871 closed	0.1213 begins to close 0.1675 closed
Hot leg blowdown (GB-LM-11-1)	0.9082 begins to open [b]	50.0880 begins to open [b]
Hot leg blowdown (GB-LM-11-2)	50.1356 begins to open 50.2249 open	0.2624 begins to open 0.3308 open
Cold leg blowdown (GB-LM-11-3)	1.0199 begins to open 1.1020 open	0.4148 begins to open 0.4916 open
	50.1804 begins to close 50.3595 closed	50.1570 begins to close 50.3290 closed
Cold leg shutoff (GB-LM-11-8)	50.1626 begins to close 50.2827 closed	50.1370 begins to close 50.2573 closed
Quench (GB-LM-11-8)	50.3865 begins to open 50.4749 open	50.3860 begins to open 50.4715 open

[a] Seconds following scram initiation.

[b] Opened indication failed (valve opens in ≈ 100 ms).

III. INSTRUMENTATION AND MEASUREMENTS

The PBF-LOCA instrumentation system was designed to measure and record the important events that occur prior to and during a LOCA test. The instrumentation required to satisfactorily describe the test fuel rod behavior during blowdown conditions is of primary importance. The instrumentation for the LOC-11 tests measures the fuel rod surface and centerline temperatures, plenum pressure and temperature, axial length change, and coolant pressure, temperature, density, and flow rate.

A geometric orientation of the four test rods and associated instrumentation is shown in Figure 10. General thermocouple construction information is supplied in Table VII.

The following instrumentation is used for measuring variables for each of the four fuel rods. The detector name is given in each case and X denotes the test rod number (1, 2, 3, or 4). Figure 11 graphically displays the relative locations of the fuel rod instrumentation.

(1) One Kaman strain gage pressure transducer, PE-4-X, is fitted with a slip fitting sleeve to protect the device from thermal transients and measures the plenum pressure of each fuel rod. The sleeve consists of a stainless steel annular jacket containing a silver cylinder pressed on the inner surface and separated from the outer surface by a helium filled gap.

(2) Four cladding surface thermocouples are laser welded to each fuel rod at 0.53 m (TE-5-X and TE-10-X) and 0.61 m (TE-8-X and TE-22-X) above the bottom of the fuel stack.

(3) One tungsten-rhenium centerline thermocouple (TE-11-X), located 0.53 m above the bottom of the fuel rod stack in a 1.91-mm hole, measures the fuel temperature of each test rod.

(4) One plenum temperature thermocouple (TE-3-X), unshielded from thermal radiation, indicates each fuel rod plenum gas temperature.

(5) One EG&G Idaho, Inc., axial length change transformer (LVDT-X) is located at the lower end of each rod. The device is not temperature compensated or thermally shielded, so it detects rather than quantifies length changes during the transient blowdown, quench, and cooling phases of the tests.

(6) Five self-powered neutron detectors, SPND-1, 2, 3, 4, and 5, are located at 0.76, 0.61, 0.46, 0.30, and 0.15 m, respectively, above the bottom of the fuel rod stack. The detectors correlate reactor power to calibrated fuel rod power and determine the axial power shape with power level.

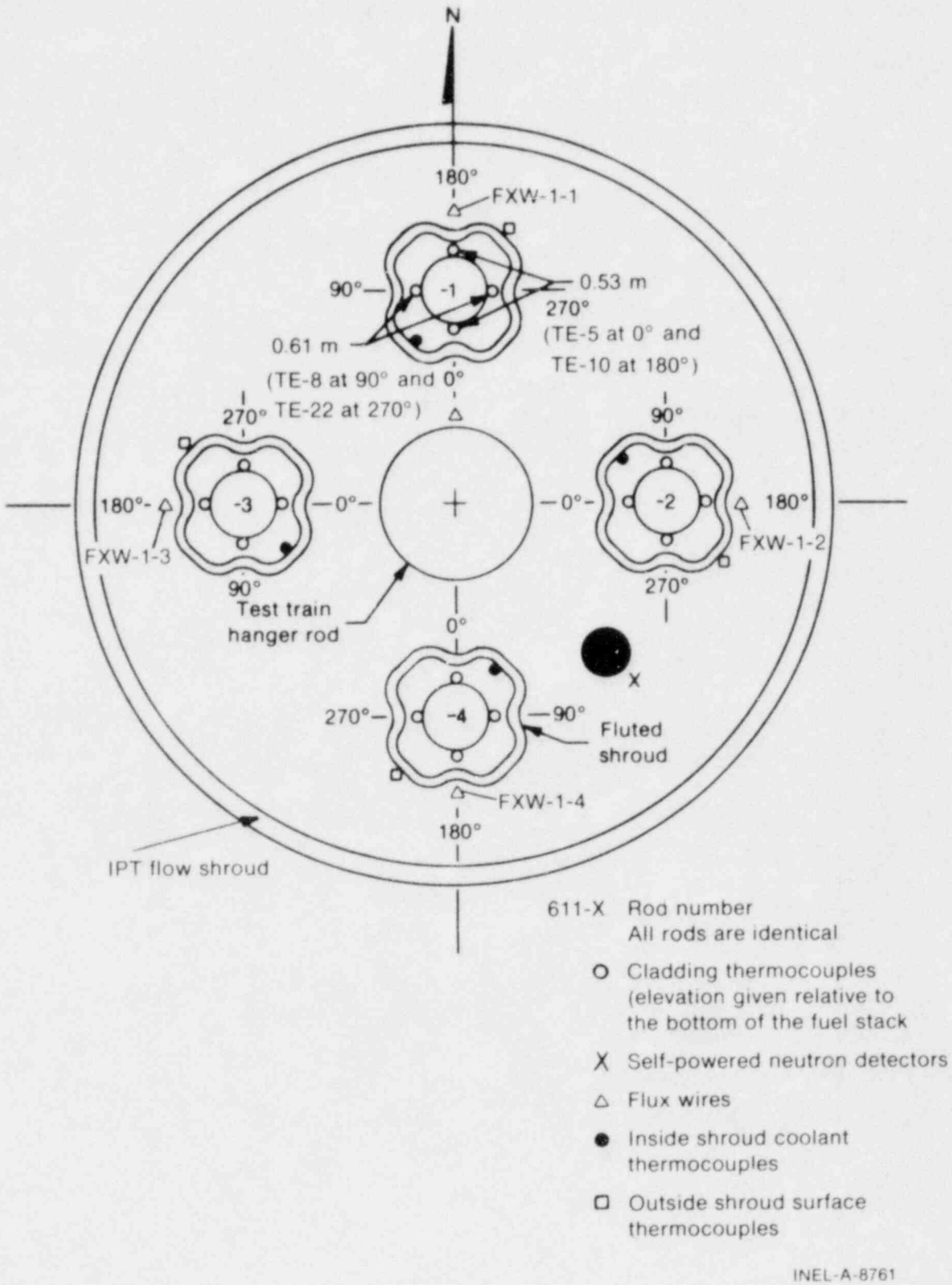

Fig. 10 LOC-11 fuel rod orientation with instrumentation.

TABLE VII

THERMOCOUPLE CONSTRUCTION FOR LOC-11 TESTS

Thermocouple	Type	Insulation	Sheath Material	Outside Diameter (mm)	Wall Thickness (mm)	Junction Type
Centerline (TE-11)	W5Re/W26Re	BeO hard fired	Ta	1.575	0.254	Grounded
Cladding surface (TE-5,8,10,22)	Type K	MgO	Ti	1.17	0.229	Ungrounded, spade tip
Coolant channel differential (ΔT-1)	Type K	MgO	SST	1.575	0.254	Ungrounded
Fuel rod plenum (TE-3)	Type K	MgO	SST	0.51	[a]	Grounded
Fuel rod coolant inlet and outlet (TE-2,14)	Type K	MgO	SST	1.575	0.254	Grounded
Inside shroud coolant (TE-6,9,13)	Type K	MgO	SST	1.02	0.203	Grounded
Shroud outer surface (TE-4,7,12)	Type K	MgO	Ti	1.17	0.229	Grounded, spade tip

[a] Wall is swaged at junction and thickness is not available.

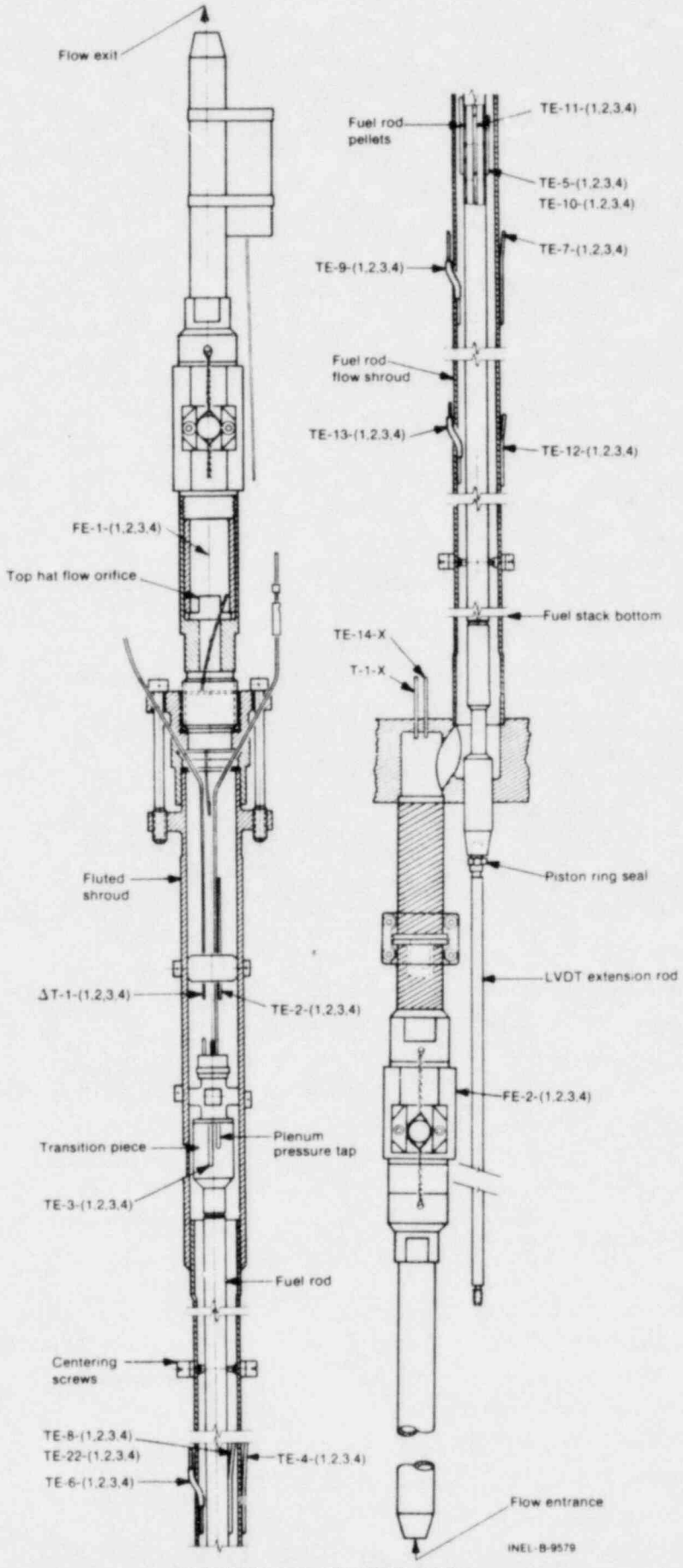

Fig. 11 LOC-11 fuel rod assembly with instrumentation.

Instrumentation for measurement of coolant variables in the in-pile tube is shown in Figure 12 and described as follows:

(1) A full-flow turbine flowmeter (Flow Technology) with graphite sleeve bearings is located at the top (FE-1-X) and bottom (FE-2-X) of each fuel rod shroud. Two pickup coils (EG&G Idaho, Inc.) are a. sociated with each turbine to determine flow direction.

(2) A pair of differential thermocouples (ΔT-1-X) measures the temperature increase across each fuel rod flow channel during steady-state operation for power calibration purposes. The junctions are located 0.18 m above the top of the fuel stack and 0.092 below the fuel stack bottom.

(3) A pair of thermocouples for each fuel rod channel measures the fuel rod flow inlet and outlet temperatures. The inlet junction (TE-14-X) is located 0.092 m below the bottom of the fuel stack and the outlet junction is (TE-2-X) 0.18 m above the fuel stack top.

(4) Three thermocouples, TE-6, 9, and 13-X, are located 0.30, 0.46, and 0.61 m above the fuel stack bottom, respectively. These detectors are positioned inside each flow shroud to measure the coolant temperature during the transient.

(5) Three thermocouples, TE-4, 7, and 12-X, are located 0.30, 0.46, and 0.61 m above the fuel stack bottom, repectively. These detectors are positioned on each fuel rod flow shroud to measure the outside surface temperature.

(6) Three thermocouples, TE-1, 19, and 18, are located in the IPT upper plenum at 0.38, 0.76, and 1.52 m above the fuel rod flow shroud outlets, respectively. These measurements aid in determining temperature gradients in the upper plenum region. The thermocouples are structurally supported by the hanger rod.

(7) One thermocouple (TE-17), located in the bypass volume at the midplane of the active fuel length, aids in the determination of the coolant condition in the bypass region.

(8) Two thermocouples, TE-15 and 16, are located in the lower plenum 0.025 and 0.22 m below the lower support plate, respectively, to aid in determining the coolant condition in the lower plenum. The lower thermocouple junction is also below the pressure transducers located in the lower plenum. A 16-mm tip is exposed to the coolant.

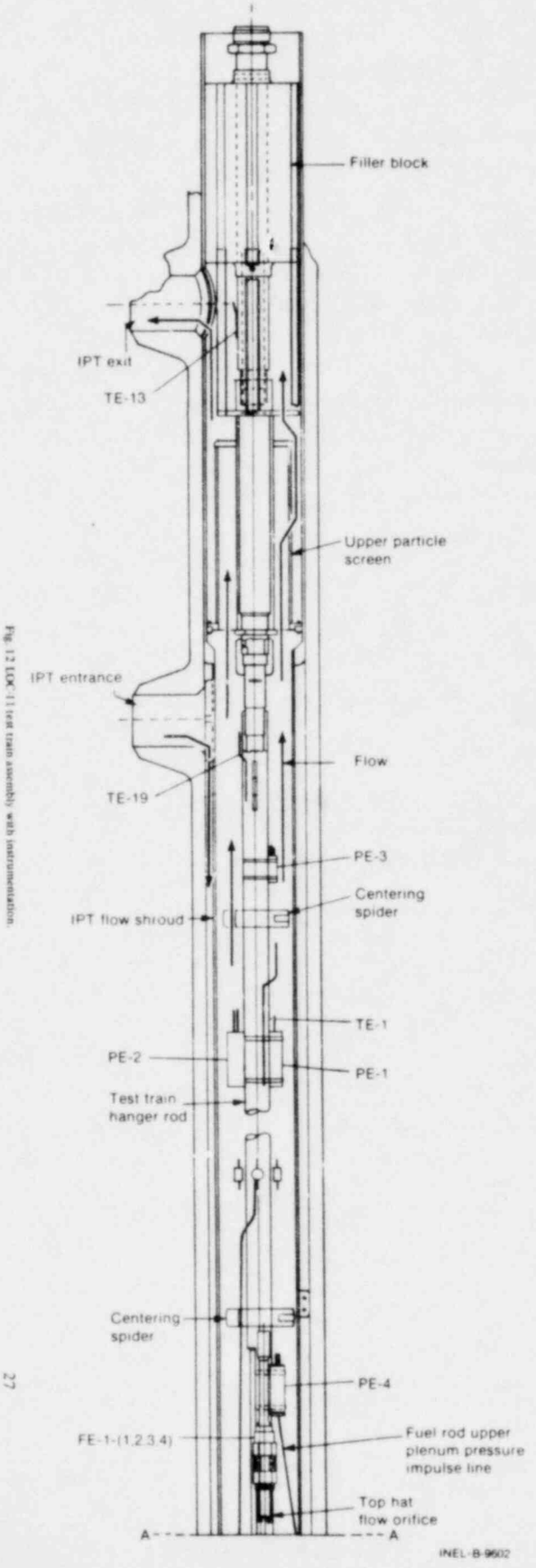

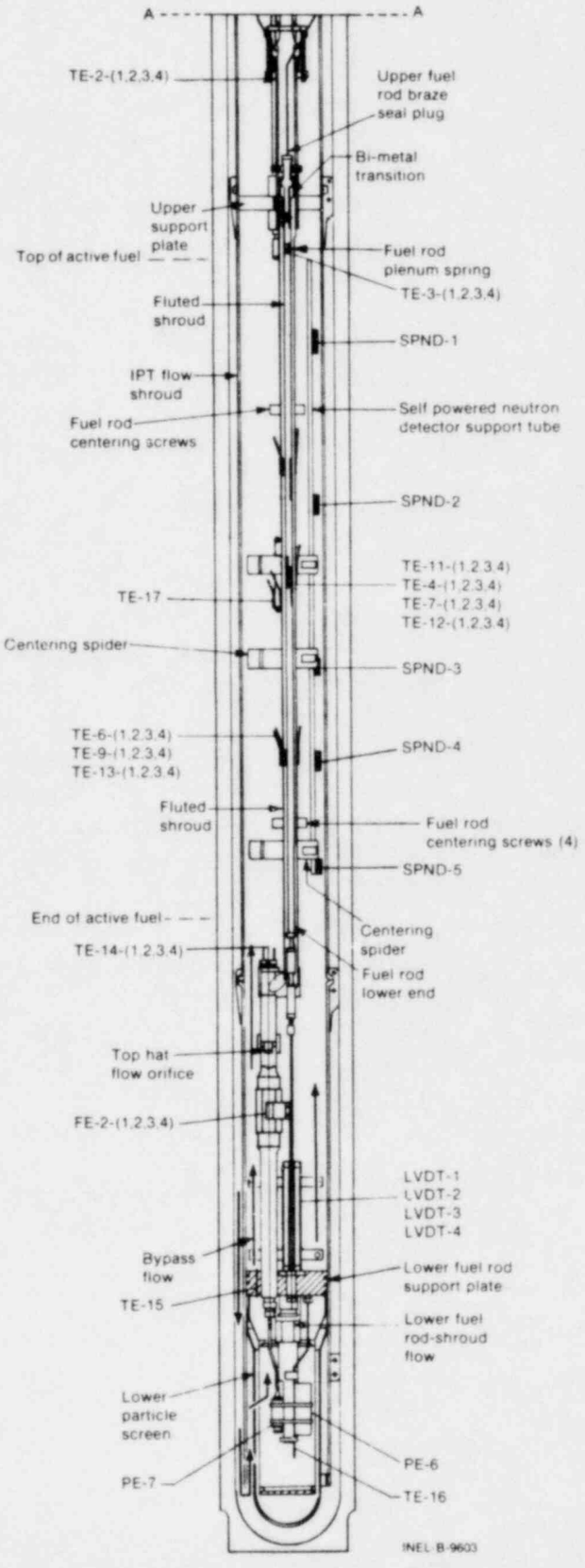

Fig. 1.2 LOFT 11 test train assembly with instrumentation.

(9) One EG&G Idaho, Inc., fast response pressure transducer, PE-3, measures large IPT overpressure transients. The transducer is located 0.68 m above the fuel rod shroud tube outlets.

(10) Two EG&G Idaho, Inc., fast response pressure transducers, PE-2 and PE-6, are located 0.41 m above the fuel rod shroud outlets and 0.19 m below the lower support plate, respectively, and measure the pressure change during the blowdown transient.

(11) Two Kaman strain gage type pressure transducers, PE-1 and PE-7, are located 0.41 m above the fuel rod shroud outlets and 0.19 m below the lower support plate, respectively, and measure the preblowdown and saturated blowdown pressure.

The three measurement spools provide additional initial conditions and blowdown instrumentation which further characterizes the blowdown coolant variables of pressure, temperature, velocity, and density in the lines leading to the Henry nozzle break planes. Schematics of the measurement spools showing associated instrumentation positions are provided in Figures 13 and 14. Instrumentation for the measurement spools is described as follows:

(1) Resistance temperature detectors (Rosemount) that measure the preblowdown temperature of the coolant in each spool are TE-20, inlet spool; TE-23, cold leg spool; and TE-26, hot leg spool.

(2) Exposed ribbon thermocouples, Type K, (Rosemount) that measure the coolant temperature in each spool during the transient are TE-21, inlet spool; TE-24, cold leg spool; and TE-25, hot leg spool.

(3) Flush mounted pressure transducers (Precise Sensors) that measure the preblowdown and subcooled decompression in each spool are PE-8, inlet spool; PE-10, cold leg spool; and PE-12, hot leg spool.

(4) Water-cooled stand-off mounted pressure transducers (Precise Sensors) measuring the preblowdown and saturated decompression in each spool are PE-9, inlet spool; PE-11, cold leg spool; and PE-13, hot leg spool.

(5) A full-flow turbine meter with graphite bearings (Flow Technology) measures preblowdown coolant velocity to the IPT in the inlet condition spool (FE-5) and blowdown velocities from the IPT in the hot (FE-9) and cold leg (FE-6) spools.

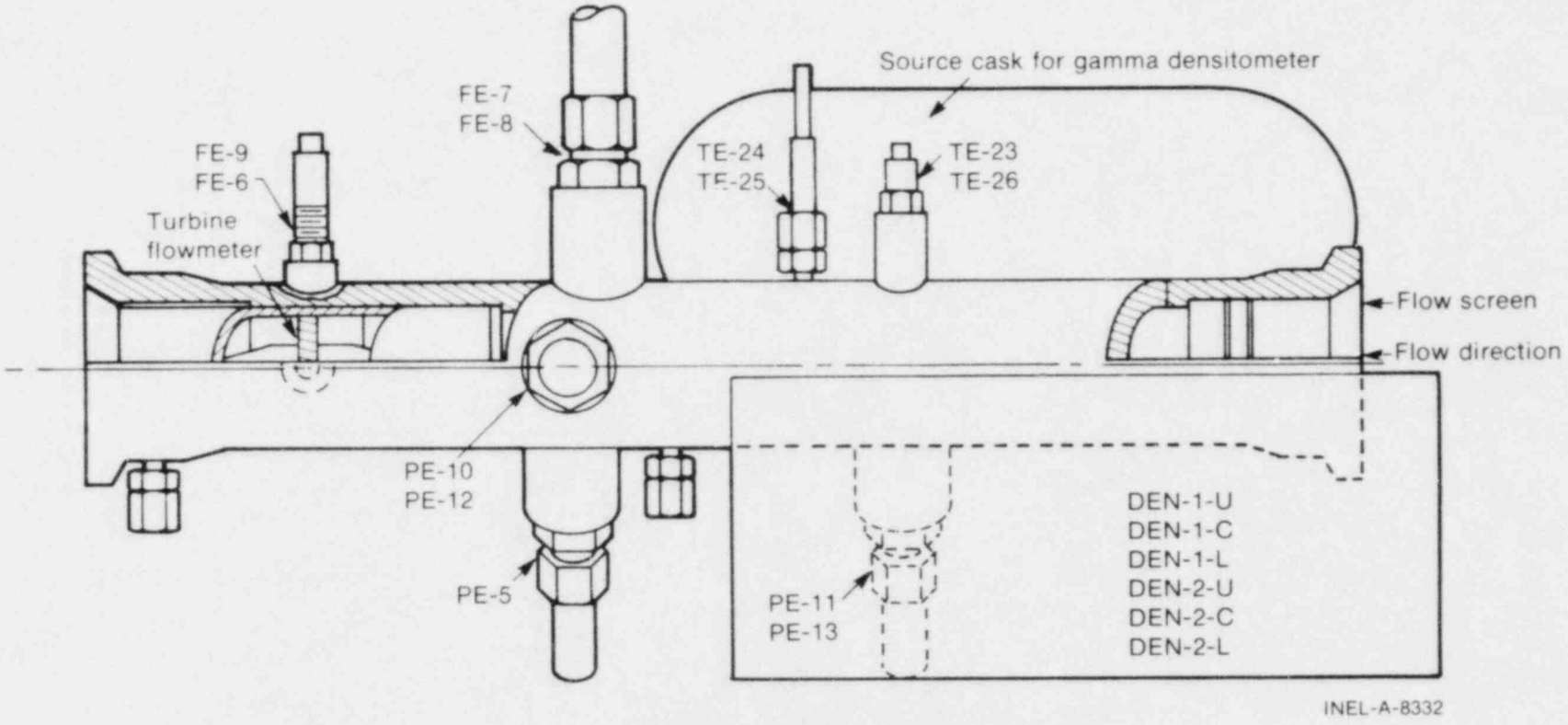

Fig. 13 LOC-11 blowdown spool with instrumentation.

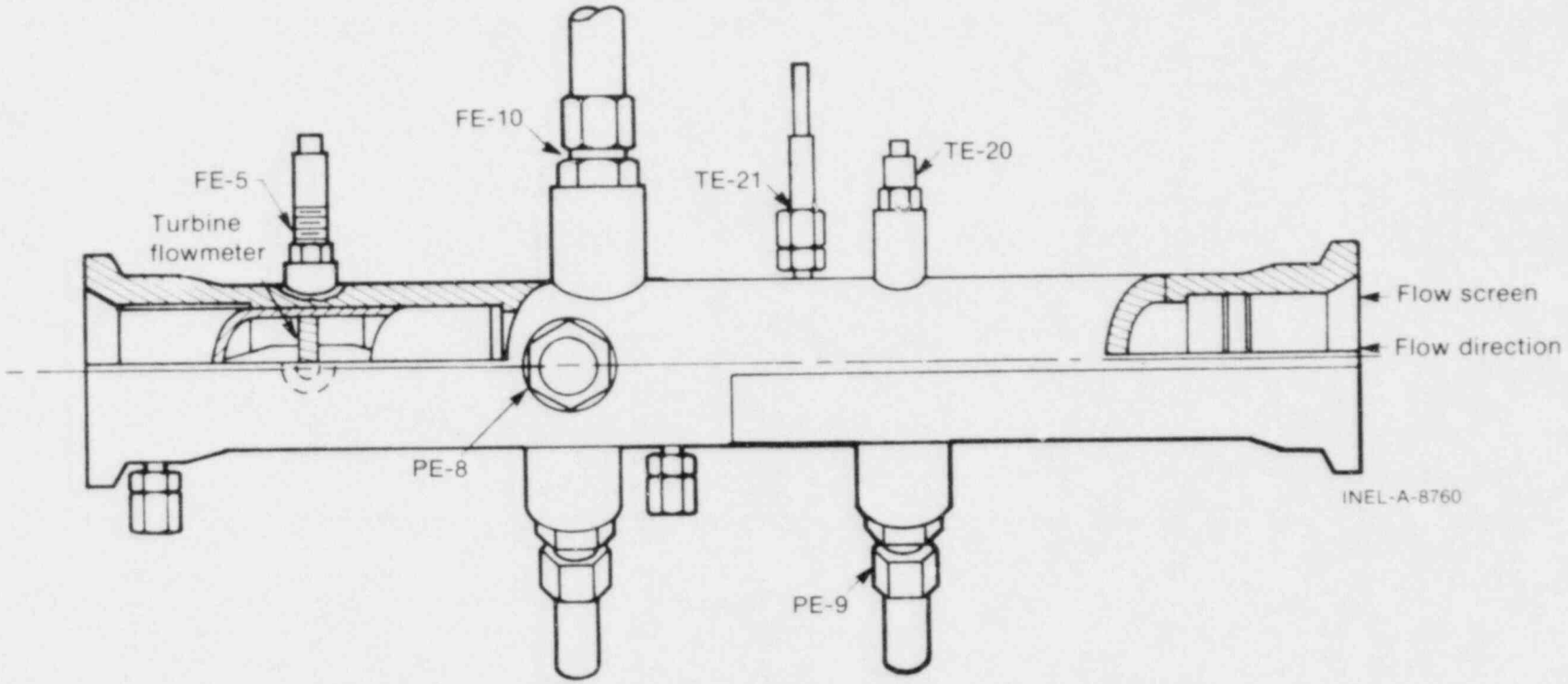

Fig. 14 LOC-11 inlet spool with instrumentation.

(6) A drag disc (Ramapo), in each hot and cold leg spool, FE-8 and FE-7, respectively, measures the coolant momentum flux during the transient. It is located in the center of the flow area and intercepts approximately 12% of the flow area.

(7) A three-beam gamma densitometer (EG&G Idaho, Inc.) on each hot and cold leg spool measures coolant density.

(8) A pressure difference transducer, ΔPE-5 (BLH), connects the hot and cold leg spools. This device measures the preblowdown pressure difference across the test train and the spool-to-spool difference during the transient.

Free-field pressure transducers, in which the sensing elements are inside a bellows arrangement, are used to eliminate connecting transmission lines and thereby produce higher frequency response without the distortion caused by the lines.

The three-beam gamma densitometers use the attenuation of gamma rays from a Cesium-137 source to sense the density of fluid within the blowdown spool. The three beams traverse the lower, middle, and upper parts of the horizontal spool pieces as shown in Figures 15 and 16. Each beam is considered to be measuring the average density along its chordal path. To calculate the total average density the vertical density gradient was assumed to be linear; then the chordal densities were fit to the model and integrated over the spool piece cross section.

In the two blowdown spools the flow regime can be considered homogeneous in most cases. The fluid is made homogeneous by flow dispersing screens located in the inlet section of the spool pieces. These screens are designed to remove fluid swirl caused by upstream piping and then disperse and homogenize the fluid. At low velocities and high void fractions, the flow will degenerate into a stratified state which introduces significant flow regime errors in the data presented.

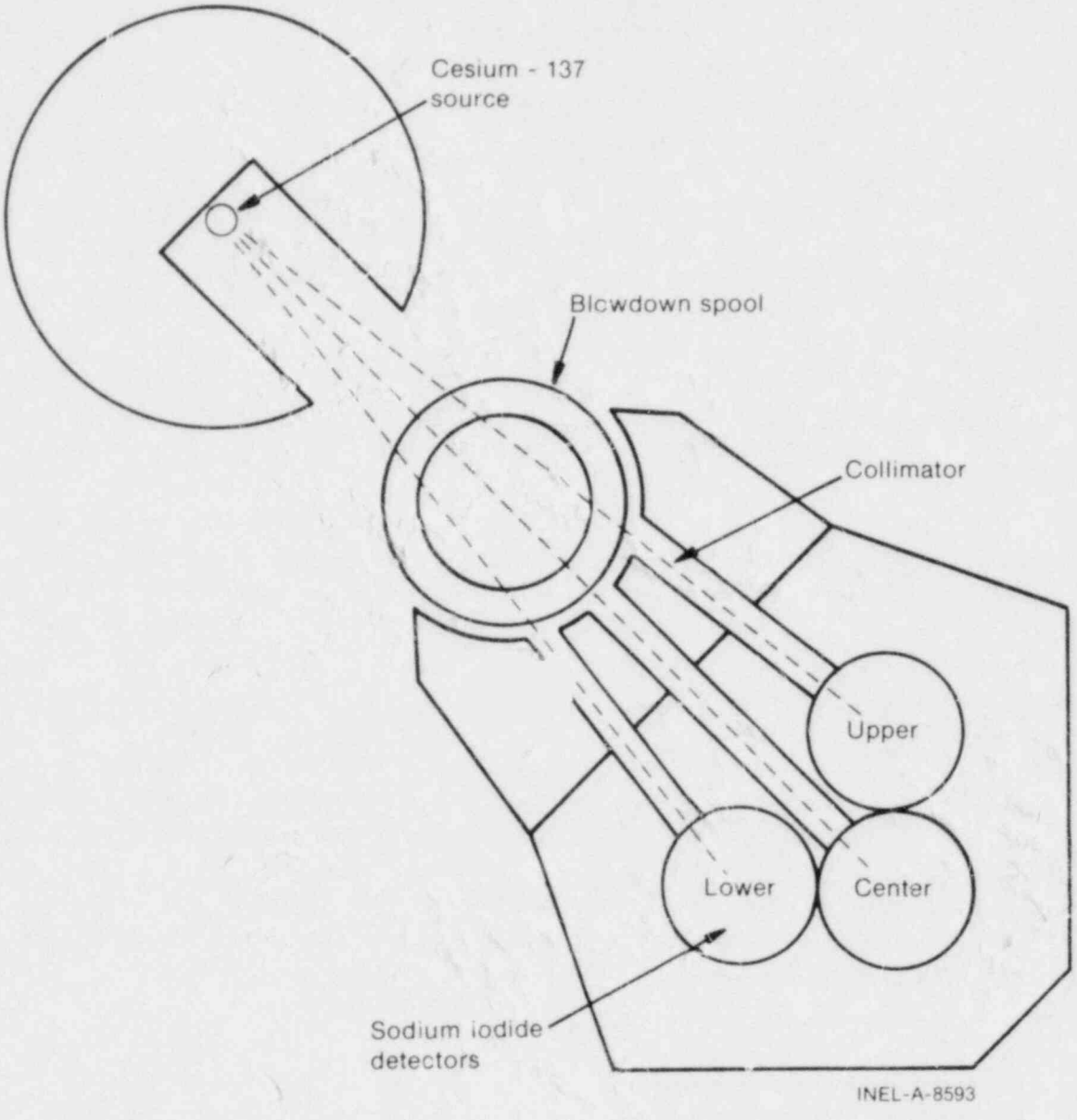

Fig. 15 Gamma beam densitometer for LOC-11 tests.

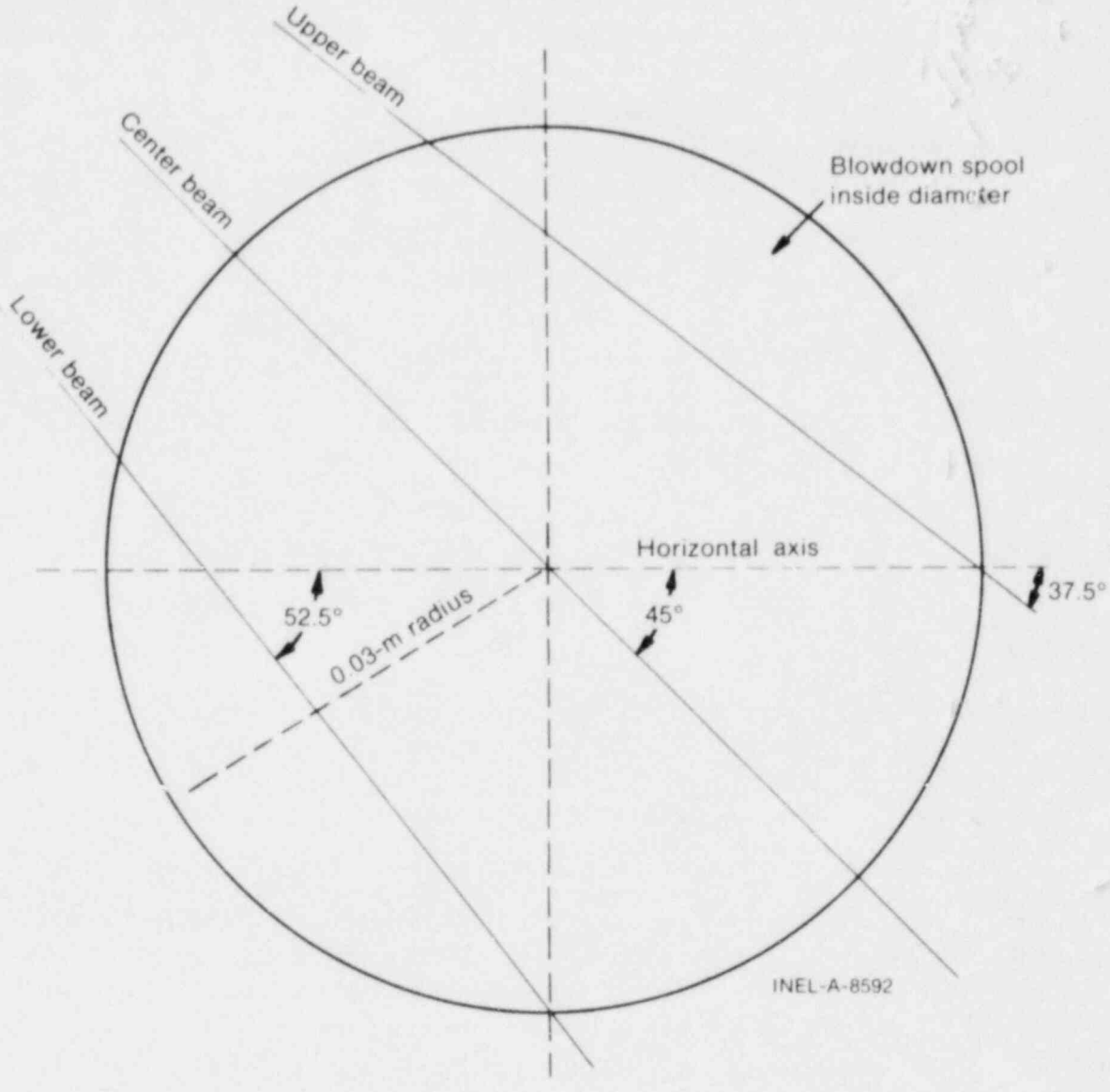

Fig. 16 Gamma beam densitometer paths through the blowdown spools.

IV. DATA PRESENTATION

The data from PBF-LOCA Tests LOC-11B and 11C are presented with brief comment. Processing analysis has been performed only to the extent necessary to obtain appropriate engineering units and to ensure that the data are reasonable and consistent. In all cases, in converting transducer output to engineering units, a homogeneous fluid was assumed. To ensure reasonable and consistent data, all the data in this report were subjected to a thorough review. Where possible, instrument channel outputs were compared with corresponding parameter channels, test predictions, calculated quantities, and preblowdown initial conditions. The results provide the basis for posttest processing and adjustments, and verification applied to these data. Appendix B describes in detail methods used to determine the adjustments that have been applied to the presented data and provides the basis for verifying or dividing the data into four categories:

(1) Verified engineering units data (Verified) – have been verified to represent the variable being measured within specified uncertainty limits.

(2) Restrained data – appear reasonable but not within uncertainty limits, or no data from an independent channel are available for comparison.

(3) Trend data – are suitable for illustrative purposes but probably not for numerical analyses.

(4) Failed data – are irretrievable due to a measurement channel failure.

Of the 119 measurements used to monitor the system performance for both Tests LOC-11B and 11C, 105 and 102 measurements, respectively, produced usable data. All detector analog output was digitized and recorded by the PBF data acquisition and reduction system (PBF/DARS). The PBF/DARS tape recording system was configured to record at four different bandwidths:

(1) dc to 10 Hz

(2) dc to 100 Hz

(3) dc to 5 kHz

(4) dc to 20 kHz.

Table VIII denotes the bandwidth used for each measurement in the LOC-11 tests. All blowdown data plots (-5 to 30 s) were recorded at a sample rate of 50 points per second. Long term data plots (-5 to 120 s) were compressed at a 4 to 1 ratio, giving an effective rate

TABLE VIII

DATA PRESENTATION FOR TESTS LOC-11B AND 11C

Measurement	Location and Comments[a]	Range[a]		Frequency Response[a]		Figure[a]	Measurement Comments
		Detector	Data Acquisition System	Detector	Data[b] Acquisition System		
PLENUM TEMPERATURE	Chromel-Alumel thermocouple						
Fuel Rod							
TE-3-1	Fuel rod plenum	0 to 1643 K	280 to 820 K	1.7 Hz	10 Hz	17 LOC-11B 122 LOC-11C C1	Restrained[b]
TE-3-2						18 LOC-11B 123 LOC-11C D1	Restrained[b]
TE-3-3						19 LOC-11B 124 LOC-11C E1	Restrained[b]
TE-3-4							Failed for LOC-11B and C
CLADDING TEMPERATURE	Chromel-Alumel thermocouples unless otherwise specified	0 to 1643 K	280 to 1530 K	7 Hz	10 Hz		
Fuel Rod							
TE-5-1	Fuel rod cladding surface thermocouple, 0.61 m above fuel stack bottom, 0°					20 LOC-11B 125 LOC-11C F1	Restrained[c]
TE-5-2						21 LOC-11B 126 LOC-11C G1	Restrained[c]
TE-5-3						22 LOC-11B 127 LOC-11C H1	Restrained[c]
TE-5-4						23 LOC-11B 128 LOC-11C I1	Restrained[c]
TE-8-1	Fuel rod cladding surface thermocouple, 0.53 m above fuel stack bottom, 90°					24 LOC-11B 129 LOC-11C J1	Restrained[c]
TE-8-2						25 LOC-11B 130 LOC-11C K1	Restrained[c]
TE-8-3						26 LOC-11B 131 LOC-11C L1	Restrained[c]
TE-8-4						27 LOC-11B 132 LOC-11C M1	Restrained[c]
TE-10-1	Fuel rod cladding surface thermocouple, 0.53 m above fuel stack bottom, 270°					28 LOC-11B 133 LOC-11C N1	Restrained[c]
TE-10-2		0 to 1643 K	280 to 1530 K	7 Hz	10 Hz	29 LOC-11B 134 LOC-11C O1	Restrained[c]
TE-10-3						30 LOC-11B 135 LOC-11C P1	Restrained[c]
TE-10-4						31 LOC-11B 136 LOC-11C B2	Restrained[c]
TE-22-1	Fuel rod cladding surface thermocouple, 0.61 m above fuel stack bottom, 270°					32 LOC-11B 137 LOC-11C C2	Trend data for LOC-11B[d] Restrained data for LOC-11C[c]
TE-22-2						33 LOC-11B 138 LOC-11C D2	Restrained[c]
TE-22-3						34 LOC-11B 139 LOC-11C E2	Restrained[c]
TE-22-4						35 LOC-11B 140 LOC-11C F2	Restrained[c]
CENTERLINE TEMPERATURE	Tungsten-rhenium thermocouple	0 to 2477 K	309 to 2750 K	1.4 Hz	10 Hz		
TE-11-1	Fuel rod centerline thermocouple, 0.53 m above fuel stack bottom					36 LOC-11B 141 LOC-11C G2	Verified

TABLE VIII (continued)

Measurement	Location and Comments[a]	Range[a]		Frequency Response[a]		Figure[a]	Measurement Comments
		Detector	Data Acquisition System	Detector	Data Acquisition System[b]		
TE-11-2		0 to 2877 K	309 to 2750 K	1.4 Hz	10 Hz	37 LOC-11B 142 LOC-11C H2	Verified
TE-11-3						38 LOC-11B 143 LOC-11C I2	Verified
TE-11-4						39 LOC-11B 144 LOC-11C J2	Verified
FLUID TEMPERATURE	Chromel-Alumel thermocouples, unless otherwise specified.						
Test Train							
TE-1	Lower upper plenum thermocouple, 0.38 m above top of active fuel.	0 to 1643 K	280 to 829 K	1.7 Hz	10 Hz	40 LOC-11B 145 LOC-11C K2	From - 10 to 45 s Verified 45 to 120 s Restrained[e]
TE-2-1	Fuel rod coolant outlet thermocouple, 0.18 m above top of active fuel.					41 LOC-11B 146 LOC-11C L2	Test LOC-11B From - 10 to 50 s Verified 50 to 120 s Restrained[e,f] Test LOC-11C From - 10 to 6 s Verified 6 to 18 s Restrained[e] 18 to 50 s Verified 50 to 120 s Restrained[f]
TE-2-2		0 to 1643 K	280 to 820 K	1.7 Hz	10 Hz	42 LOC-11B 147 LOC-11C M2	Test LOC-11B From - 10 to 50 s Verified 50 to 120 s Restrained[f] Test LOC-11C - 10 to 6 s Verified 6 to 18 s Restrained[e] 18 to 50 s Verified 50 to 120 s Restrained[f]
TE-2-3							Channel failed
TE-2-4						43 LOC-11B 148 LOC-11C N2	Test LOC-11B From - 10 to 50 s Verified 50 to 120 s Restrained[f] Test LOC-11C From - 10 to 7 s Verified 7 to 120 s Restrained[e]
TE-6-1	Inside shroud coolant thermocouple, 0.61 m above fuel stack bottom.					44 LOC-11B 149 LOC-11C O2	Test LOC-11B From - 10 to 8 s Verified 8 to 18 s Restrained[e] 18 to 27 s Verified 27 to 120 s Restrained[e] Test LOC-11C From - 10 to 4 s Verified 4 to 120 s Restrained[e]
TE-6-2							Channel failed
TE-6-3						45 LOC-11B 150 LOC-11C P2	Test LOC-11B From - 10 to 8 s Verified 8 to 10 s Restrained[e] 18 to 42 s Verified 42 to 120 s Restrained[e] Test LOC-11C From - 10 to 4 s Verified 4 to 120 s Restrained[e]
TE-6-4						46 LOC-11B 151 LOC-11C Q2	Test LOC-11B From - 10 to 6 s Verified 6 to 18 s Restrained[e] 12 to 31 s Verified 31 to 120 s Restrained[e] Test LOC-11C From - 10 to 4 s Verified 4 to 120 s Restrained[e]
TE-9-1	Inside shroud coolant thermocouple, 0.46 m above fuel stack bottom.					47 LOC-11B 152 LOC-11C C3	Test LOC-11B From - 10 to 6 s Verified 6 to 20 s Restrained[e] 20 to 30 s Verified 30 to 120 s Restrained[e] Test LOC-11C From - 10 to 4 s Verified 4 to 120 s Restrained[e]
TE-9-2						48 LOC-11B 153 LOC-11C D3	Test LOC-11B From - 10 to 6 s Verified 6 to 20 s Restrained[e] 20 to 30 s Verified 30 to 120 s Restrained[e] Test LOC-11C From - 10 to 4 s Verified 4 to 120 s Restrained[e]

TABLE VIII (continued)

Measurement	Location and Comments[a]	Range[a]		Frequency Response[a]		Figure[a]	Measurement Comments
		Detector	Data Acquisition System	Detector	Data Acquisition System[b]		
Test Train (continued)							
TE-9-3		0 to 1643 K	280 to 820 K	1.7 Hz	10 Hz	49 LOC-11B 154 LOC-11C E3	Test LOC-11B From - 10 to 6 s Verified 6 to 20 s Restrained[e] 20 to 30 s Verified 30 to 120 s Restrained[e] Test LOC-11C From - 10 to 4 s Verified 4 to 120 s Restrained[e]
TE-9-4						50 LOC-11B 155 LOC-11C F3	Test LOC-11B From - 10 to 6 s Verified 6 to 20 s Restrained[e] 20 to 30 s Verified 30 to 120 s Restrained[e] Test LOC-11C From - 10 to 4 s Verified 4 to 120 s Restrained[e]
TE-13-1	Inside shroud coolant thermocouple, 0.30 m above fuel stack bottom.					51 LOC-11B 156 LOC-11C G3	Test LOC-11B From - 10 to 8 s Verified 8 to 18 s Restrained[e] 18 to 28 s Verified 28 to 120 s Restrained[e] Test LOC-11C From - 10 to 6 s Verified 6 to 120 s Restrained[e]
TE-13-2						52 LOC-11B 157 LOC-11C H3	Test LOC-11B From - 10 to 8 s Verified 8 to 18 s Restrained[e] 18 to 28 s Verified 28 to 120 s Restrained[e] Test LOC-11C From - 10 to 6 s Verified 6 to 120 s Restrained[e]
TE-13-3							Channel failed
TE-13-4						53 LOC-11B 158 LOC-11C J3	Test LOC-11B From - 10 to 8 s Verified 8 to 18 s Restrained[e] 18 to 28 s Verified 28 to 120 s Restrained[e] Test LOC-11C From - 10 to 6 s Verified 6 to 120 s Restrained[e]
TE-14-1	Fuel rod coolant inlet thermocouple, 0.092 m below bottom of fuel stack.	0 to 1643 K	0 to 1539 K	1.7 Hz	10 Hz	54 LOC-11B 159 LOC-11C J3	Test LOC-11B From - 10 to 16 s Verified 16 to 19 s Restrained[e] 19 to 25 s Verified 25 to 120 s Restrained[e] Test LOC-11C From - 10 to 14 s Verified 14 to 120 s Restrained[e]
TE-14-2							Channel failed
TE-14-3						55 LOC-11B 160 LOC-11C K3	Test LOC-11B From - 10 to 16 s Verified 16 to 19 s Restrained[e] 19 to 25 s Verified 25 to 120 s Restrained[e] Test LOC-11C From - 10 to 14 s Verified 14 to 120 s Restrained[e]
TE-14-4						56 LOC-11B 161 LOC-11C L3	Test LOC-11B From - 10 to 19 s Verified 19 to 21 s Restrained[e] 21 to 28 s Verified 28 to 120 s Restrained[e] Test LOC-11C From - 10 to 11 s Verified 11 to 120 s Restrained[e]
TE-15	Lower plenum thermocouple, 0.025 m below support plate.					57 LOC-11B 162 LOC-11C M3	Test LOC-11B From - 10 to 35 s Verified 35 to 120 s Restrained[e] Test LOC-11C From - 10 to 25 s Verified 25 to 120 s Restrained[e]
TE-16	Lower plenum thermocouple, 0.22 m below support plate and near particle screen	0 to 1643 K	280 to 820 K	1.7 Hz	10 Hz	58 LOC-11B 163 LOC-11C N3	Tests LOC-11B and 11C From - 10 to 50 s Verified 50 to 120 s Restrained[f]
TE-17	Bypass volume thermocouple, located in the midplane of the active fuel, 0.46 m above the fuel stack bottom.					59 LOC-11B 164 LOC-11C O3	Tests LOC-11B and 11C From - 10 to 50 s Verified 50 to 120 s Restrained[f]
TE-18	Upper plenum exit thermocouple, 1.52 m above top of fuel rod shroud outlet.					60 LOC-11B 165 LOC-11C P3	Test LOC-11B From - 10 to 30 s Verified 30 to 50 s Restrained[e,f] 50 to 120 s Restrained[f]

TABLE VIII (continued)

Measurement	Location and Comments[a]	Range[a]		Frequency Response[a]		Figure[a]	Measurement Comments
		Detector	Data Acquisition System	Detector	Data Acquisition System[b]		
Test Train (continued)							
TE-18		0 to 1643 K	280 to 820 K	1.7 Hz	10 Hz		Test LOC-11C From - 10 to 22 s Verified 22 to 120 s Restrained[e]
TE-19	Upper plenum exit thermocouple, 0.76 m above top of fuel rod shroud outlet.					61 LOC-11B 166 LOC-11C B4	Test LOC-11B From - 10 to 20 s Verified 20 to 50 s Restrained[e,f] 50 to 120 s Restrained[e] Test LOC-11C From - 10 to 16 s Verified 16 to 120 s Restrained[e]
Inlet Spool							
TE-20	Resistance temperature detector.		280 to 766 K	1.4 Hz	10 Hz	52 LOC-11B 167 LOC-11C E4	Test LOC-11B From - 10 to 12 Verified 12 to 120 s Restrained[e] Test LOC-11C From - 10 to 10 s Verified 10 to 120 Restrained[e]
TE-21	Exposed ribbon thermocouple.		280 to 820 K	17.5 Hz	100 Hz	63 LOC-11B 169 LOC-11C D4	Test LOC-11B From - 10 to 39 s Verified 39 to 120 s Restrained[e] Test LOC-11C From - 10 to 30 s Verified 30 to 120 s Restrained[e]
Blowdown Spool							
TE-23	Resistance temperature detector.		280 to 766 K	17.5 Hz	100 Hz	64 LOC-11B 169 LOC-11C E4	Test LOC-11B From - 10 to 18 s Verified 18 to 120 s Restrained[e] Test LOC-11C From - 10 to 15 s Verified 15 to 120 s Restrained[e]
TE-24	Exposed ribbon thermocouple, cold leg outlet spool.		280 to 820 K	17.5 Hz	100 Hz	65 LOC-11B 170 LOC-11C F4	Test LOC-11B From - 10 to 18 s Verified 18 to 120 s Restrained[e] Test LOC-11C From - 10 to 15 s Verified 15 to 120 s Restrained[e]
TE-25	Exposed ribbon thermocouple, hot leg inlet spool.					66 LOC-11B G4 LOC-11B	Test LOC-11B From - 10 to 14 s Verified 14 to 120 s Restrained[e] Channel failed for LOC-11C
TE-26	Resistance temperature detector, hot leg inlet spool.		280 to 766 K	1.4 Hz	10 Hz	67 LOC-11B 171 LOC-11C H4 LOC-11B G4 LOC-11C	Test LOC-11C From - 10 to 14 s Verified 14 to 120 s Restrained[e] Test LOC-11C From - 10 to 11 s Verified 11 to 120 s Restrained[e]
DIFFERENTIAL TEMPERATURE							
ΔT-1-1	Fuel rod coolant temperature rise thermocouple, 0.18 m above top of active fuel.	0 to 1643 K	280 to 766 K	1.7 Hz	100 Hz	68 LOC-11B 172 LOC-11C I4 LOC-11B H4 LOC-11C	Test LOC-11B From - 10 to 1 s Verified 1 to 120 s Restrained[g] Test LOC-11C From - 10 to 1 s Verified 1 to 10 s Restrained[g] 10 to 16 s Failed[h] 16 to 18 s Restrained[g] 18 to 50 s Failed[h] 50 to 120 s Restrained[g]
ΔT-1-2		0 to 1643 K	280 to 766 K	1.7 Hz	100 Hz	69 LOC-11B 173 LOC-11C J4 LOC-11B I4 LOC-11C	Test LOC-11B From - 10 to 1 s Verified 1 to 120 s Restrained[g] Test LOC-11C From - 10 to 1 s Verified 1 to 10 s Restrained[g] 10 to 16 s Failed[h] 16 to 18 s Restrained[g] 18 to 50 s Failed[h] 50 to 120 s Restrained[g]
ΔT-1-3						70 LOC-11B 174 LOC-11C K4 LOC-11B J4 LOC-11C	Test LOC-11B From - 10 to 1 s Verified 1 to 120 s Restrained[g] Test LOC-11C From - 10 to 1 s Verified 1 to 9 s Restrained[g] 9 to 16 s Failed[h] 16 to 120 s Restrained[g]
ΔT-1-4						71 LOC-11B 175 LOC-11C L4 LOC-11B	Test LOC-11B From - 10 to 1 s Verified 1 to 120 s Restrained[g]

TABLE VIII (continued)

Measurement	Location and Comments[a]	Range[a]		Frequency Response[a]		Figure[a]	Measurement Comments
		Detector	Data Acquisition System	Detector	Data[b] Acquisition System		
ΔT-1-4 (continued)		0 to 1643 K	280 to 766 K	1.7 Hz	100 Hz	K4 LOC-11C	Test LOC-11C From - 10 to 1 s Verified 1 to 10 s Restrained[g] 10 to 16 s Failed[h] 16 to 53 s Restrained[g] 53 to 54 s Failed[h] 54 to 120 s Restrained[g]
MATERIAL TEMPERATURE	Chromel-Alumel thermocouples.						
TE-4-1	Outside shroud surface thermocouples, 0.61 m above fuel stack bottom.	0 to 1643 K	280 to 1530 K	1.7 Hz	100 Hz	72 LOC-11B 176 LOC-11C M4 LOC-11B L4 LOC-11C	Restrained[c]
TE-4-2						73 LOC-11B 177 LOC-11C N4 LOC-11B M4 LOC-11C	Restrained[c]
TE-4-3						74 LOC-11B 178 LOC-11C O4 LOC-11B N4 LOC-11C	Trend data for LOC-11B[d] Restrained for LOC-11C[c]
TE-4-4						75 LOC-11B 179 LOC-11C P4 LOC-11B O4 LOC-11C	Trend data for LOC-11B[d] Restrained for LOC-11C[c]
TE-7-1	Outside shroud surface thermocouples, 0.46 m above fuel stack bottom.					76 LOC-11C 180 LOC-11C B5 LOC-11B P4 LOC-11C	Restrained[c]
TE-7-2						77 LOC-11B 181 LOC-11C C5 LOC-11B B5 LOC-11C	Restrained[c]
TE-7-3						78 LOC-11B 182 LOC-11C D5 LOC-11B C5 LOC-11C	Restrained[c]
TE-7-4						79 LOC-11B 183 LOC-11C E5 LOC-11B D5 LOC-11C	Restrained[c]
TE-12-1	Outside shroud surface thermocouple, 0.30 m above fuel stack bottom.	0 to 1643 K	280 to 1530 K	1.7 Hz	100 Hz	80 LOC-11B 184 LOC-11C F5 LOC-11B E5 LOC-11C	Restrained[c]
TE-12-2						81 LOC-11B 185 LOC-11C G5 LOC-11B F5 LOC-11C	Restrained[c]
TE-12-3						82 LOC-11B 186 LOC-11C H5 LOC-11B G5 LOC-11C	Restrained[c]
TE-12-4						83 LOC-11B 187 LOC-11C I5 LOC-11B H5 LOC-11C	Restrained[c]
PRESSURE							
Fuel Rod							
PE-4-1	Fuel rod plenum pressure, Kaman Eddy current type.	0 to 24 MPa	0 to 20.7 MPa	23.3 Hz	10 Hz		
PE-4-2							
PE-4-3							
PE-4-4							Channel failed
Test Train							
PE-1	Upper free field pressure transducer, 0.41 m above top of fuel rod shroud outlet (Kaman).				10 Hz	84 LOC-11C 188 LOC-11C I5 LOC-11B I5 LOC-11C	Restrained[i]
PE-2	Upper free field pressure transducer (EG&G Idaho, Inc.) 0.41 m above top of fuel rod shroud outlet.			3.5 kHz			Channel failed

TABLE VIII (continued)

Measurement	Location and Comments[a]	Range[a] Detector	Range[a] Data Acquisition System	Frequency Response[a] Detector	Frequency Response[a] Data[b] Acquisition System	Figure[a]	Measurement Comments
Test Train (continued)							
PE-3	Overpressure free field pressure transducer (EG&G Idaho, Inc.) 0.68 m above top of fuel rod shroud outlet.	0 to 70 MPa	0 to 68.9 MPa	3.5 kHz	10 Hz 5 Hz	85 LOC-11B 189 LOC-11C K5 LOC-11B J5 LOC-11C	 Restrained for LOC-11B[j] Verified for LOC-11C
PE-6	Lower free field pressure transducer (EG&G Idaho, Inc.) 0.19 m below lower support plate.	0 to 24 MPa	0 to 17.2 MPa	3.5 kHz	100 Hz	86 LOC-11B 190 LOC-11C L5 LOC-11B K5 LOC-11C	From - 10 to 22 s Restrained - LOC-11B[j] 22 to 120 s Failed Restrained data for LOC-11C[j]
PE-7	Lower free field pressure transducer (Kaman) 0.19 m below lower support plate.	0 to 24 MPa	0 to 17.2 MPa	11.7 Hz	10 Hz		Channel failed
Inlet Spool							
PE-8	Pressure transducer, flush mounted, bonded strain gauge.	0 to 24 MPa	0 to 20.7 MPa	23.3 kHz	100 Hz 20 kHz		Channel failed
PE-9	Pressure transducer, water-cooled stand-off, bonded strain gauge.					87 LOC-11B 191 LOC-11C M5 LOC-11B L5 LOC-11C	Verified
Blowdown Spool							
PE-10	Pressure transducer, flush mounted bonded strain gauge.					88 LOC-11B 192 LOC-11C N5 LOC-11B M5 LOC-11C	Verified for LOC-11B Restrained for LOC-11C[k] For Test LOC-11C an accurate offset could not be determined or applied because of noisy data.
PE-11	Pressure transducer, water-cooled stand-off, bonded strain gauge, cold leg.	0 to 24 MPa	0 to 20.7 MPa	23.3 kHz	100 Hz 20 kHz	89 LOC-11B 193 LOC-11C O5 LOC-11B N5 LOC-11C	Verified LOC-11B and 11C
PE-12	Pressure transducer, flush mounted, bonded strain gauge, hot leg.					90 LOC-11B 194 LOC-11C P5 LOC-11B O5 LOC-11C	Verified LOC-11B and 11C
PE-13	Pressure transducer, flush mounted, water-cooled stand-off, bonded strain gauge, hot leg.					91 LOC-11B 195 LOC-11C B6 LOC-11B P5 LOC-11C	Verified LOC-11B and 11C
ΔPE-5	Inter-spool pressure difference transducer.			35 Hz		92 LOC-11B 196 LOC-11C C6 LOC-11B B6 LOC-11C	Restrained data for LOC-11B and 11C[l]
VOLUMETRIC FLOW							
Test Train							
FE-1-1	Upper fuel rod shroud flow turbine (bidirectional), Rod 1.	0.6 to 0.8 x/s	0.8 to 0.95 x/s	11.7 Hz	100 Hz	93 LOC-11B 197 LOC-11C D6 LOC-11B C6 LOC-11C	Verified for LOC-11B Test LOC-11C - 10 to 60 s Verified 60 to 90 s Restrained[h] 90 to 120 s Verified
FE-1-2	Upper fuel rod shroud flow turbine (bidirectional), Rod 2.					94 LOC-11B 198 LOC-11C E6 LOC-11B D6 LOC-11C	Verified for LOC-11B - 10 to 60 s LOC-11C 60 to 85 s Restrained[h] 85 to 120 s Verified
FE-1-3	Upper fuel rod shroud flow turbine (bidirectional), Rod 3.					95 LOC-11C 199 LOC-11C E6 LOC-11B E6 LOC-11C	Verified for LOC-11B Test LOC-11C - 10 to 68 s Verified 68 to 80 s Restrained[h] 80 to 85 s Verified 85 to 87 s Restrained[h] 87 to 120 s Verified
FE-1-4	Upper fuel rod shroud flow turbine (bidirectional), Rod 4.					96 LOC-11B 200 LOC-11C G6 LOC-11B F6 LOC-11C	Verified for LOC-11B Test LOC-11C - 10 to 68 s Verified 68 to 80 s Restrained[h] 80 to 85 s Verified 85 to 87 s Restrained[h] 87 to 120 s Verified
FE-2-1	Lower fuel rod shroud flow turbine (bidirectional), Rod 1.					97 LOC-11B 201 LOC-11C H6 LOC-11B	Test LOC-11B From - 10 to 27 s Verified Test LOC-11C From - 10 to 16 s Verified 16 to 36 s Restrained[n] 36 to 120 s Verified 27 to 42 s Restrained[n] 42 to 120 s Verified

TABLE VIII (continued)

Measurement	Location and Comments[a]	Range[a]		Frequency Response[a]		Figure[a]	Measurement Comments
		Detector	Data Acquisition System	Detector	Data Acquisition System[b]		
Test Train (continued)							
FE-2-2	Lower fuel rod shroud flow turbine (bidirectional), Rod 2.		0.8 to 0.95 m/s	17.5 Hz	100 Hz	98 LOC-11B 202 LOC-11C J6 LOC-11B H6 LOC-11C	Test LOC-11B From - 10 to 30 s Verified 30 to 34 s Failed[h] 34 to 120 s Verified Verified for LOC-11C
FE-2-3	Lower fuel and shroud flow turbine (bidirectional), Rod 3.	0.6 to 0.8 m/s				99 LOC-11B 203 LOC-11C J6 LOC-11B J6 LOC-11C	Test LOC-11B From - 10 to 25 s Verified 25 to 30 s Failed[h] Test LOC-11C 30 to 120 s Verified
FE-2-4	Lower fuel rod shroud flow turbine (bidirectional), Rod 4.					100 LOC-11B 204 LOC-11C K6 LOC-11B J6 LOC-11C	Test LOC-11B From - 10 to 25 s Verified 25 to 27 s Failed[h] 27 to 40 s Restrained[n] 40 to 120 s Verified Test LOC-11C From - 10 to 26 s Verified 26 to 36 s Restrained[n] 36 to 120 s Verified
FE-5	Turbine flowmeter in inlet spool.			21.3 kHz		101 LOC-11B 205 LOC-11C L6 LOC-11B K6 LOC-11C	Restrained for LOC-11B and 11C[l]
FE-6	Turbine flowmeter in blowdown spool cold leg.					102 LOC-11B 206 LOC-11C M6 LOC-11B L6 LOC-11C	Test LOC-11B From - 10 to 60 s Verified 60 to 120 s Failed[m] Test LOC-11C From - 10 to 53 s Verified 53 to 120 s Failed[m]
FE-9	Turbine flowmeter in blowdown spool hot leg.					103 LOC-11B 207 LOC-11C N6 LOC-11B 06 LOC-11C	Test LOC-11B From - 10 to 1 s Failed[k] 1 to 120 s Verified[o] Test LOC-11C From - 10 to 0.5 s Failed[k] 0.5 to 120 s Verified[o]
MOMENTUM FLUX							
FE-7	Drag disc in blowdown spool cold leg.					104 LOC-11B 208 LOC-11C 06 LOC-11B H6 LOC-11C	Test LOC-11B From - 10 to 1 s Failed[p] 1 to 120 s Verified Test LOC-11C From - 10 to 0.5 s Failed[p] 0.5 to 120 s Verified
FE-8	Drag disc in blowdown spool hot leg.					105 LOC-11B 209 LOC-11C P6 LOC-11B N6 LOC-11C	Test LOC-11B From - 10 to 1 s Failed[p] 1 to 120 s Verified Test LOC-11C From - 10 to 0.5 s Failed[p] 0.5 to 120 s Verified
DENSITY							
DEN-1-U	Gamma densitometer, upper beam. Located in cold leg blowdown spool					106 LOC-11B 210 LOC-11C B7 LOC-11B P6 LOC-11C	Verified data for LOC-11B and 11C
DEN-1-C	Gamma densitometer, center beam. Located in cold leg blowdown spool.						Channel failed
DEN-1-L	Gamma densitometer, lower beam. Located in cold leg blowdown spool.					107 LOC-11B C7 LOC-11B	Verified for LOC-11B Channel failed for LOC-11C
DEN-2-U	Gamma densitometer, upper beam. Located in hot leg blowdown spool.					108 LOC-11B 211 LOC-11C D7 LOC-11B B7 LOC-11C	Verified
DEN-2-C	Gamma densitometer, center beam. Located in hot leg of the blowdown spool.					109 LOC-11B 212 LOC-11C E7 LOC-11B C7 LOC-11C	Verified data for LOC-11B and 11C
DEN-2-L	Gamma densitometer, lower beam. Located in hot leg of the blowdown spool.					110 LOC-11B 213 LOC-11C F7 LOC-11B D7 LOC-11C	Verified data for LOC-11B and 11C
DEN-2-AVE	Gamma densitometer. Average of upper, center and lower beams.					111 LOC-11B 214 LOC-11C G7 LOC-11B E7 LOC-11C	Verified data for LOC-11B and 11C

TABLE VIII (continued)

Measurement	Location and Comments[b]	Range[a]		Frequency Response[a]		Figure[a]	Measurement Comments
		Detector	Data Acquisition System	Detector	Data Acquisition System		
CLADDING DISPLACEMENT							
LVDT-1	Fuel rod axial length change transformer, mounted on rod bottom, Rod 1.	0 ± 12.7 mm	0 ± 12.7 mm	35 Hz		112 LOC-11B 215 LOC-11C H7 LOC-11B F7 LOC-11C	Trend data for LOC-11B and 11C[1]
LVDT-2	Fuel rod axial length change transformer, mounted on rod bottom, Rod 2.					113 LOC-11B 216 LOC-11C I7 LOC-11B G7 LOC-11C	Trend data for 10C-11B and 11C[1]
LVDT-3	Fuel rod axial length change transformer, mounted on rod bottom, Rod 3.					114 LOC-11B 217 LOC-11C J7 LOC-11B H7 LOC-11C	Trend data for LOC-11B and 11C[1]
LVDT-4	Fuel rod axial length change transformer, mounted on rod bottom, Rod 4.					115 LOC-11B 218 LOC-11C K7 LOC-11B I7 LOC-11C	Trend data for LOC-11B and 11C[1]
REACTOR POWER							
PPS-1	Ion chamber located outside reactor core.					116 LOC-11B 219 LOC-11C L7 LOC-11B J7 LOC-11C	Verified data for LOC-11B and 11C
SPND POWER							
SPND-1	Self-powered neutron detector, 0.76 m above fuel stack bottom.	1 to 10 μA	1 to 10 μA	1.2 Hz	100 Hz	117 220 M7 K7	Trend data for LOC-11B and 11C[1]
SPND-2	Self-powered neutron detector, 0.61 m above fuel stack bottom.					118 221 N7 L7	Trend data for LOC-11B and 11C[1]
SPND-3	Self-powered neutron detector, 0.46 m above fuel stack bottom.					119 07	Trend data for LOC-11B[1] Channel Failed for LOC-11C
SPND-4	Self-powered neutron detector, 0.30 m above fuel stack bottom.					120 LOC-11B 222 P7 M7	Trend data for LOC-11B and 11C[1]
SPND-5	Self-powered neutron detector, 0.15 m above fuel stack bottom					121 223 B8 N7	Trend data for LOC-11B and 11C[1]

[a] Statements at the beginning of a measurement category regarding location and comments, range, and figures apply to all subsequent measurements within the given category unless specified otherwise.

[b] The rod plenum thermocouples are unshielded and will probably experience some radiation effects.

[c] It is expected that the surface thermocouple will be reading lower than the actual cladding or shroud surface temperature because of fin cooling and mounting effects.

[d] An extreme offset has been applied to produce reasonable data.

[e] The thermocouple (or RTD) has dried out and is reading a combination of steam temperature and pipe wall radiation effects.

[f] Quench injection begins at 50 s and the thermocouple may be reading superheated steam.

[g] The upper or lower junction of the differential thermocouple may be reading superheated steam or pipe wall radiation effects rather than fluid temperature.

[h] A signal conditioning amplifier has saturated.

[i] The Kaman pressure transducer is subject to severe temperature transient effects that have not been quantified.

[j] The temperature sensitivity has not been removed from the data.

[k] The data are extremely noisey.

[l] No independent measurement is available for comparison.

[m] The flow should be zero at this point but the turbine is reading 1.9 ℓ/s. This corresponds to a pick-up frequency of 58 Hz so it is believed to be reading line noise.

[n] The turbine appears to be triggering on line frequency (see [m]).

[o] The spike at 0.5 s is real but may be clipped due to instrument response.

[p] The data is drifting during this steady-state segment.

of 12.5 points per second. The fast response pressure transducer data plots (-0.1 to 1.0 s and 1.6 s) were recorded at 500 points per second. The parameter scales selected for the graphs do not reflect the obtainable resolution of the data.

Table VIII lists all measurements included in this data report and groups them according to measurement type. The table identifies the specific measurement location, lists the detector range and frequency response, notes the PBF/DARS recording ranges and bandwidth, provides brief comments reflecting the usability and verification of the data, and references the measurement and comments to the corresponding figures.

The data graphs are presented according to the following groups:

Description	Time Span	Figures	
LOC-11B blowdown data	-5 to 30 s	17-121	Hard copy
LOC-11C blowdown data	-5 to 30 s	122-223	Hard copy
LOC-11B blowdown plus quench phase data	-5 to 120 s	C1-B8	Microfiche
LOC-11C blowdown plus quench phase data	-5 to 120 s	C1-N7	Microfiche
LOC-11B fast reponse pressure transducer data	-0.1 to 1.0 s	C8-F8	Microfiche
LOC-11C fast response pressure transducer data	-0.1 to 1.0 s	07-B8	Microfiche

Time zero for all data plots is the time of reactor scram initiation (blowdown for each test was initiated within one second following the reactor shutdown scram). Plots are presented in both hard copy and microfiche as noted.

Appendix C is an analysis of selected data which provides a guide to an uncertainty associated with data measurements in the PBF system.

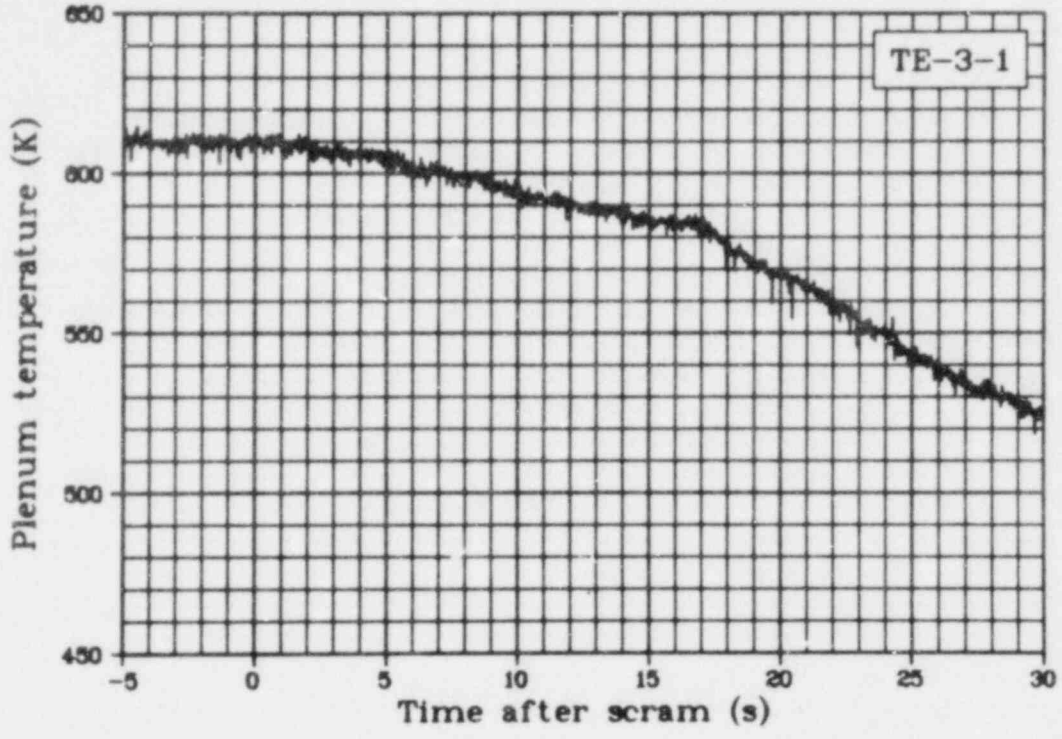

Fig. 17 Plenum temperature in fuel Rod 1 (TE-3-1), Test LOC-11B.

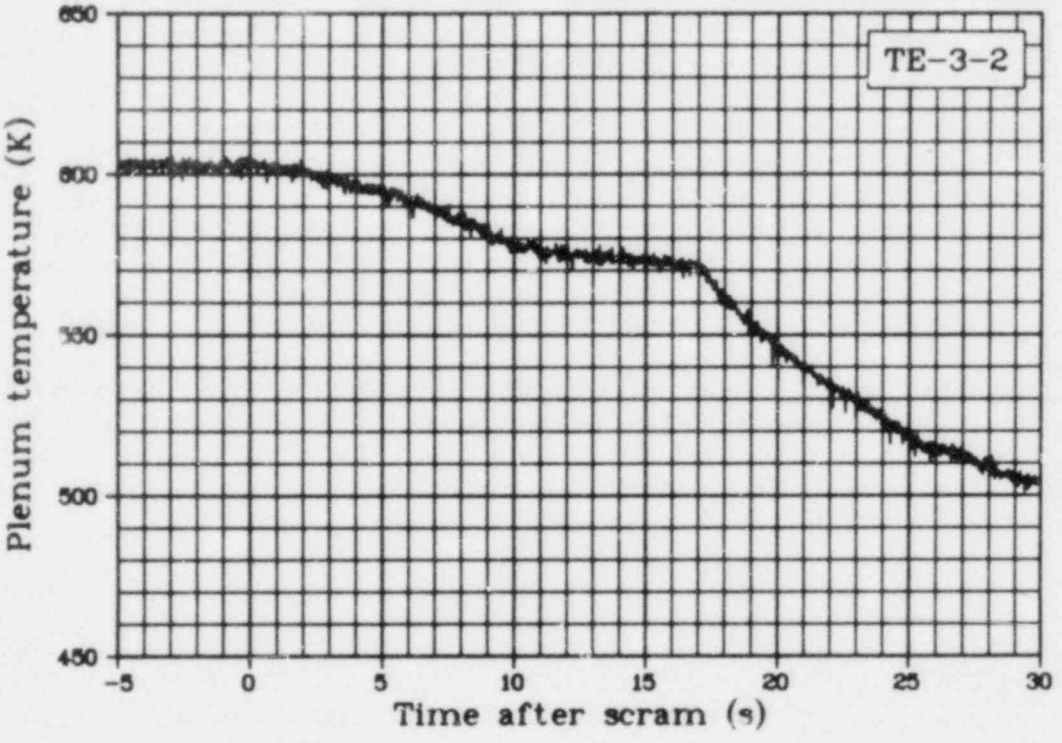

Fig. 18 Plenum temperature in fuel Rod 2 (TE-3-2), Test LOC-11B.

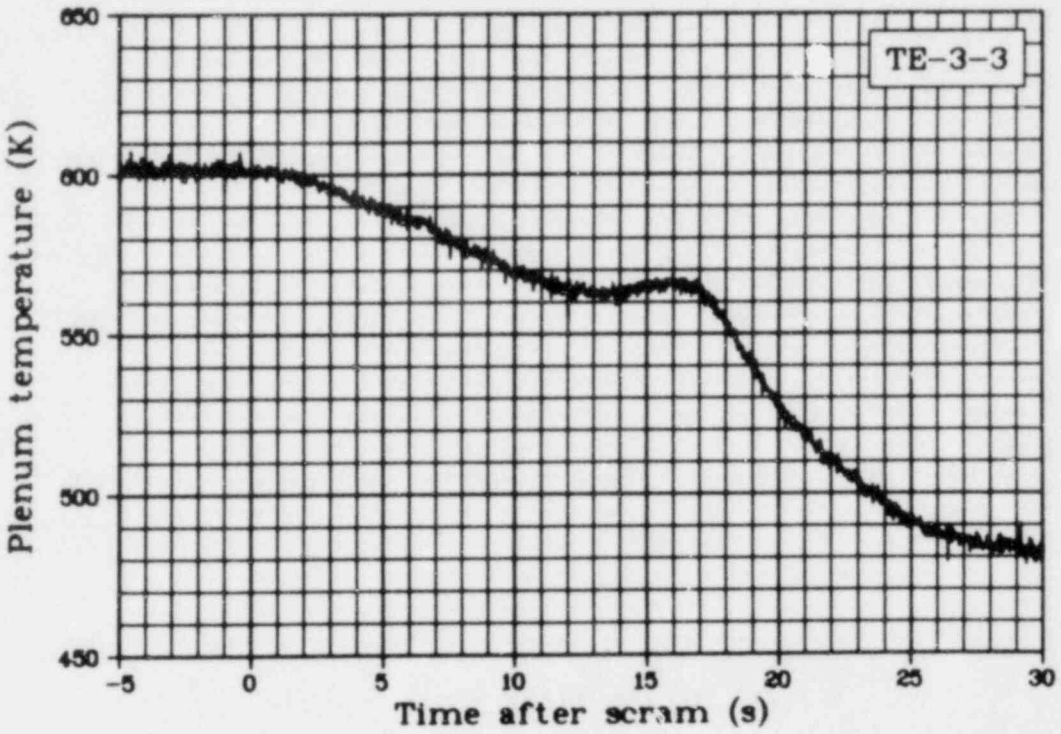

Fig. 19 Plenum temperature in fuel Rod 3 (TE-3-3), Test LOC-11B.

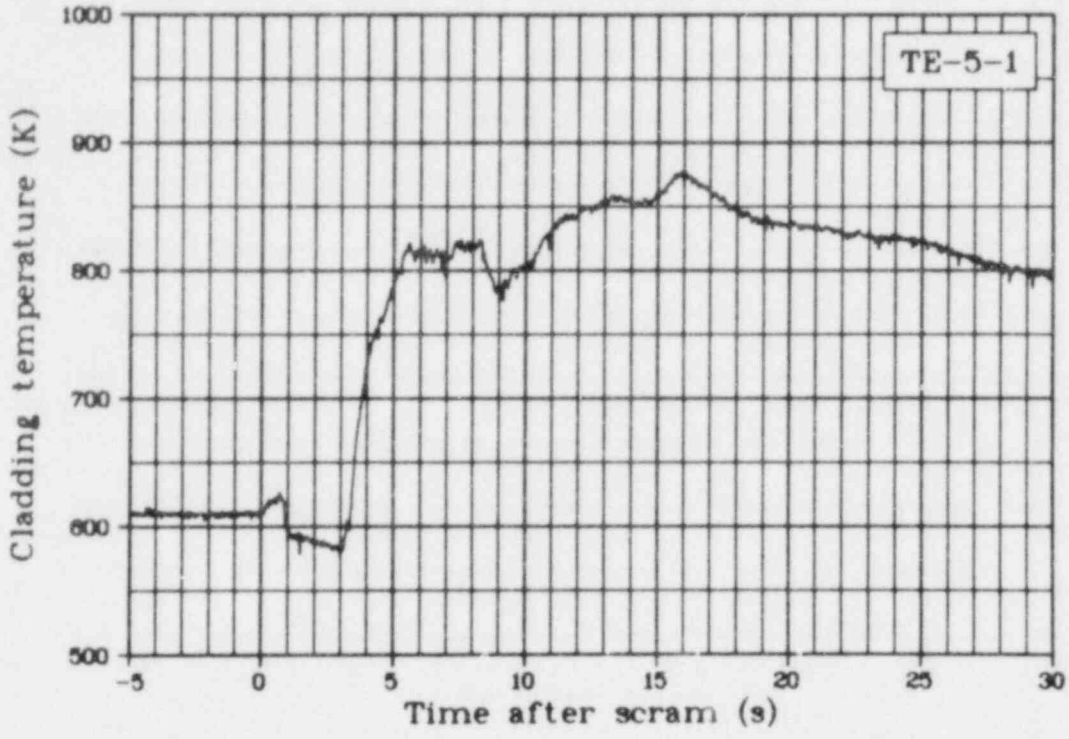

Fig. 20 Cladding temperature Rod 1, 0.53 m above bottom of fuel stack (TE-5-1), Test LOC-11B.

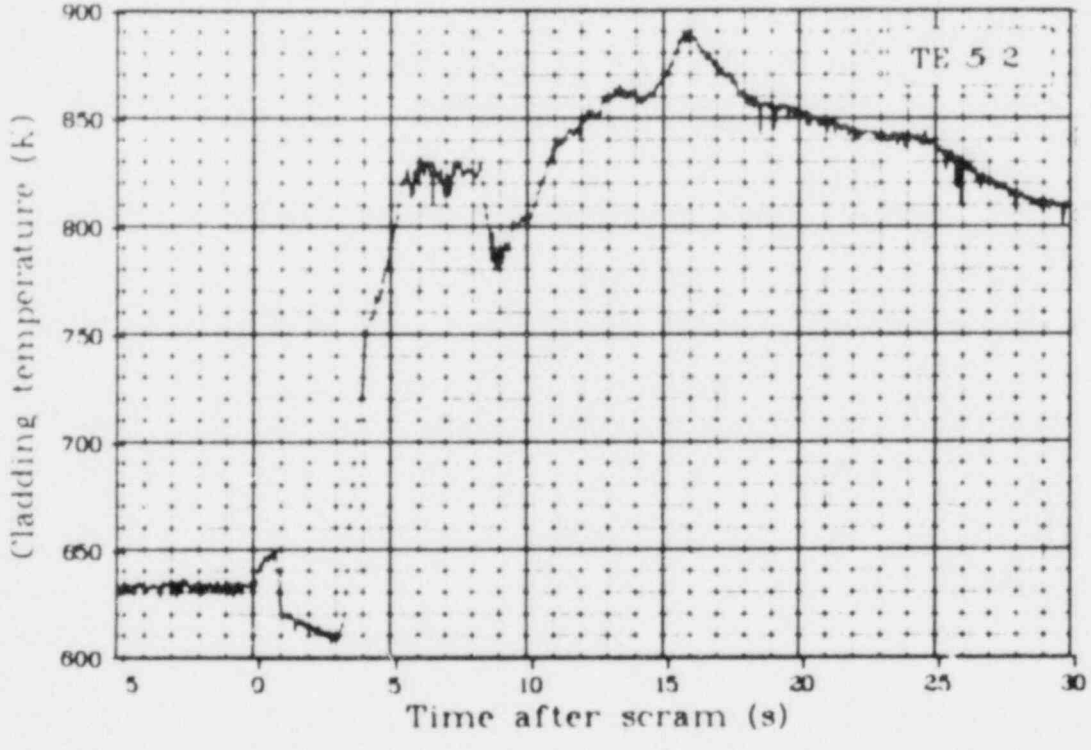

Fig. 21 Cladding temperature Rod 2, 0.53 m above bottom of fuel stack (TE-5-2), Test LOC-11B.

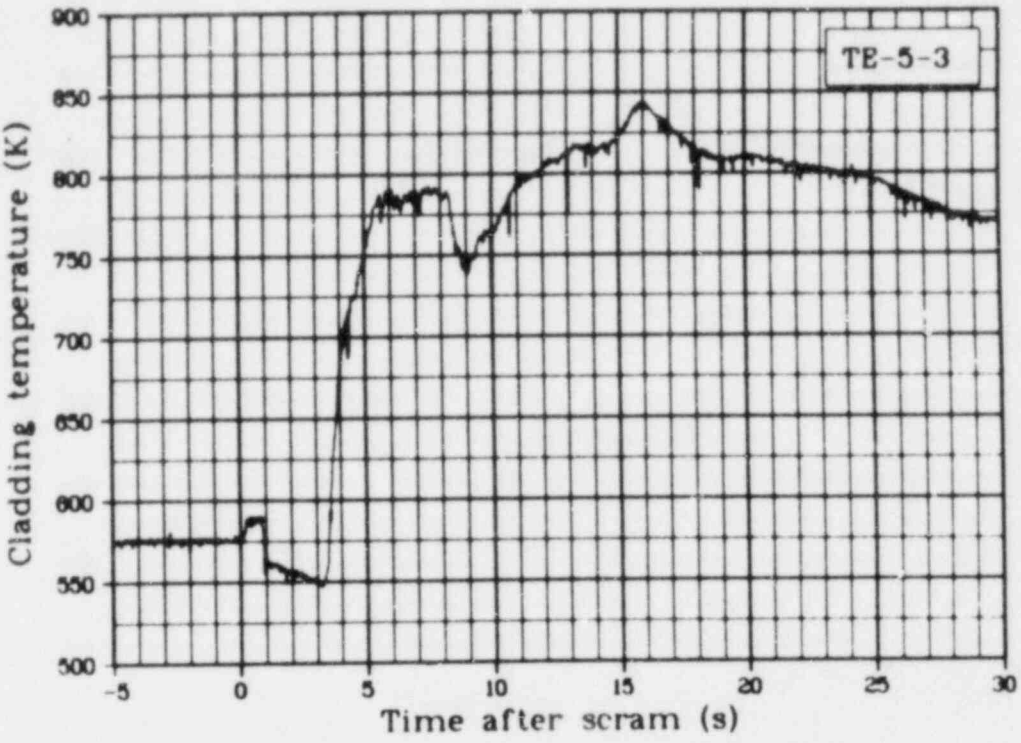

Fig. 22 Cladding temperature Rod 3, 0.53 m above bottom of fuel stack (TE-5-3), Test LOC-11B.

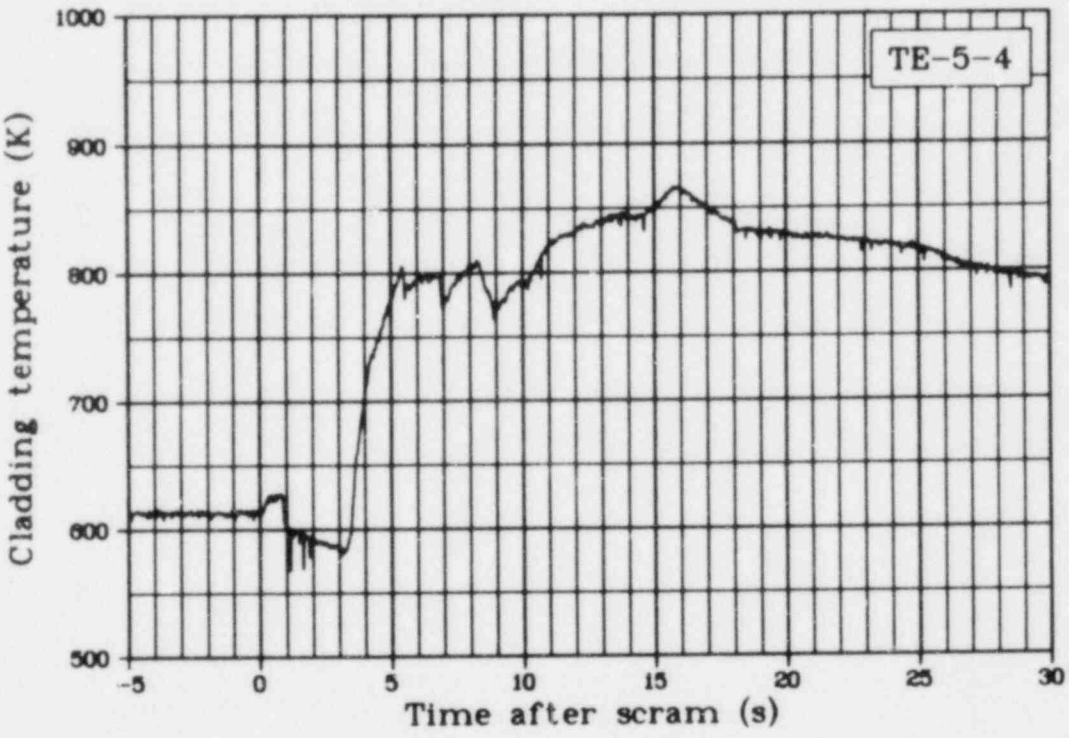

Fig. 23 Cladding temperature Rod 4, 0.53 m above bottom of fuel stack (TE-5-4), Test LOC-11B.

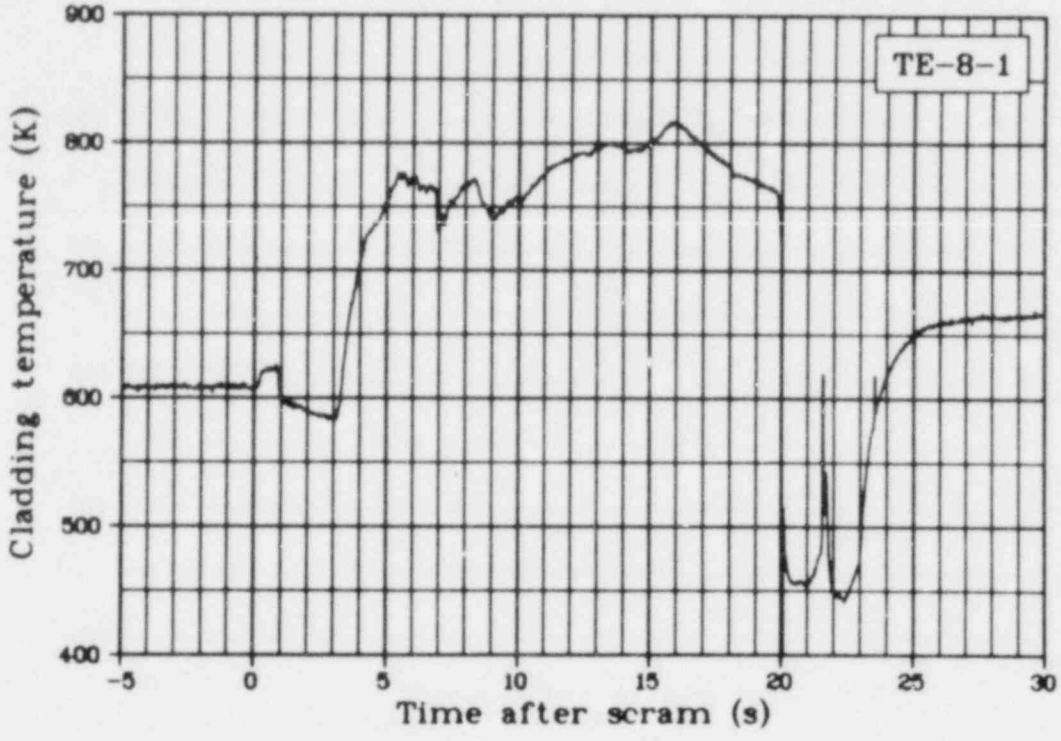

Fig. 24 Cladding temperature Rod 1, 0.61 m above bottom of fuel stack (TE-8-1), Test LOC-11B.

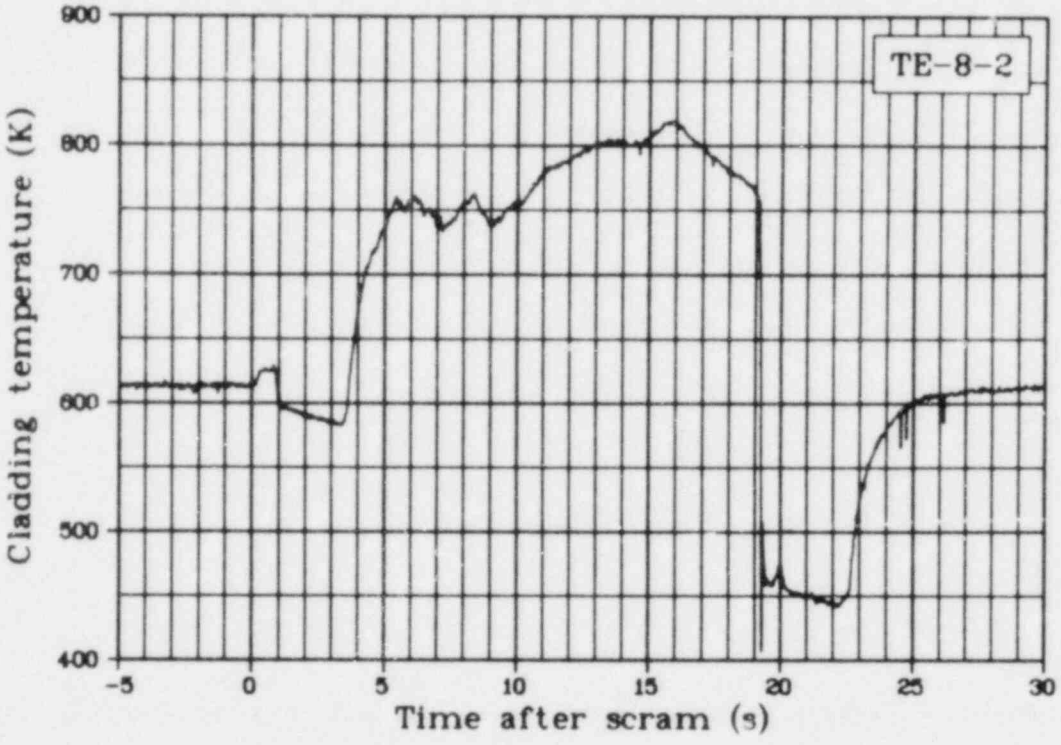

Fig. 25 Cladding temperature Rod 2, 0.61 m above bottom of fuel stack (TE-8-2), Test LOC-11B.

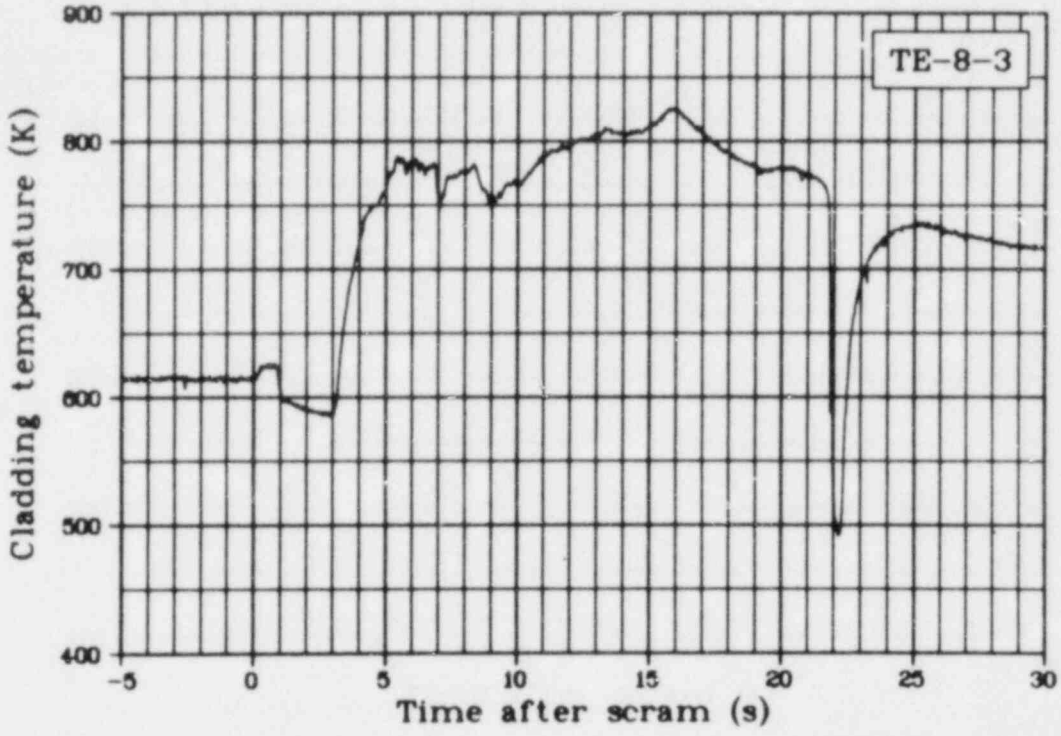

Fig. 26 Cladding temperature Rod 3, 0.61 m above bottom of fuel stack (TE-8-3), Test LOC-11B.

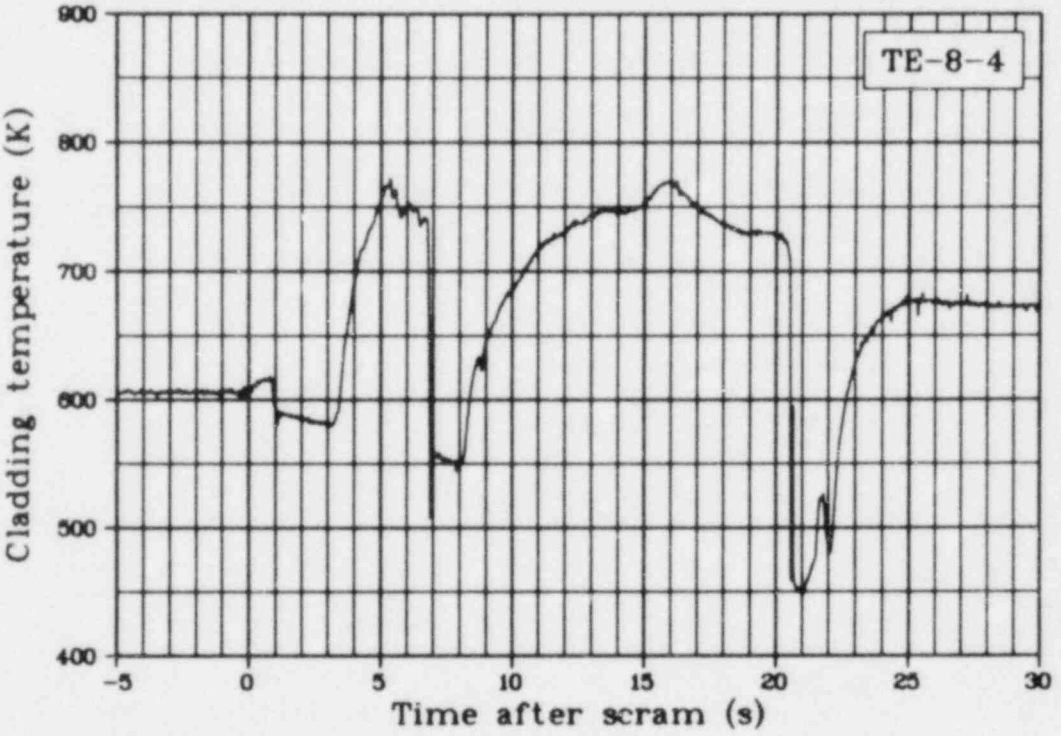

Fig. 27 Cladding temperature Rod 4, 0.61 m above bottom of fuel stack (TE-8-4), Test LOC-11B.

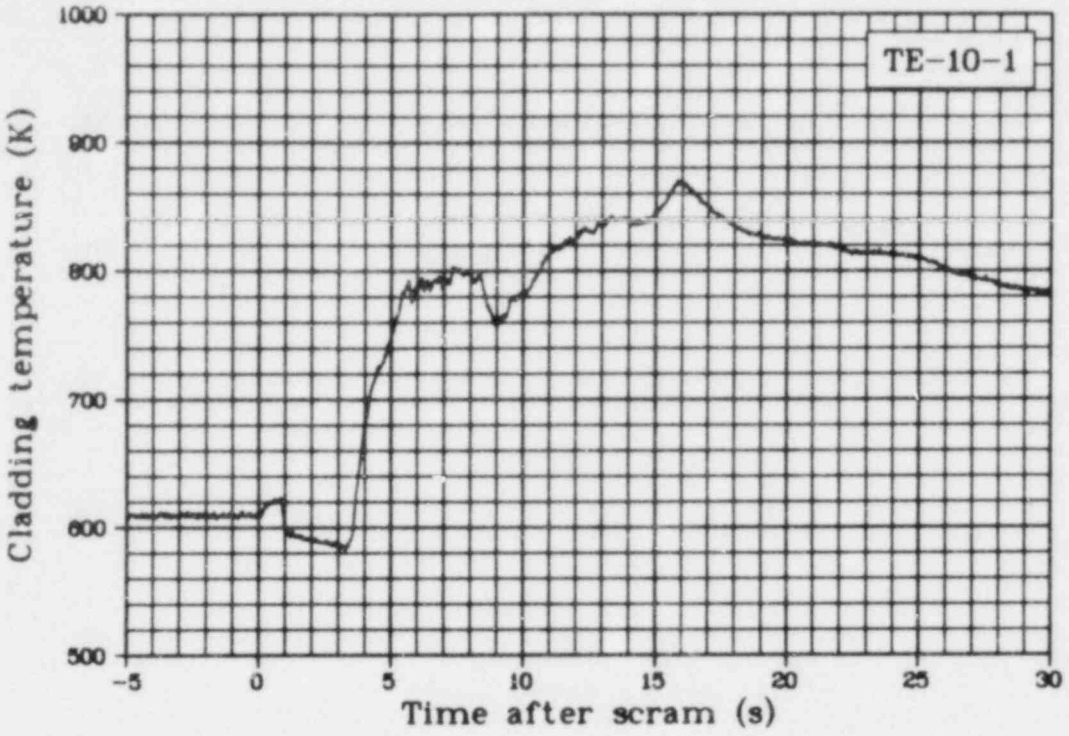

Fig. 28 Cladding temperature Rod 1, 0.53 m above bottom of fuel stack (TE-10-1), Test LOC-11B.

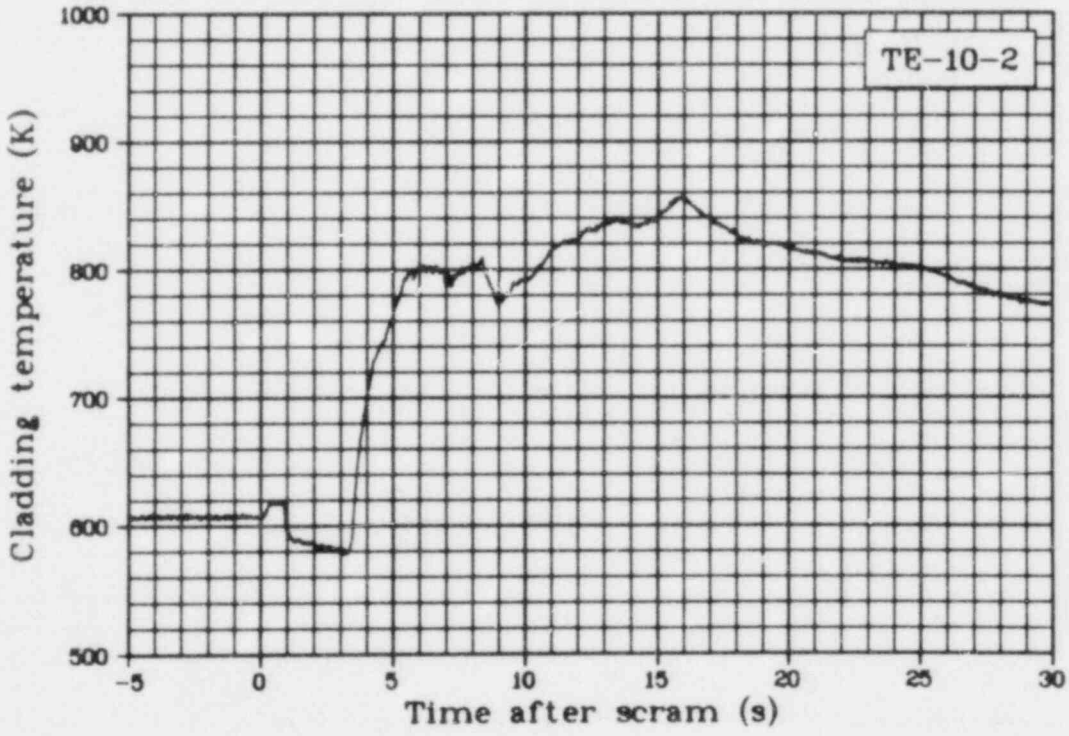

Fig. 29 Cladding temperature Rod 2, 0.53 m above bottom of fuel stack (TE-10-2), Test LOC-11B.

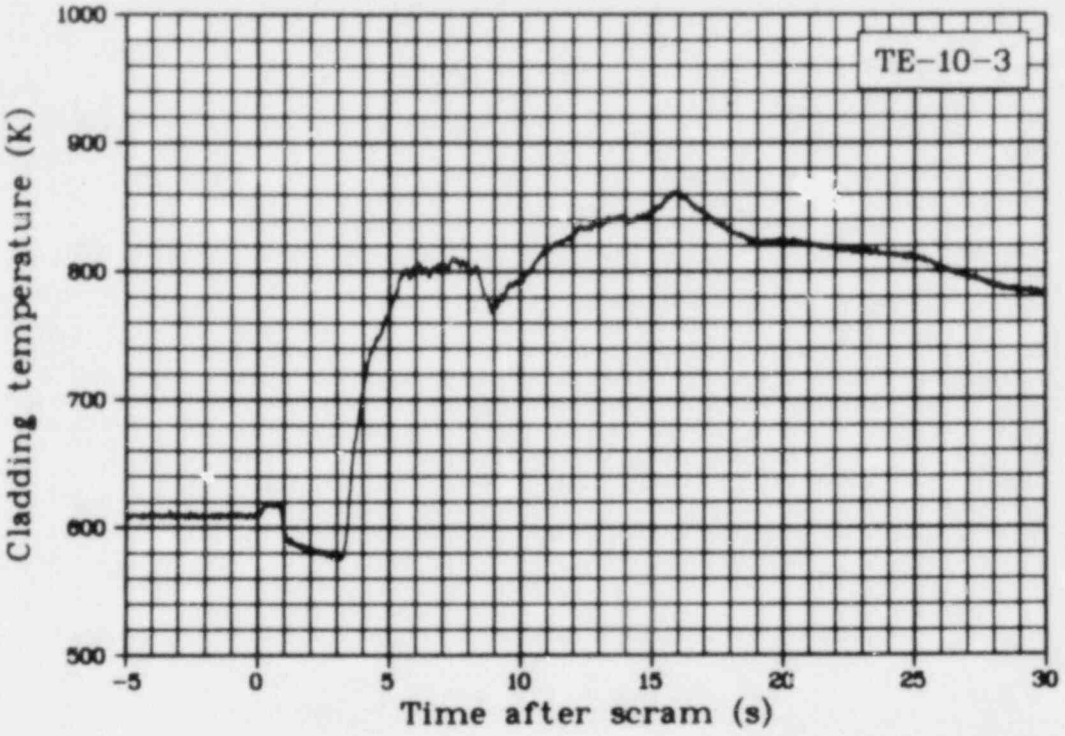

Fig. 30 Cladding temperature Rod 3, 0.53 m above bottom of fuel stack (TE-10-3), Test LOC-11B.

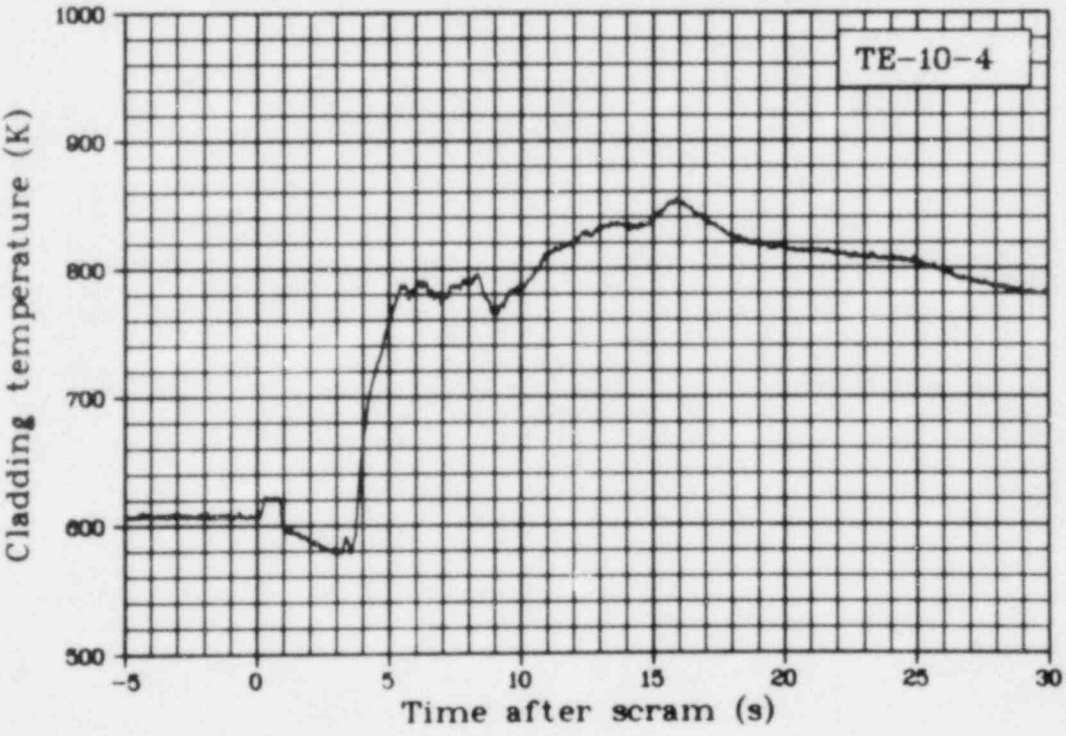

Fig. 31 Cladding temperature Rod 4, 0.53 m above bottom of fuel stack (TE-10-4), Test LOC-11B.

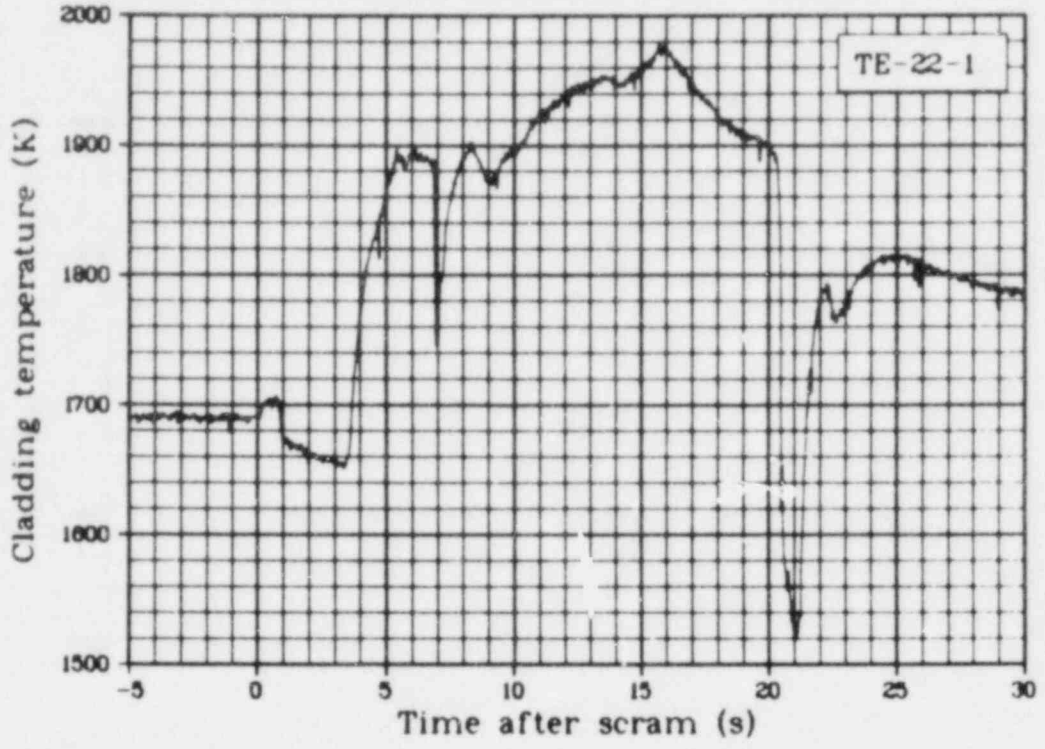

Fig. 32 Cladding temperature Rod 1, 0.61 m above bottom of fuel stack (TE-22-1), Test LOC-11B.

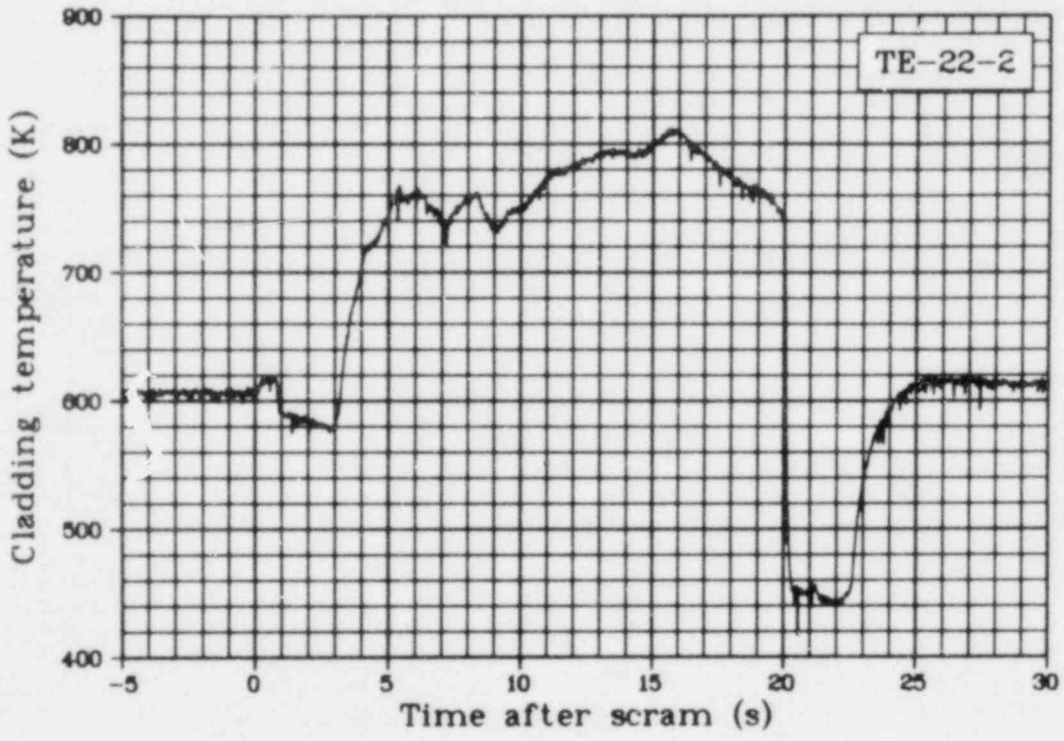

Fig. 33 Cladding temperature Rod 2, 0.61 m above bottom of fuel stack (TE-22-2), Test LOC-11B.

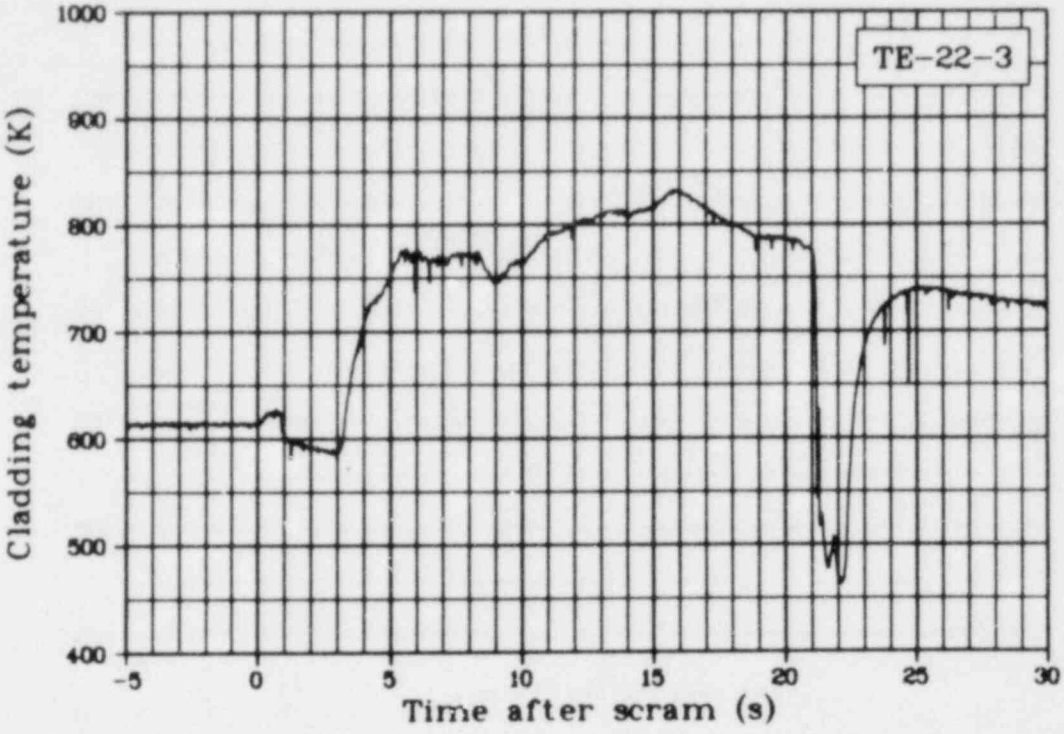

Fig. 34 Cladding temperature Rod 3, 0.61 m above bottom of fuel stack (TE-22-3), Test LOC-11B.

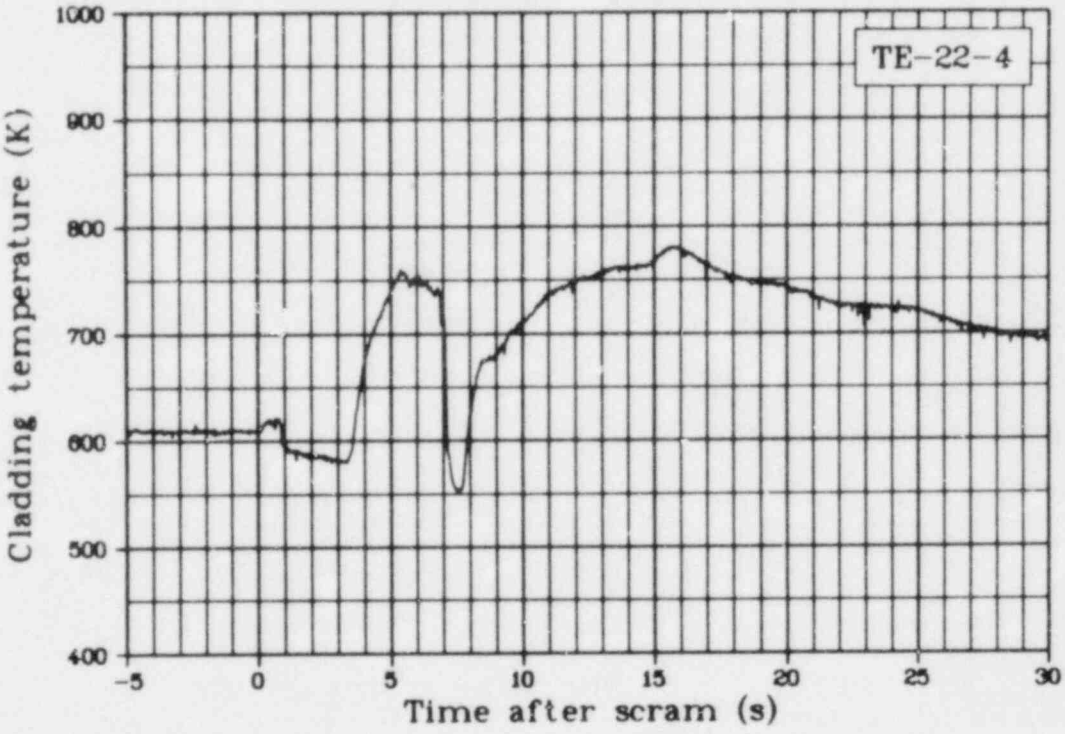

Fig. 35 Cladding temperature Rod 4, 0.61 m above bottom of fuel stack (TE-22-4), Test LOC-11B.

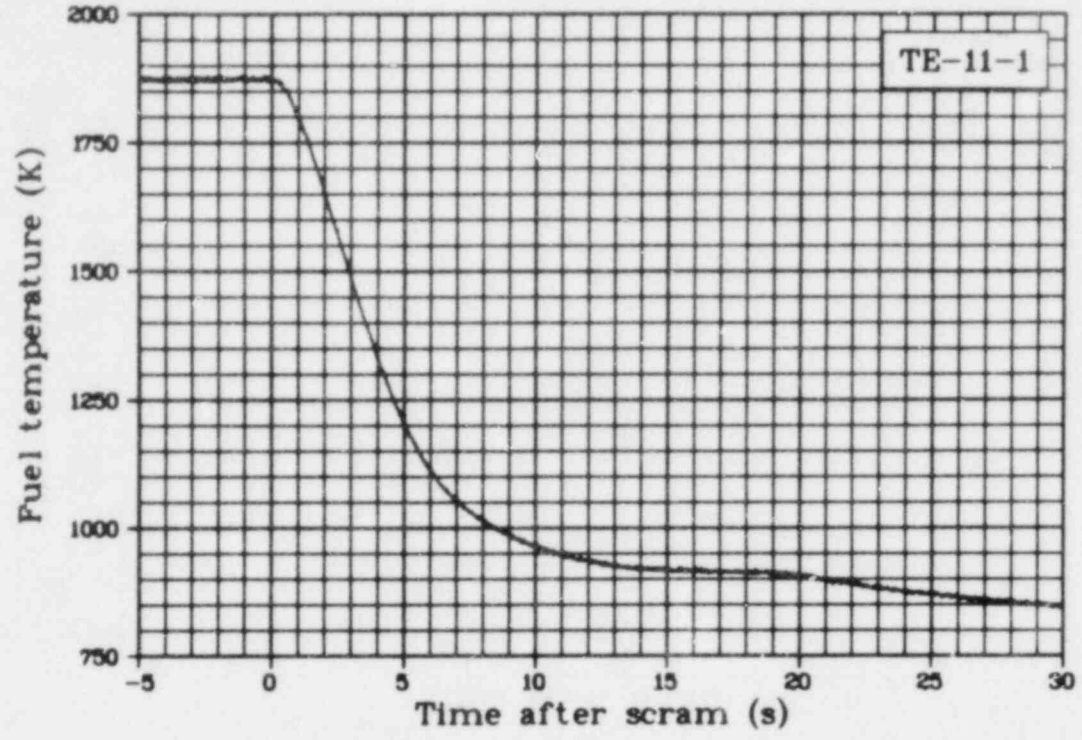

Fig. 36 Fuel temperature Rod 1, 0.53 m above bottom of fuel stack (TE-11-1), Test LOC-11B.

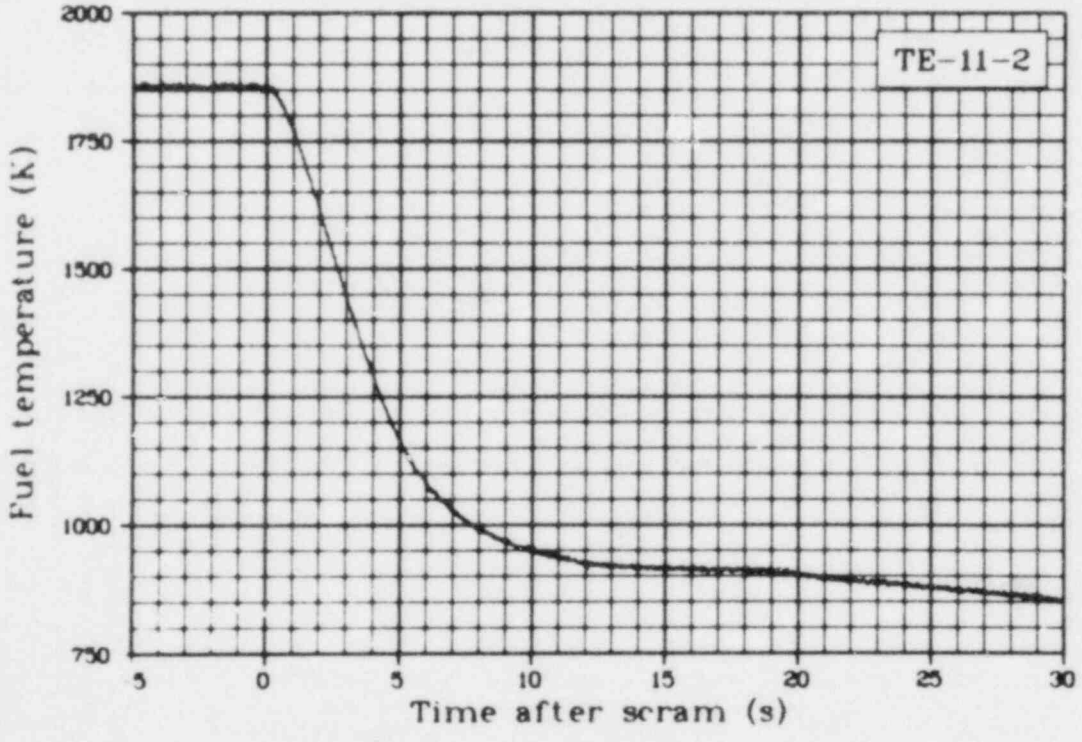

Fig. 37 Fuel temperature Rod 2, 0.53 m above bottom of fuel stack (TE-11-2), Test LOC-11B.

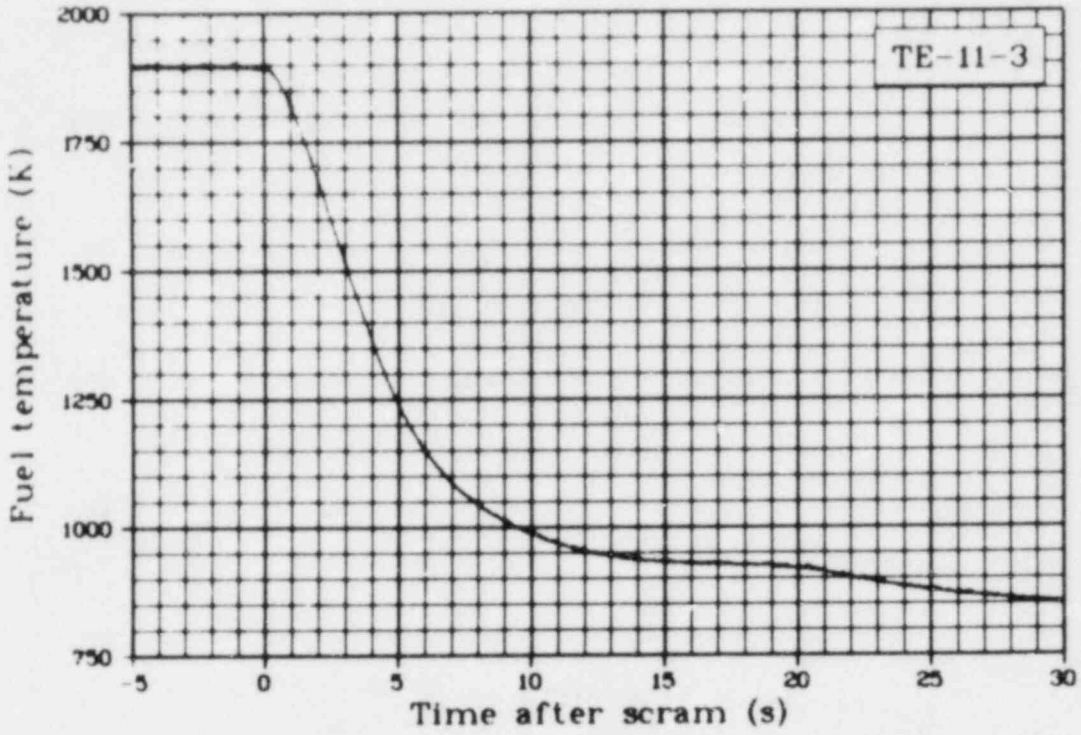

Fig. 38 Fuel temperature Rod 3, 0.53 m above bottom of fuel stack (TE-11-3), Test LOC-11B.

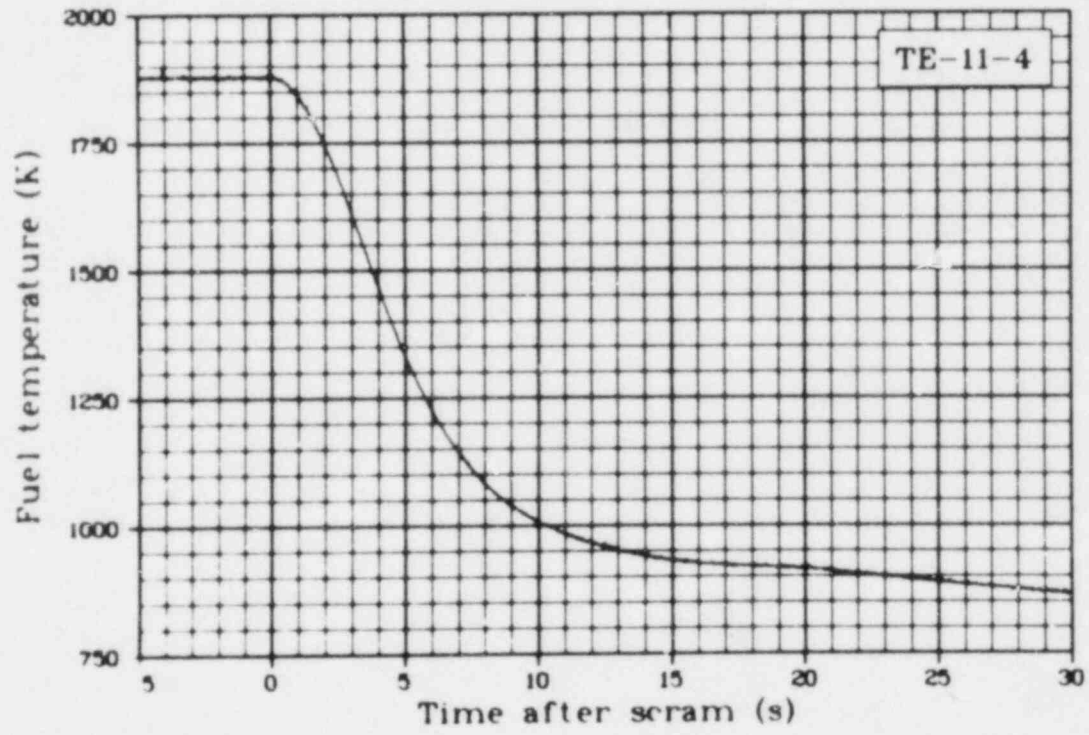

Fig. 39 Fuel temperature Rod 4, 0.53 m above bottom of fuel stack (TE-11-4), Test LOC-11B.

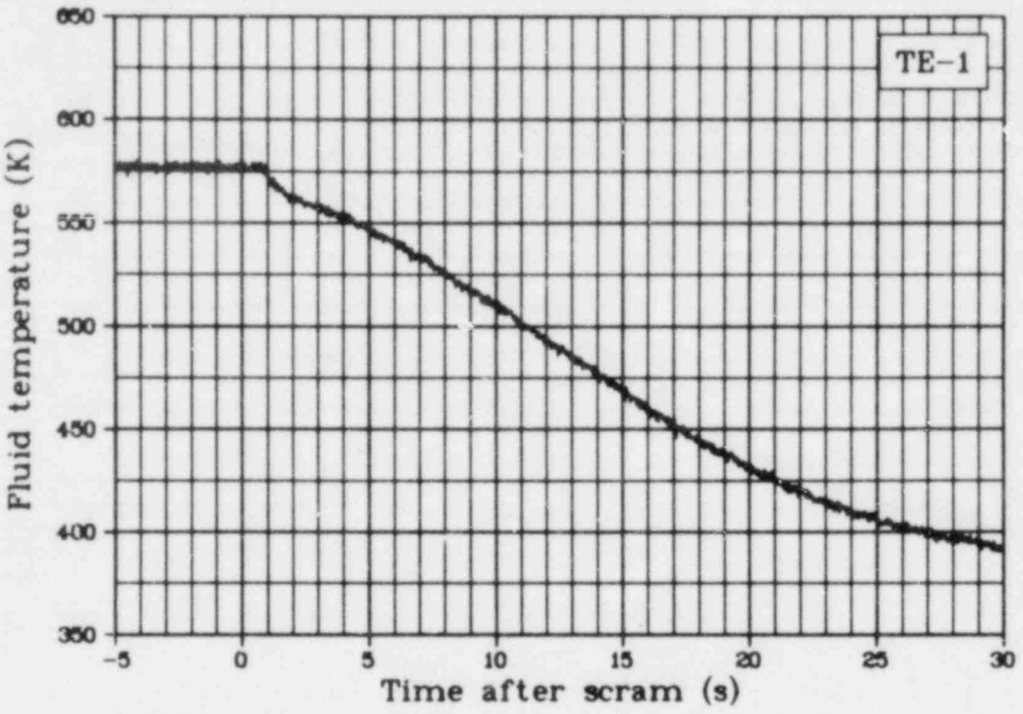

Fig. 40 Fluid temperature in lower upper plenum (TE-1), Test LOC-11B.

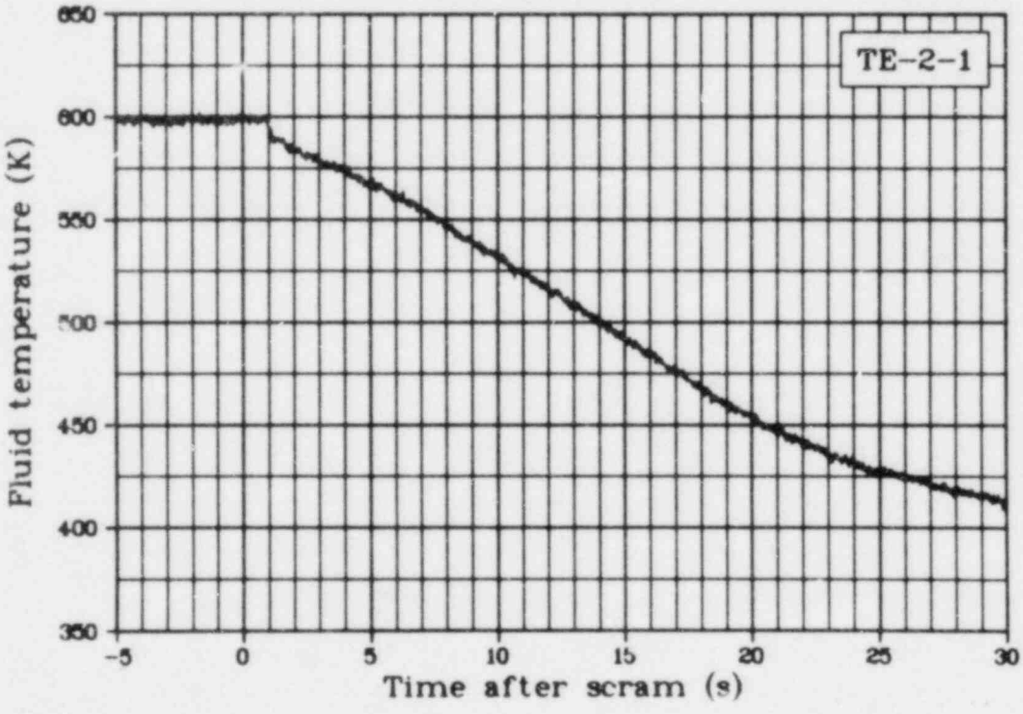

Fig. 41 Fluid temperature of Rod 1 coolant outlet (TE-2-1), Test LOC-11B.

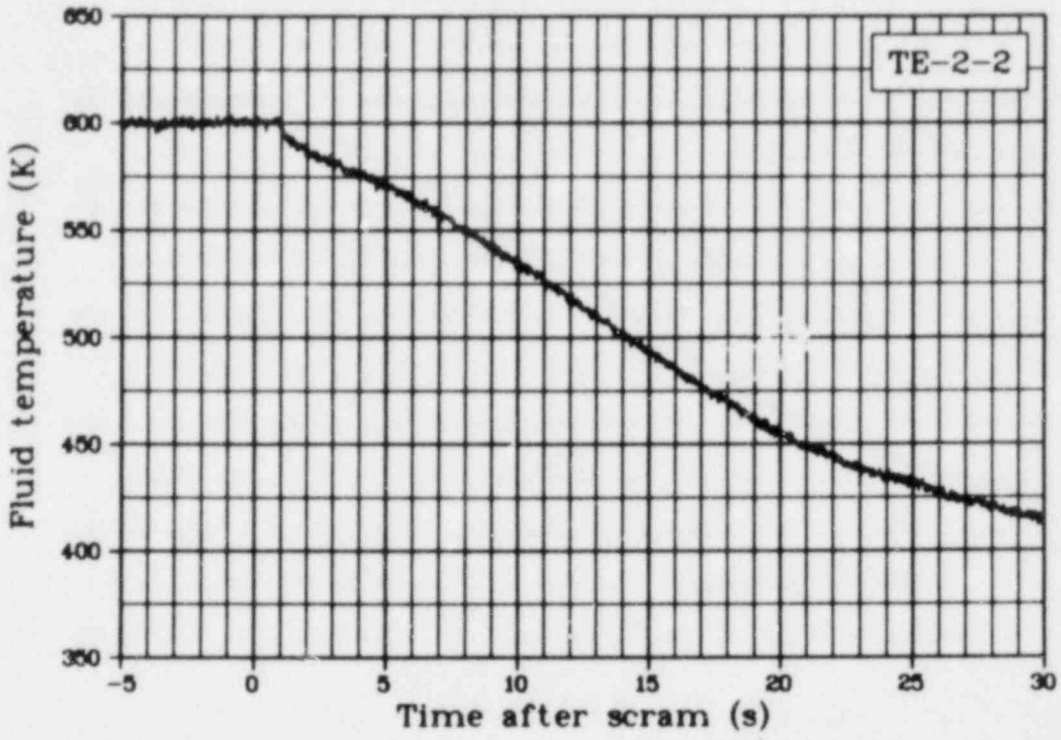

Fig. 42 Fluid temperature of Rod 2 coolant outlet (TE-2-2), Test LOC-11B.

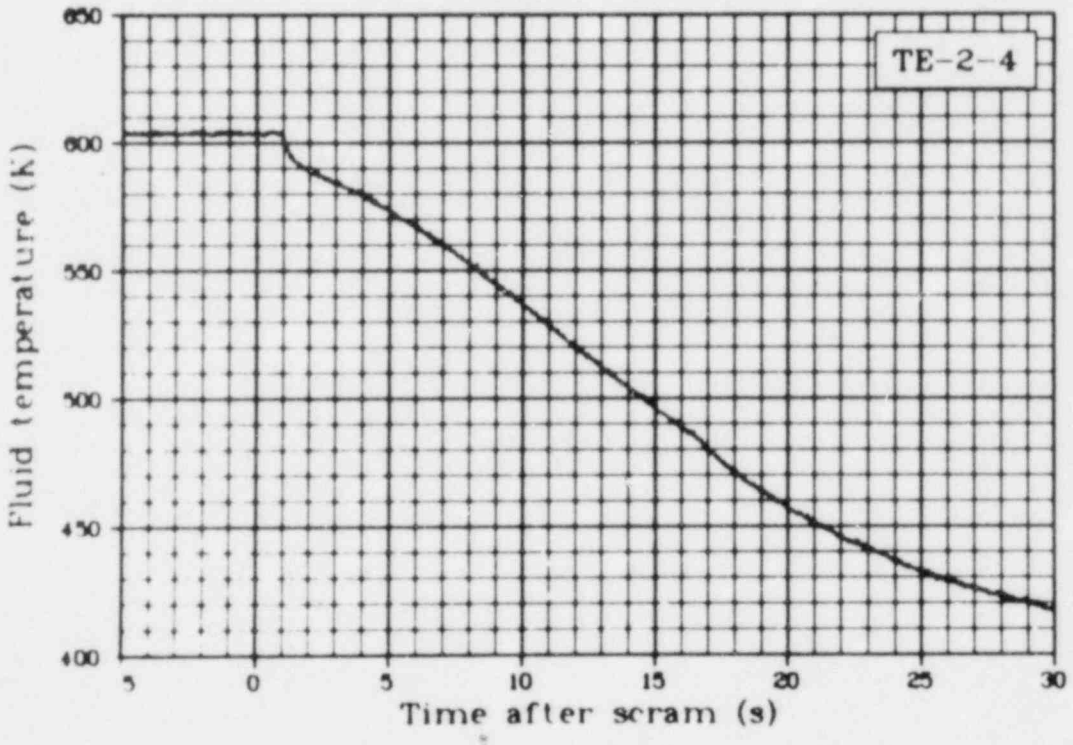

Fig. 43 Fluid temperature of Rod 4 coolant outlet (TE-2-4), Test LOC-11B.

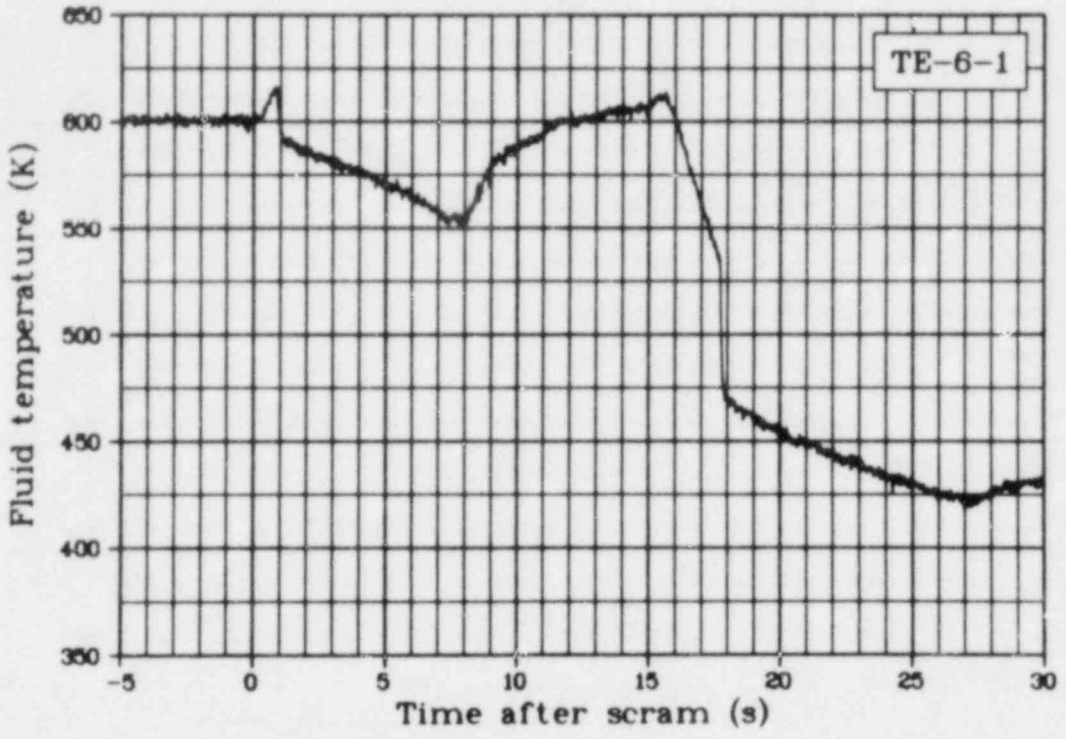

Fig. 44 Fluid temperature of Rod 1, 0.61 m above bottom of fuel stack (TE-6-1), Test LOC-11B.

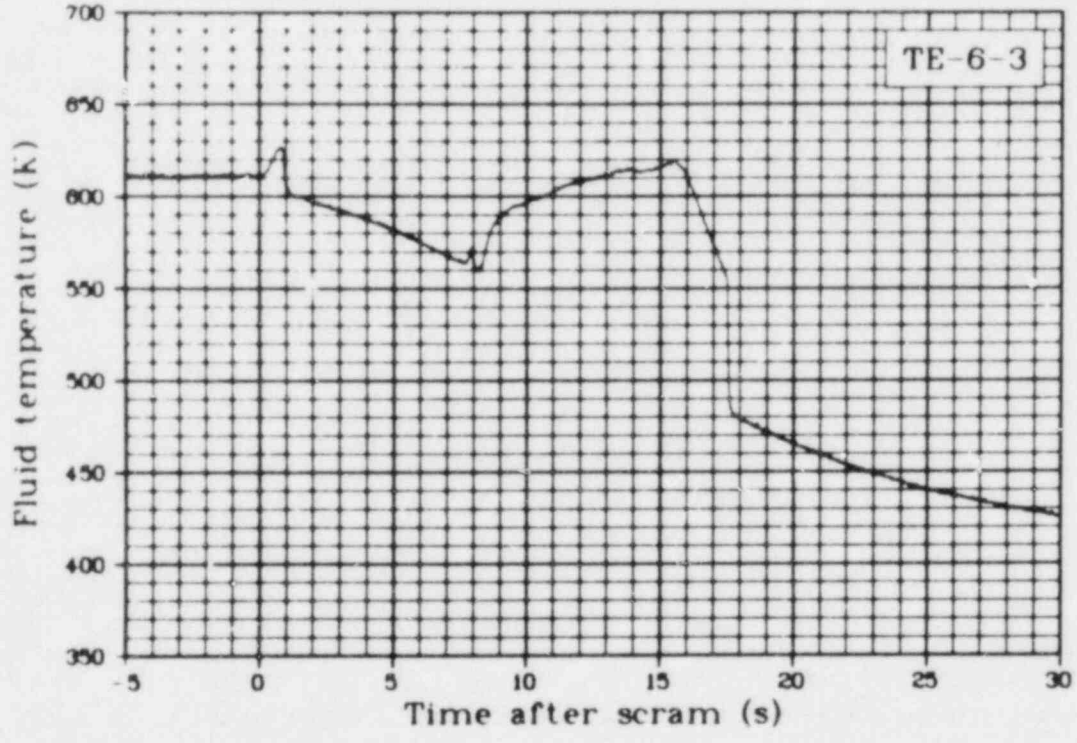

Fig. 45 Fluid temperature of Rod 3, 0.61 m above bottom of fuel stack (TE-6-3), Test LOC-11B.

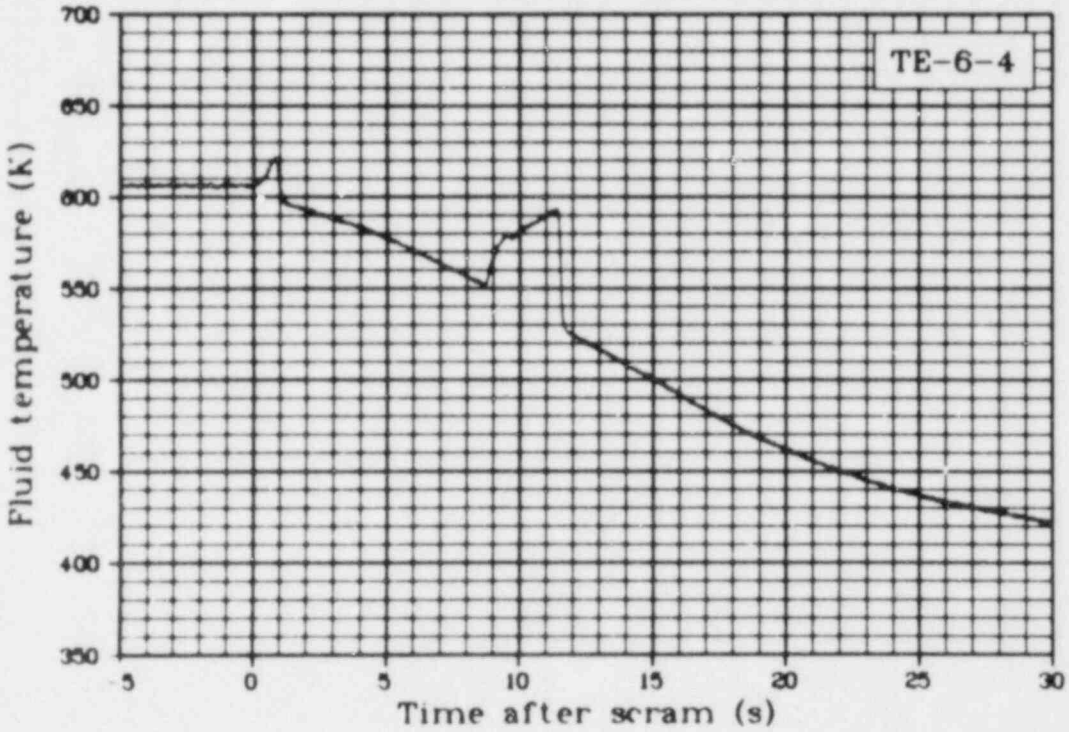

Fig. 46 Fluid temperature of Rod 4, 0.61 m above bottom of fuel stack (TE-6-4), Test LOC-11B.

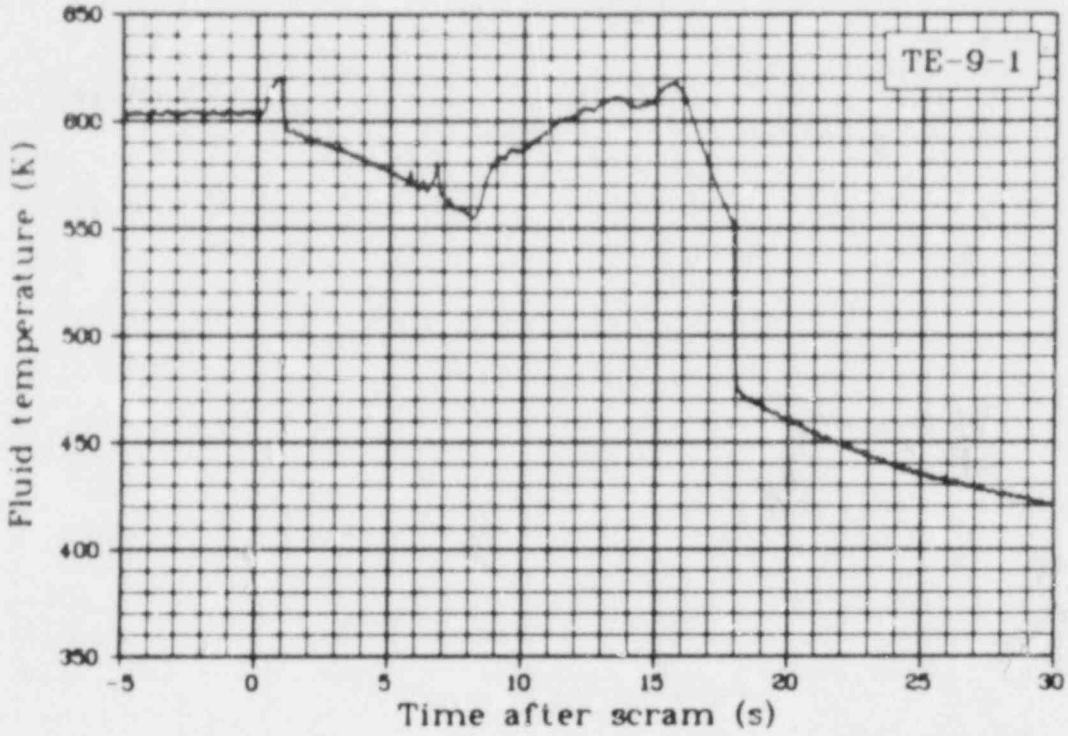

Fig. 47 Fluid temperature of Rod 1, 0.46 m above bottom of fuel stack (TE-9-1), Test LOC-11B.

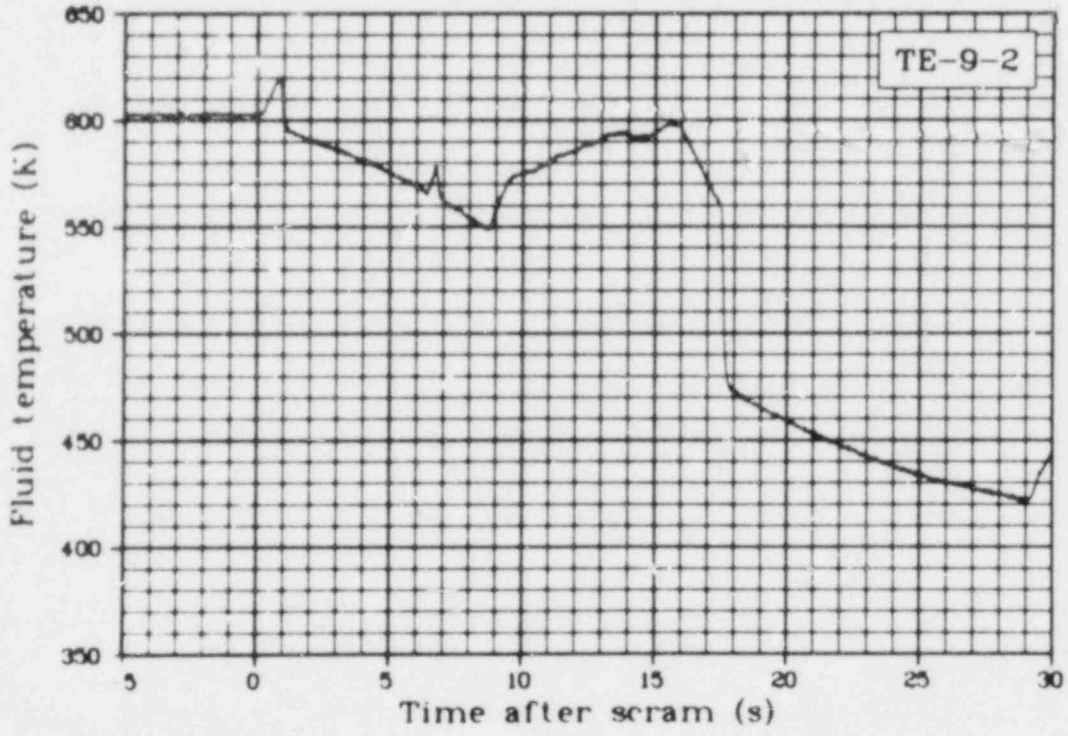

Fig. 48 Fluid temperature of Rod 2, 0.46 m above bottom of fuel stack (TE-9-2), Test LOC-11B.

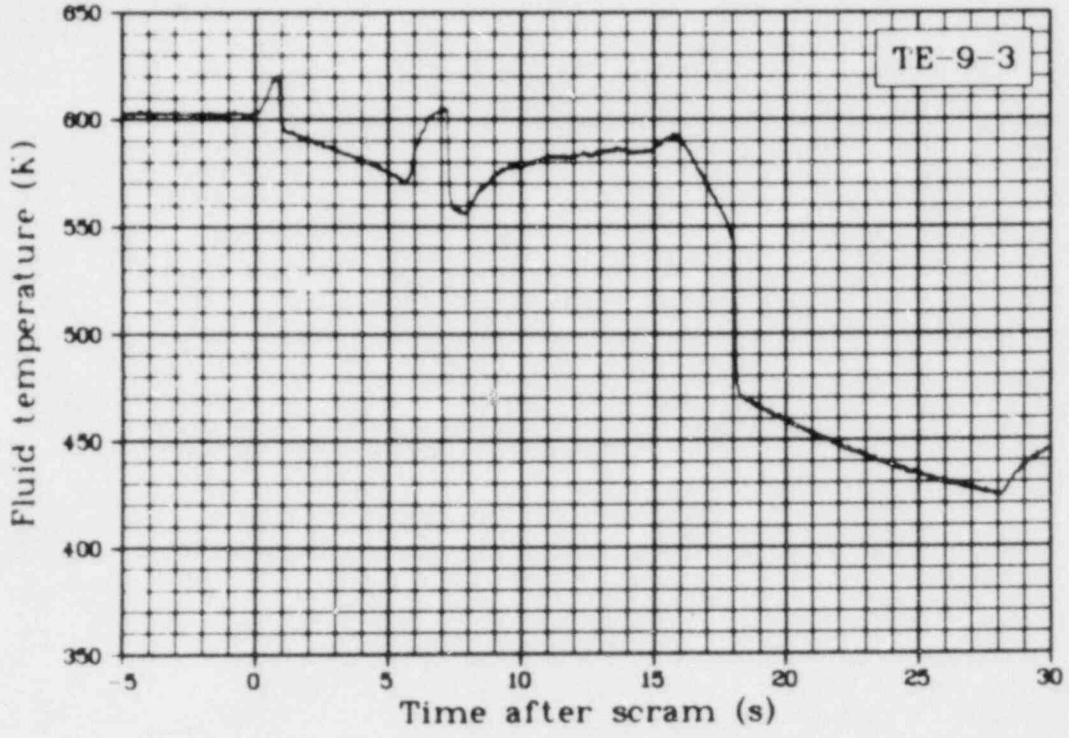

Fig. 49 Fluid temperature of Rod 3, 0.46 m above bottom of fuel stack (TE-9-3), Test LOC-11B.

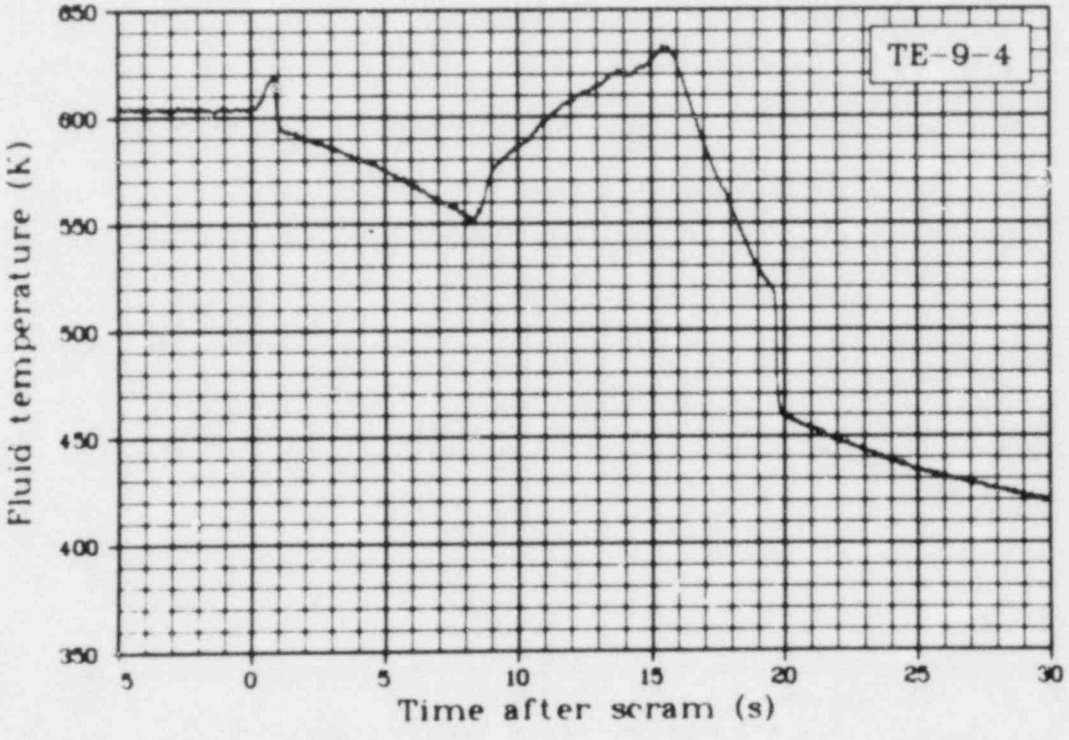

Fig. 50 Fluid temperature of Rod 4, 0.46 m above bottom of fuel stack (TE-9-4), Test LOC-11B.

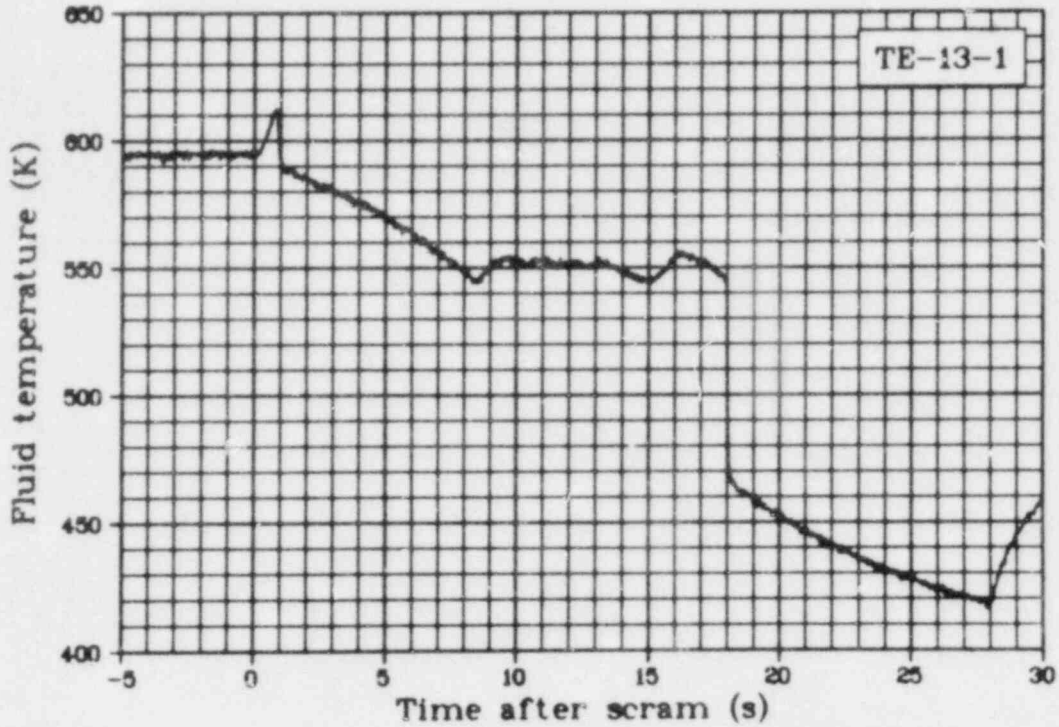

Fig. 51 Fluid temperature of Rod 1, 0.30 m above fuel stack bottom (TE-13-1), Test LOC-11B.

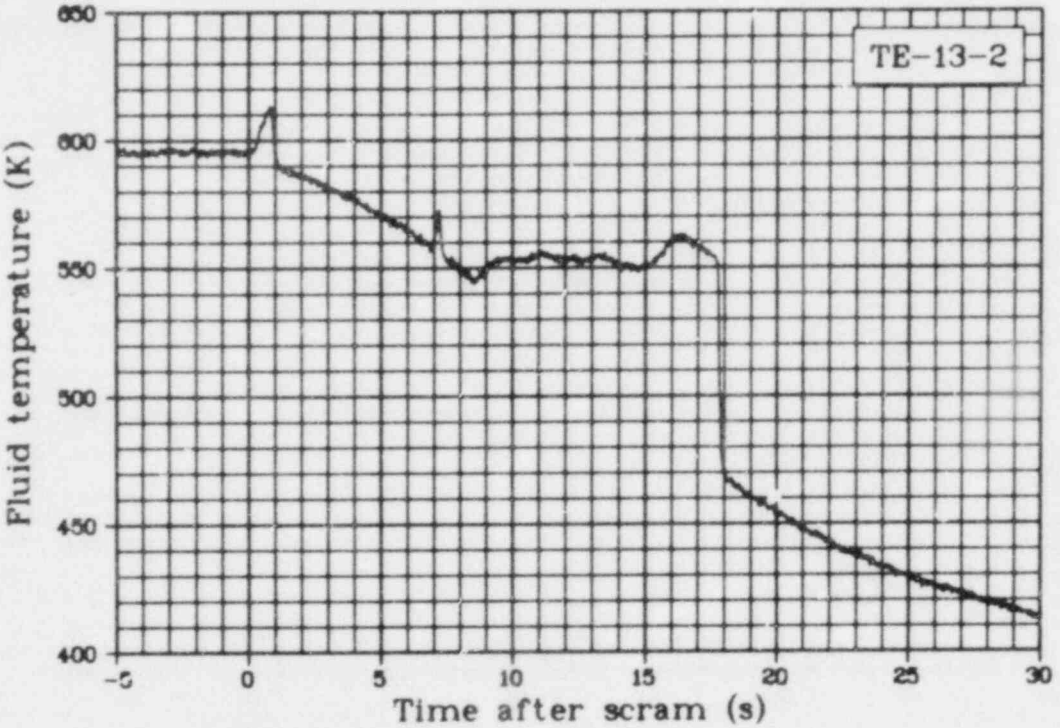

Fig. 52 Fluid temperature of Rod 2, 0.30 m above fuel stack bottom (TE-13-2), Test LOC-11B.

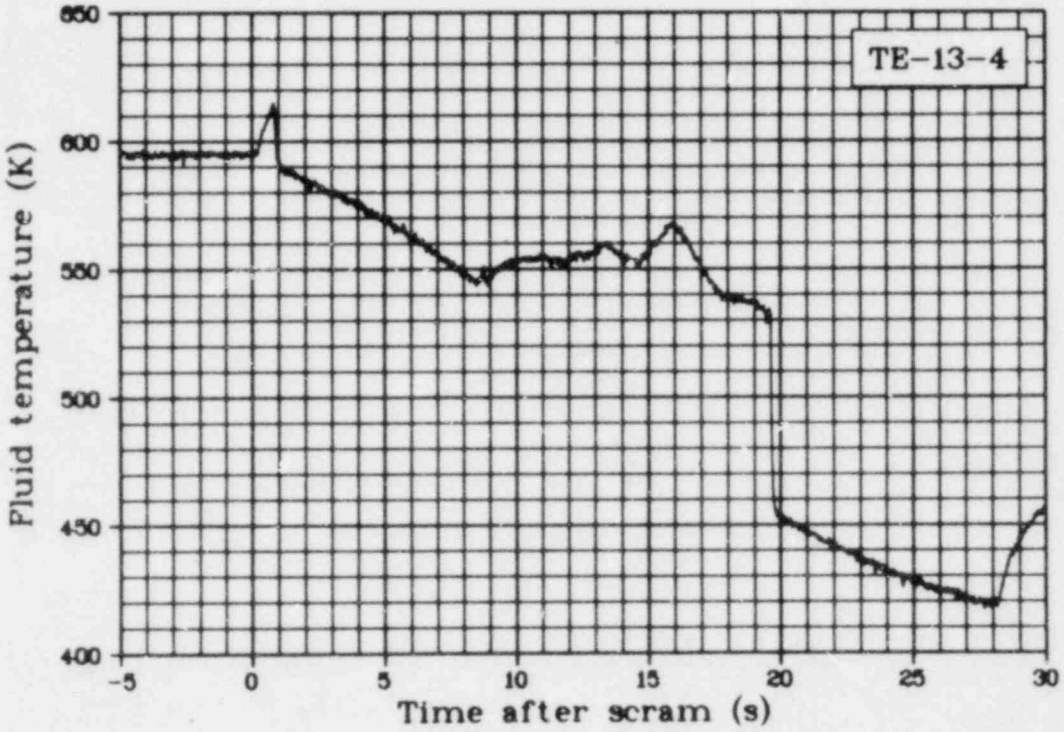

Fig. 53 Fluid temperature of Rod 4, 0.30 m above fuel stack bottom (TE-13-4), Test LOC-11B.

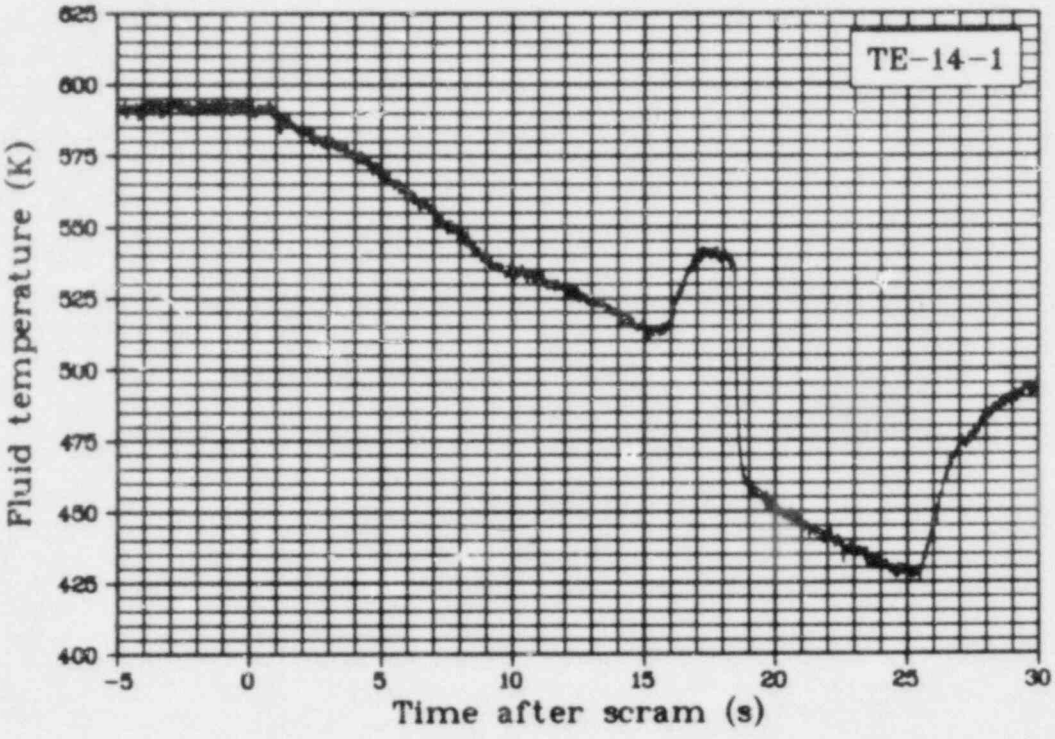

Fig. 54 Fluid temperature of Rod 1 inlet coolant (TE-14-1), Test LOC-11B.

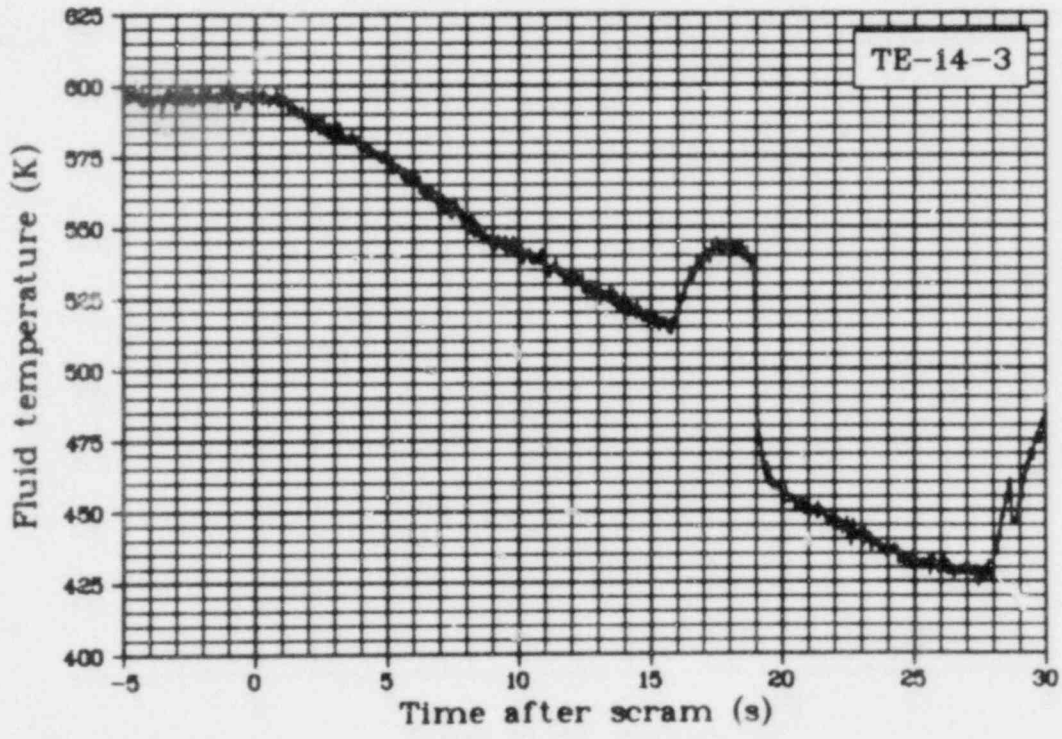

Fig. 55 Fluid temperature of Rod 3 inlet coolant (TE-14-3), Test LOC-11B.

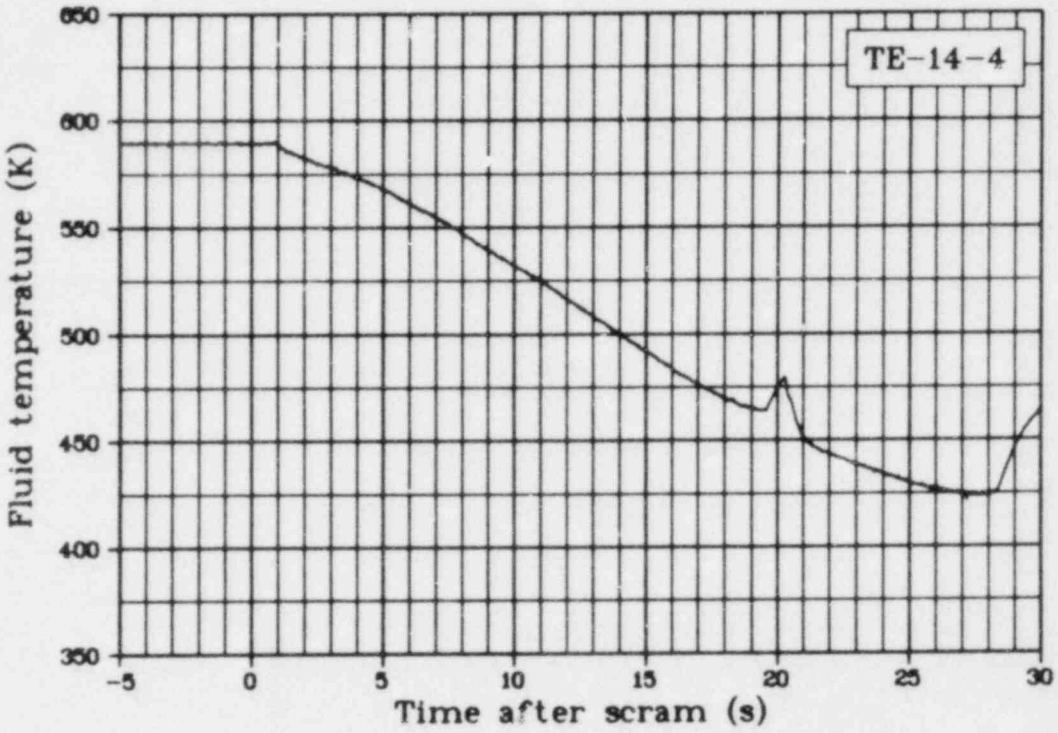

Fig. 56 Fluid temperature of Rod 4 inlet coolant (TE-14-4), Test LOC-11B.

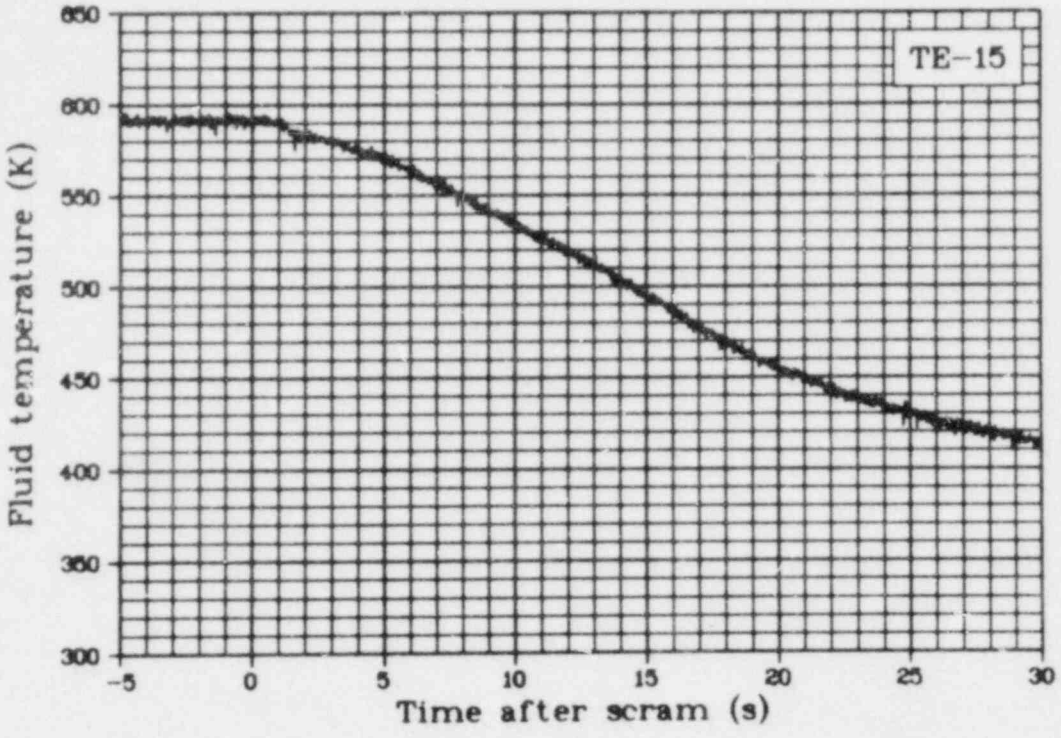

Fig. 57 Fluid temperature in test train lower particle screen (TE-15), Test LOC-11B.

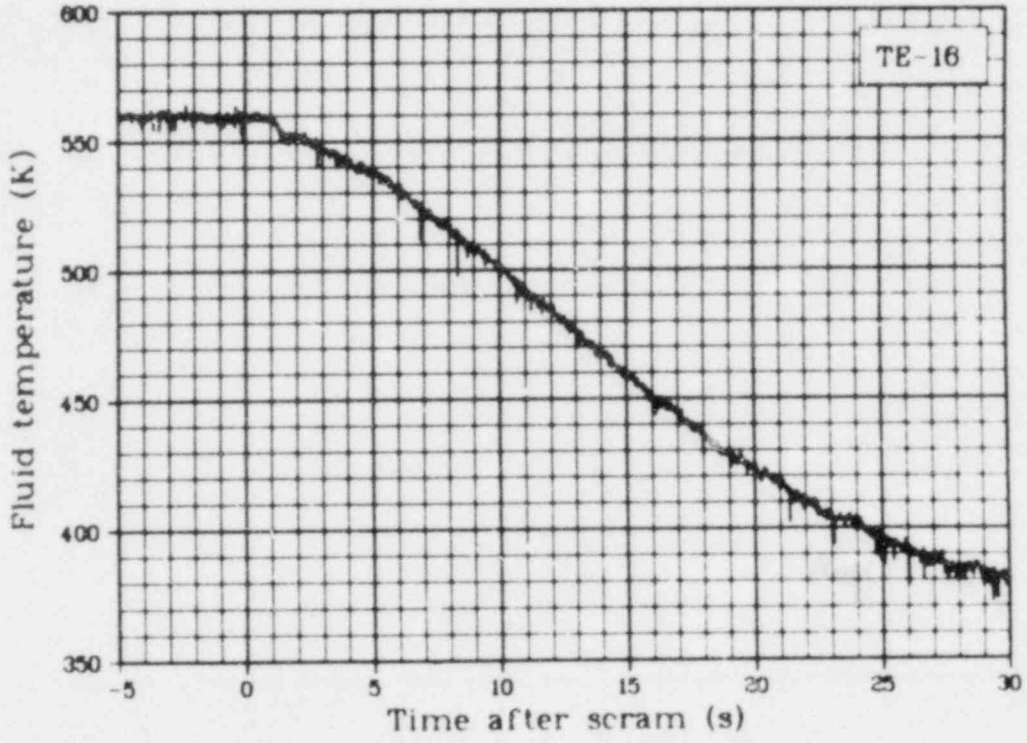

Fig. 58 Fluid temperature in test train lower particle screen (TE-16), Test LOC-11B.

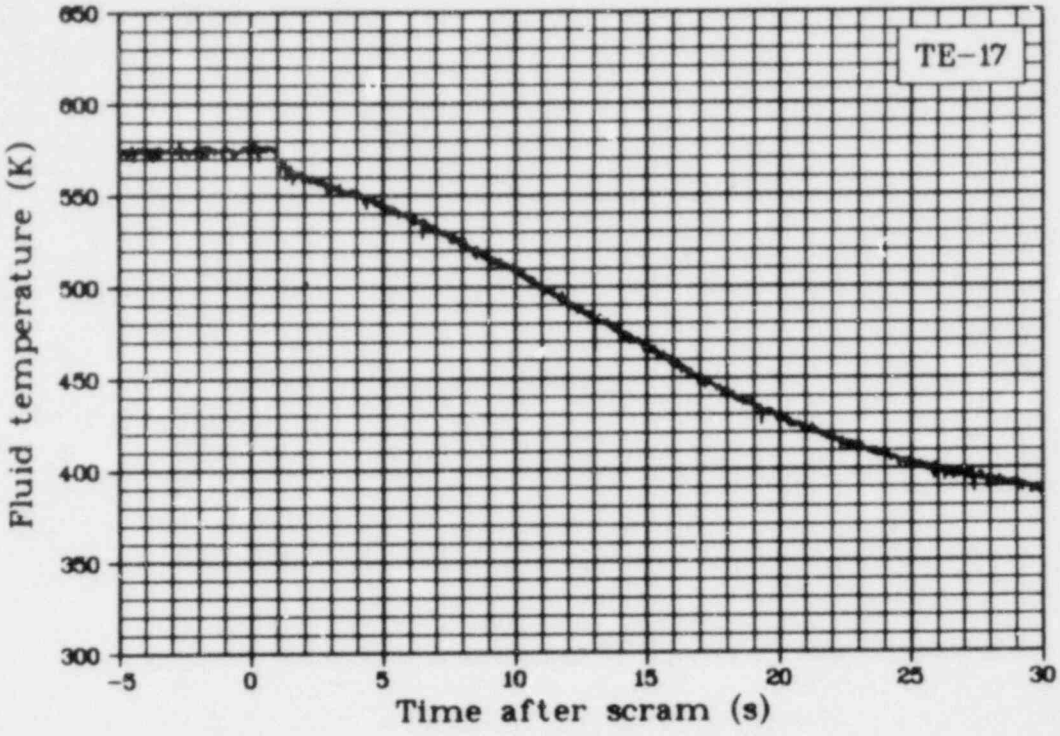

Fig. 59 Fluid temperature in test train bypass flow (TE-17), Test LOC-11B.

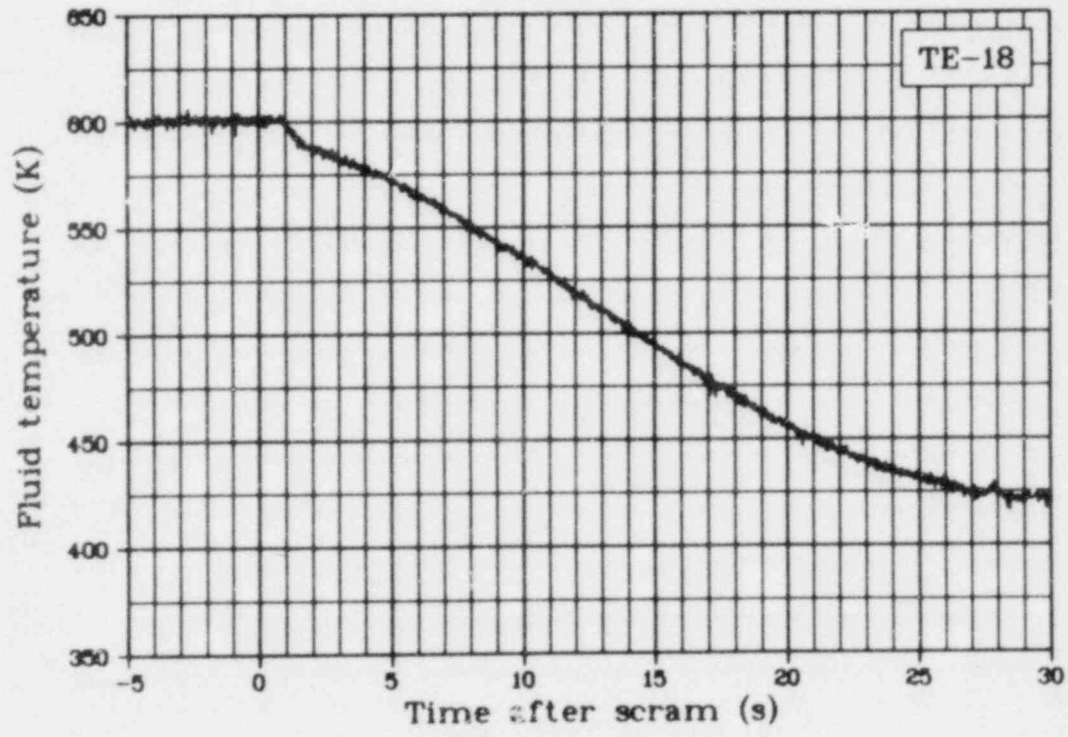

Fig. 60 Fluid temperature in upper plenum exit (TE-18), Test LOC-11B.

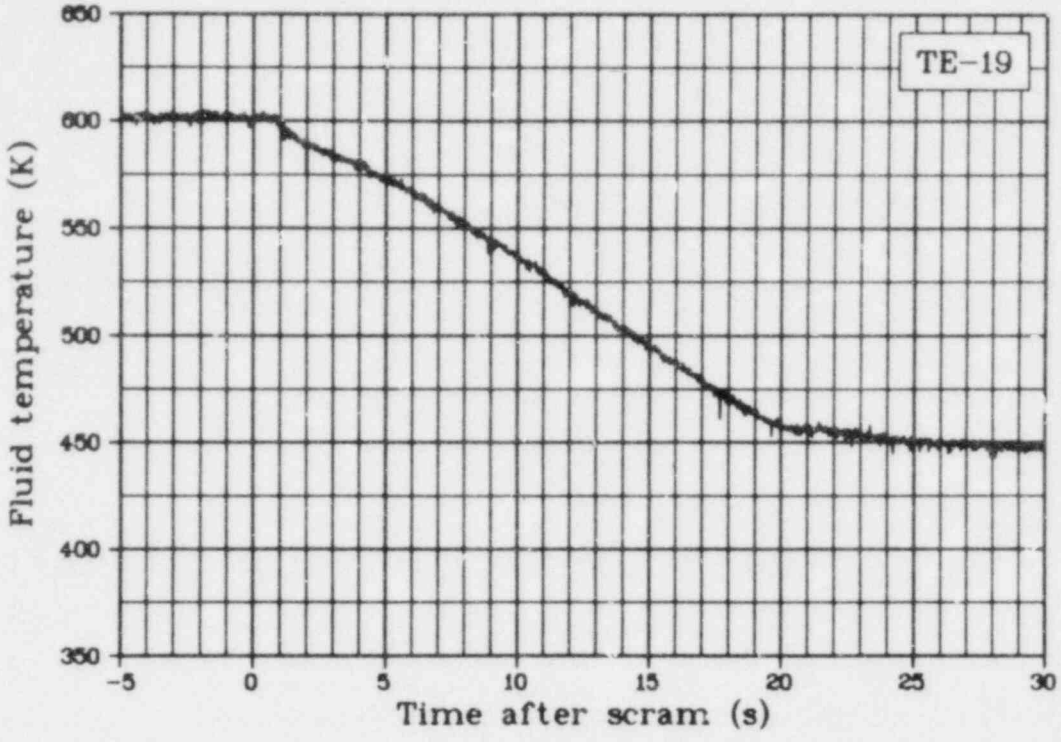

Fig. 61 Fluid temperature in upper plenum (TE-19), Test LOC-11B.

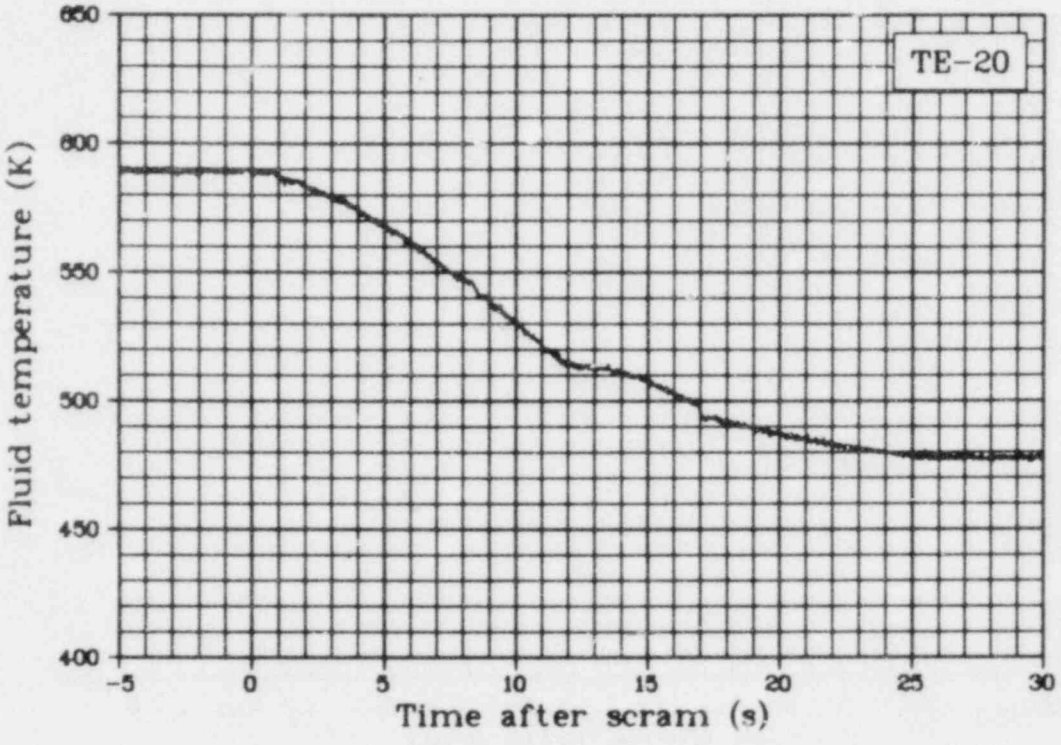

Fig. 62 Fluid temperature inlet spool (TE-20), Test LOC-11B.

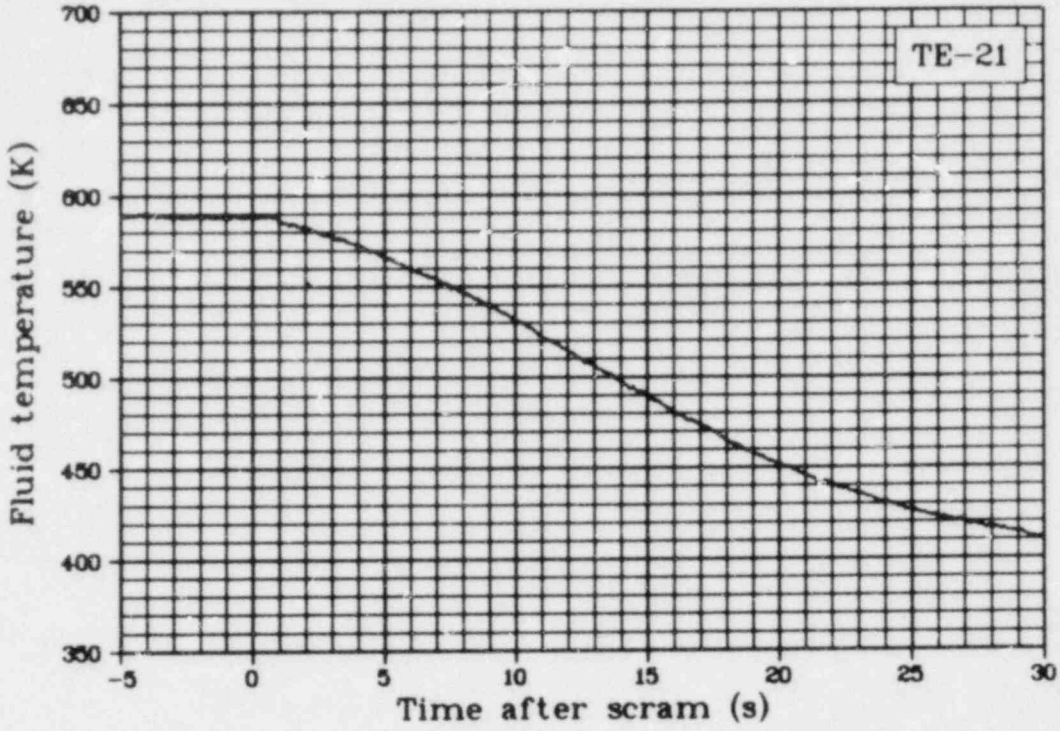

Fig. 63 Fluid temperature inlet spool (TE-21), Test LOC-11B.

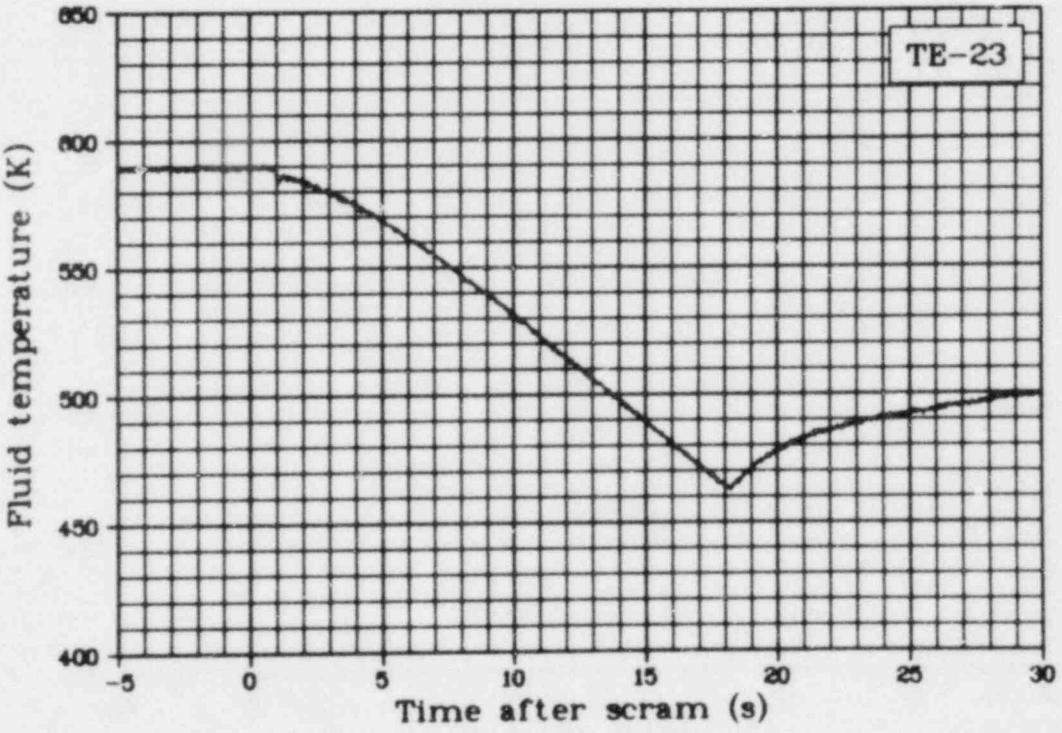

Fig. 64 Fluid temperature in cold leg blowdown spool (TE-23), Test LOC-11B.

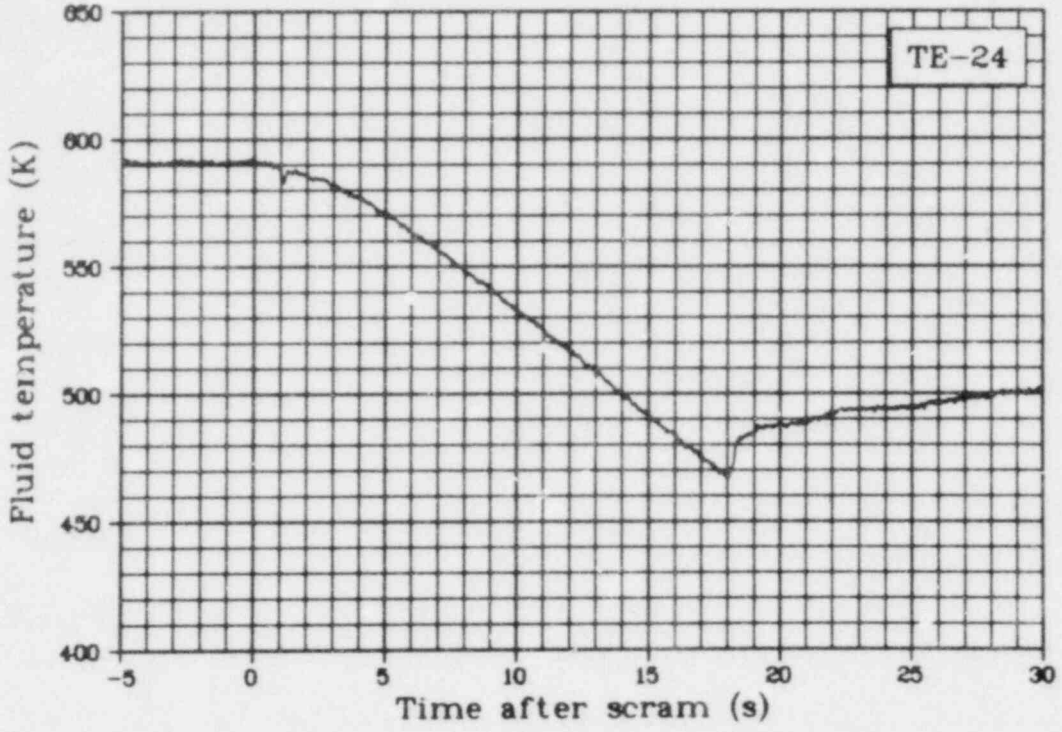

Fig. 65 Fluid temperature in cold leg blowdown spool (TE-24), Test LOC-11B.

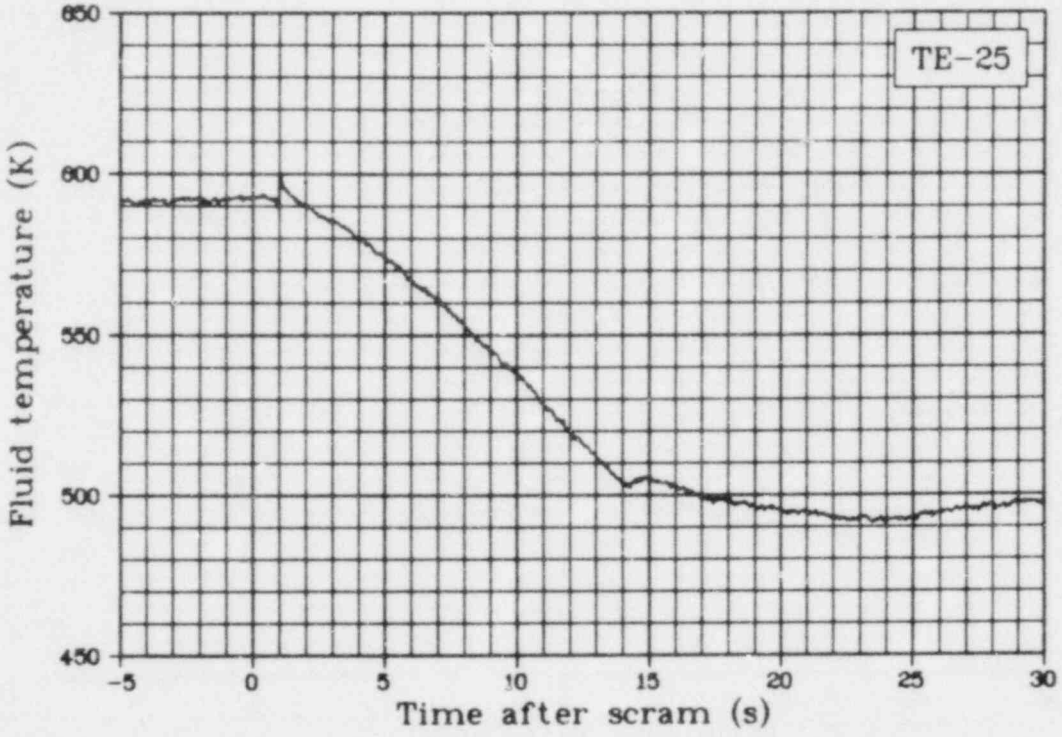

Fig. 66 Fluid temperature in hot leg blowdown spool (TE-25), Test LOC-11B.

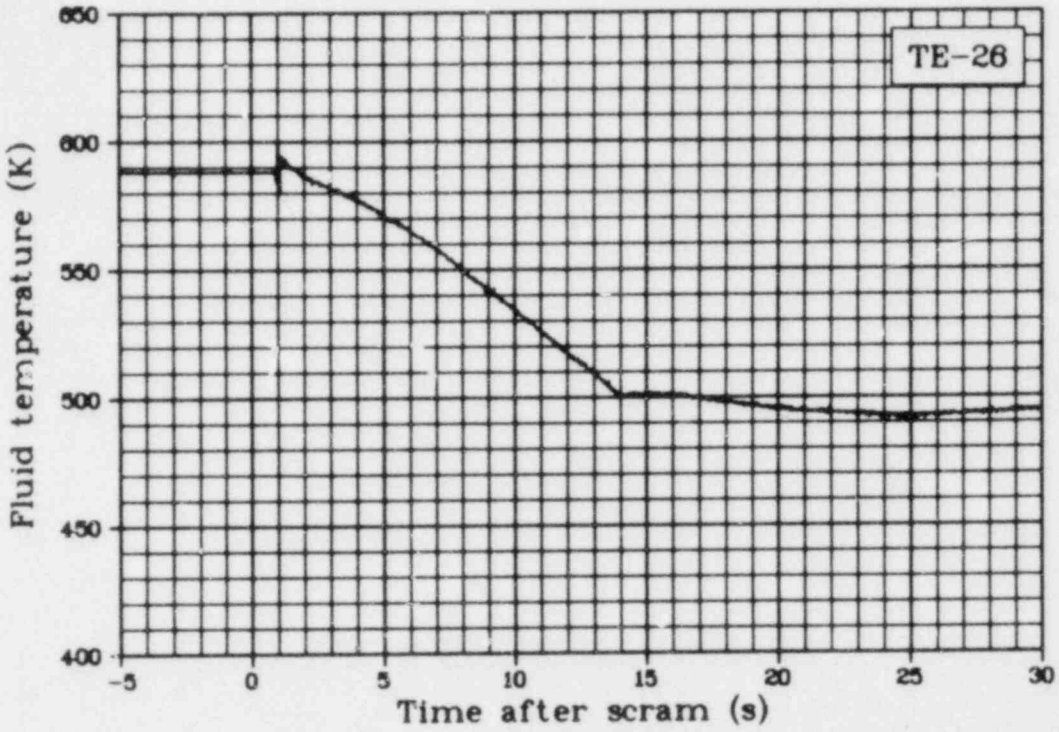

Fig. 67 Fluid temperature in hot leg blowdown spool (TE-26), Test LOC-11B.

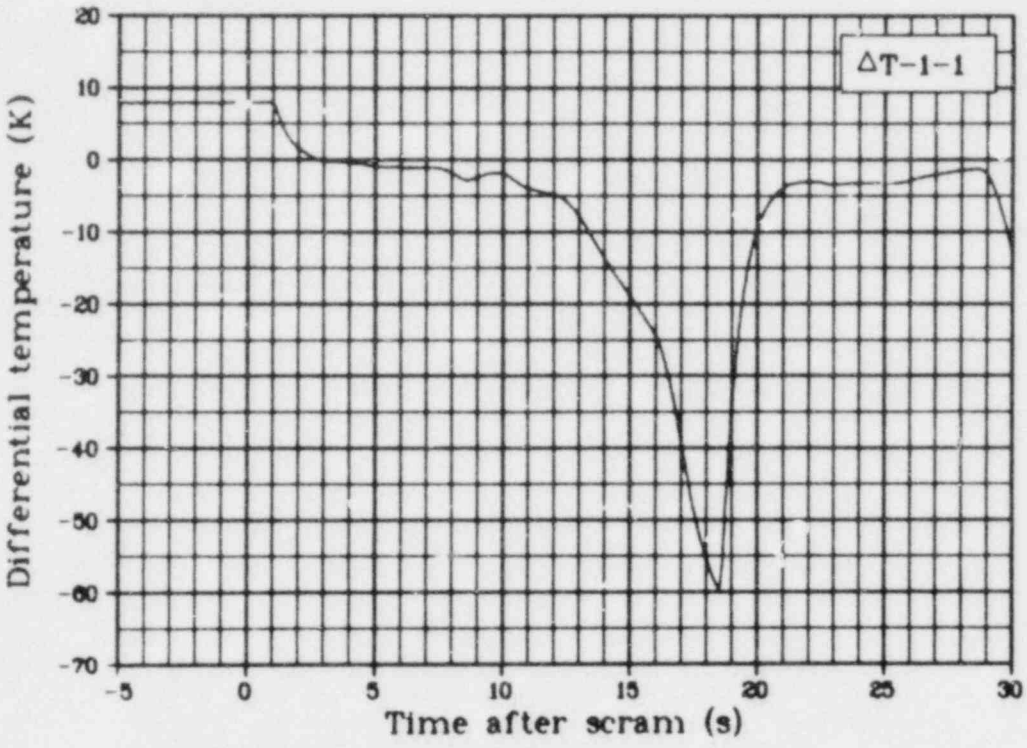

Fig. 68 Differential temperature at fuel inlet and outlet Rod 1 (ΔT-1-1), Test LOC-11B.

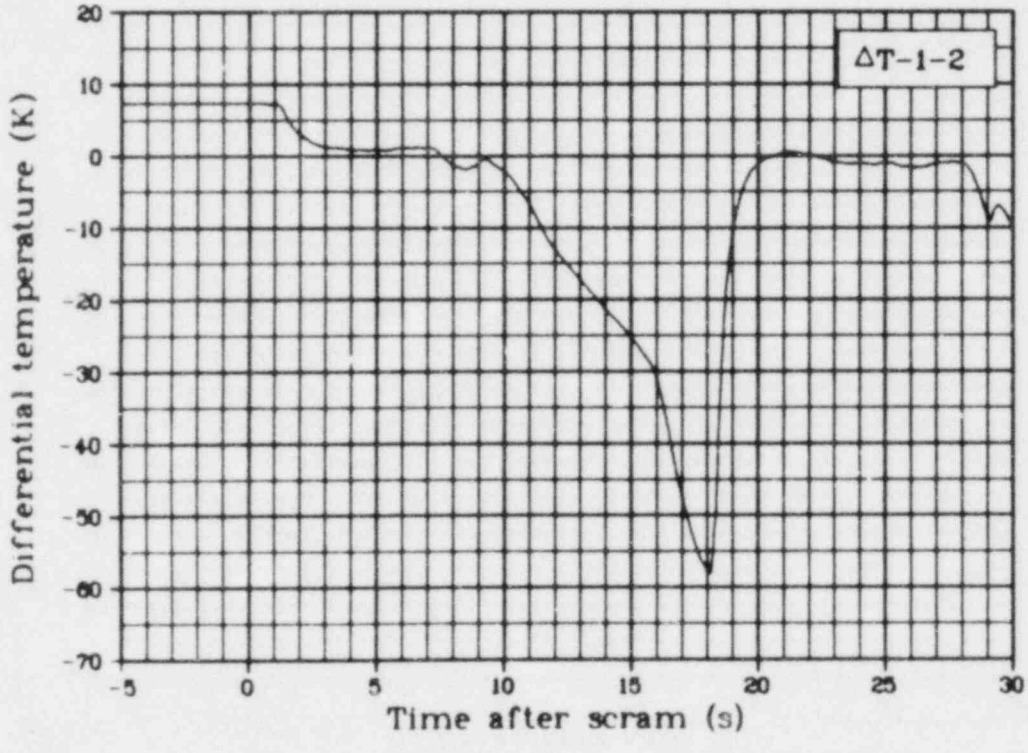

Fig. 69 Differential temperature at fuel inlet and outlet Rod 2 (ΔT-1-2), Test LOC-11B.

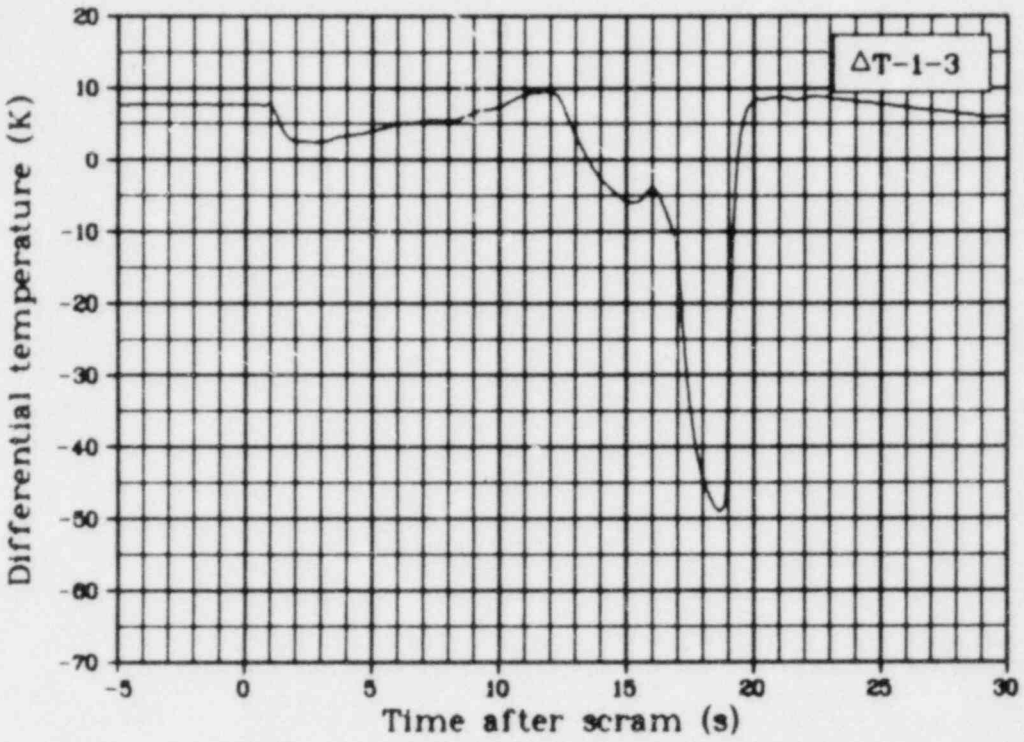

Fig. 70 Differential temperature at fuel inlet and outlet Rod 3 (ΔT-1-3), Test LOC-11B.

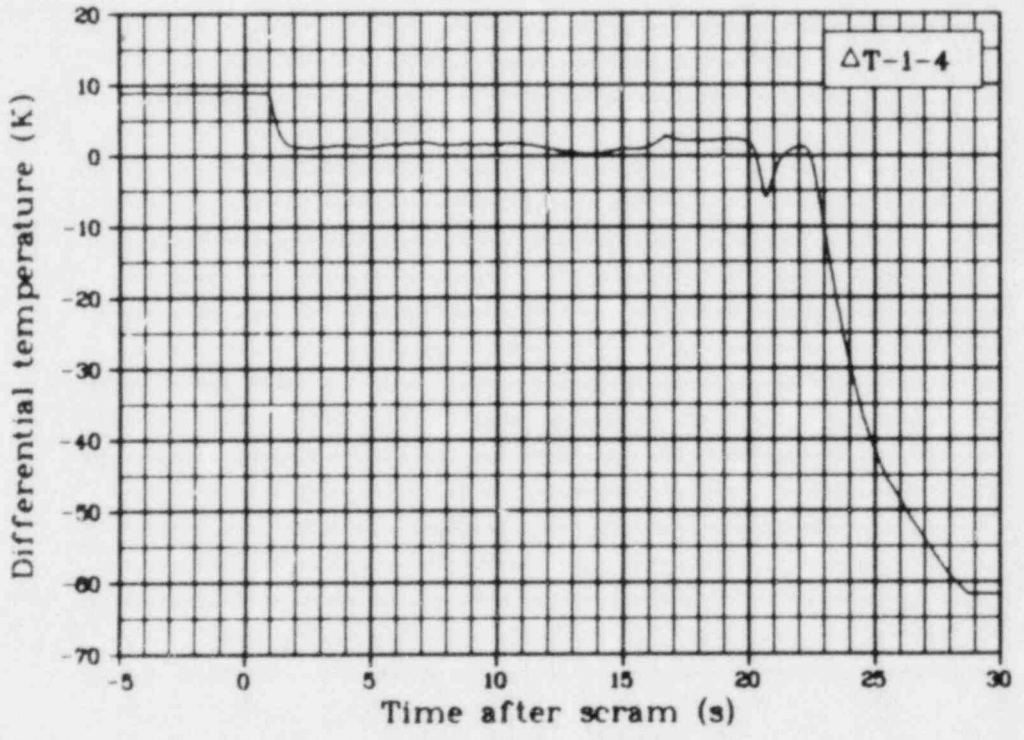

Fig. 71 Differential temperature at fuel inlet and outlet Rod 4 (ΔT-1-4), Test LOC-11B.

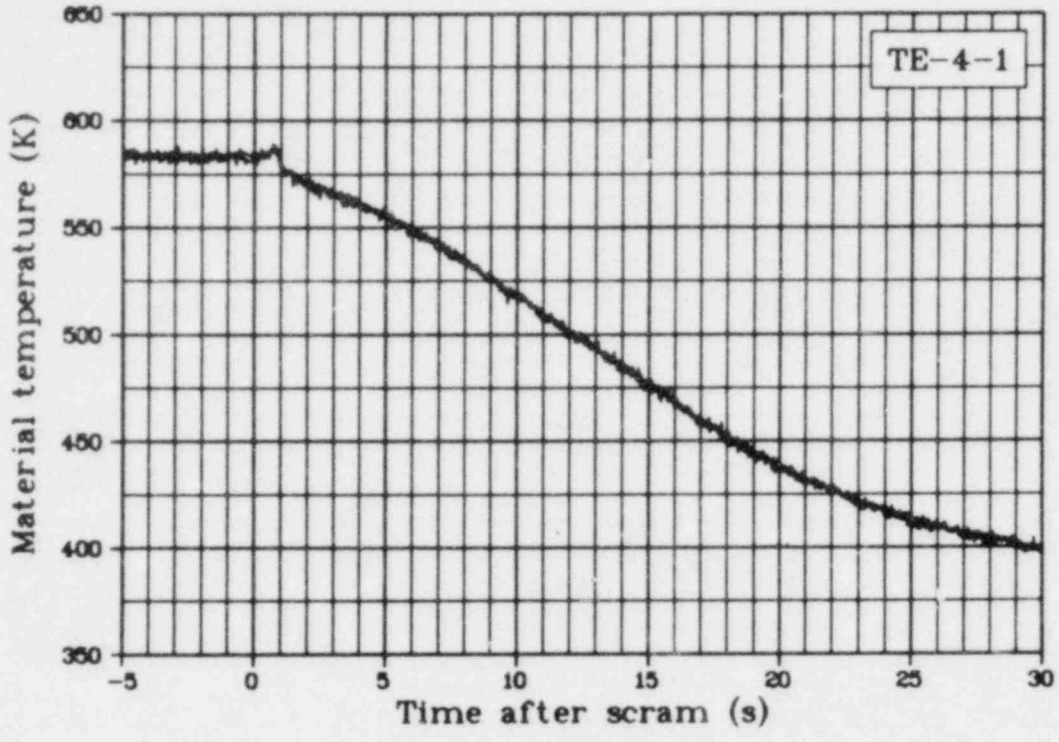

Fig. 72 Material temperature Rod 1, 0.61 m above fuel stack bottom (TE-4-1), Test LOC-11B.

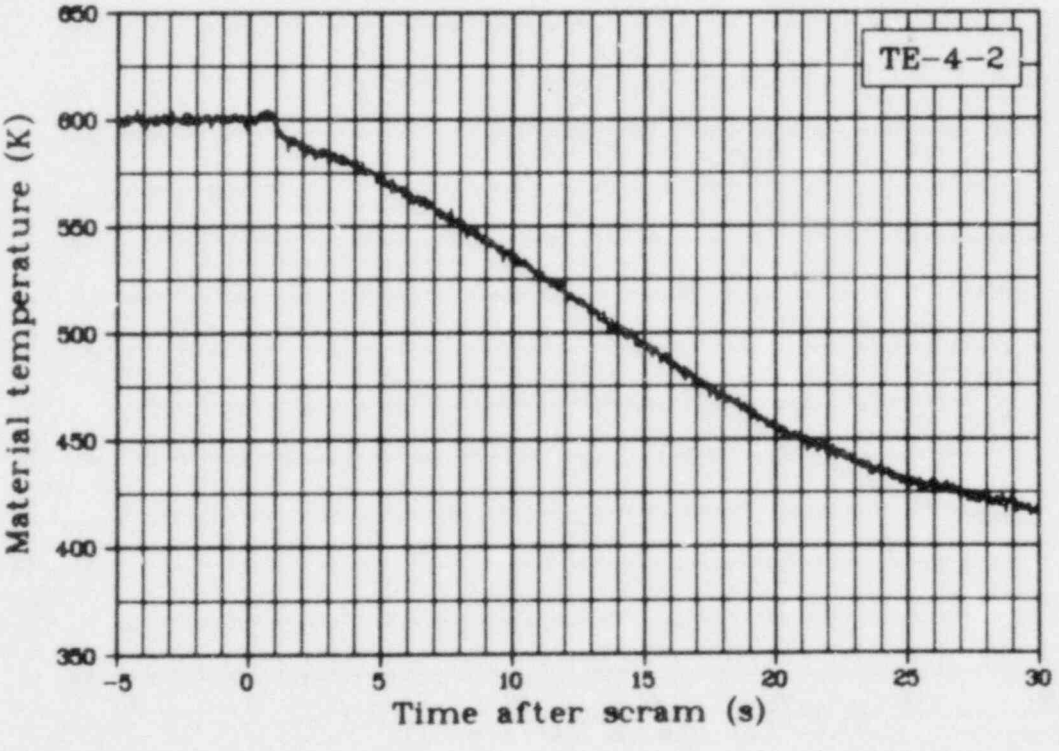

Fig. 73 Material temperature Rod 2, 0.61 m above fuel stack bottom (TE-4-2), Test LOC-11B.

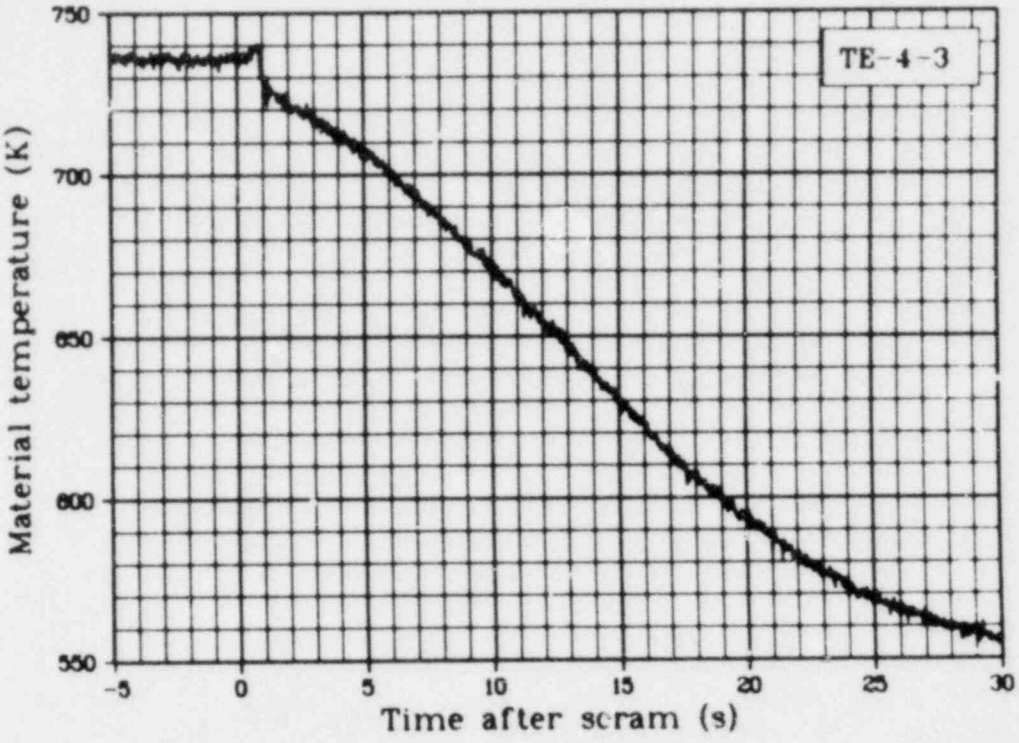

Fig. 74 Material temperature Rod 3, 0.61 m above fuel stack bottom (TE-4-3), Test LOC-11B.

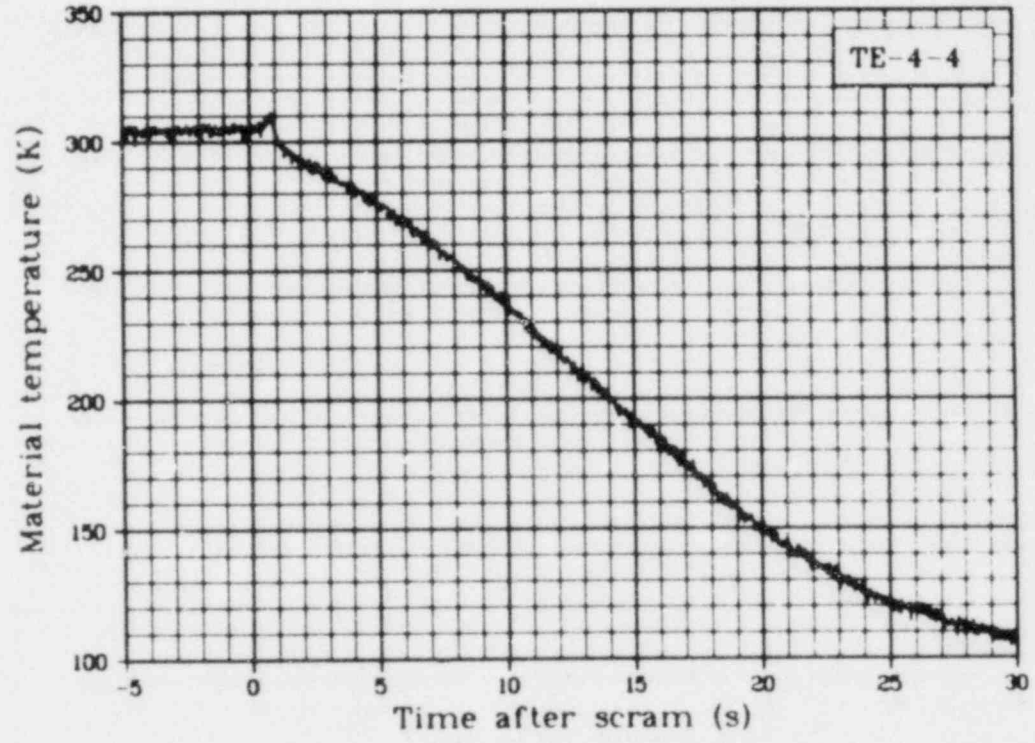

Fig. 75 Material temperature Rod 4, 0.61 m above fuel stack bottom (TE-4-4), Test LOC-11B.

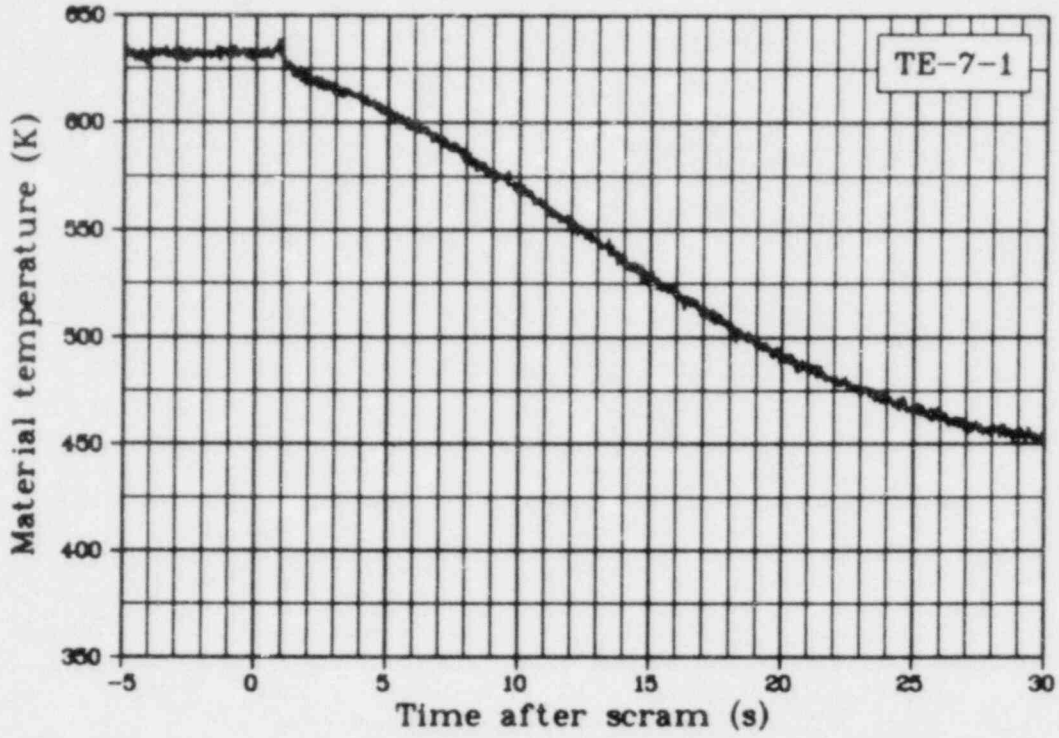

Fig. 76 Material temperature Rod 1, 0.46 m above fuel stack bottom (TE-7-1), Test LOC-11B.

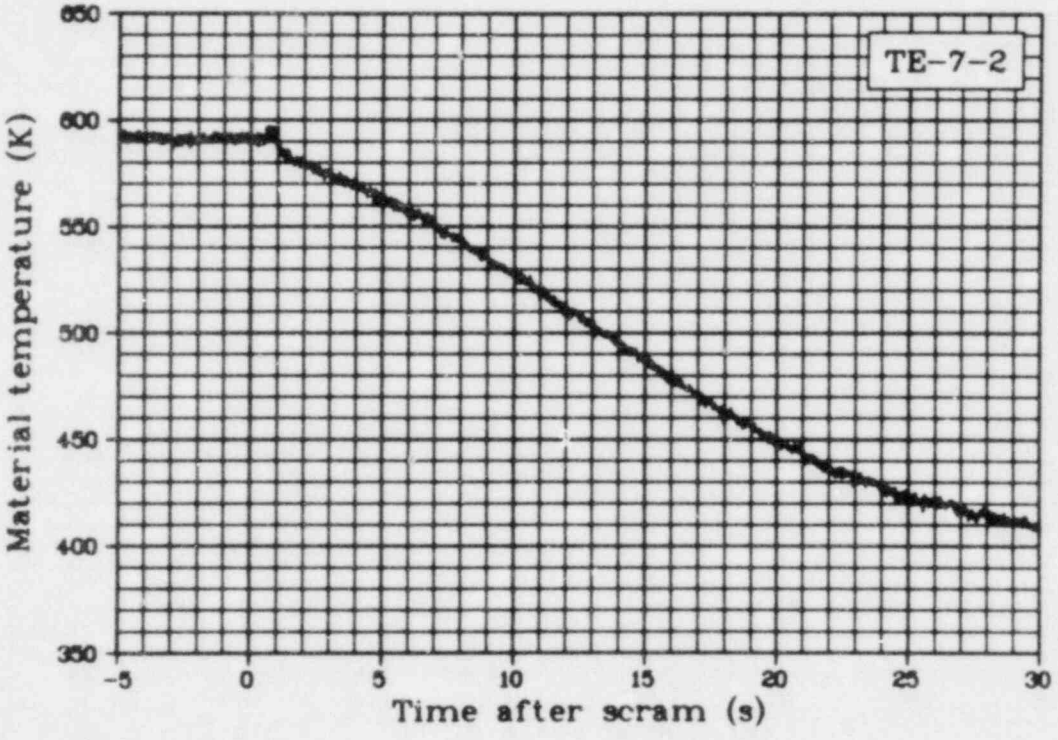

Fig. 77 Material temperature Rod 2, 0.46 m above fuel stack bottom (TE-7-2), Test LOC-11B.

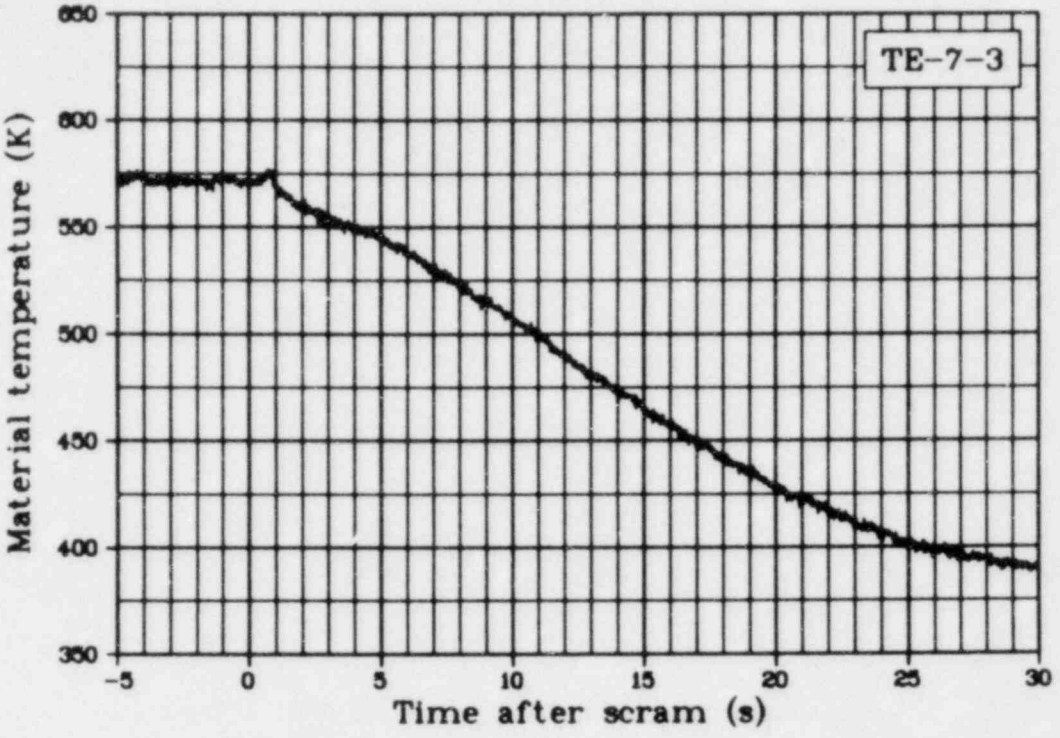

Fig. 78 Material temperature Rod 3, 0.46 m above fuel stack bottom (TE-7-3), Test LOC-11B.

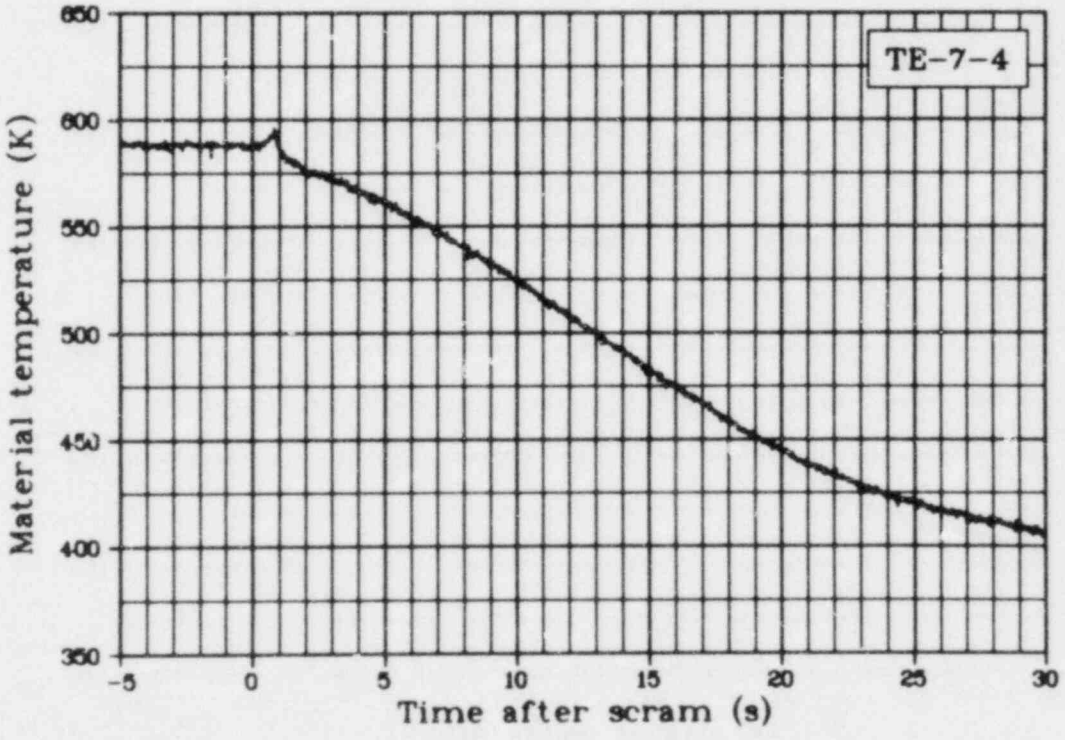

Fig. 79 Material temperature Rod 4, 0.46 m above fuel stack bottom (TE-7-4), Test LOC-11B.

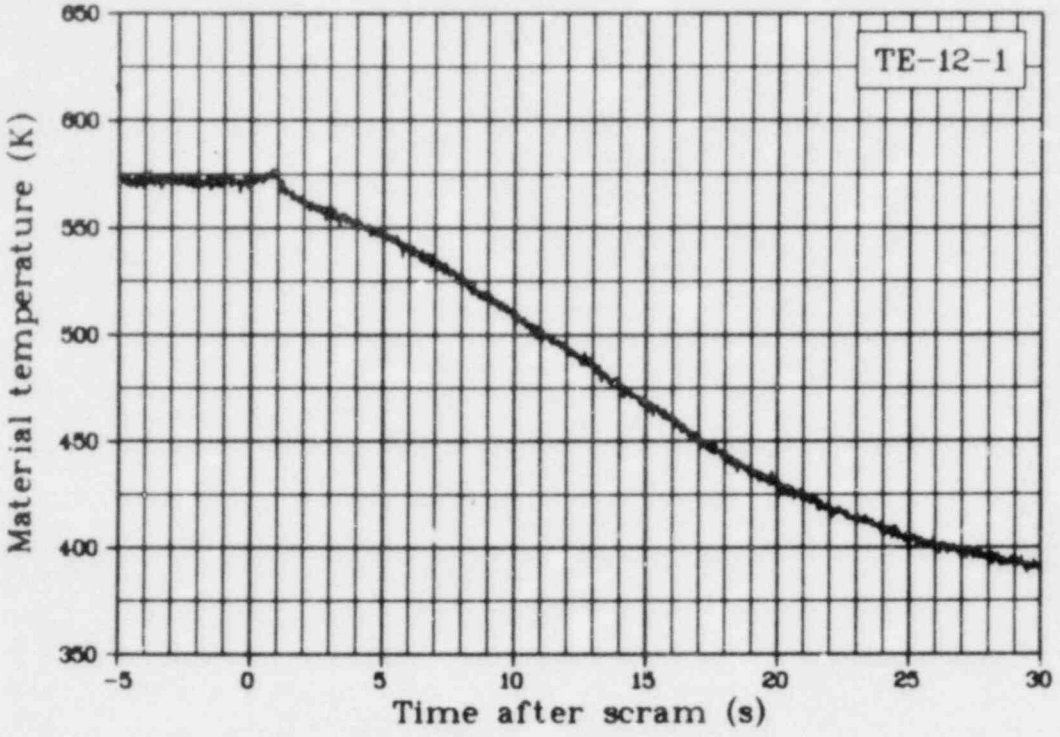

Fig. 80 Material temperature Rod 1, 0.30 m above fuel stack bottom (TE-12-1), Test LOC-11B.

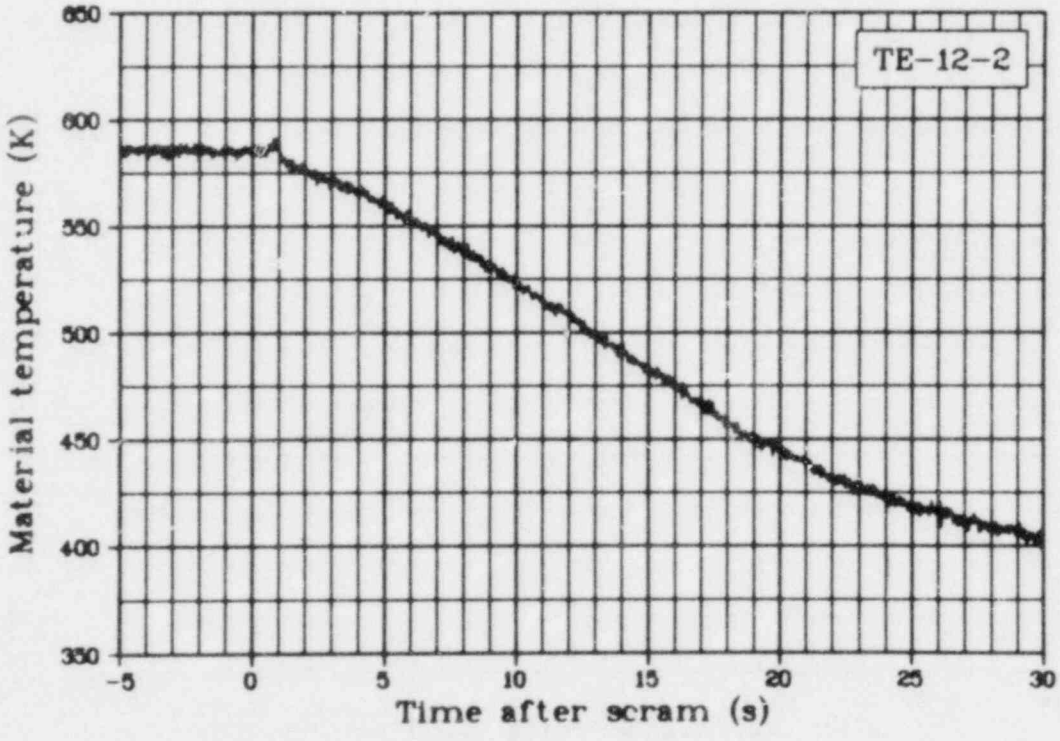

Fig. 81 Material temperature Rod 2, 0.30 m above fuel stack bottom (TE-12-2), Test LOC-11B.

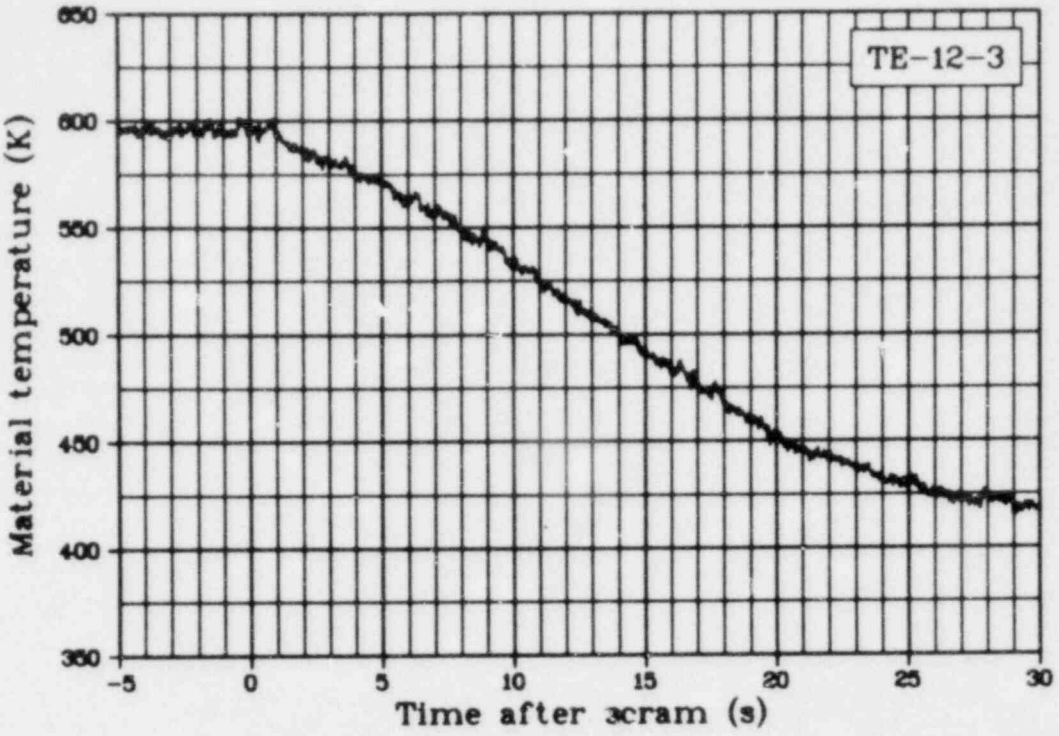

Fig. 82 Material temperature Rod 3, 0.30 m above fuel stack bottom (TE-12-3), Test LOC-11B.

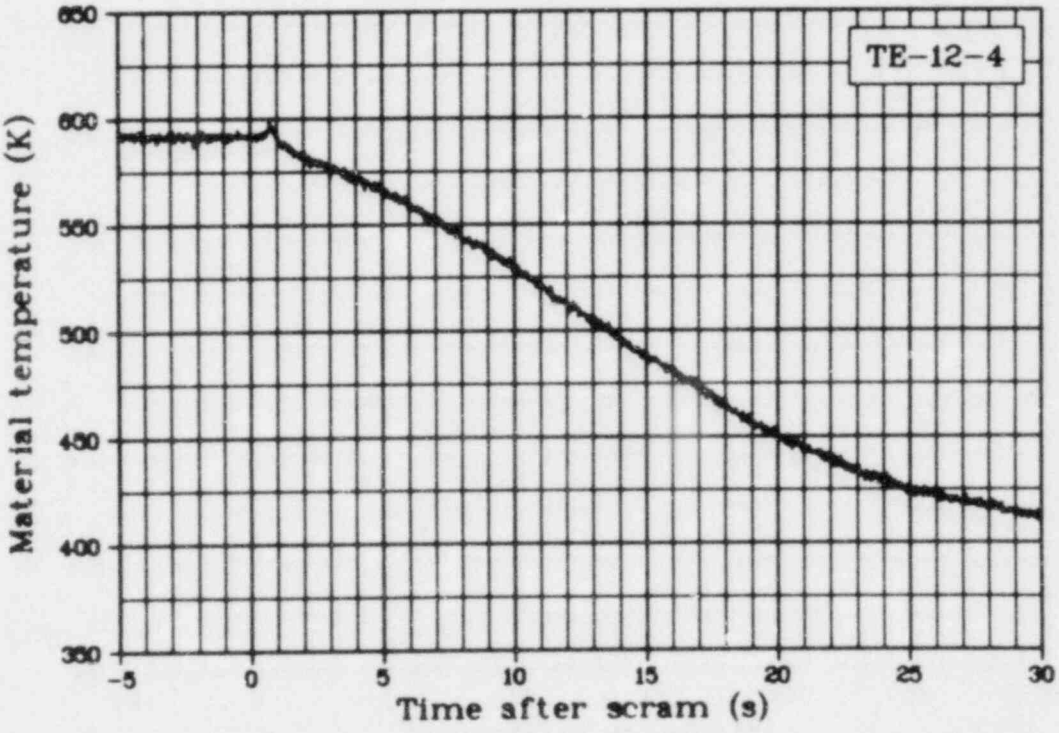

Fig. 83 Material temperature Rod 4, 0.30 m above fuel stack bottom (TE-12-4), Test LOC-11B.

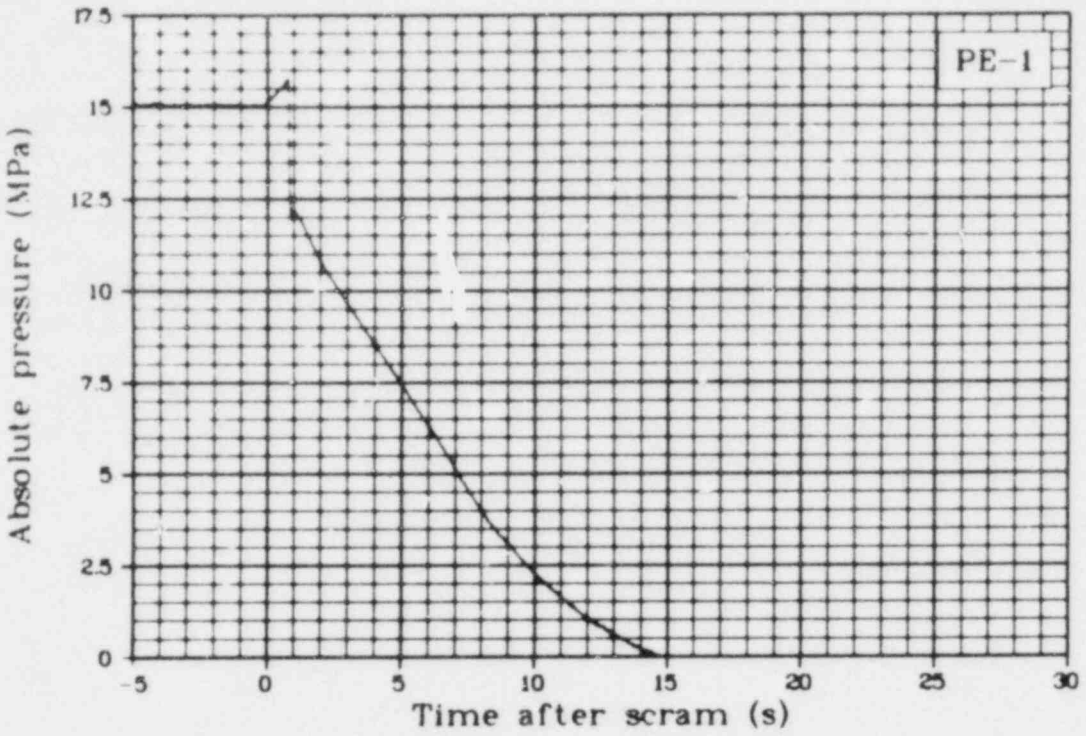

Fig. 84 Absolute pressure in upper test train (PE-1), Test LOC-11B.

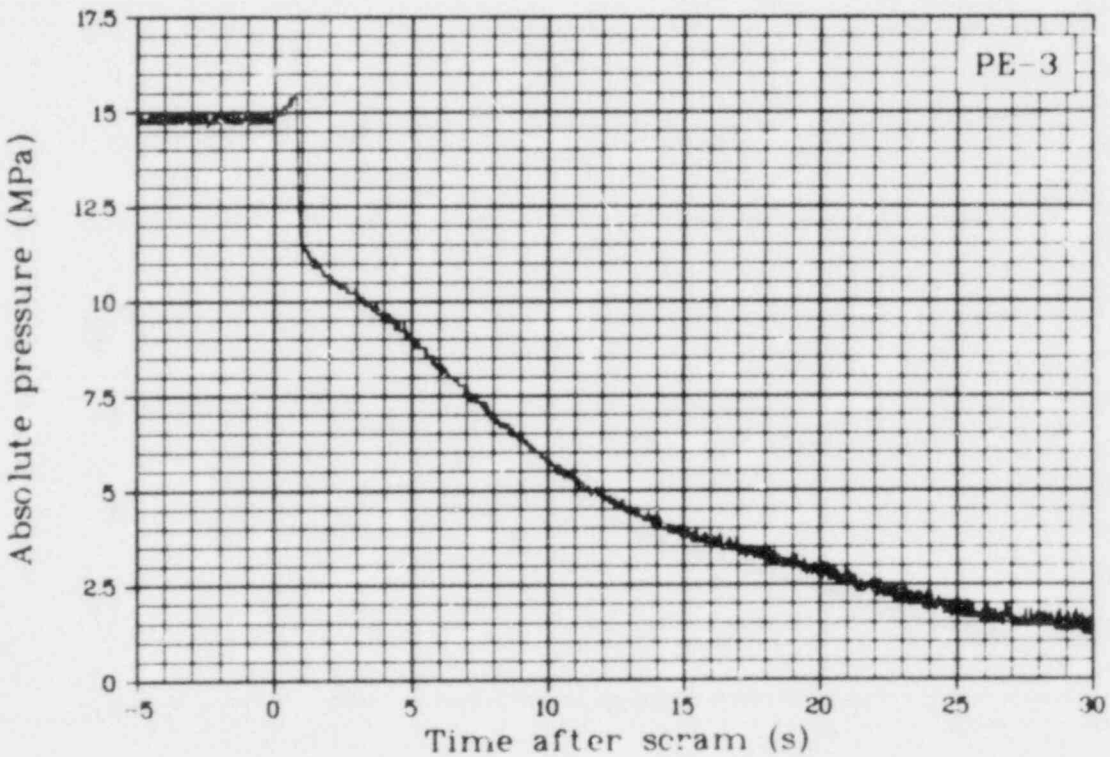

Fig. 85 Absolute pressure in upper test train (PE-3), Test LOC-11B.

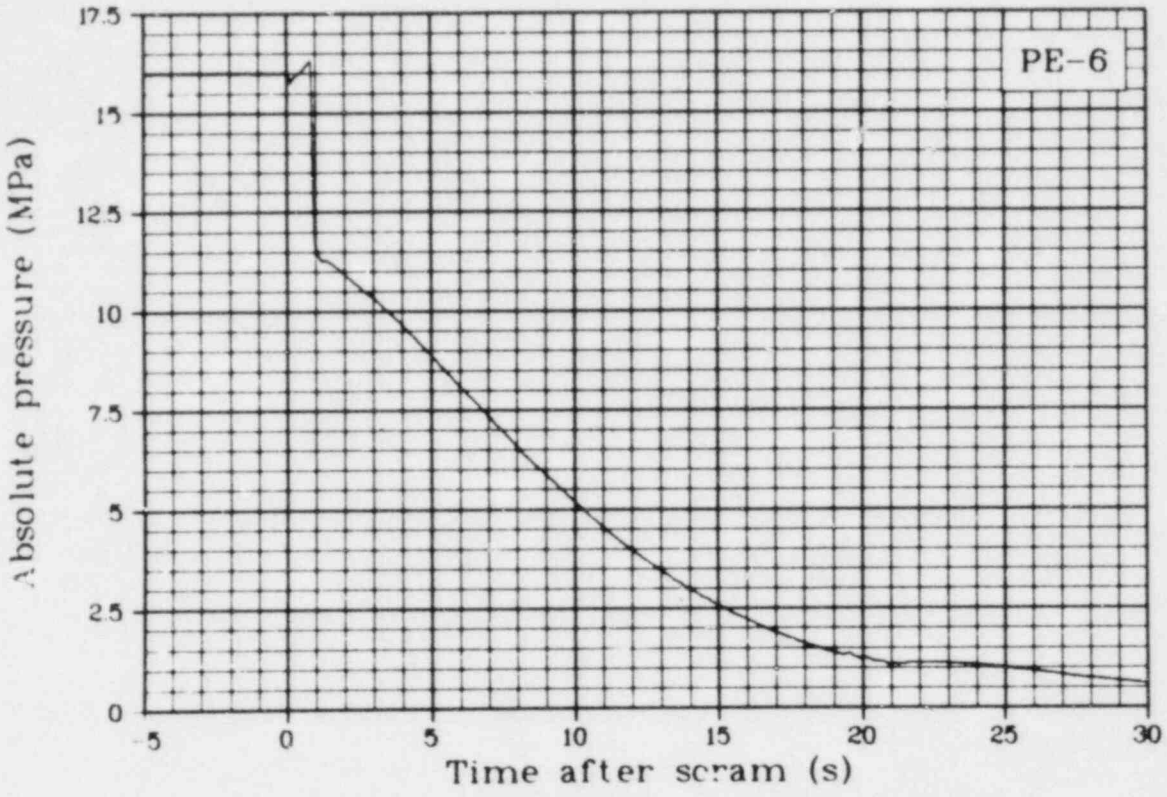

Fig. 86 Absolute pressure below test train fuel rod (PE-6), Test LOC-11B.

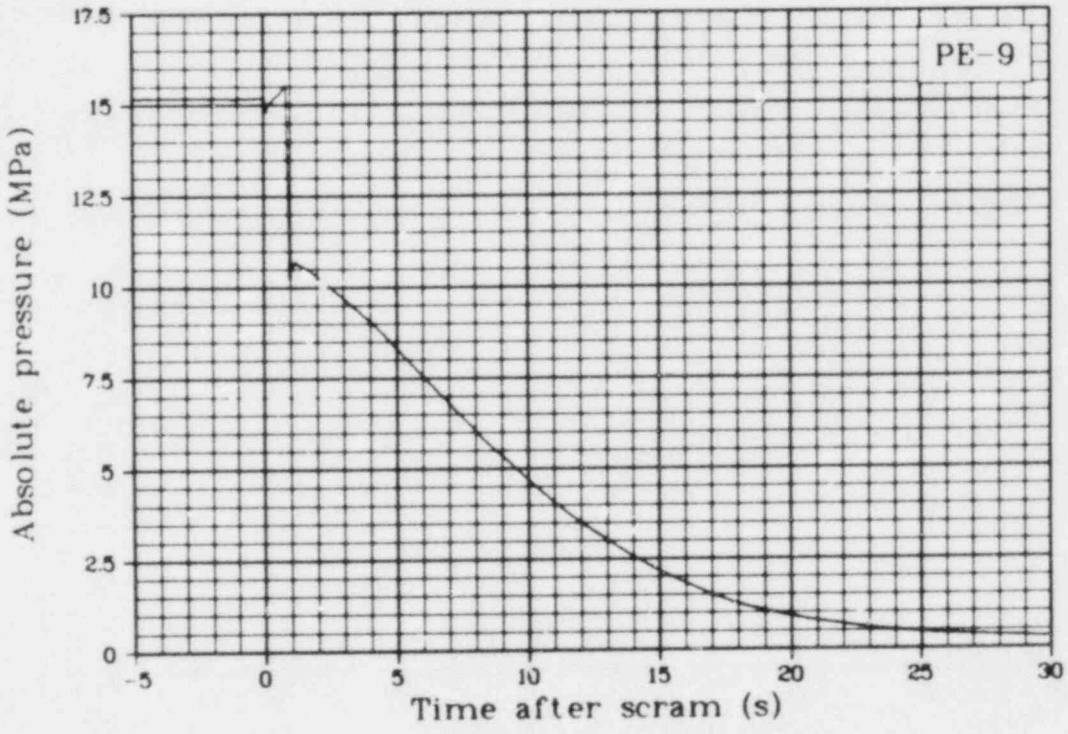

Fig. 87 Absolute pressure in inlet spool (PE-9), Test LOC-11B.

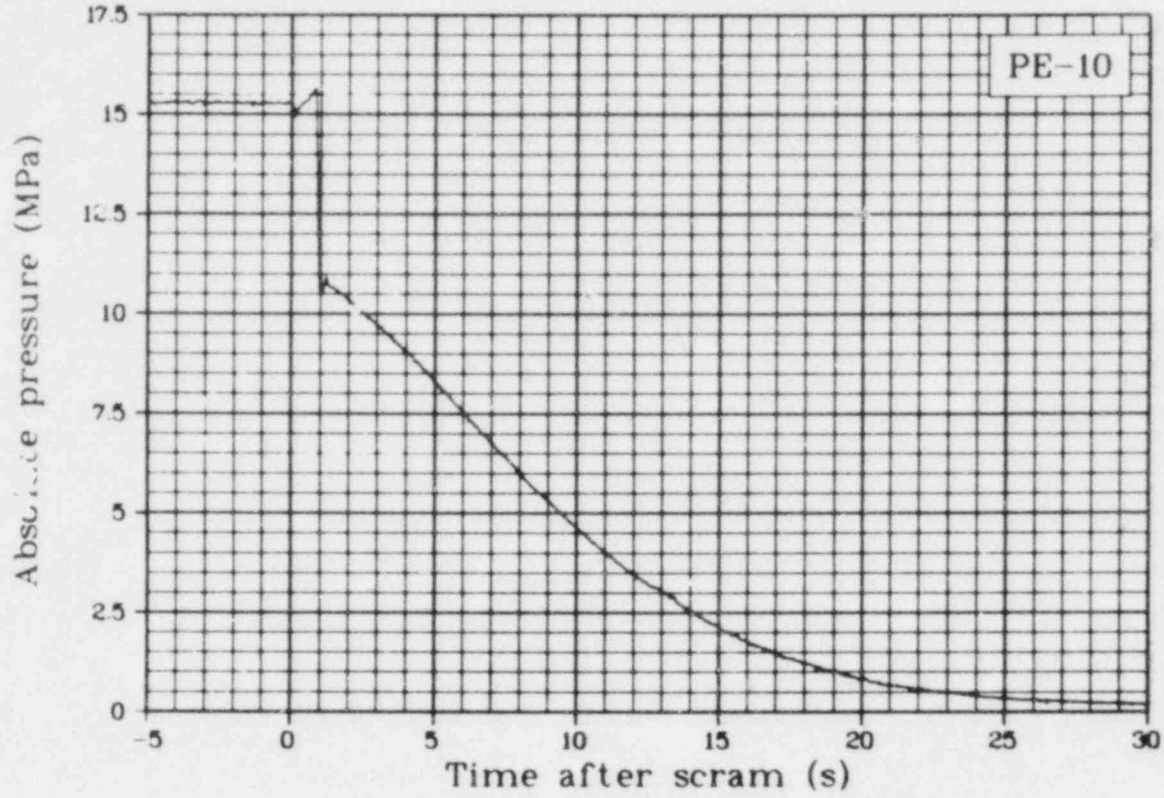

Fig. 88 Absolute pressure in cold leg blowdown spool (PE-10), Test LOC-11B.

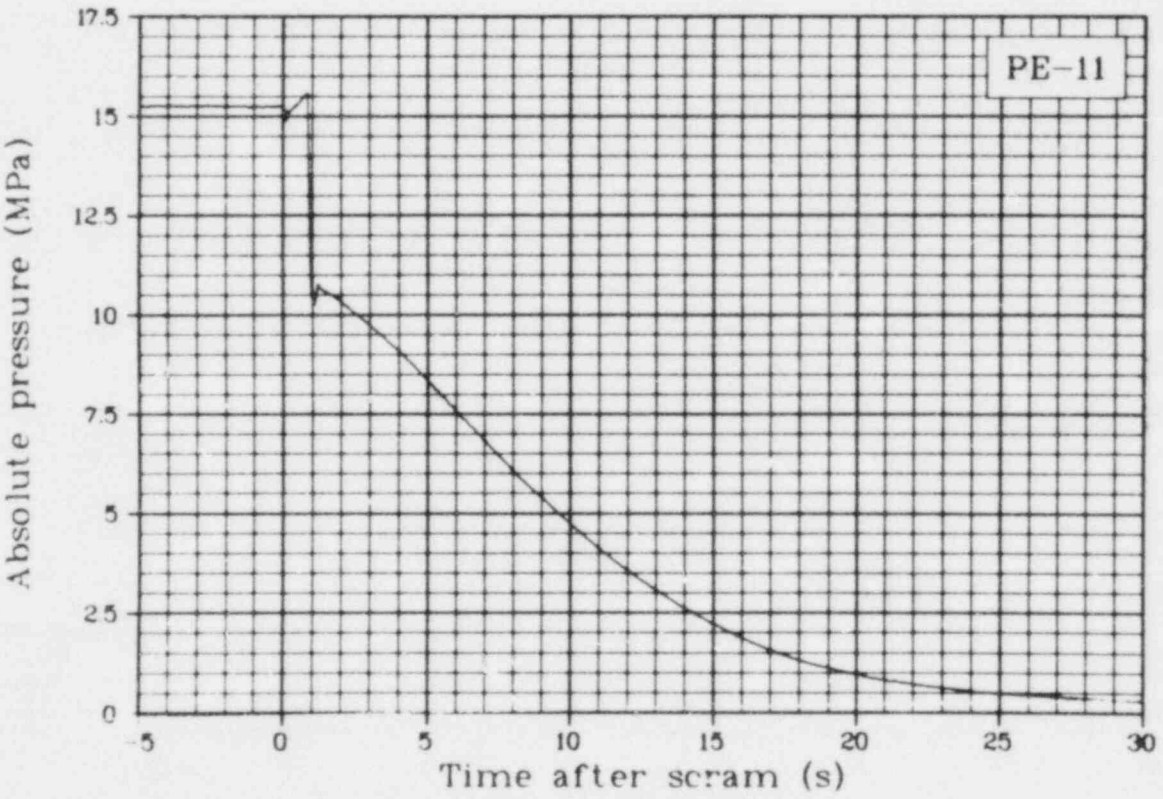

Fig. 89 Absolute pressure in cold leg blowdown spool (PE-11), Test LOC-11B.

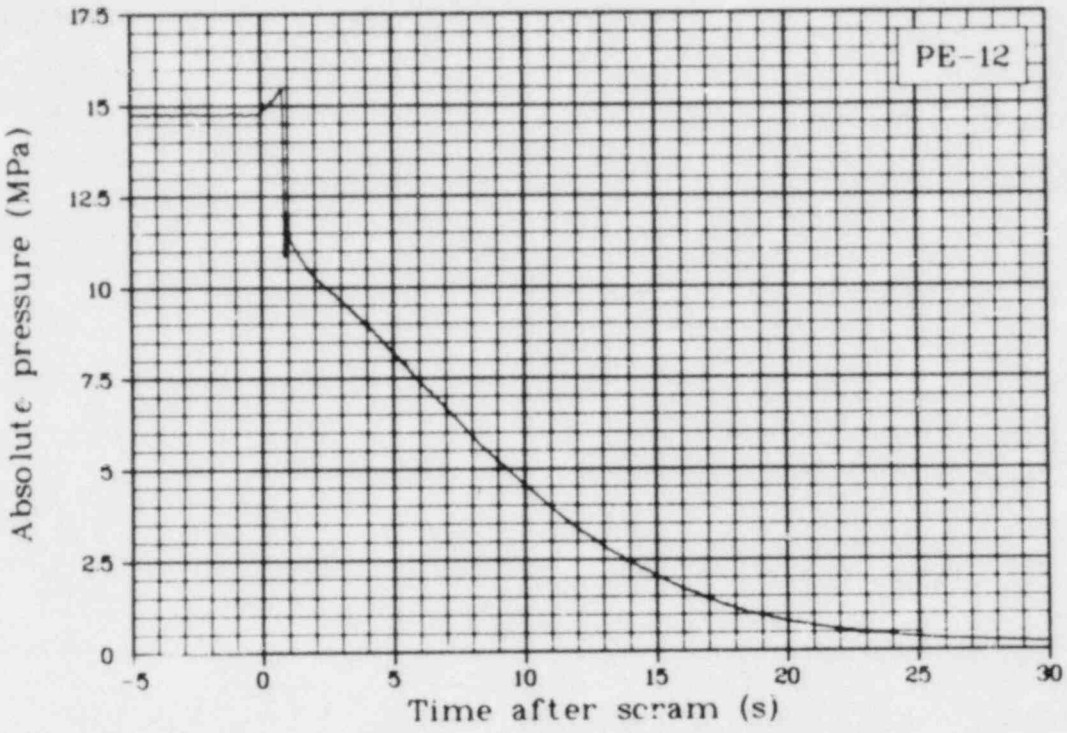

Fig. 90 Absolute pressure in hot leg blowdown spool (PE-12), Test LOC-11B.

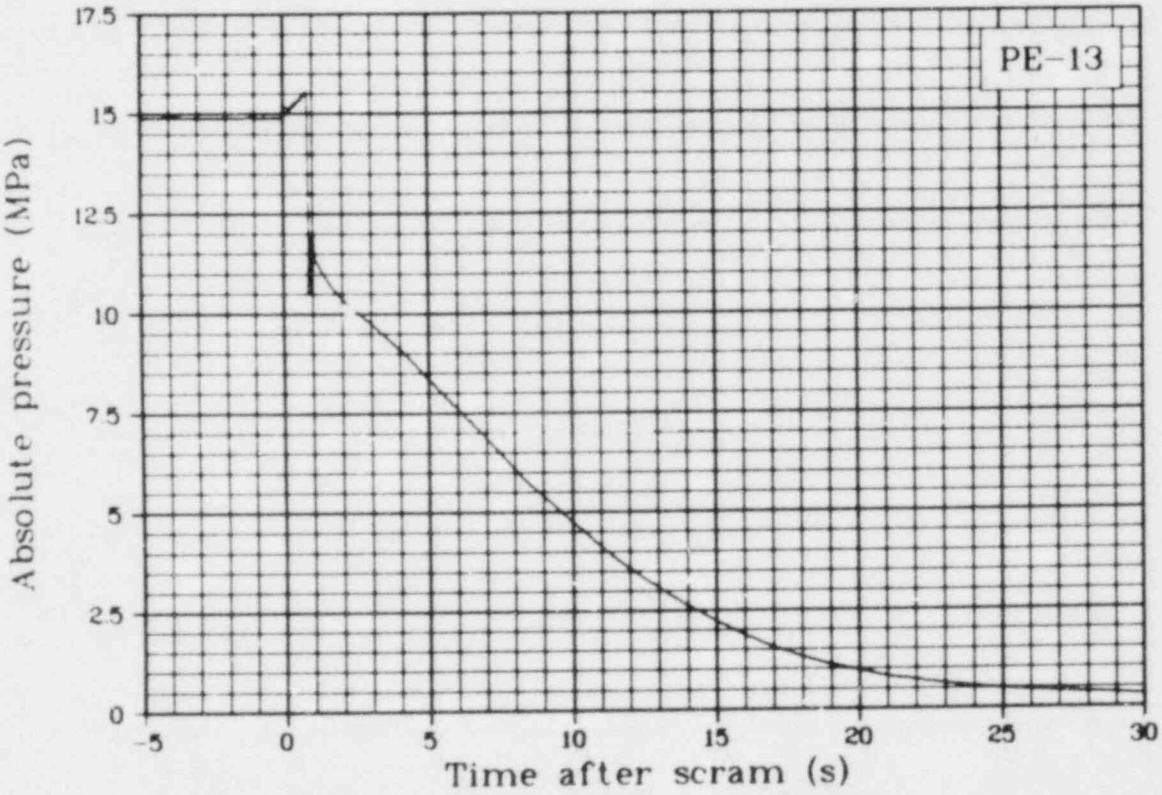

Fig. 91 Absolute pressure in hot leg blowdown spool (PE-13), Test LOC-11B.

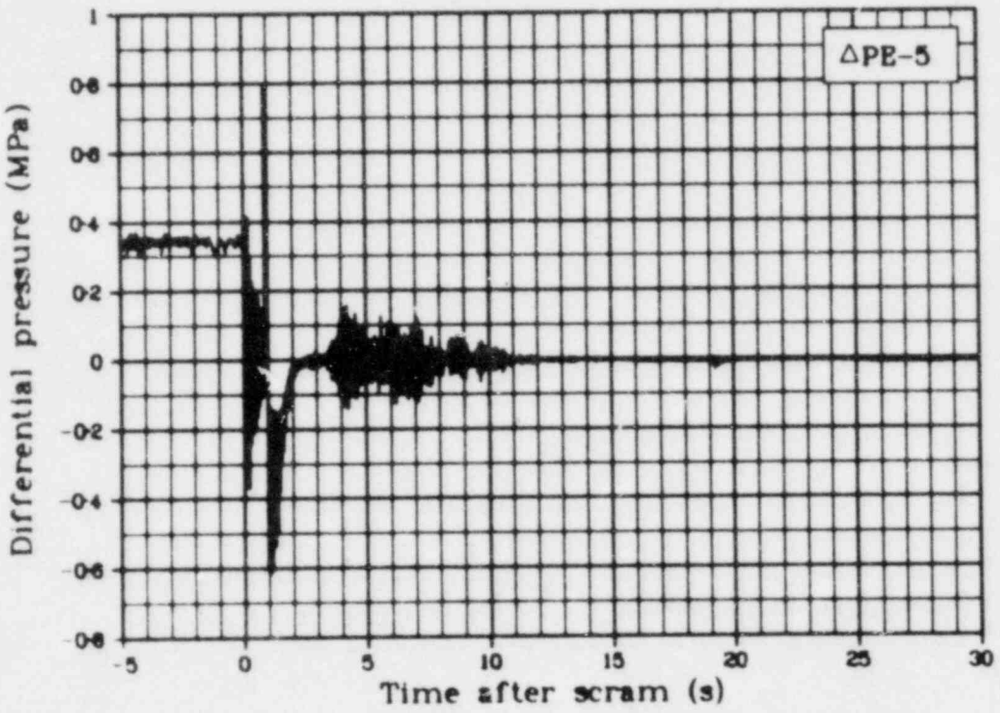

Fig. 92 Differential pressure between blowdown spools (ΔPE-5), Test LOC-11B.

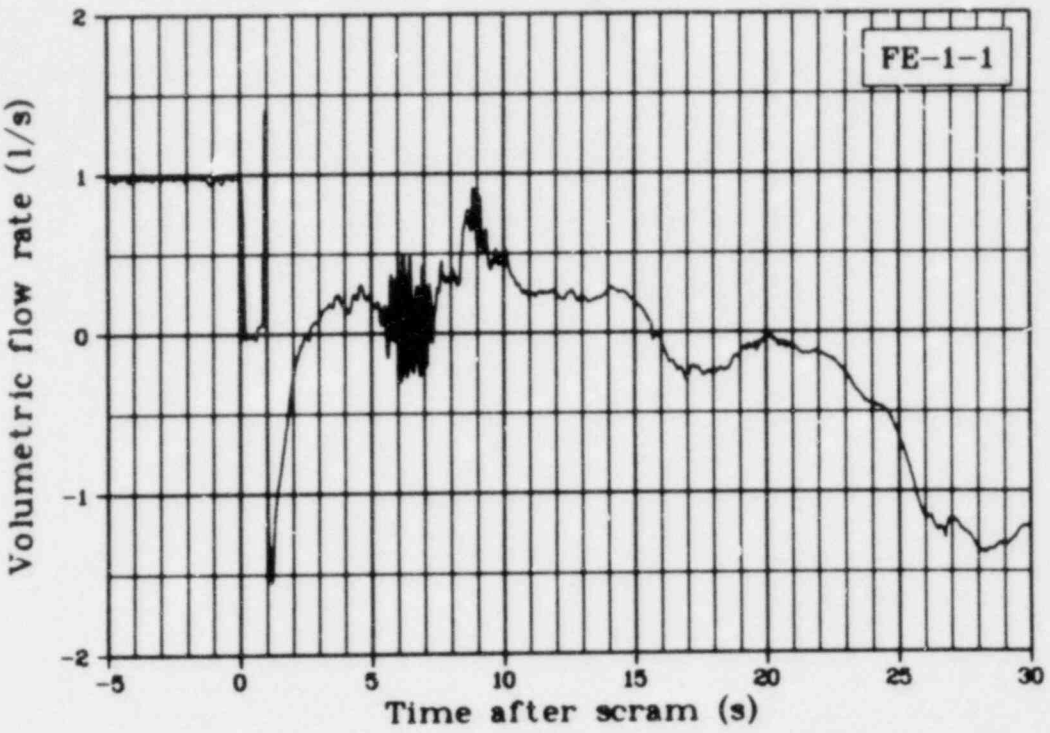

Fig. 93 Volumetric flow rate in fuel Rod 1 upper shroud (FE-1-1), Test LOC-11B.

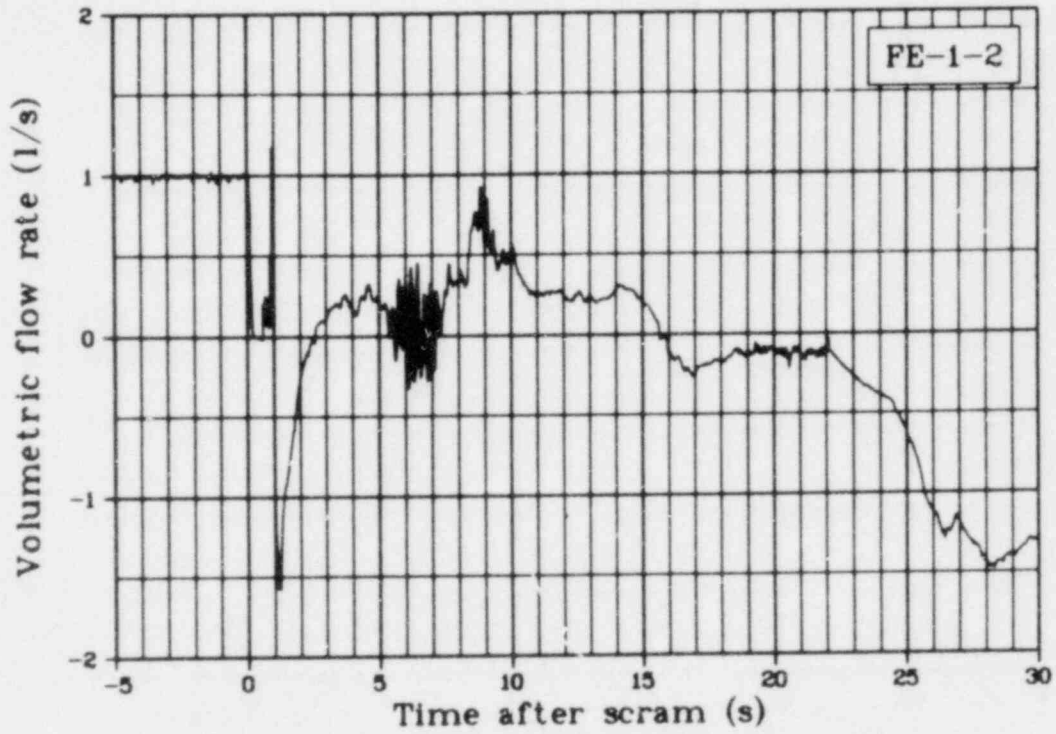

Fig. 94 Volumetric flow rate in fuel Rod 2 upper shroud (FE-1-2), Test LOC-11B.

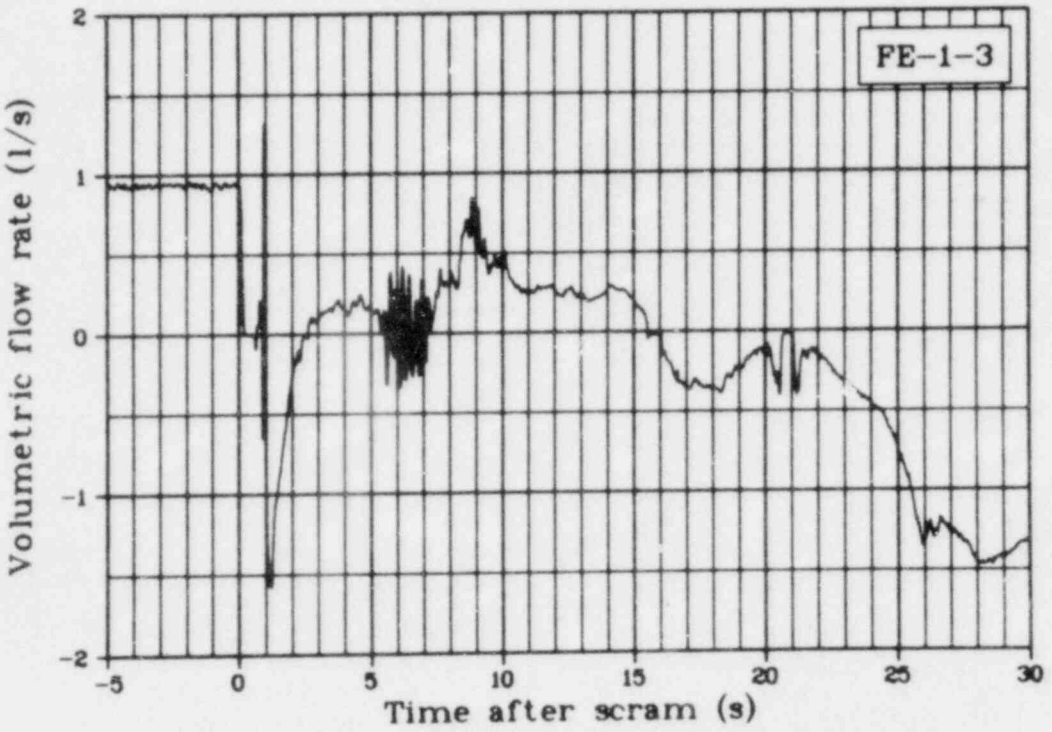

Fig. 95 Volumetric flow rate in fuel Rod 3 upper shroud (FE-1-3), Test LOC-11B.

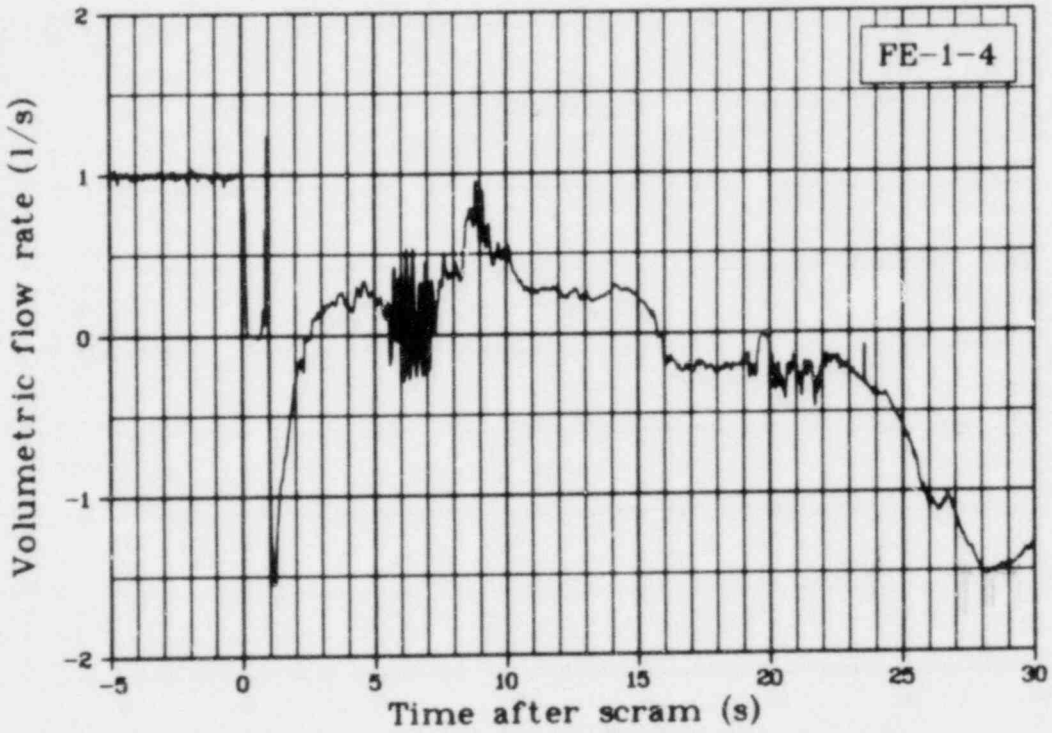

Fig. 96 Volumetric flow rate in fuel Rod 4 upper shroud (FE-1-4), Test LOC-11B.

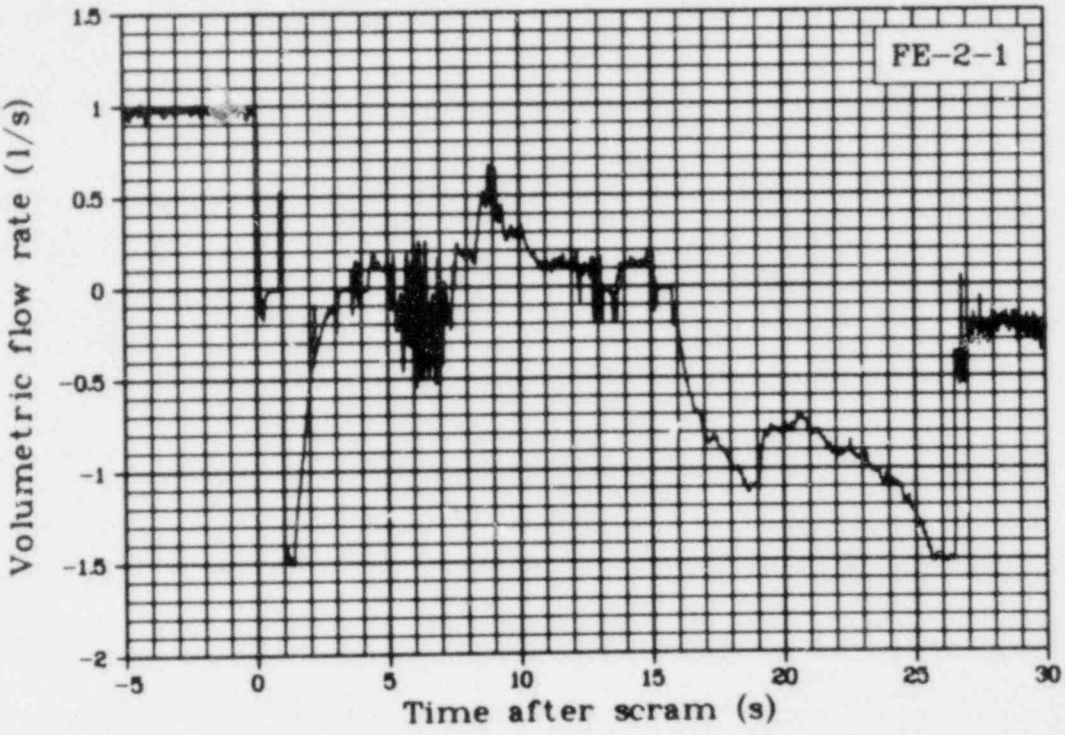

Fig. 97 Volumetric flow rate in fuel Rod 1 lower shroud (FE-2-1), Test LOC-11B.

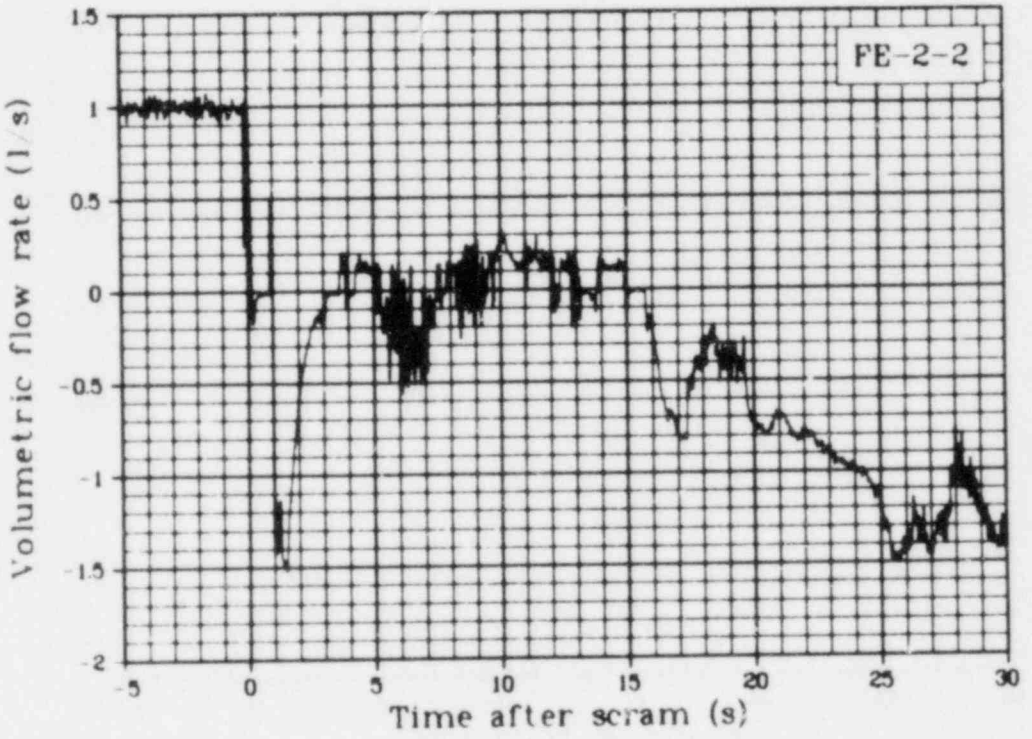

Fig. 98 Volumetric flow rate in fuel Rod 2 lower shroud (FE-2-2), Test LOC-11B.

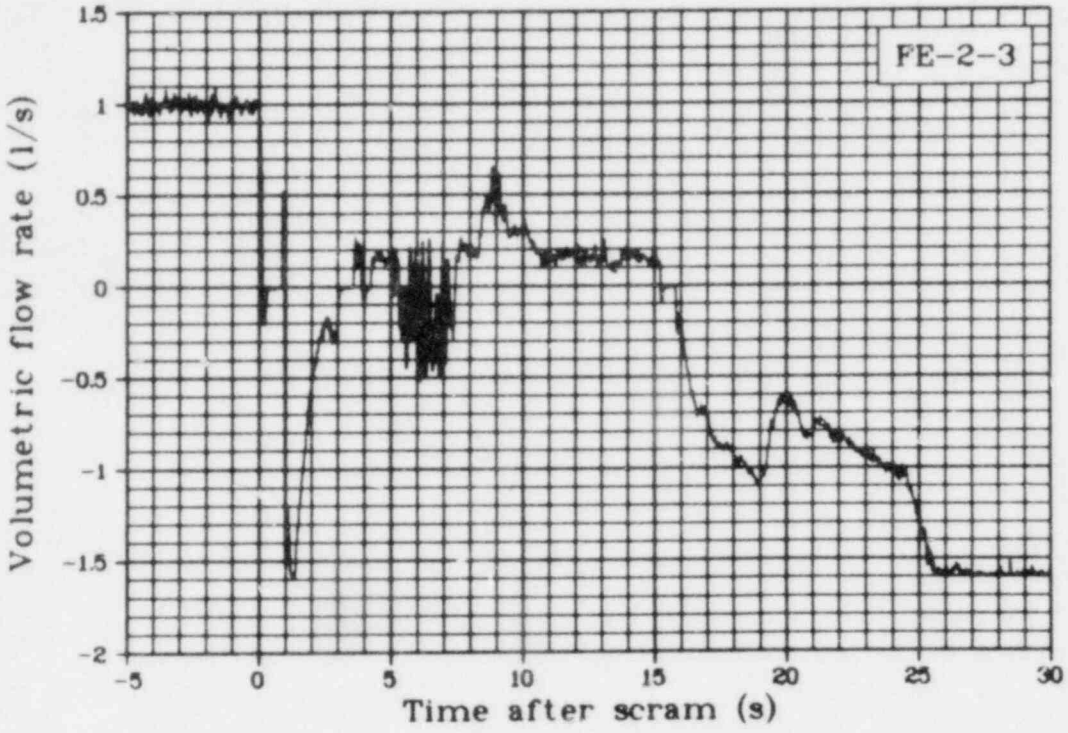

Fig. 99 Volumetric flow rate in fuel Rod 3 lower shroud (FE-2-3), Test LOC-11B.

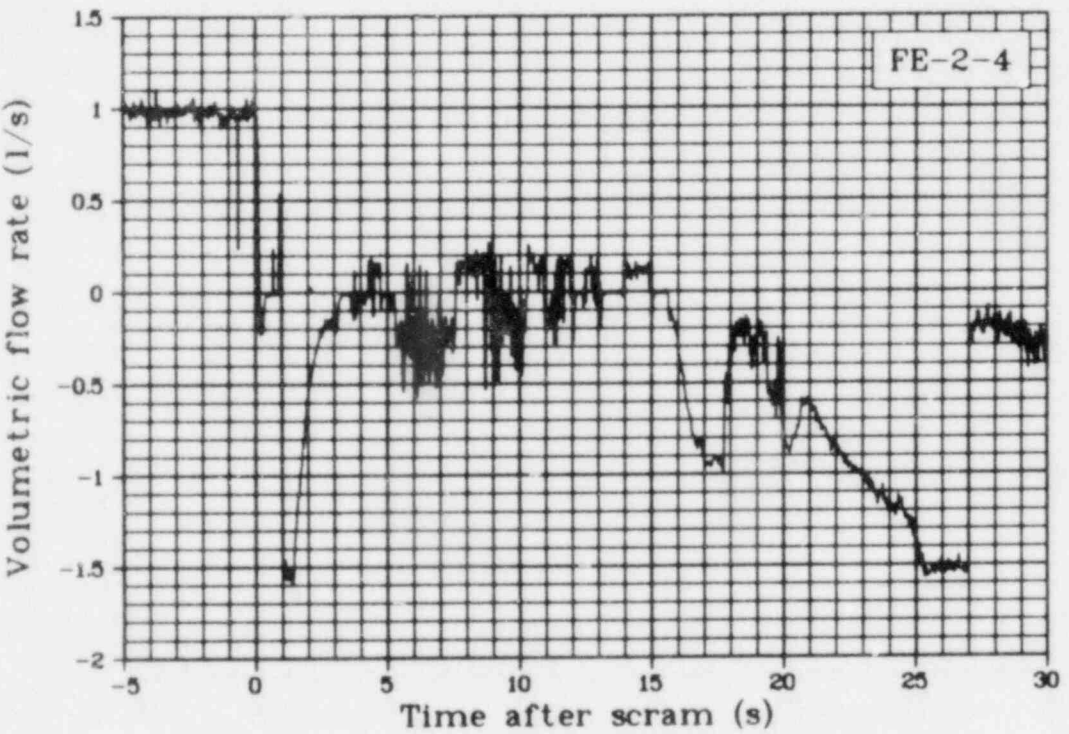

Fig. 100 Volumetric flow rate in fuel Rod 4 lower shroud (FE-2-4), Test LOC-11B.

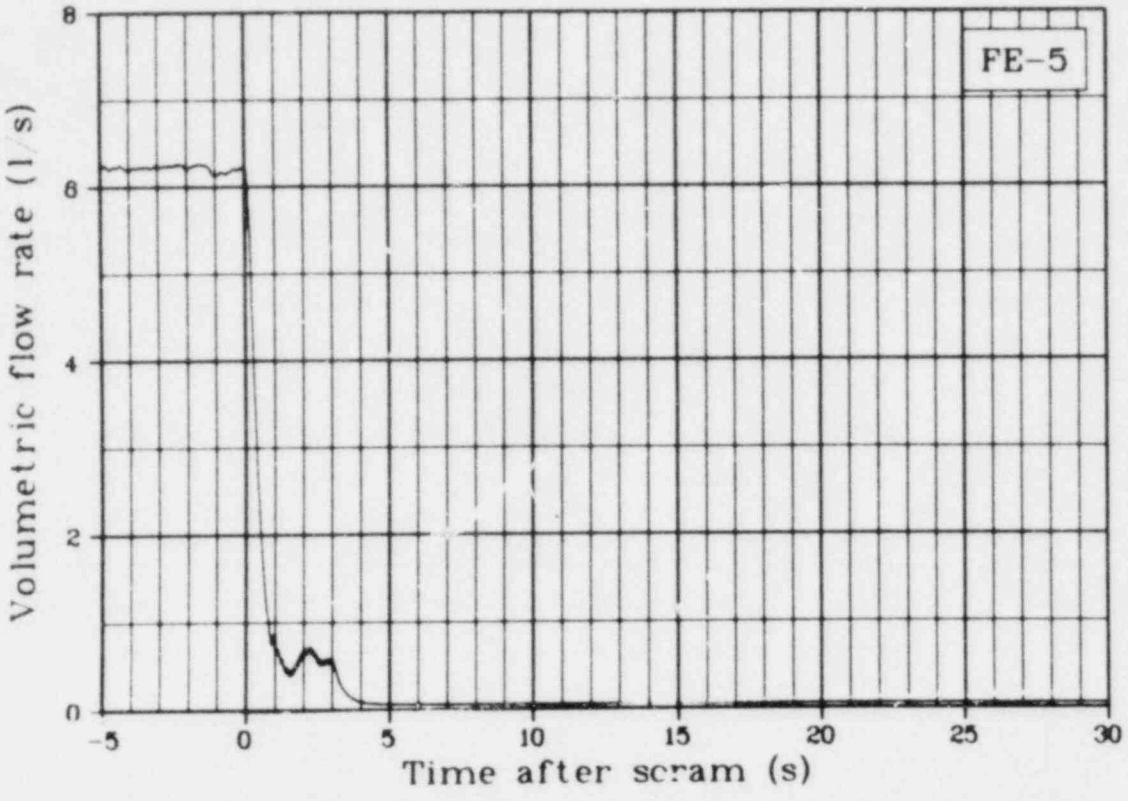

Fig. 101 Volumetric flow rate from flowmeter in inlet spool (FE-5), Test LOC-11B.

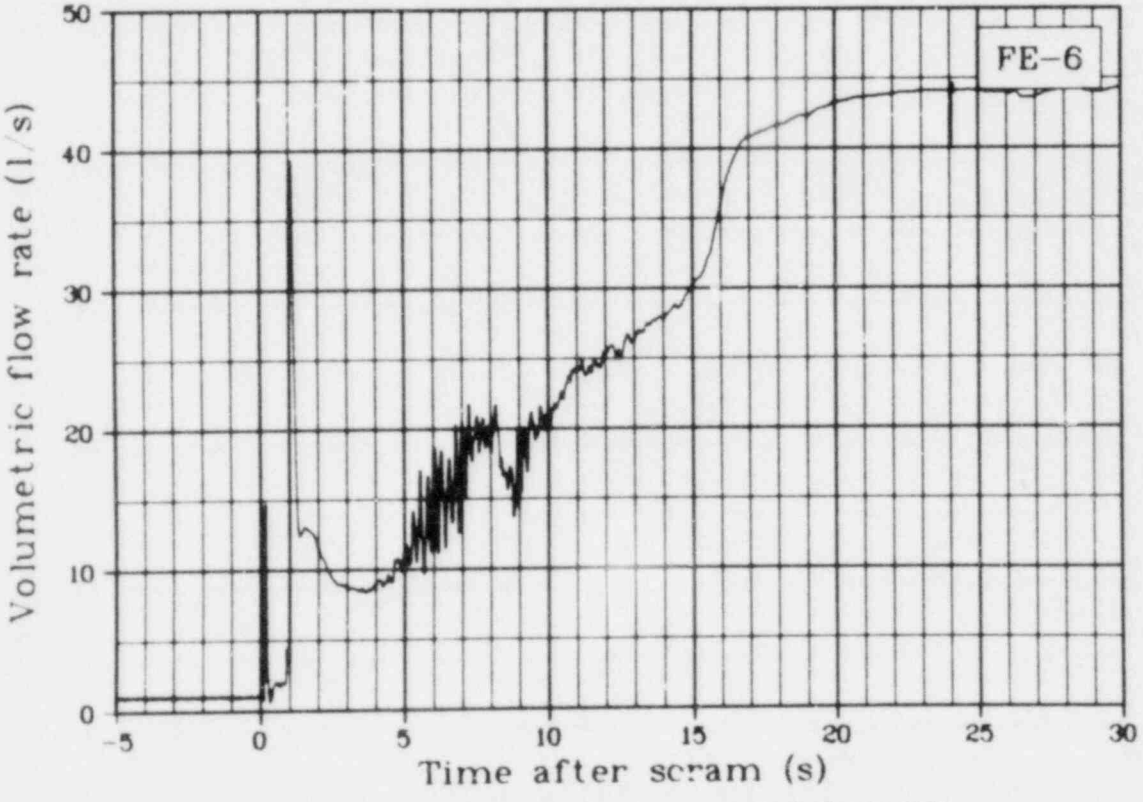

Fig. 102 Volumetric flow rate in cold leg blowdown spool (FE-6), Test LOC-11B.

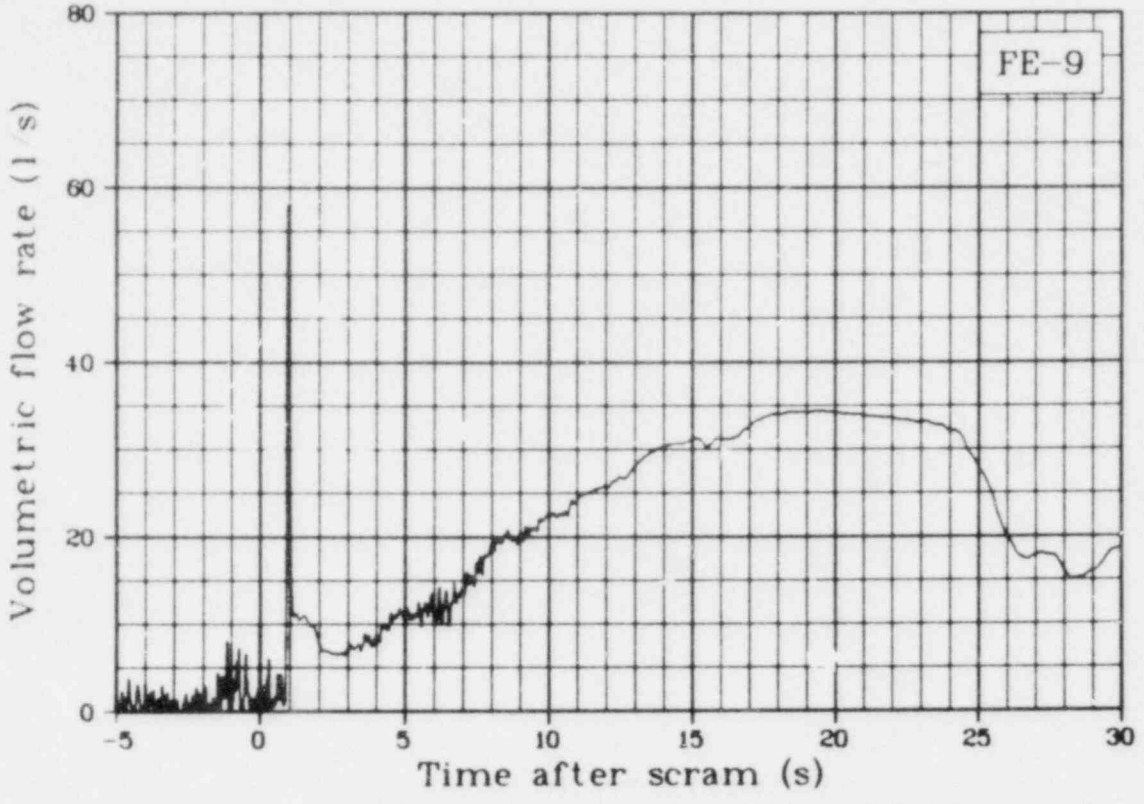

Fig. 103 Volumetric flow rate in hot leg blowdown spool (FE-9), Test LOC-11B.

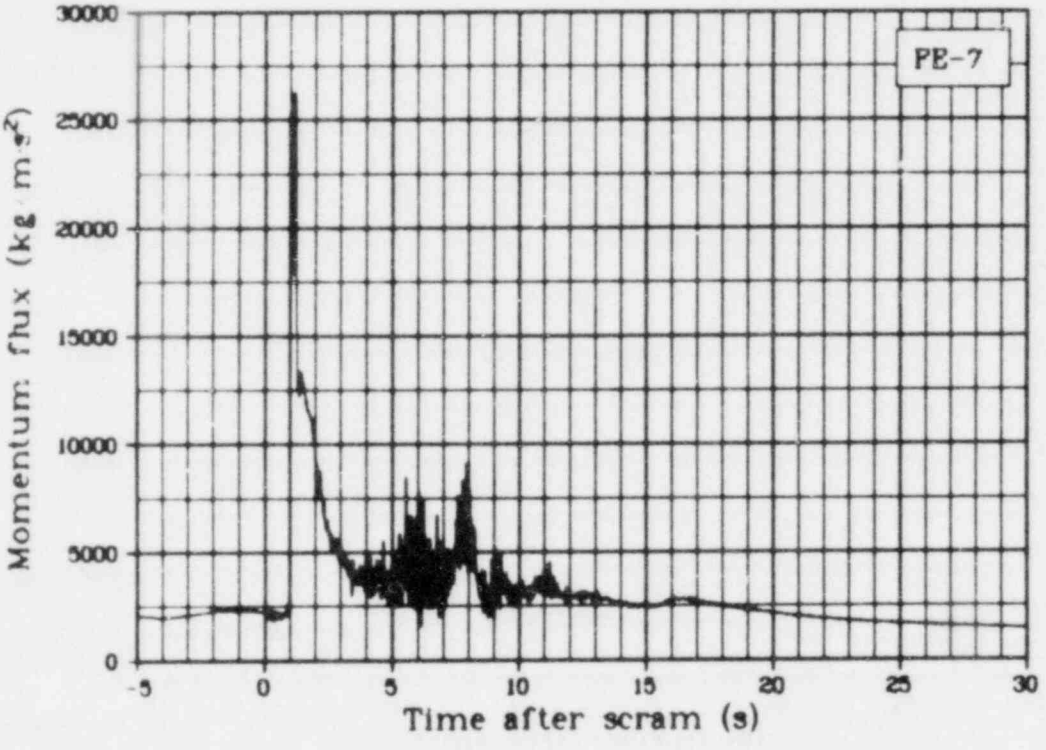

Fig. 104 Momentum flux in cold leg blowdown spool (FE-7), Test LOC-11B.

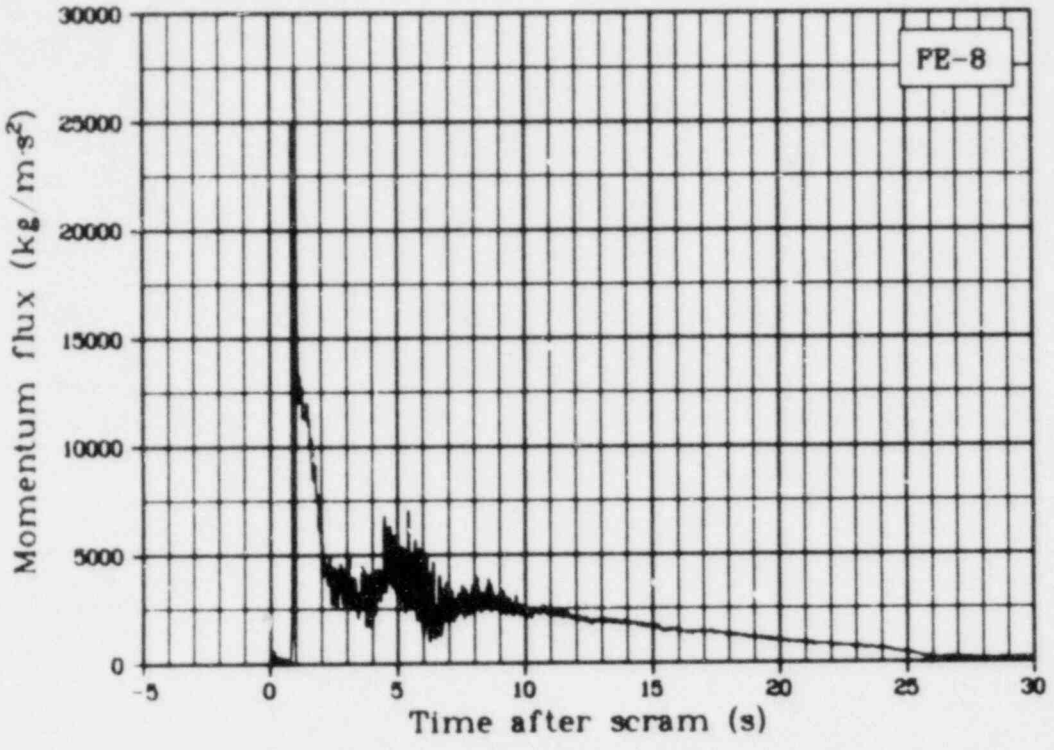

Fig. 105 Momentum flux in hot leg blowdown spool (FE-8), Test LOC-11B.

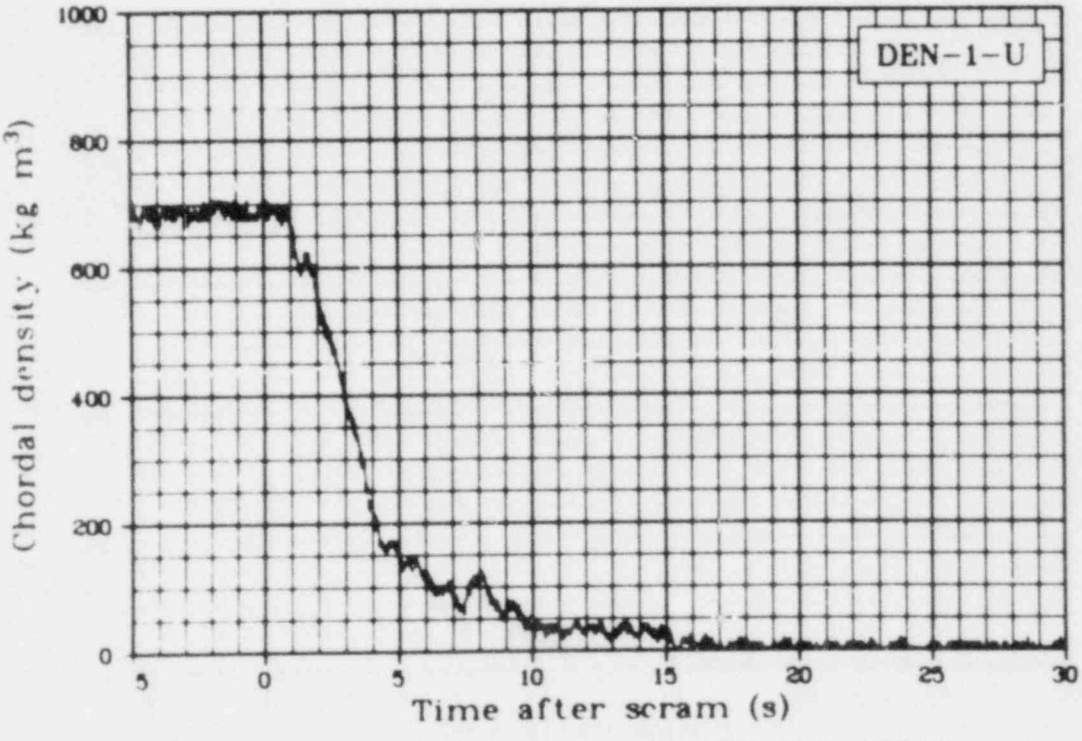

Fig. 106 Chordal density in upper gamma beam in cold leg (DEN-1-U), Test LOC-11B.

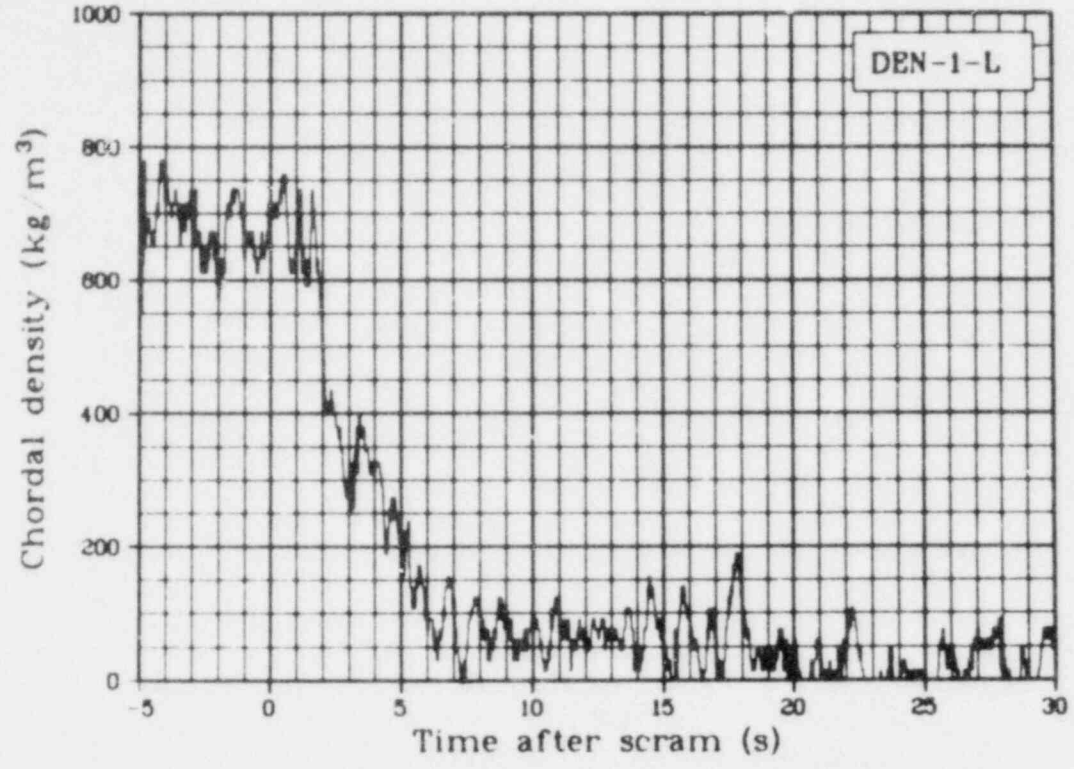

Fig. 107 Chordal density in lower gamma beam in cold leg (DEN-1-L), Test LOC-11B.

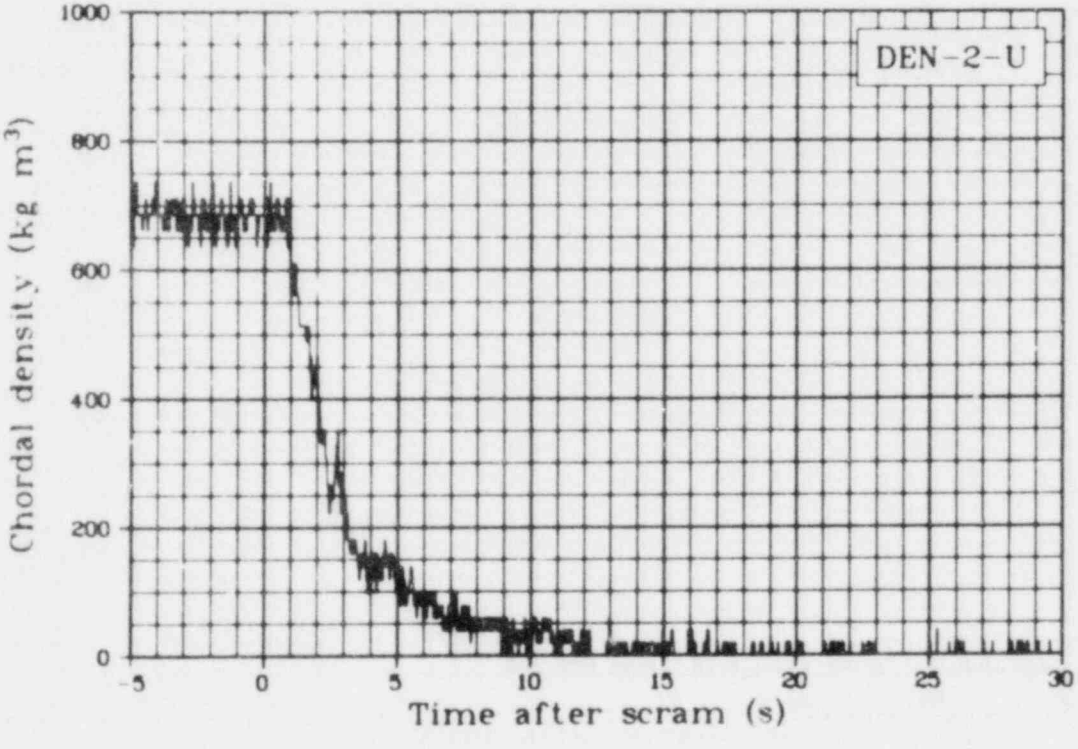

Fig. 108 Chordal density in upper gamma beam in hot leg blowdown spool (DEN-2-U), Test LOC-11B.

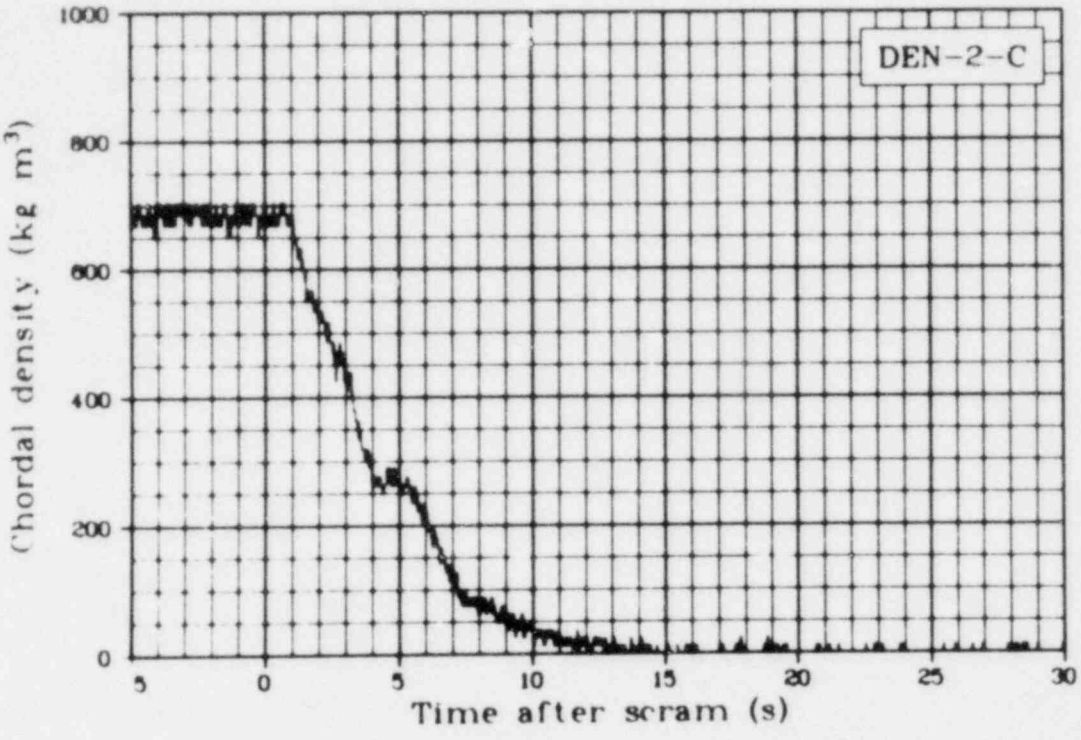

Fig. 109 Chordal density in center gamma beam in hot leg blowdown spool (DEN-2-C), Test LOC-11B.

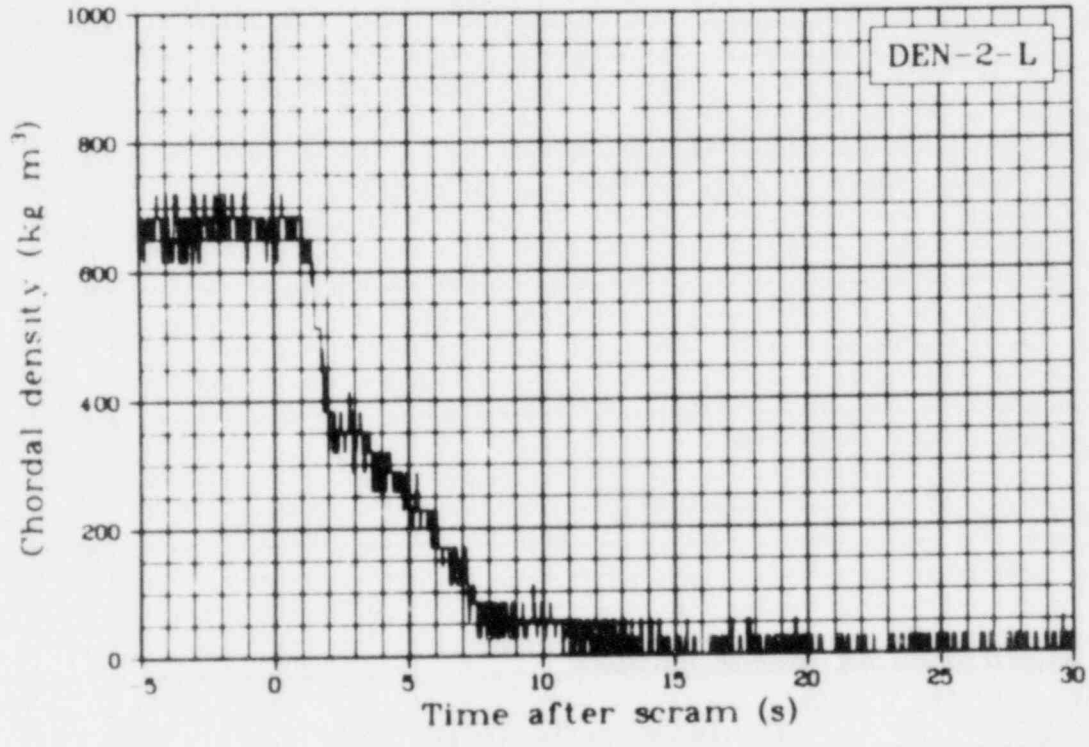

Fig. 110 Chordal density in lower gamma beam in hot leg blowdown spool (DEN-2-L), Test LOC-11B.

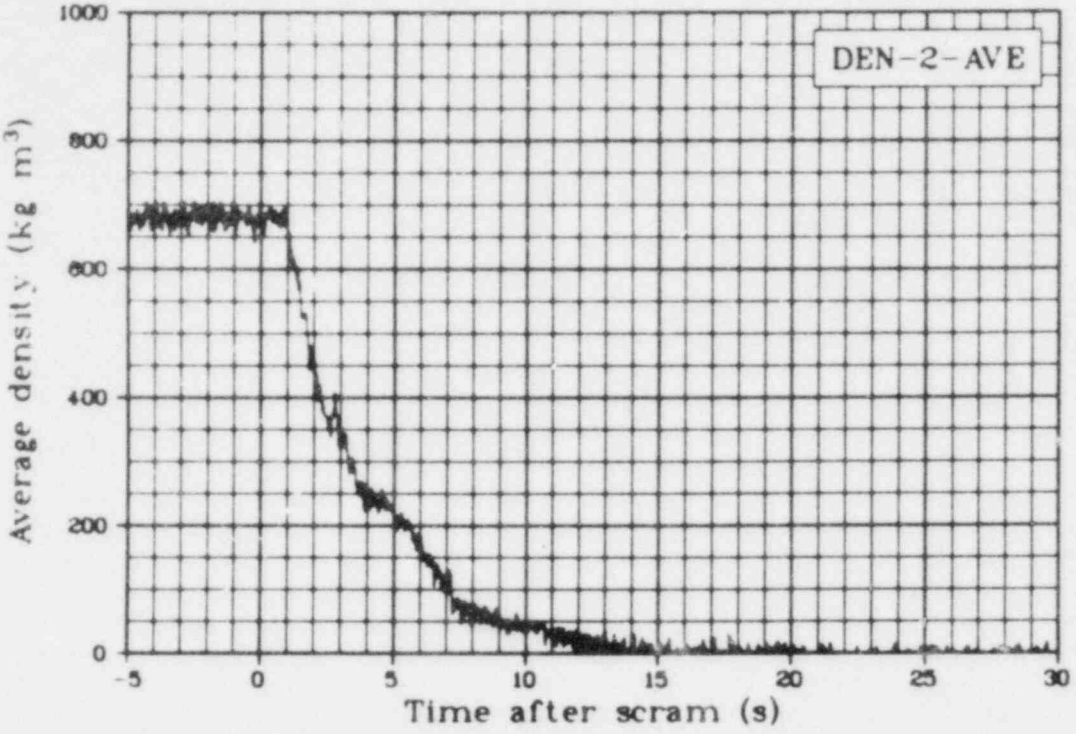

Fig. 111 Average density of hot leg blowdown spool (DEN-2-AVE), Test LOC-11B.

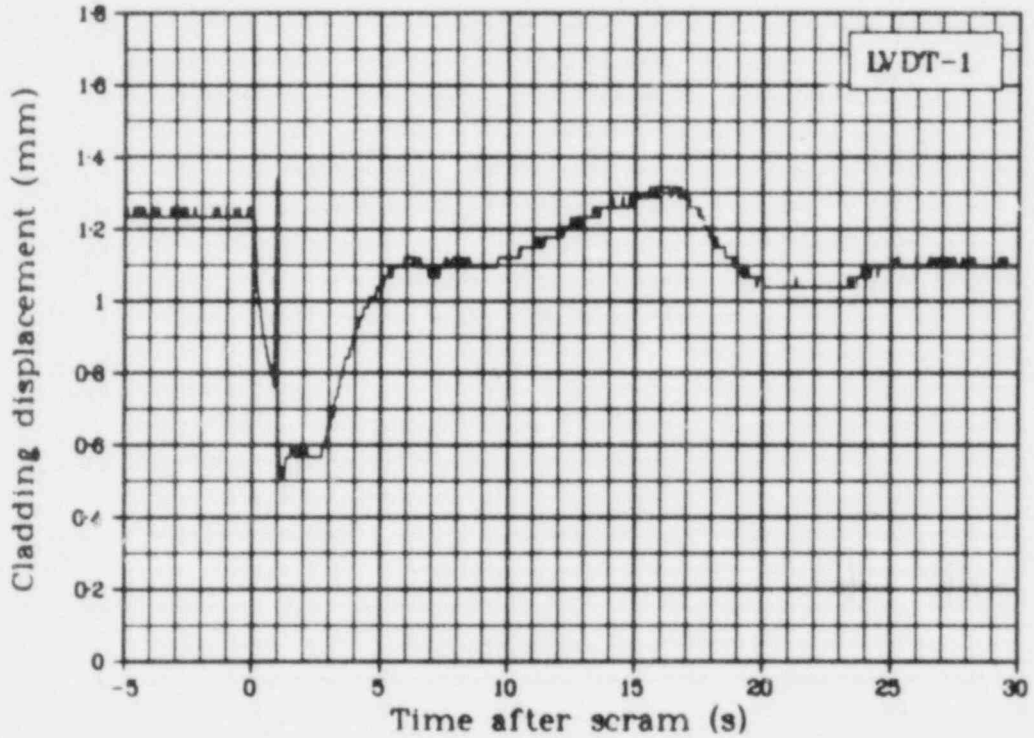

Fig. 112 Cladding displacement of Rod 1 (LVDT-1), Test LOC-11B.

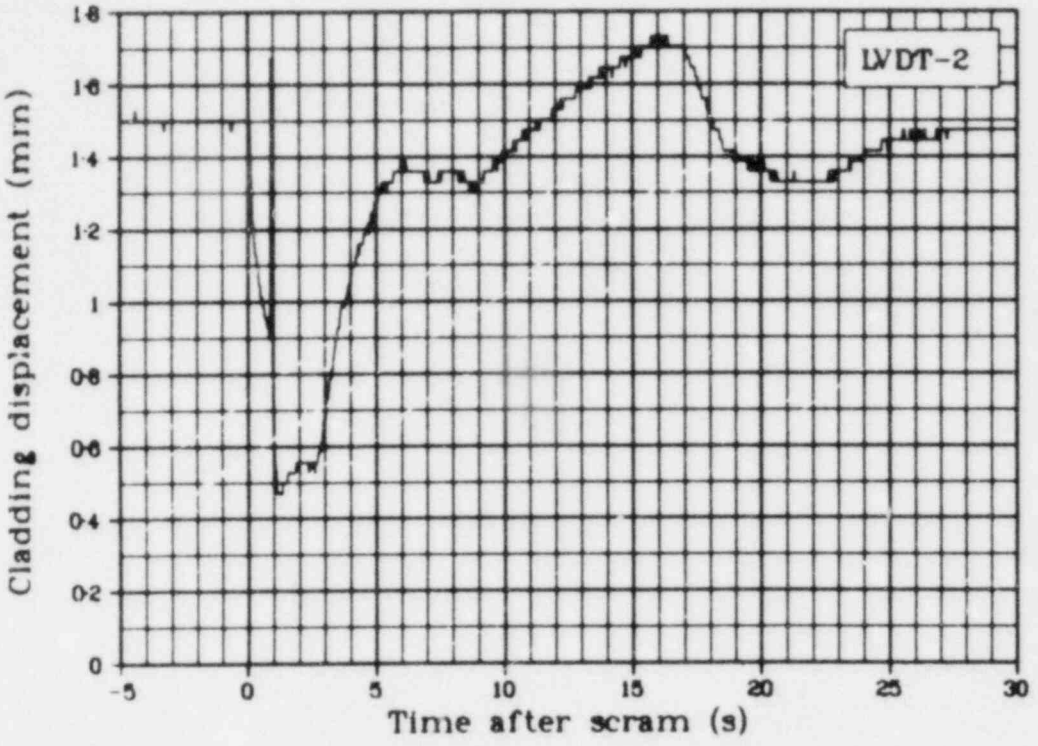

Fig. 113 Cladding displacement of Rod 2 (LVDT-2), Test LOC-11B.

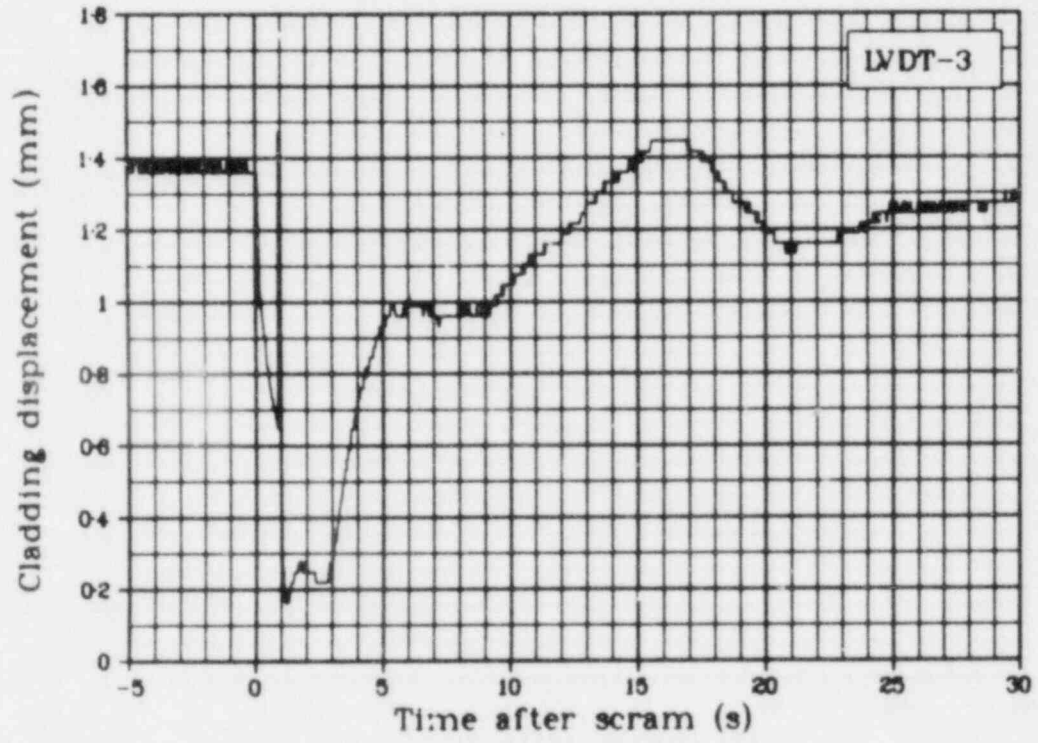

Fig. 114 Cladding displacement of Rod 3 (LVDT-3), Test LOC-11B.

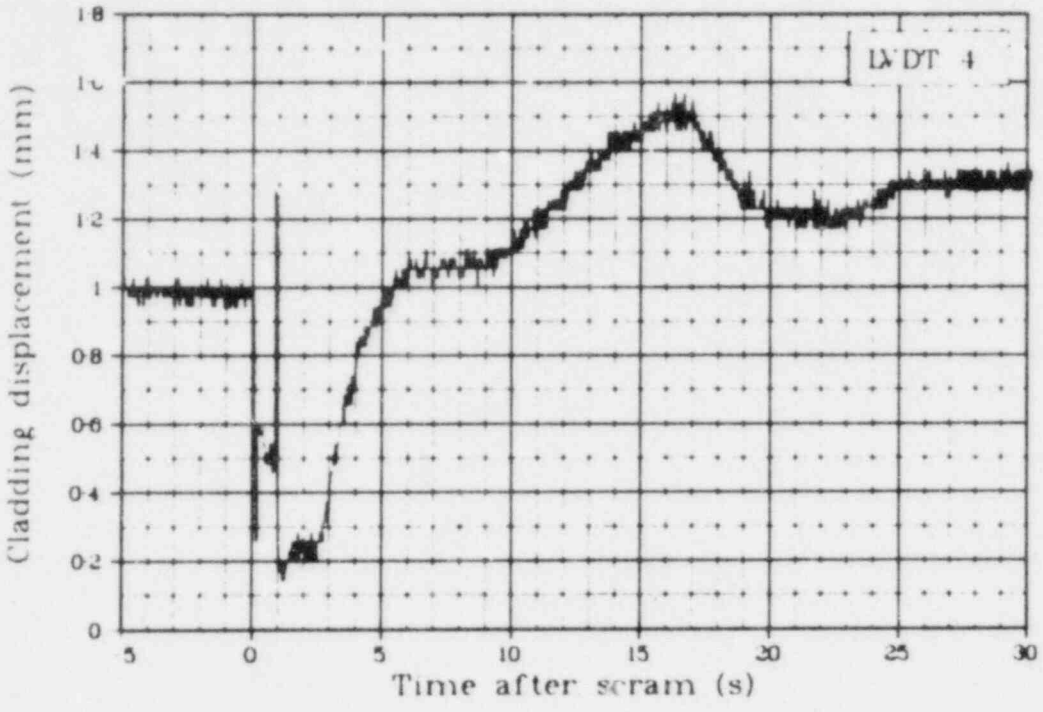

Fig. 115 Cladding displacement of Rod 4 (LVDT-4), Test LOC-11B.

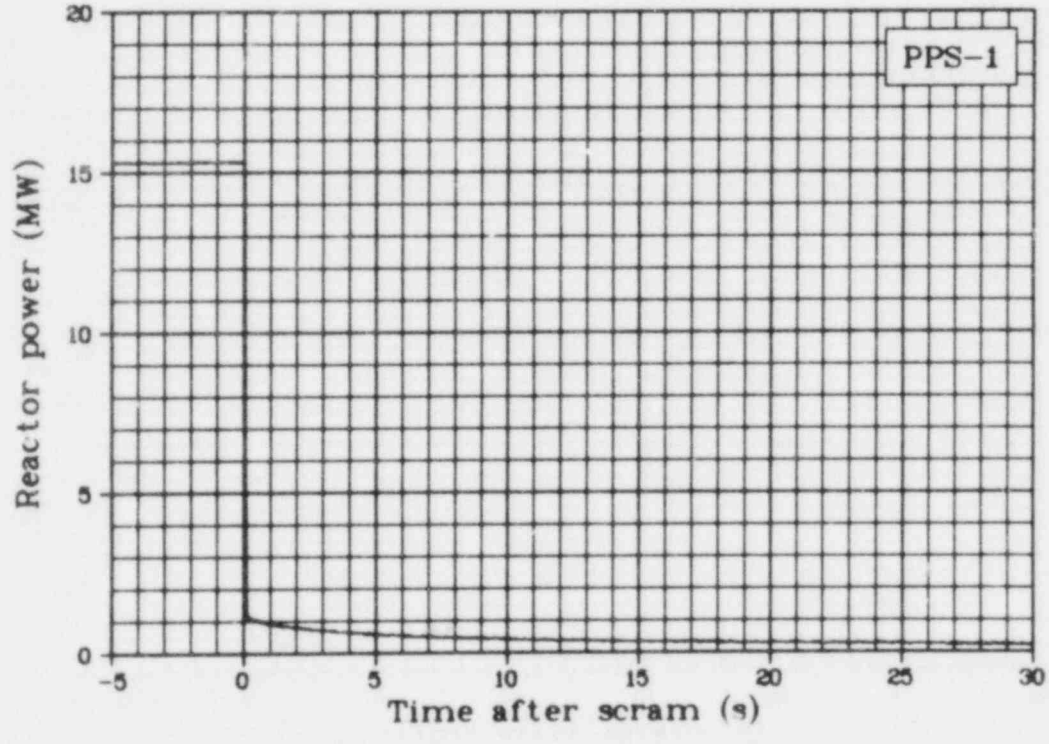

Fig. 116 Reactor power from plant protective system (PPS-1), Test LOC-11B.

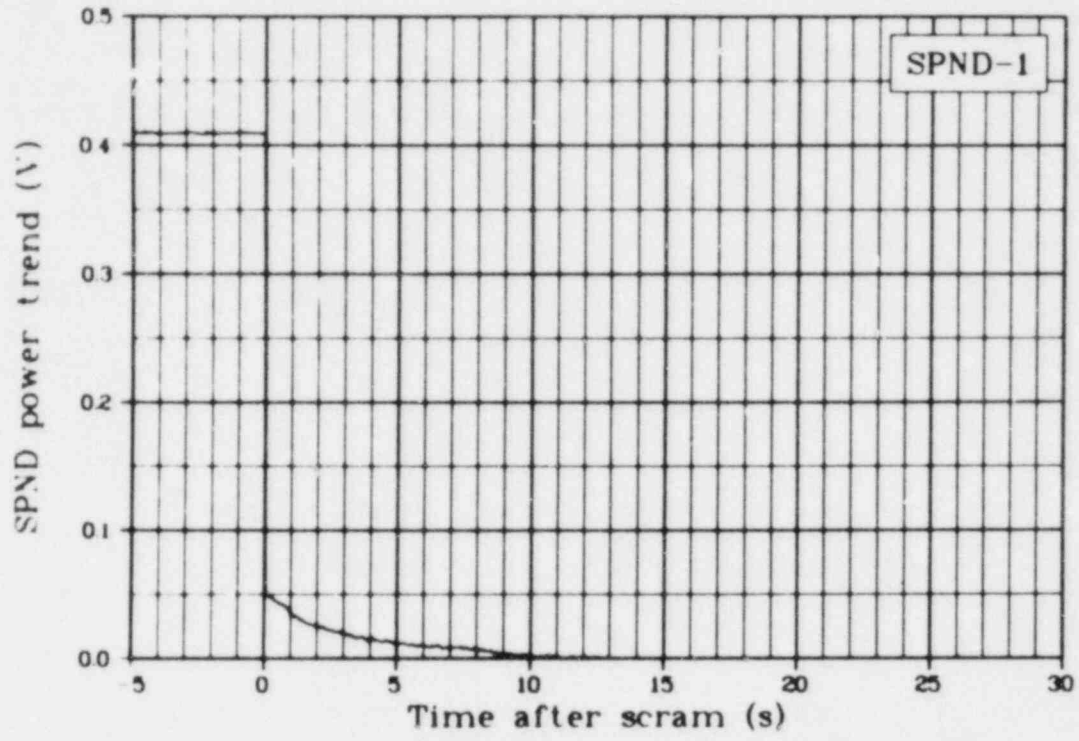

Fig. 117 SPND power trend 0.76 m above fuel stack bottom (SPND-1), Test LOC-11B.

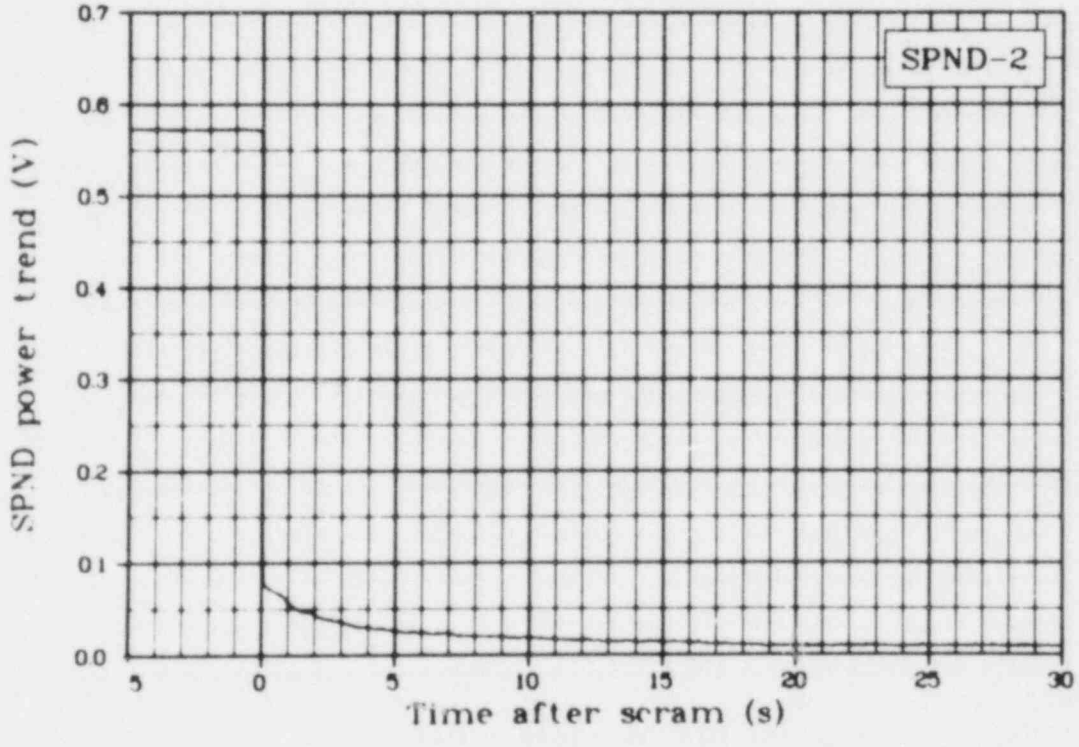

Fig. 118 SPND power trend 0.61 m above fuel stack bottom (SPND-2), Test LOC-11B.

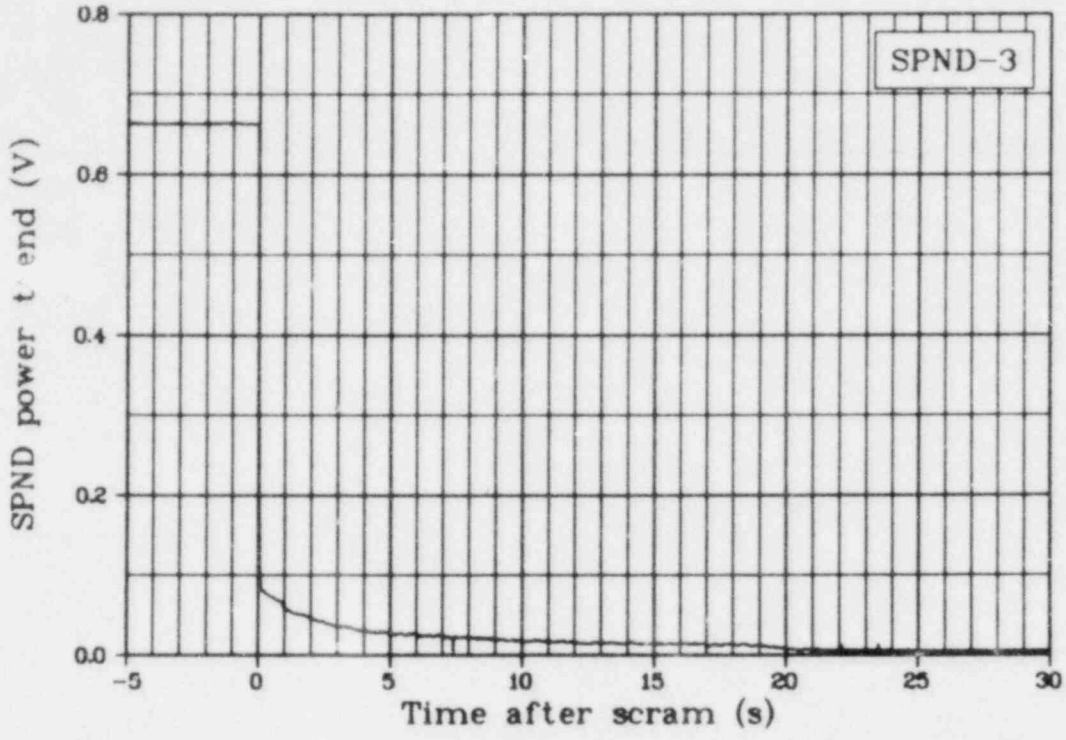

Fig. 119 SPND power trend 0.46 m above fuel stack bottom (SPND-3), Test LOC-11B.

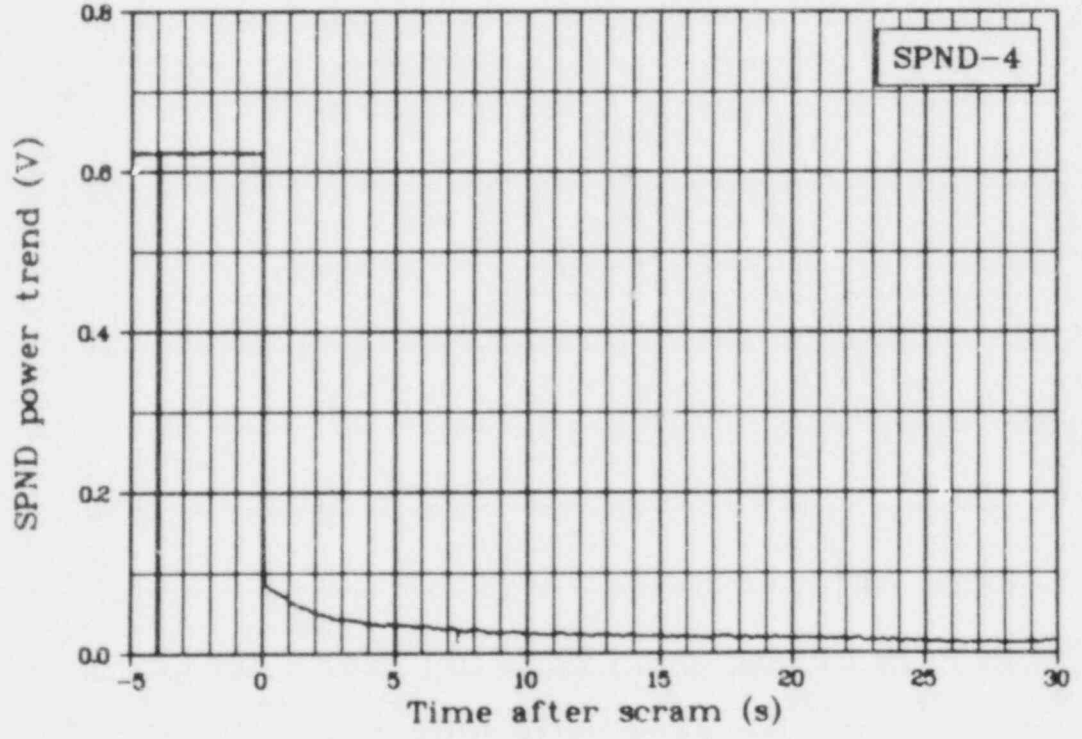

Fig. 120 SPND power trend 0.30 m above fuel stack bottom (SPND-4), Test LOC-11B.

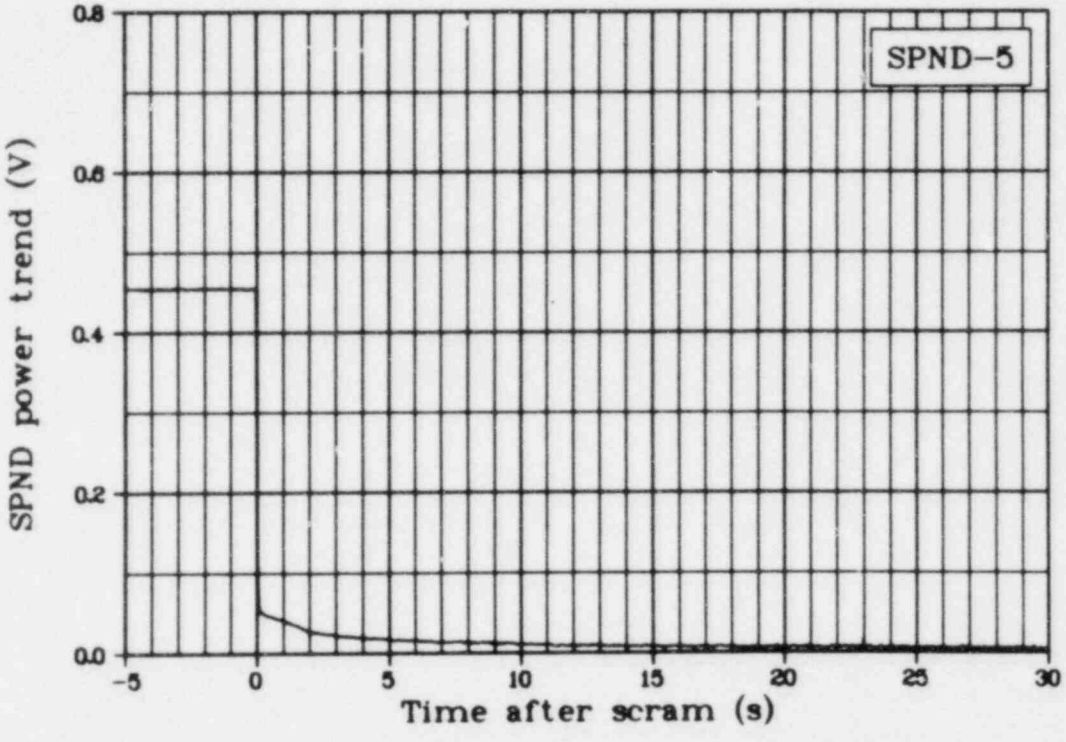

Fig. 121 SPND power trend 0.15 m above fuel stack bottom (SPND-5), Test LOC-11B.

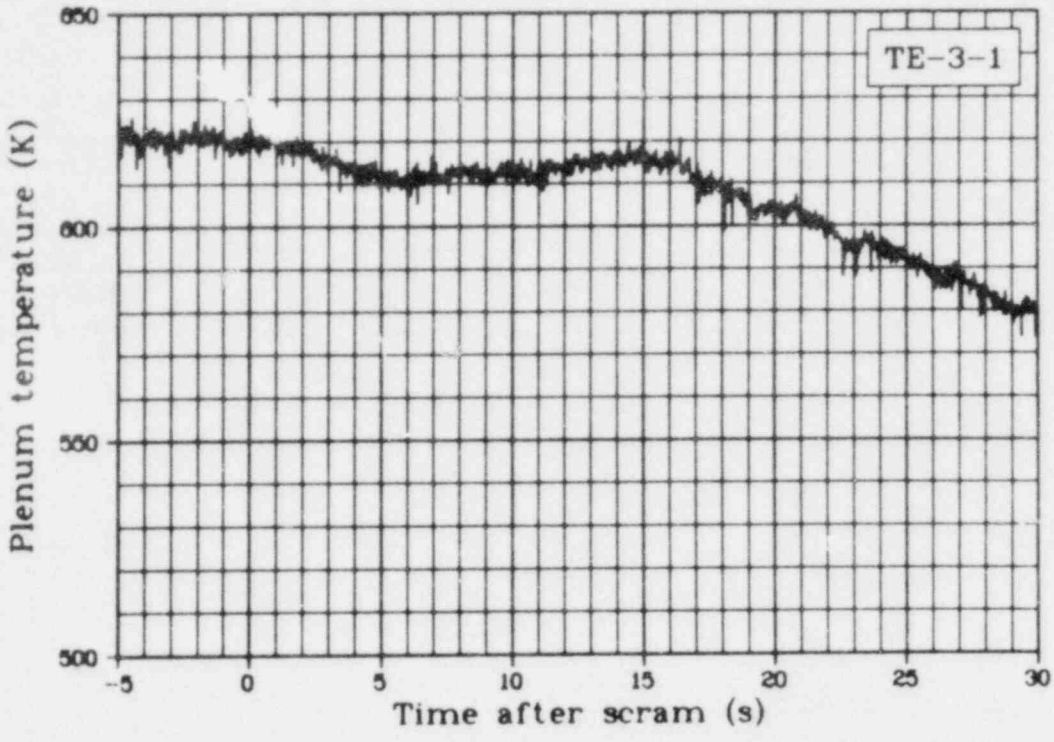

Fig. 122 Plenum temperature in fuel Rod 1 (TE-3-1), Test LOC-11C.

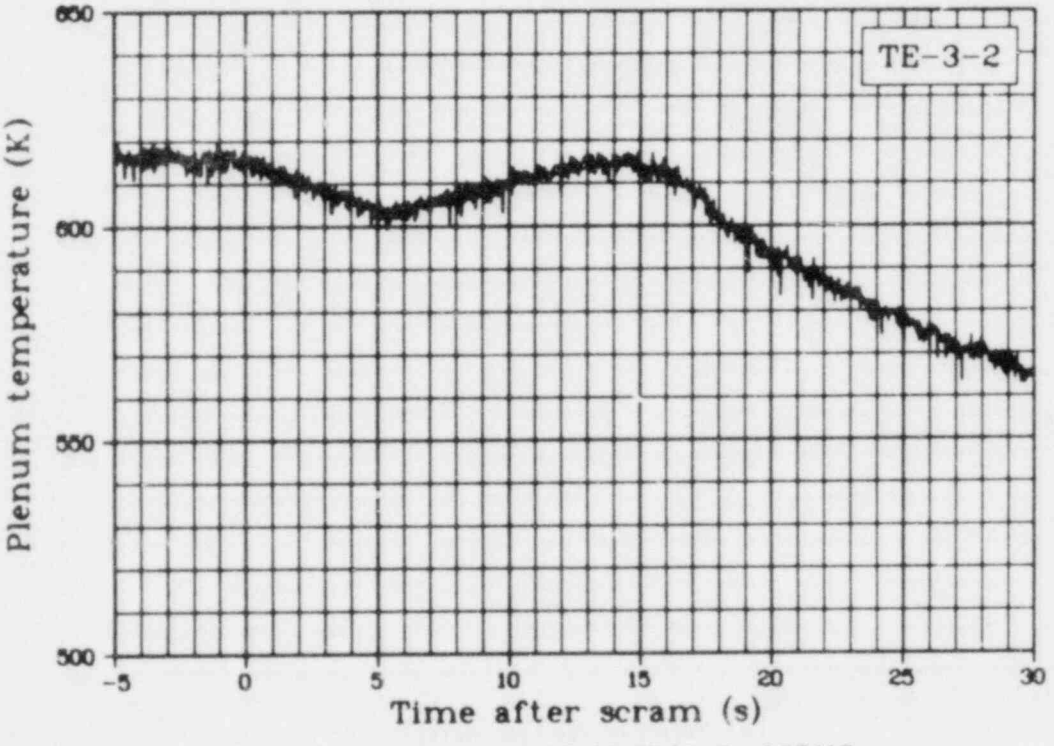

Fig. 123 Plenum temperature in fuel Rod 2 (TE-3-2), Test LOC-11C.

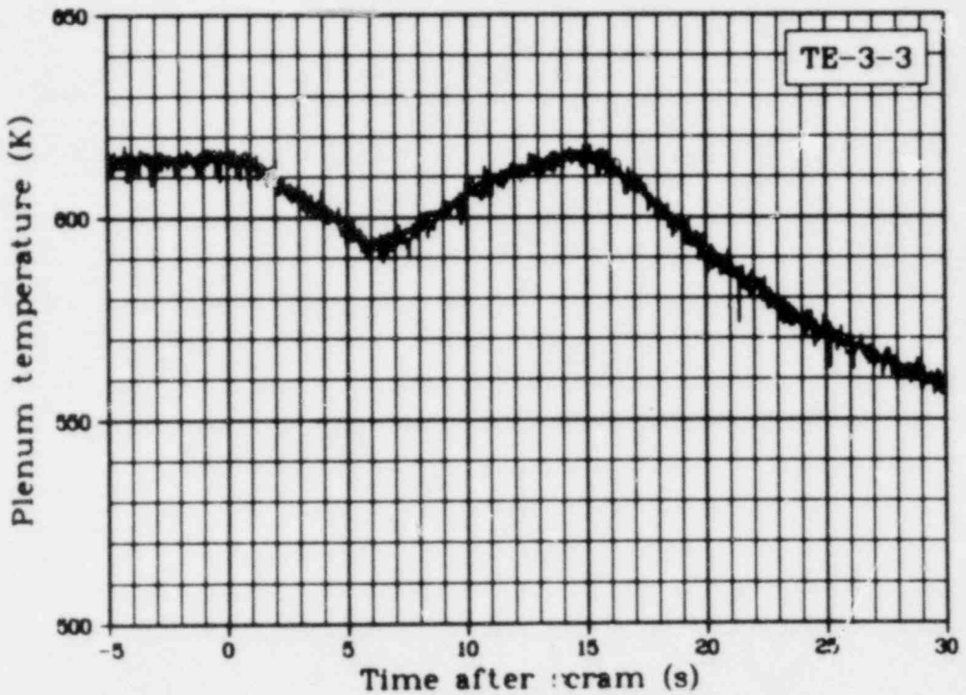

Fig. 124 Plenum temperature in fuel Rod 3 (TE-3-3), Test LOC-11C.

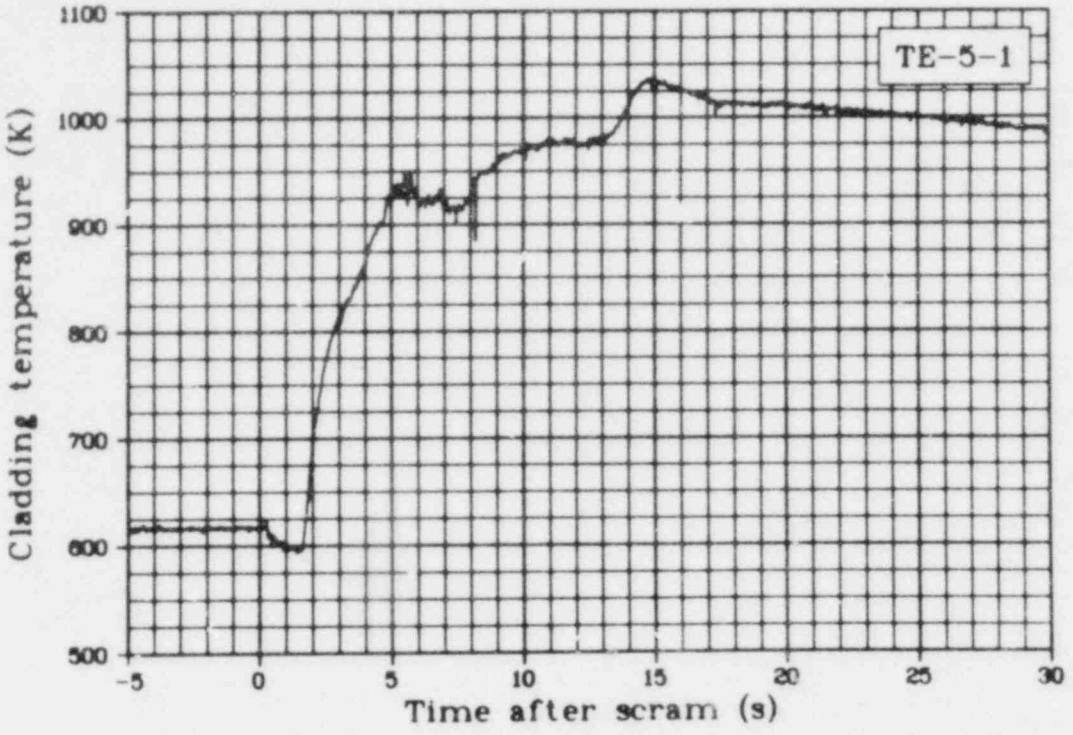

Fig. 125 Cladding temperature Rod 1, 0.53 m above bottom of fuel stack (TE-5-1), Test LOC-11C.

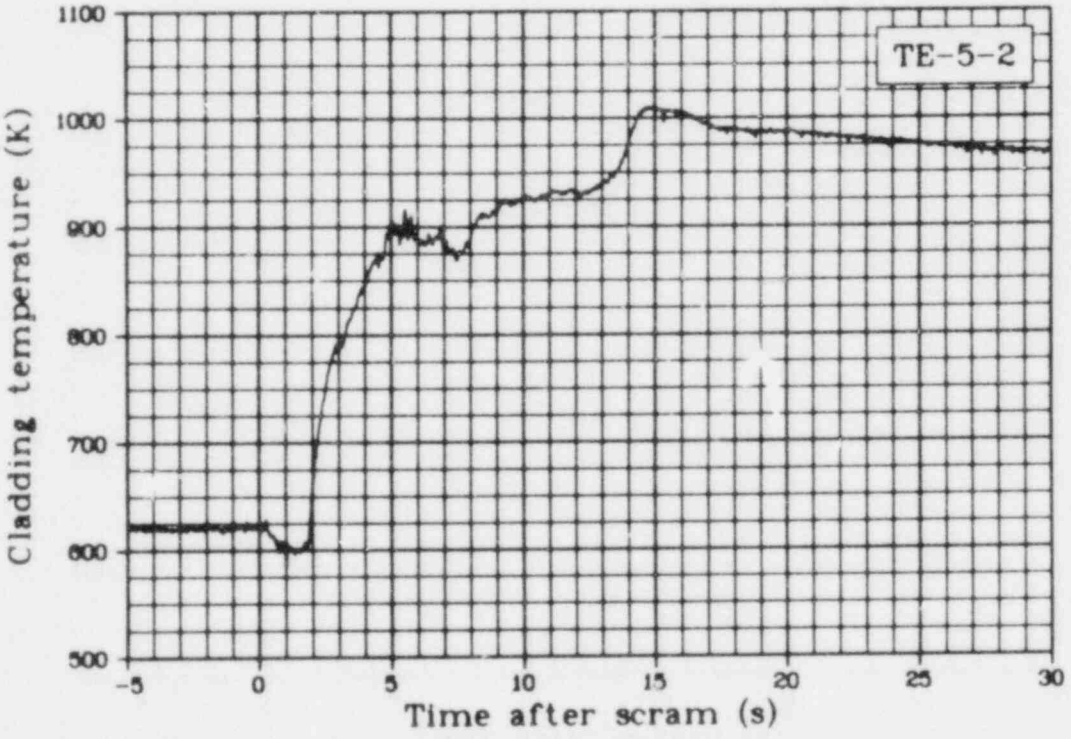

Fig. 126 Cladding temperature Rod 2, 0.53 m above bottom of fuel stack (TE-5-2), Test LOC-11C.

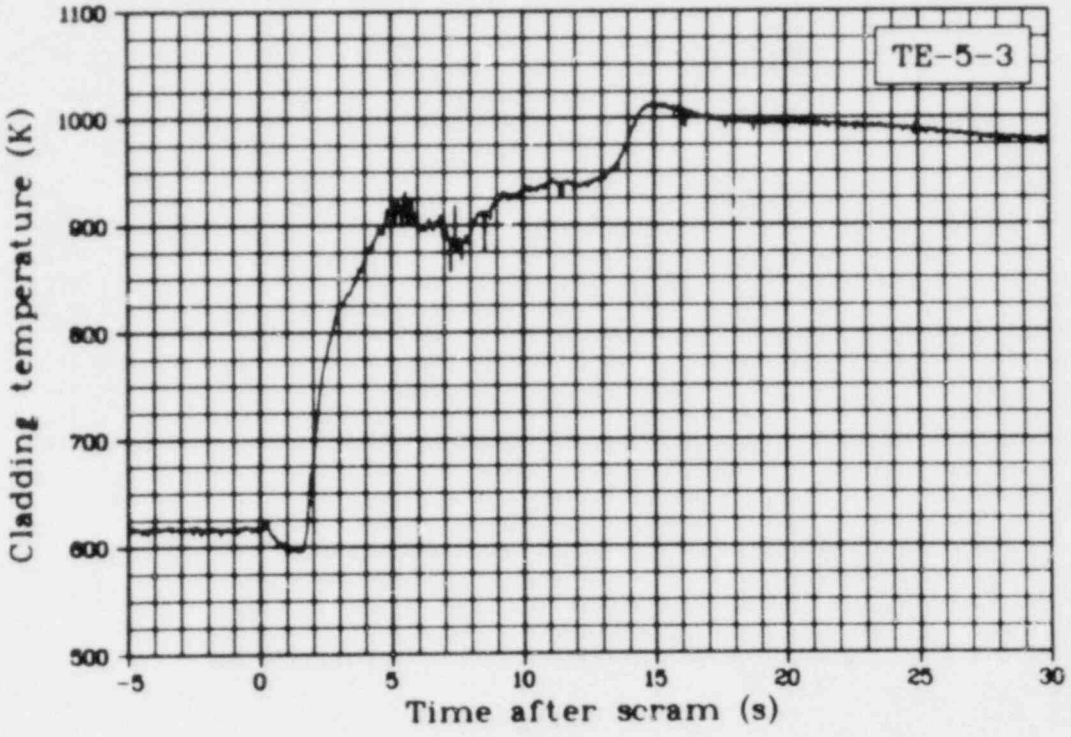

Fig. 127 Cladding temperature Rod 3, 0.53 m above bottom of fuel stack (TE-5-3), Test LOC-11C.

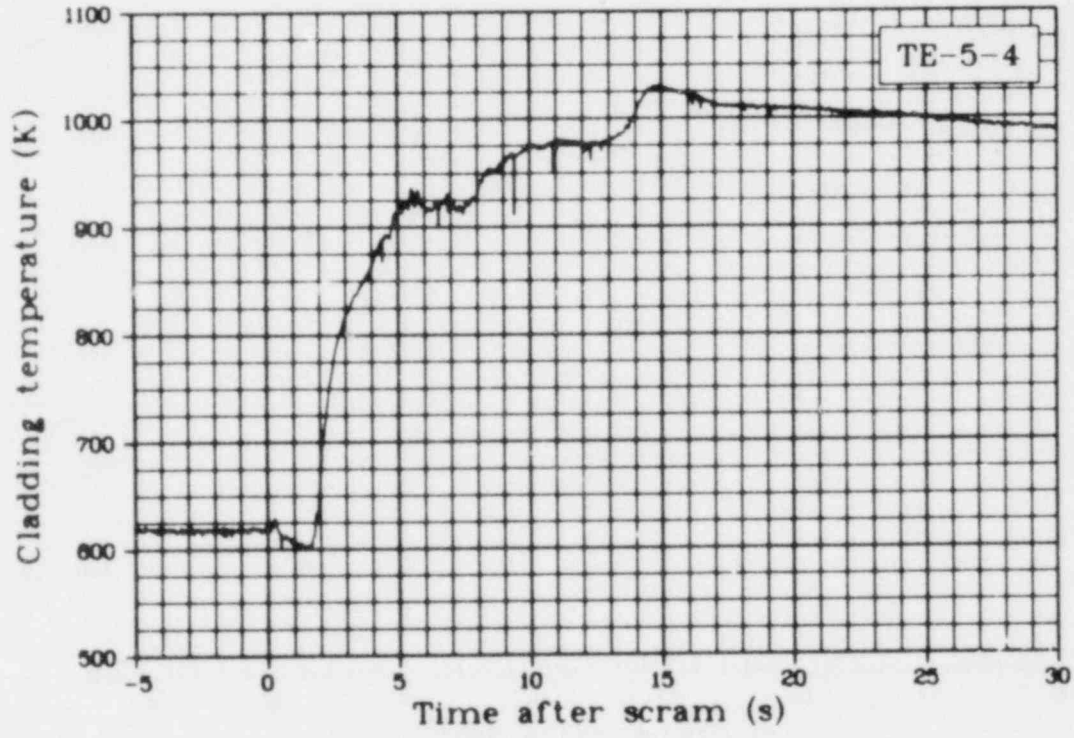

Fig. 128 Cladding temperature Rod 4, 0.53 m above bottom of fuel stack (TE-5-4), Test LOC-11C.

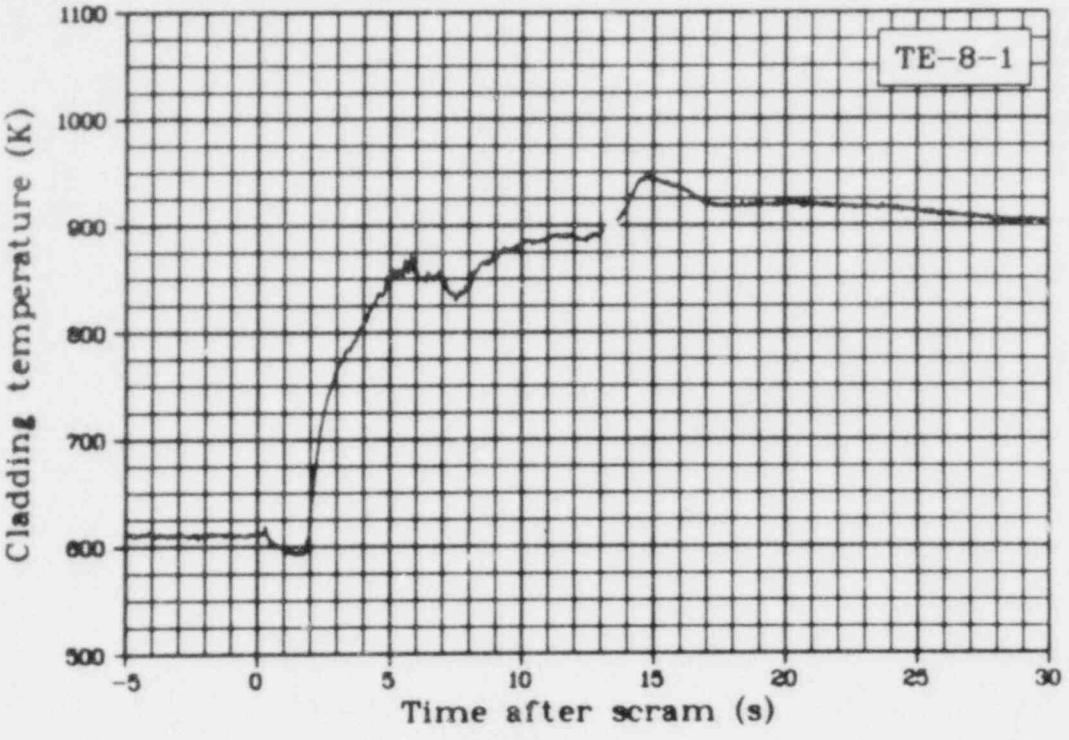

Fig. 129 Cladding temperature Rod 1, 0.61 m above bottom of fuel stack (TE-8-1), Test LOC-11C.

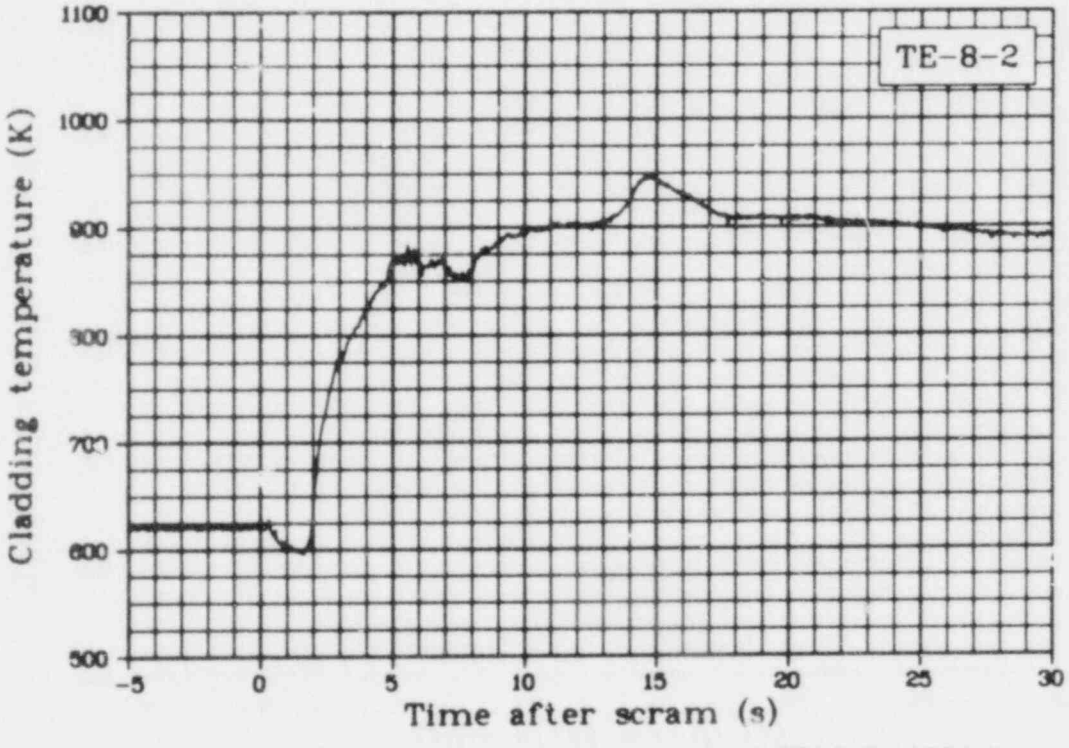

Fig. 130 Cladding temperature Rod 2, 0.61 m above bottom of fuel stack (TE-8-2), Test LOC-11C.

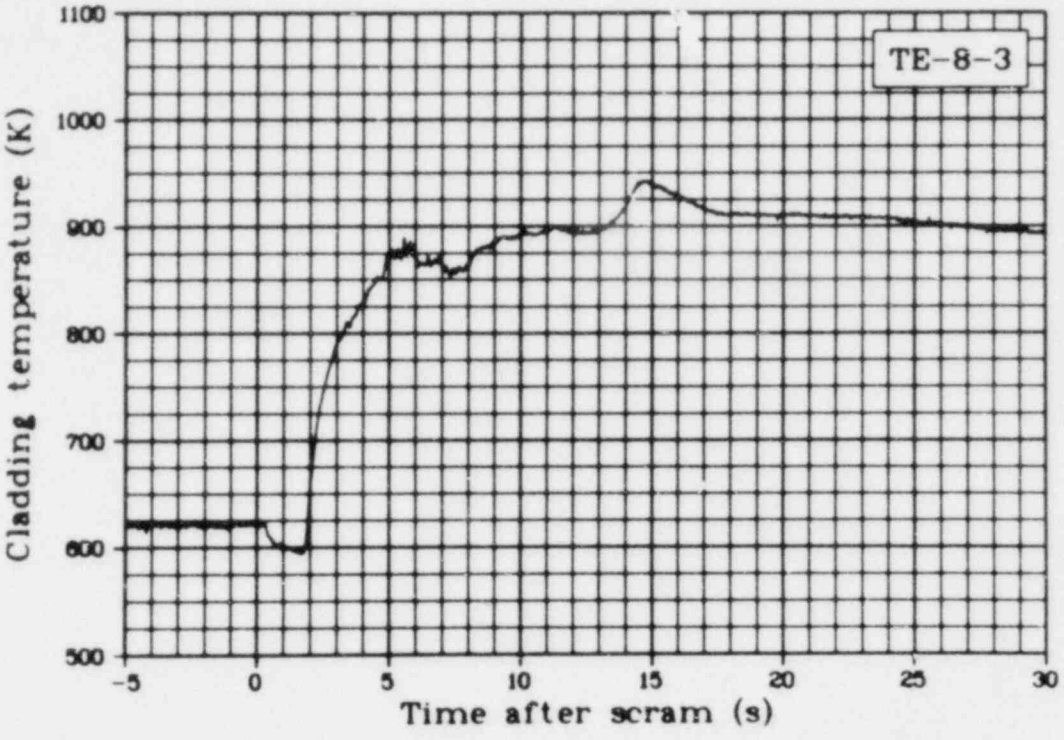

Fig. 131 Cladding temperature Rod 3, 0.61 m above bottom of fuel stack (TE-8-3), Test LOC-11C.

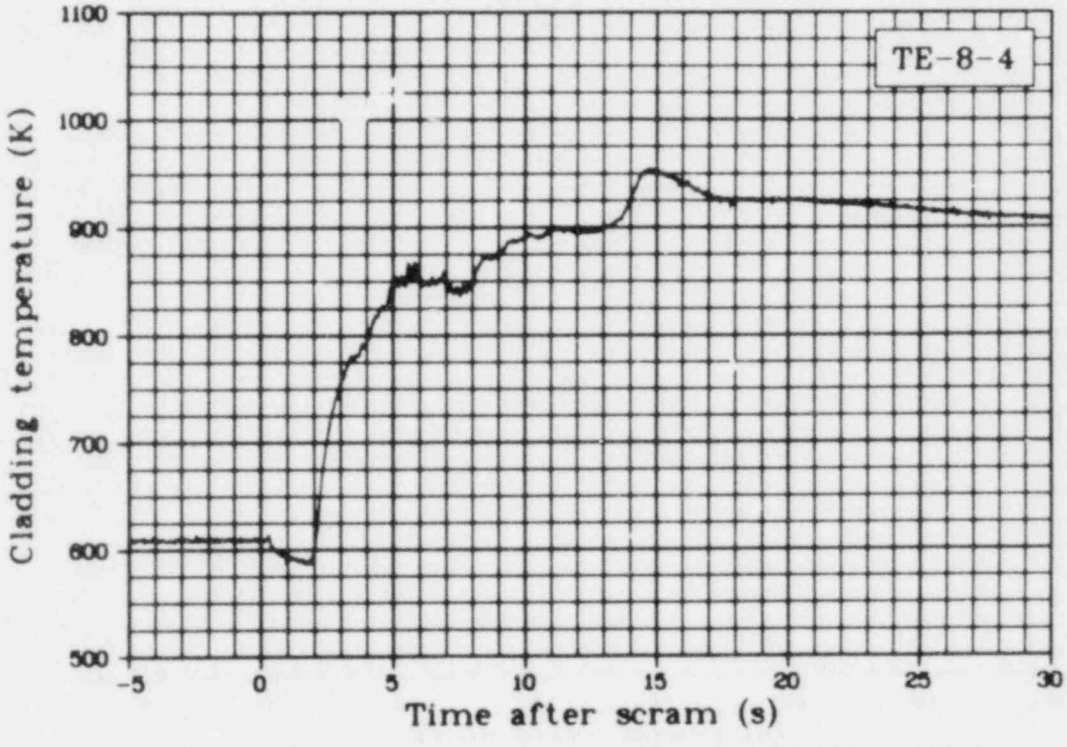

Fig. 132 Cladding temperature Rod 4, 0.61 m above bottom of fuel stack (TE-8-4), Test LOC-11C.

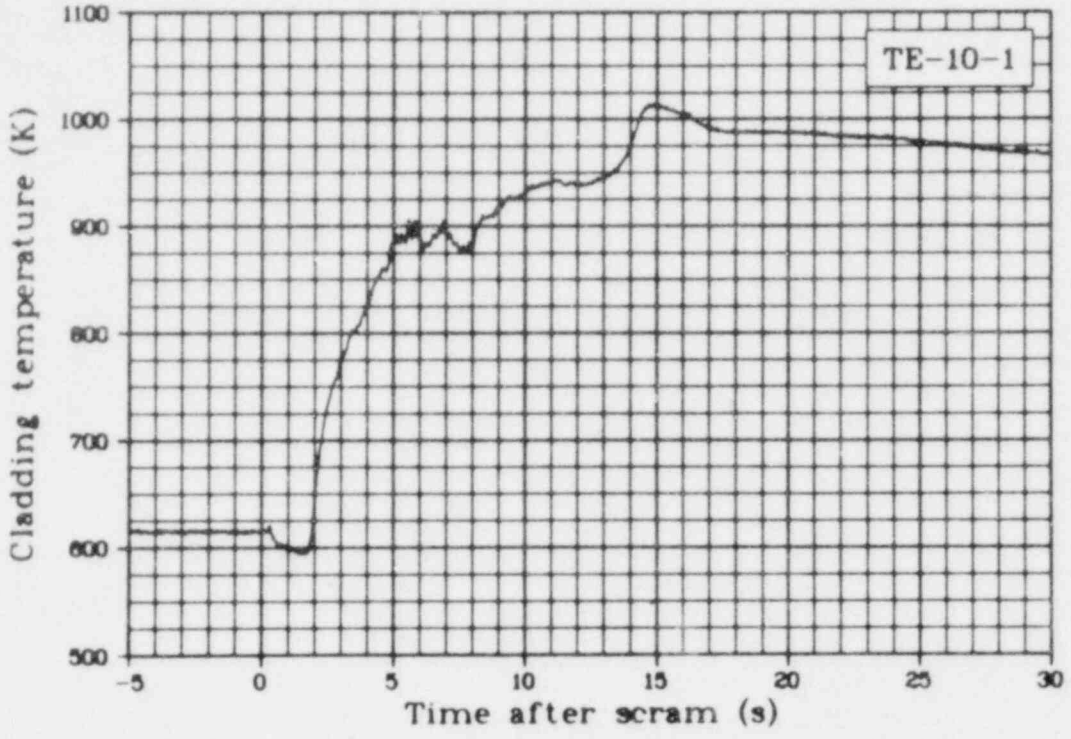

Fig. 133 Cladding temperature Rod 1, 0.53 m above bottom of fuel stack (TE-10-1), Test LOC-11C.

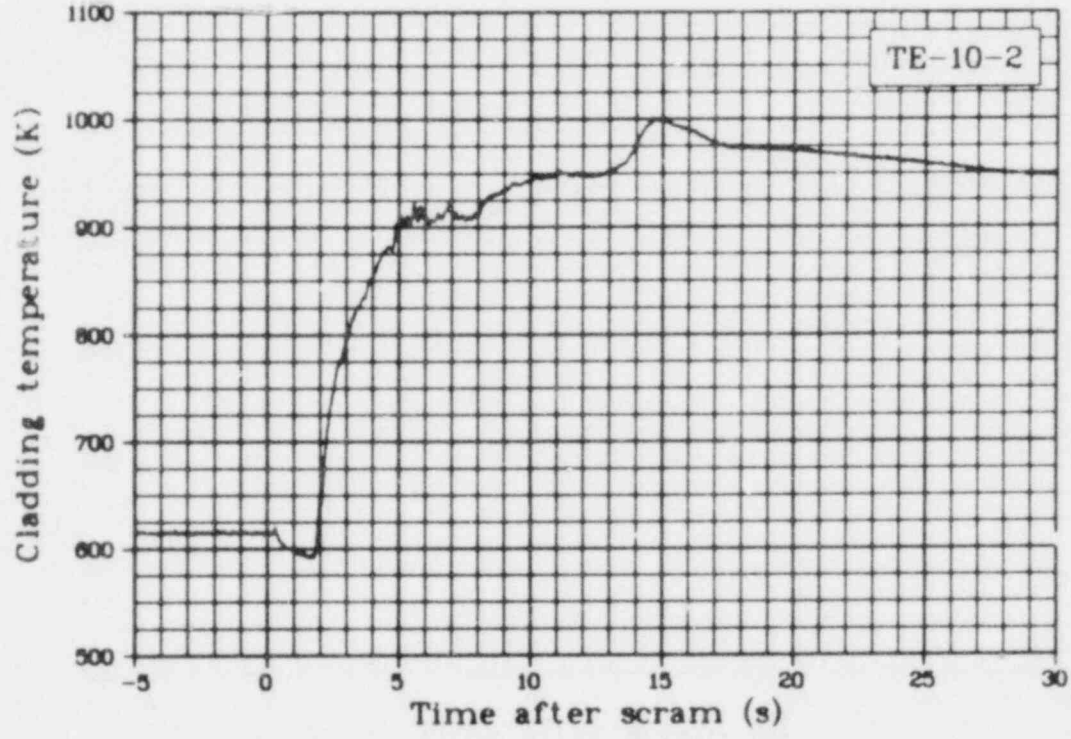

Fig. 134 Cladding temperature Rod 2, 0.53 m above bottom of fuel stack (TE-10-2), Test LOC-11C.

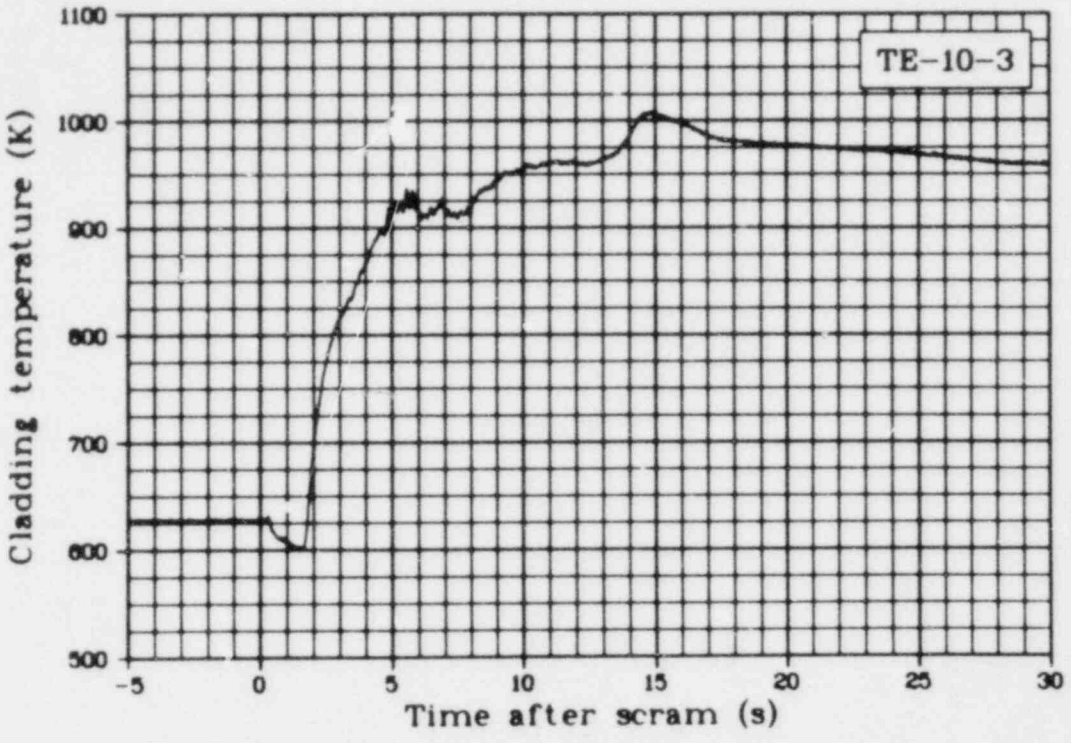

Fig. 135 Cladding temperature Rod 3, 0.53 m above bottom of fuel stack (TE-10-3), Test LOC-11C.

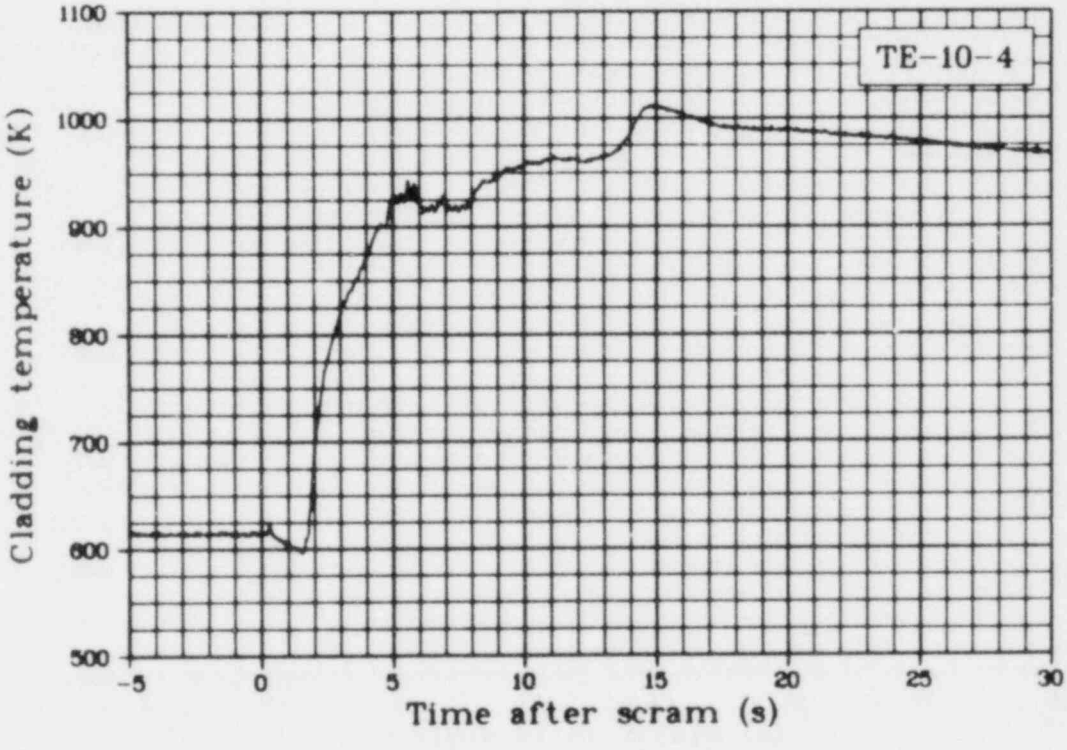

Fig. 136 Cladding temperature Rod 4, 0.53 m above bottom of fuel stack (TE-10-4), Test LOC-11C.

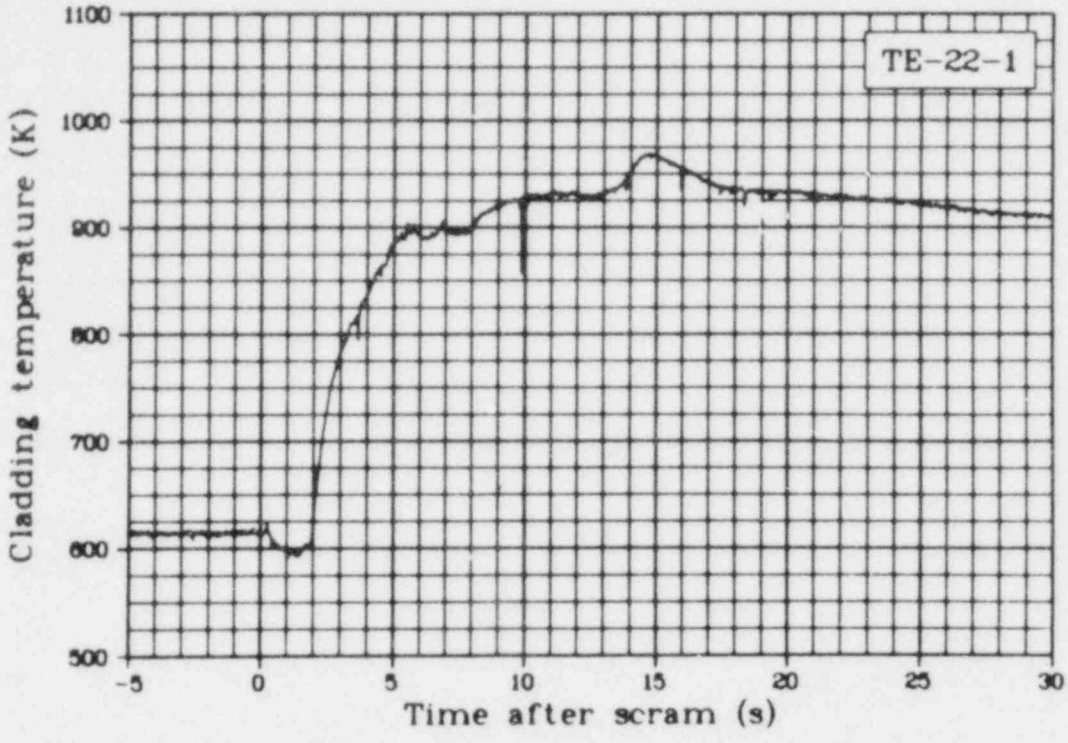

Fig. 137 Cladding temperature Rod 1, 0.61 m above bottom of fuel stack (TE-22-1), Test LOC-11C.

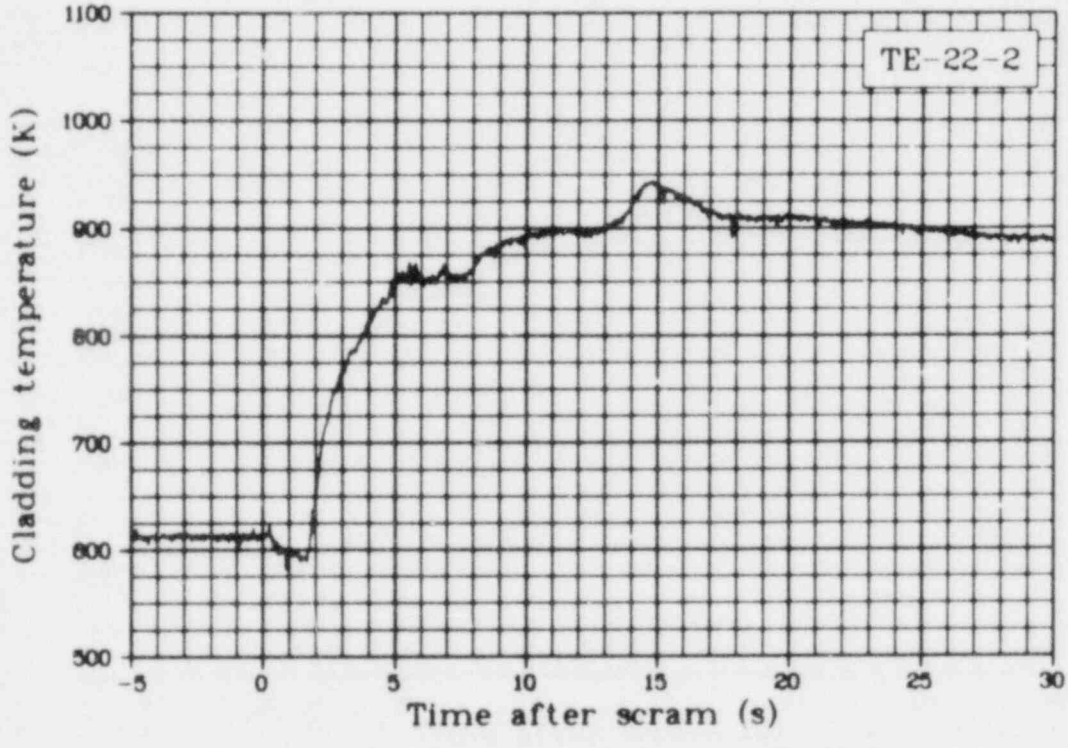

Fig. 138 Cladding temperature Rod 2, 0.61 m above bottom of fuel stack (TE-22-2), Test LOC-11C.

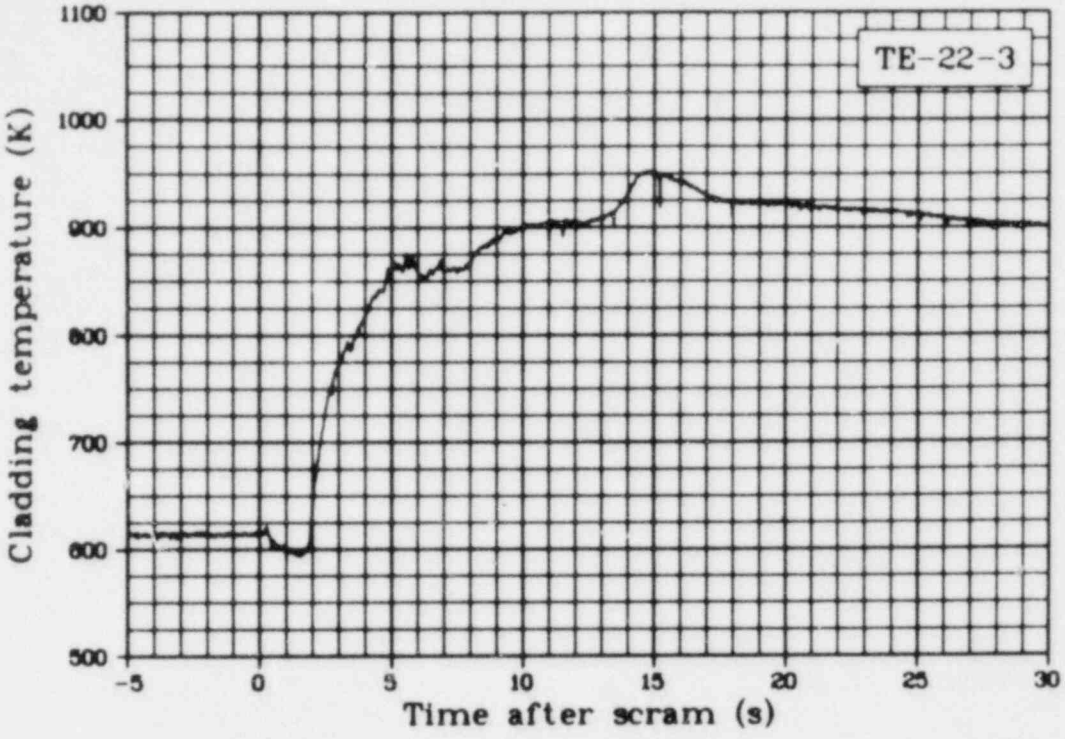

Fig. 139 Cladding temperature Rod 3, 0.61 m above bottom of fuel stack (TE-22-3), Test LOC-11C.

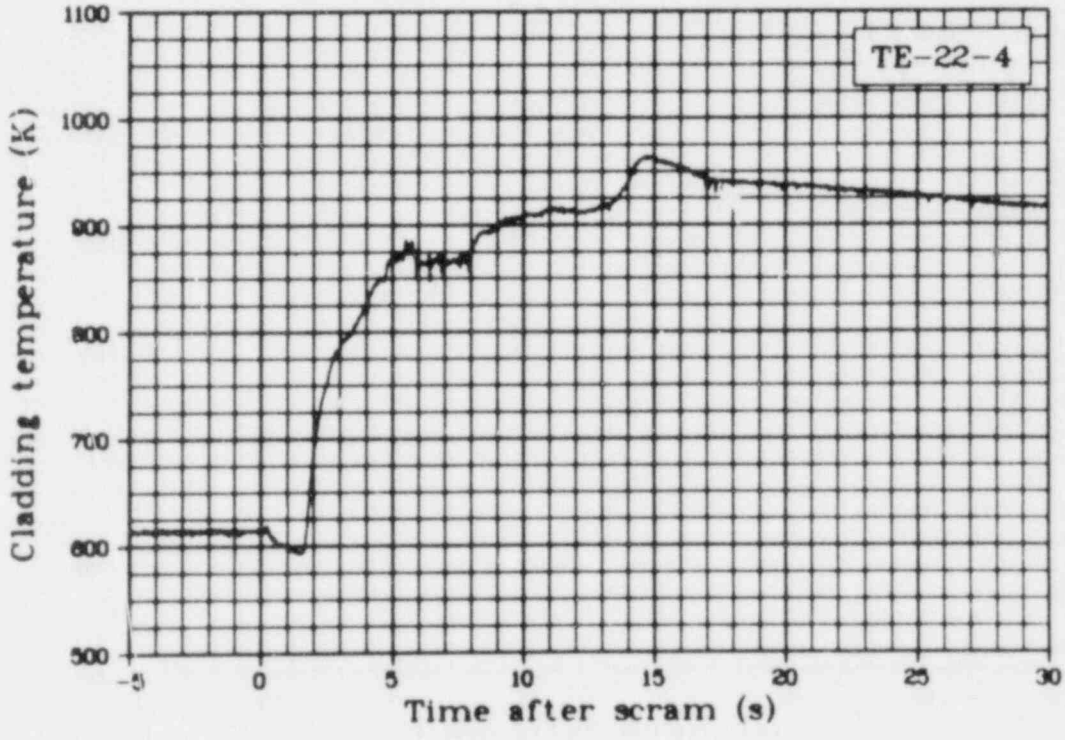

Fig. 140 Cladding temperature Rod 4, 0.61 m above bottom of fuel stack (TE-22-4), Test LOC-11C.

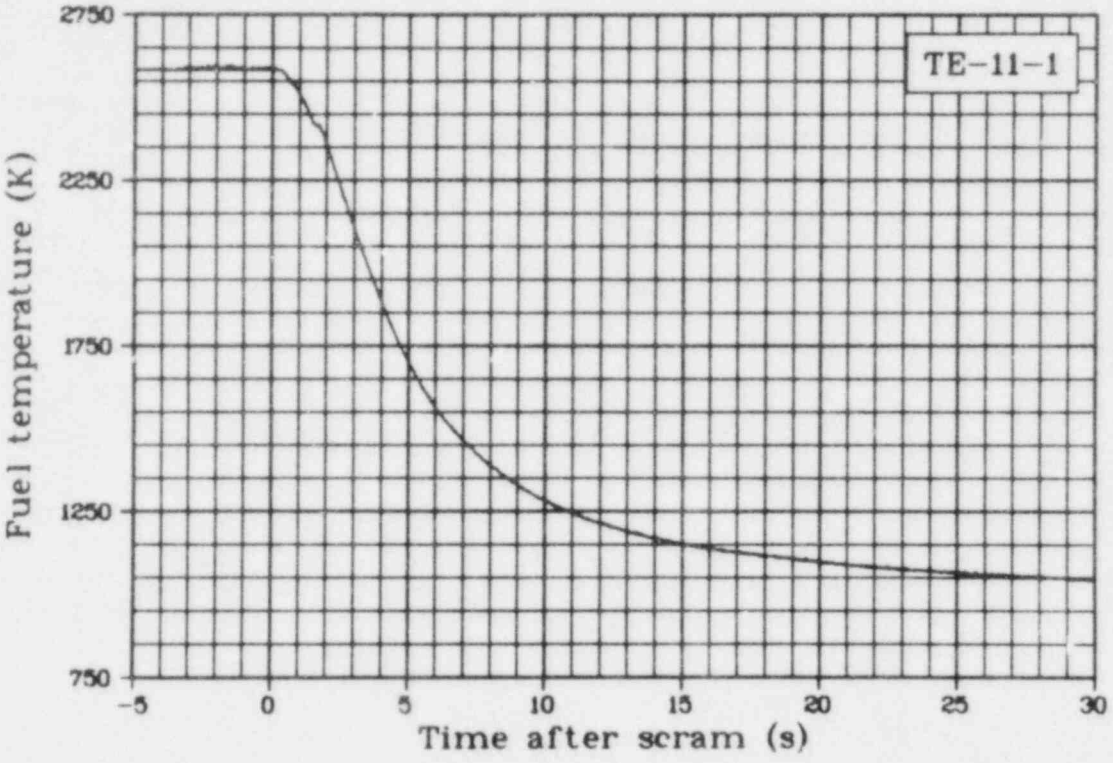

Fig. 141 Fuel temperature Rod 1, 0.53 m above bottom of fuel stack (TE-11-1), Test LOC-11C.

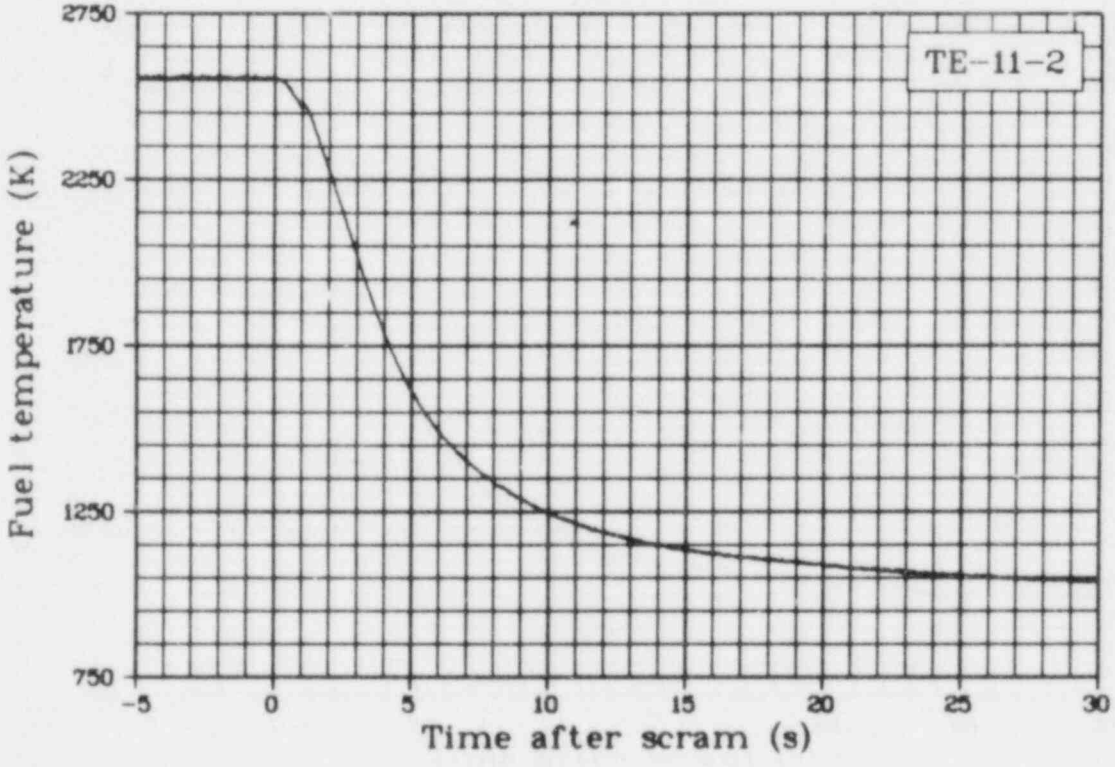

Fig. 142 Fuel temperature Rod 2, 0.53 m above bottom of fuel stack (TE-11-2), Test LOC-11C.

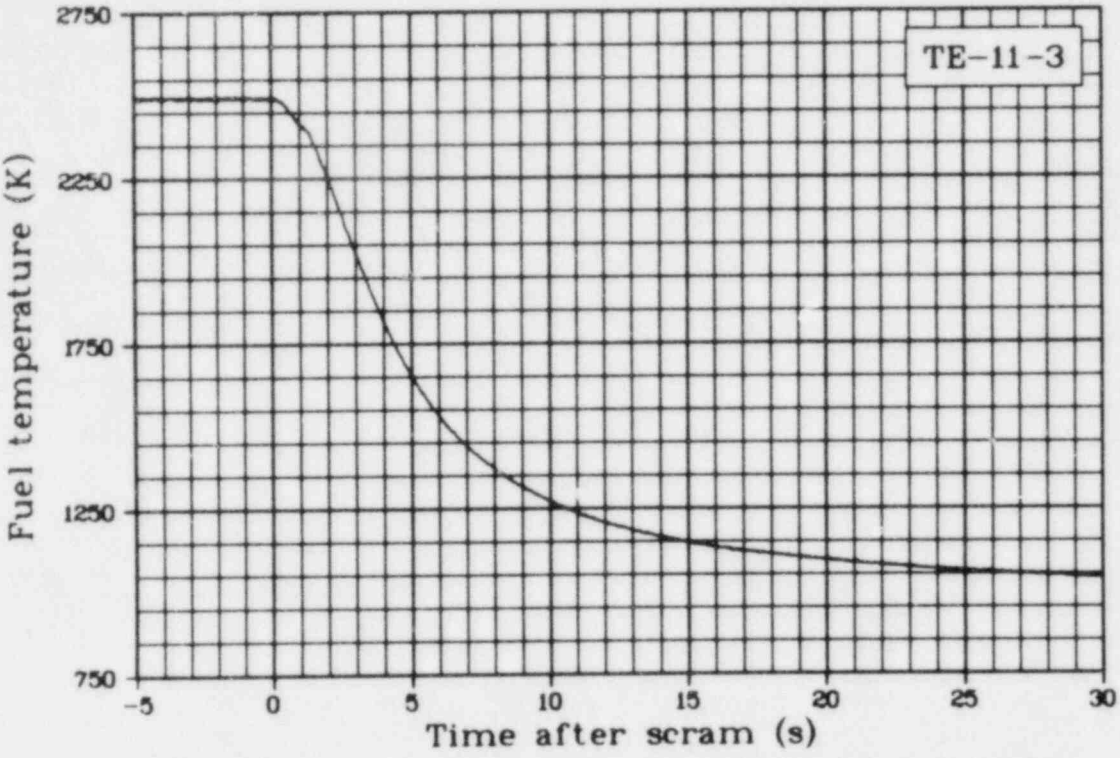

Fig. 143 Fuel temperature Rod 3, 0.53 m above bottom of fuel stack (TE-11-3), Test LOC-11C.

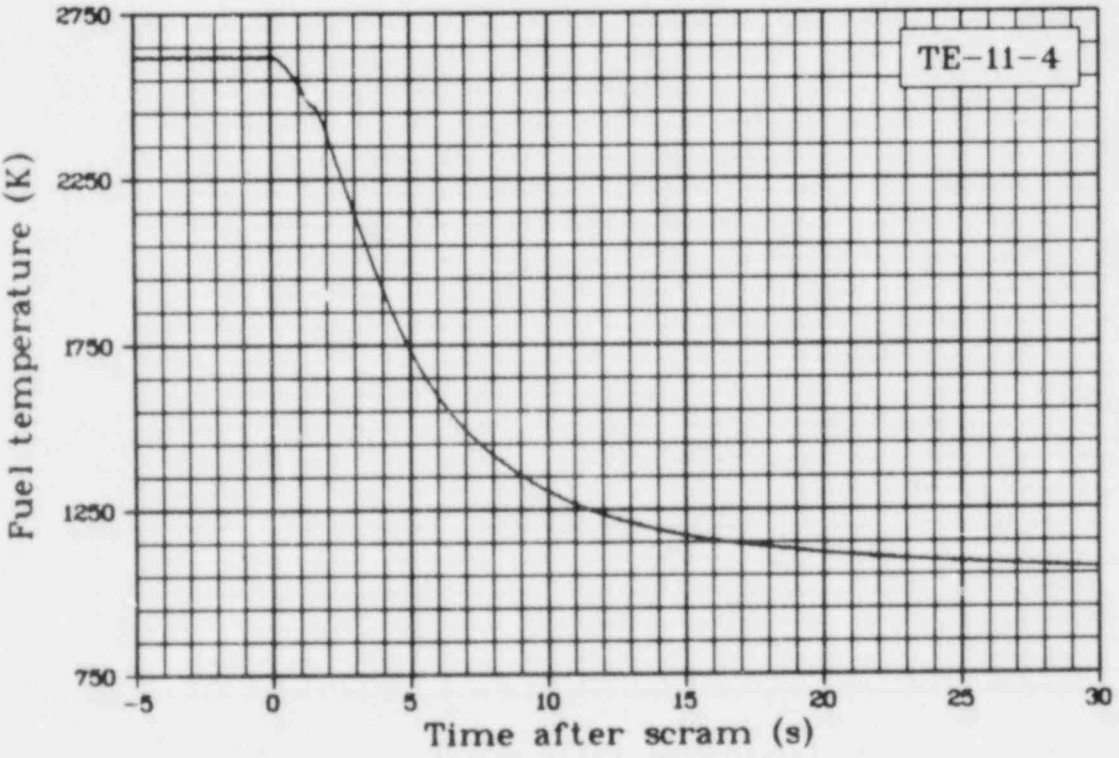

Fig. 144 Fuel temperature Rod 4, 0.53 m above bottom of fuel stack (TE-11-4), Test LOC-11C.

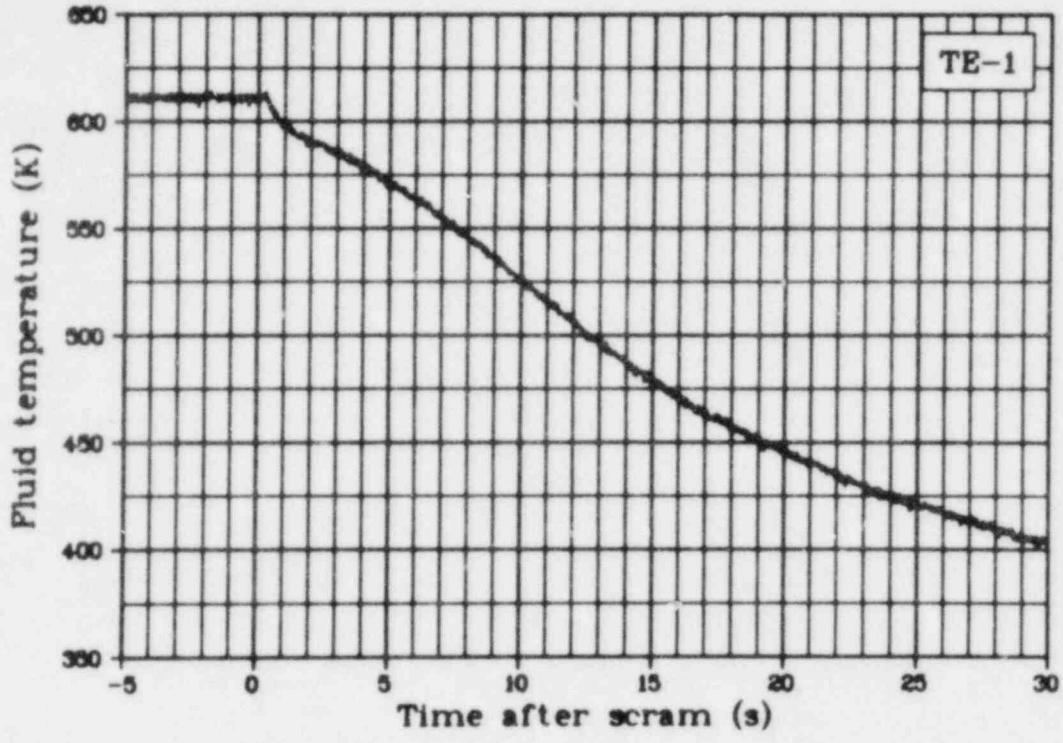

Fig. 145 Fluid temperature in lower upper plenum (TE-1), Test LOC-11C.

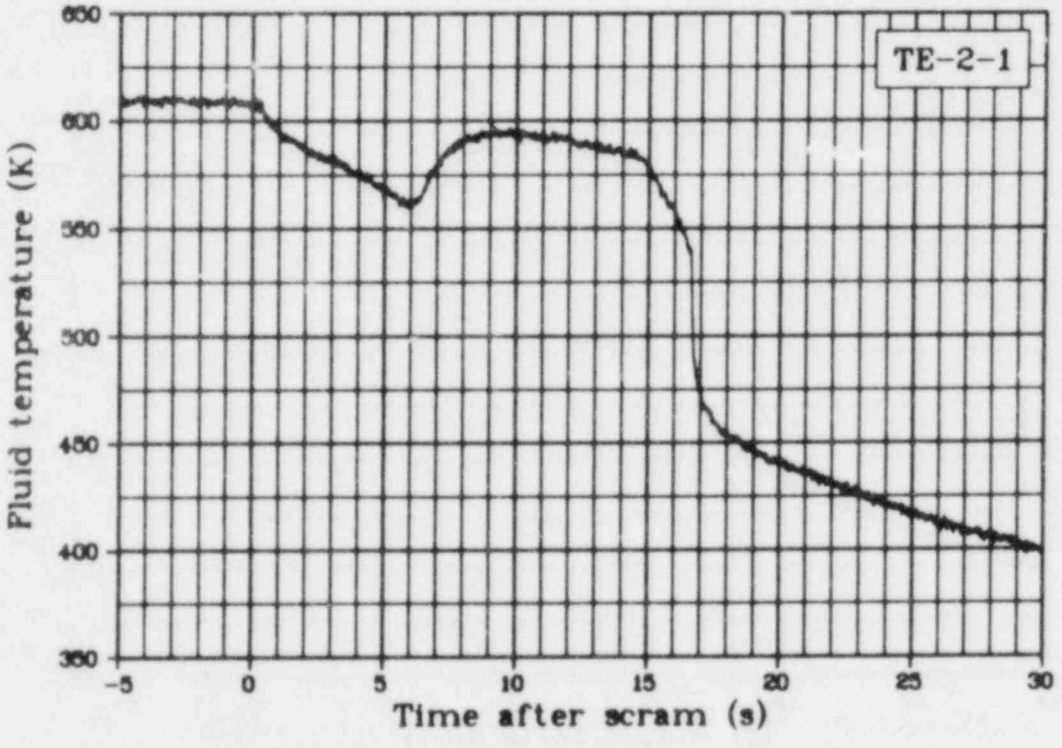

Fig. 146 Fluid temperature of Rod 1 coolant outlet (TE-2-1), Test LOC-11C.

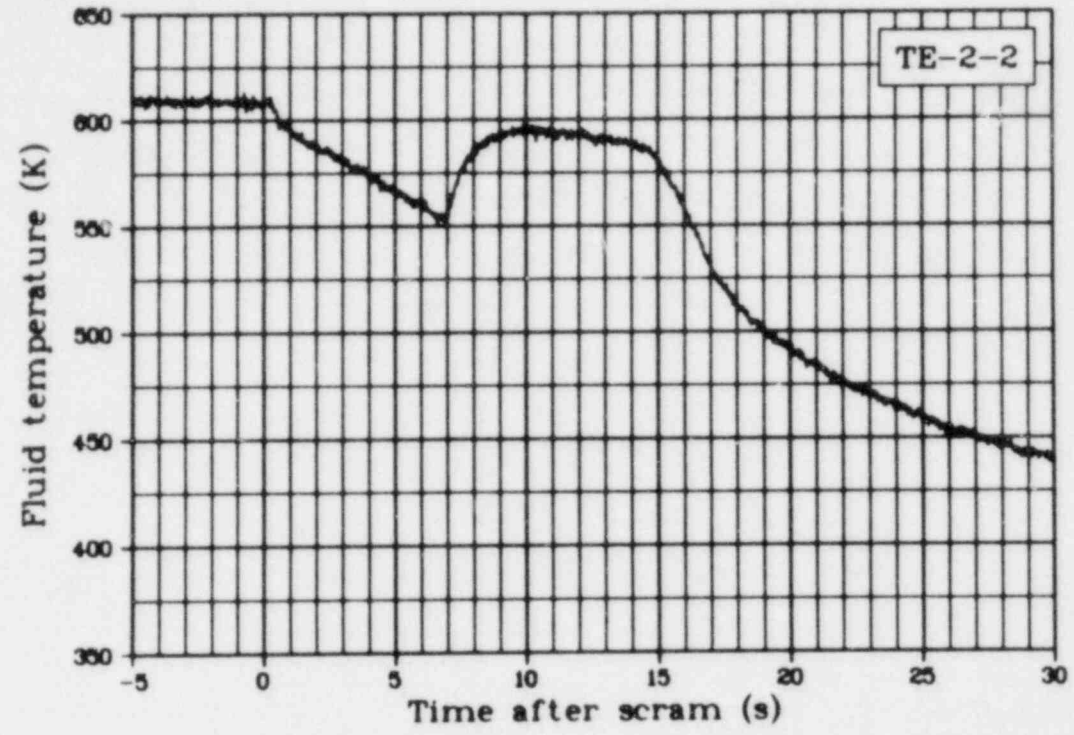

Fig. 147 Fluid temperature of Rod 2 coolant outlet (TE-2-2), Test LOC-11C.

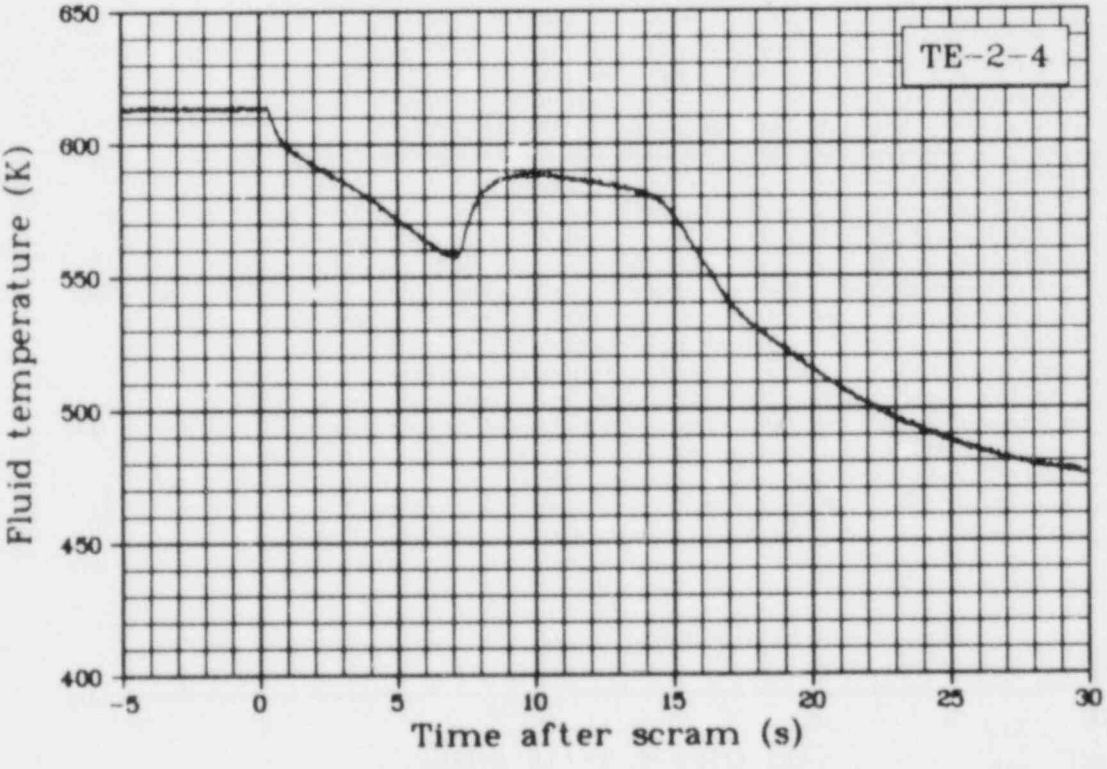

Fig. 148 Fluid temperature of Rod 4 coolant outlet (TE-2-4), Test LOC-11C.

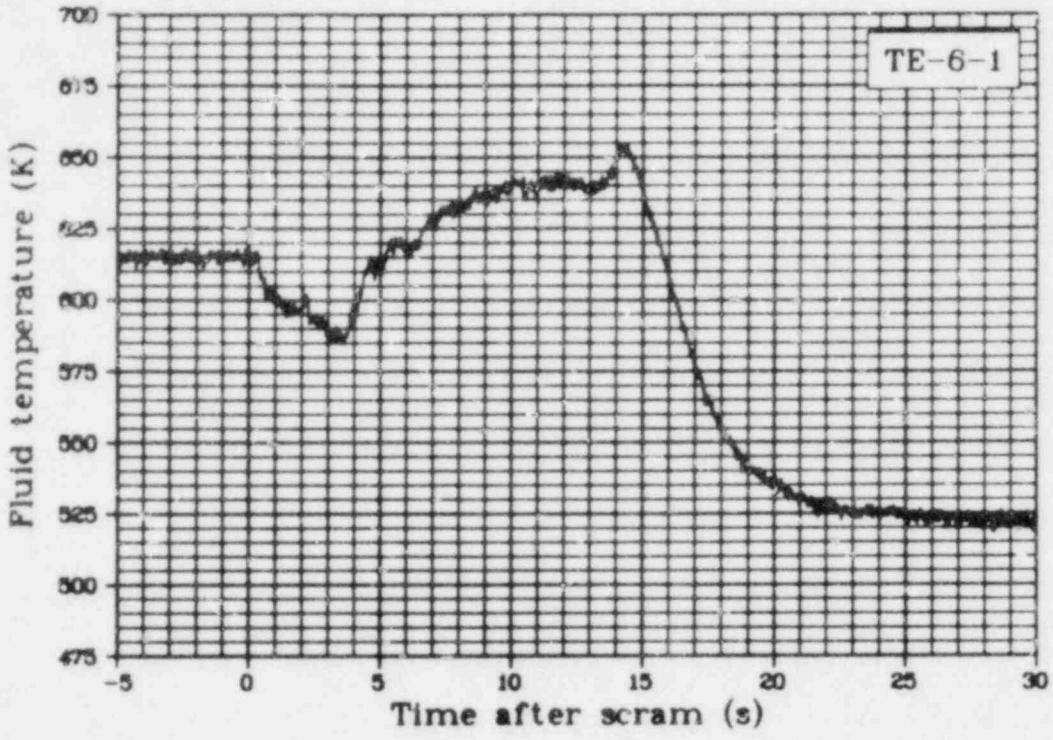

Fig. 149 Fluid temperature of Rod 1, 0.61 m above bottom of fuel stack (TE-6-1), Test LOC-11C.

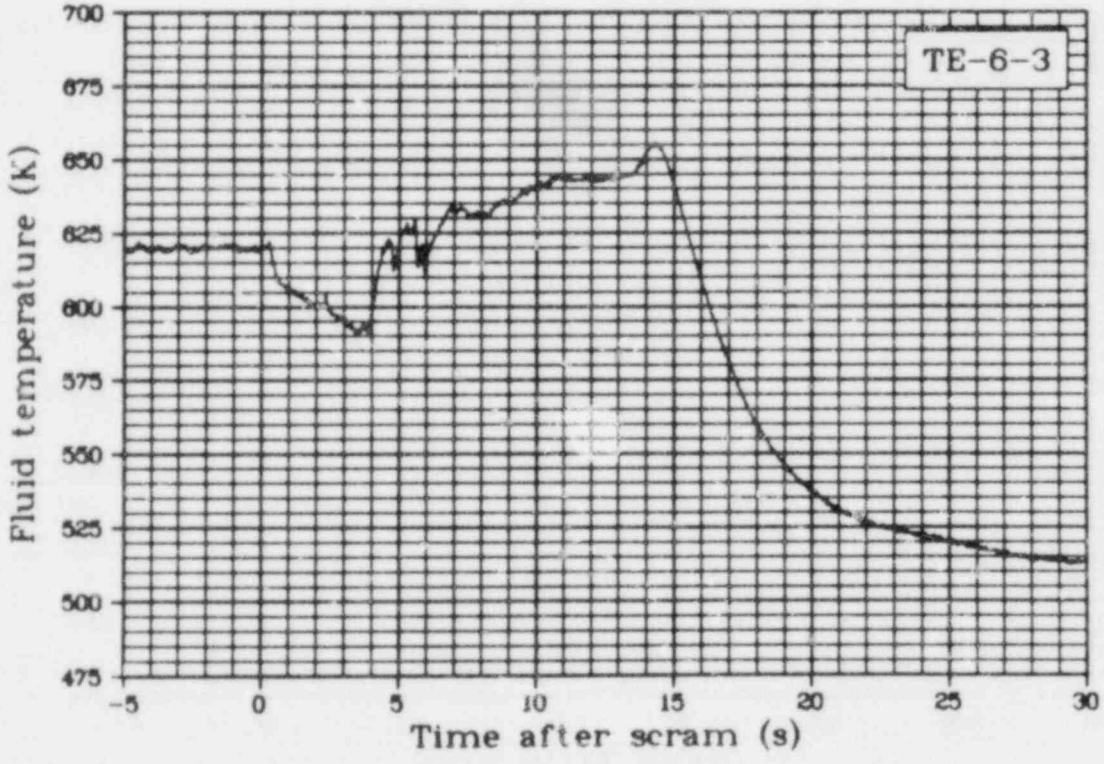

Fig. 150 Fluid temperature of Rod 3, 0.61 m above bottom of fuel stack (TE-6-3), Test LOC-11C.

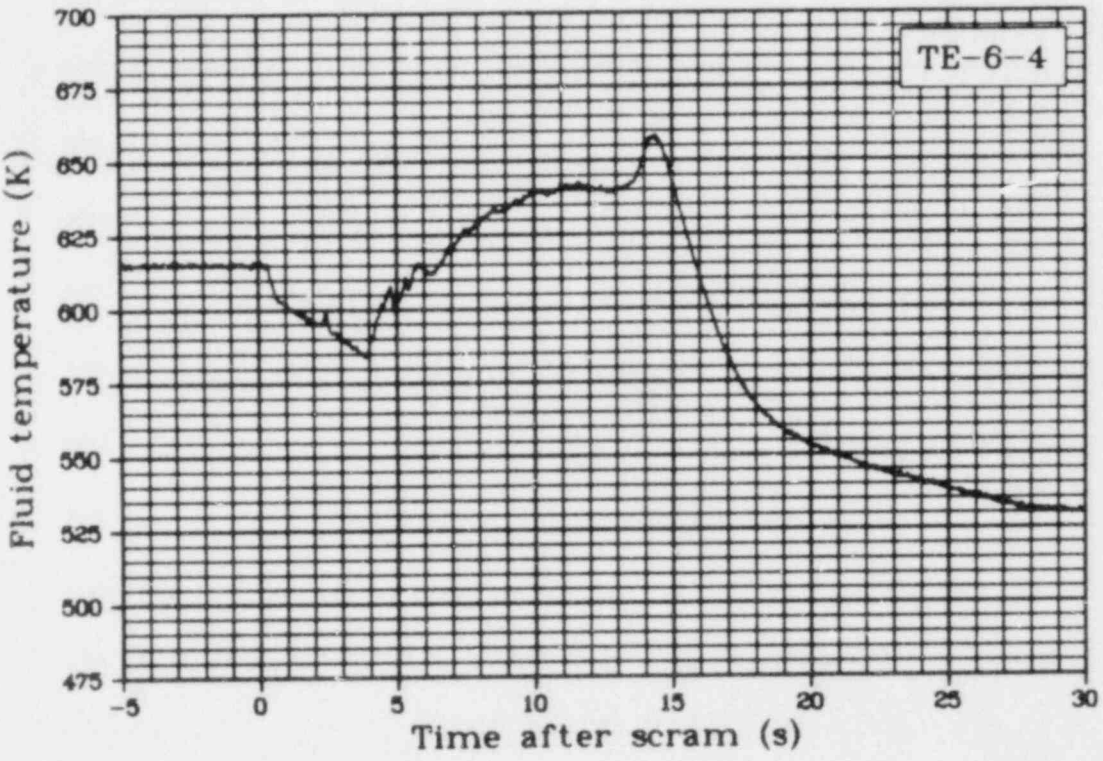

Fig. 151 Fluid temperature of Rod 4, 0.61 m above bottom of fuel stack (TE-6-4), Test LOC-11C.

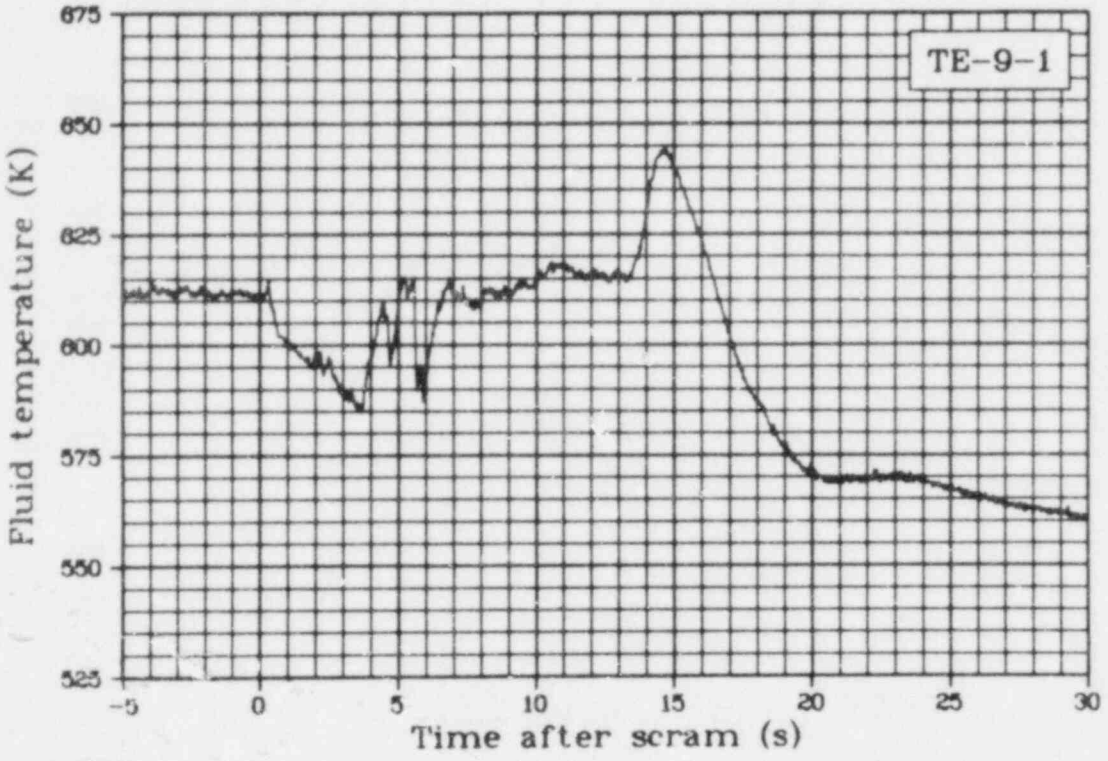

Fig. 152. Fluid temperature of Rod 1, 0,46 m above bottom of fuel stack (TE-9-1), Test LOC-11C.

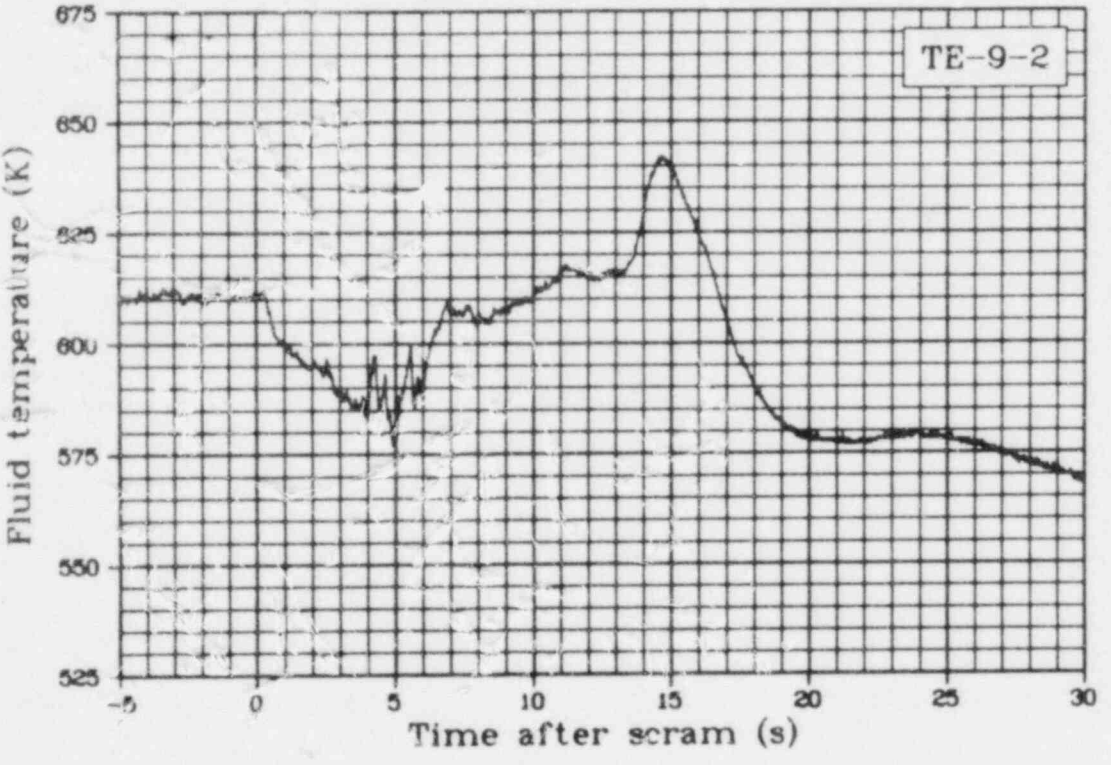

Fig. 153 Fluid temperature of Rod 2, 0,46 m above bottom of fuel stack (TE-9-2), Test LOC-11C.

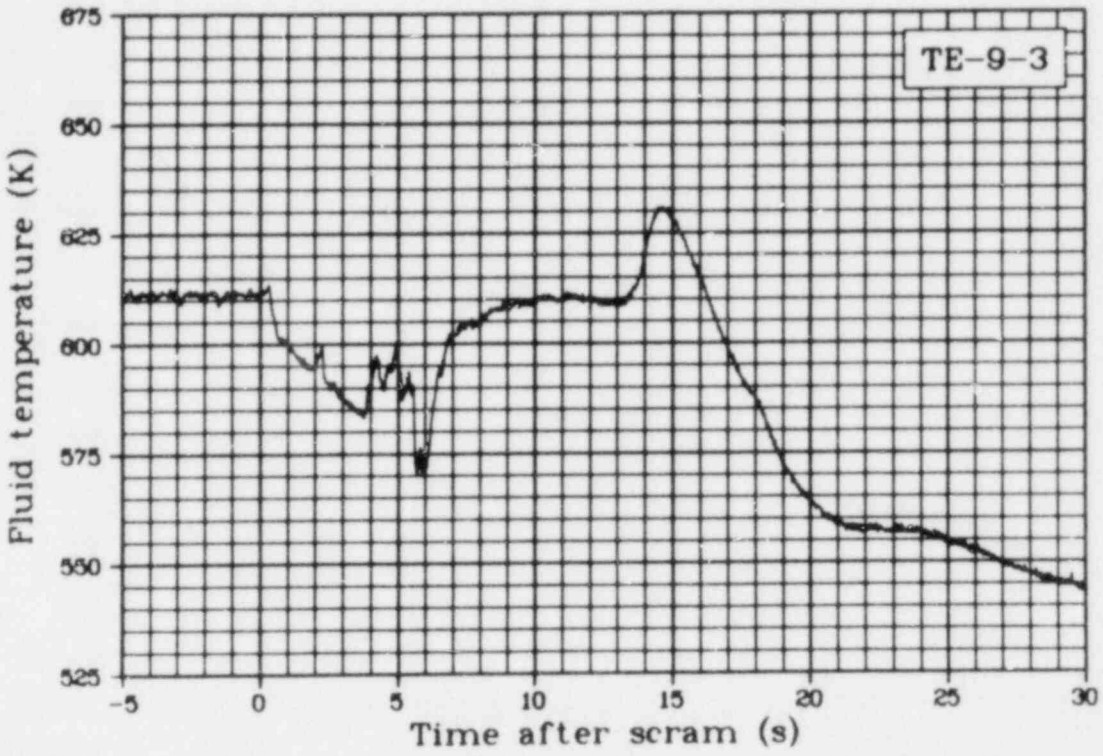

Fig. 154 Fluid temperature of Rod 3, 0.46 m above bottom of fuel stack (TE-9-3), Test LOC-11C.

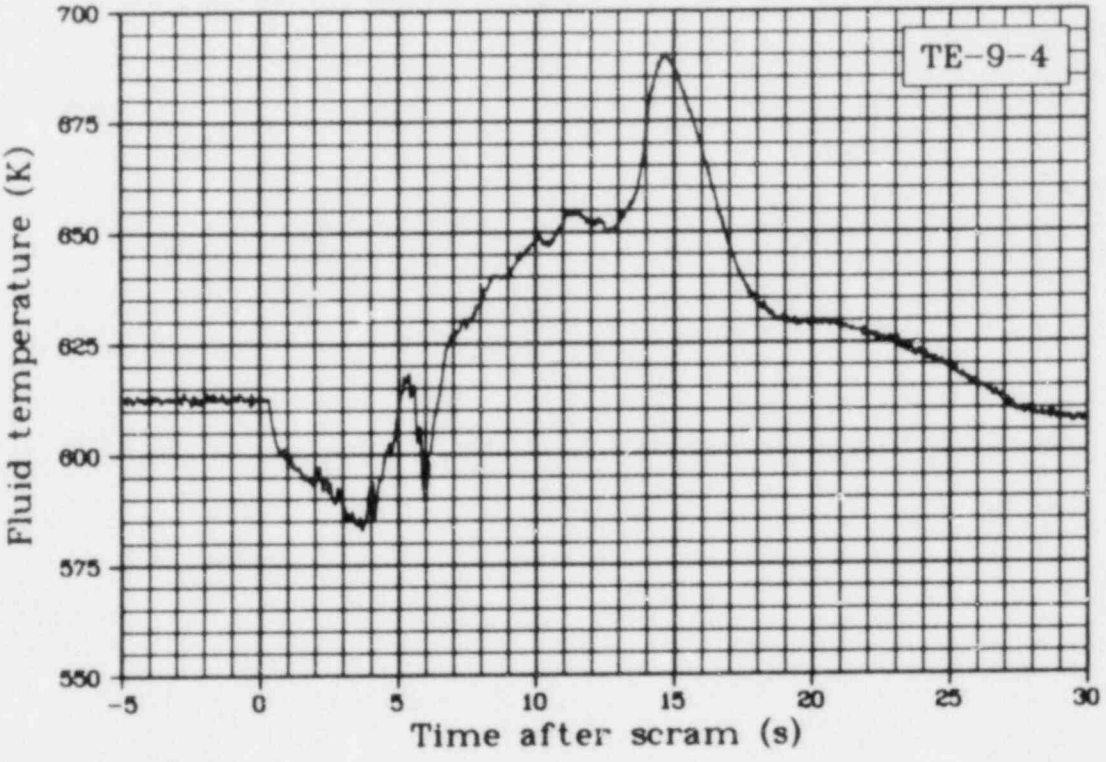

Fig. 155 Fluid temperature of Rod 4, 0.46 m above bottom of fuel stack (TE-9-4), Test LOC-11C.

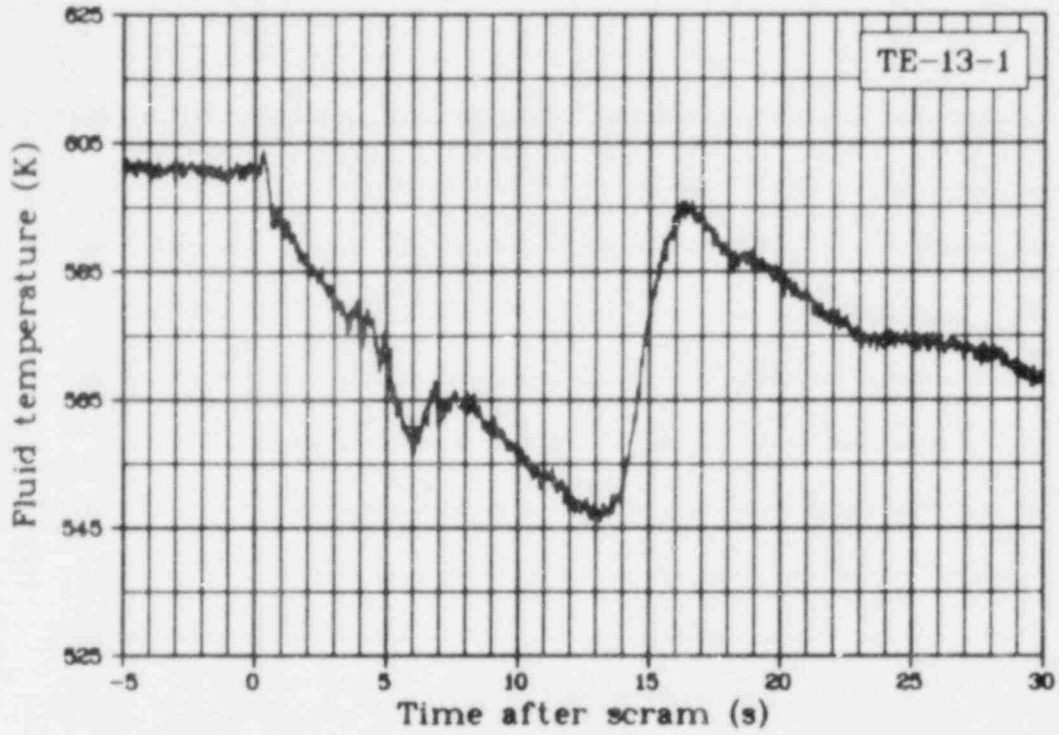

Fig. 156 Fluid temperature of Rod 1, 0.30 m above fuel stack bottom (TE-13-1), Test LOC-11C.

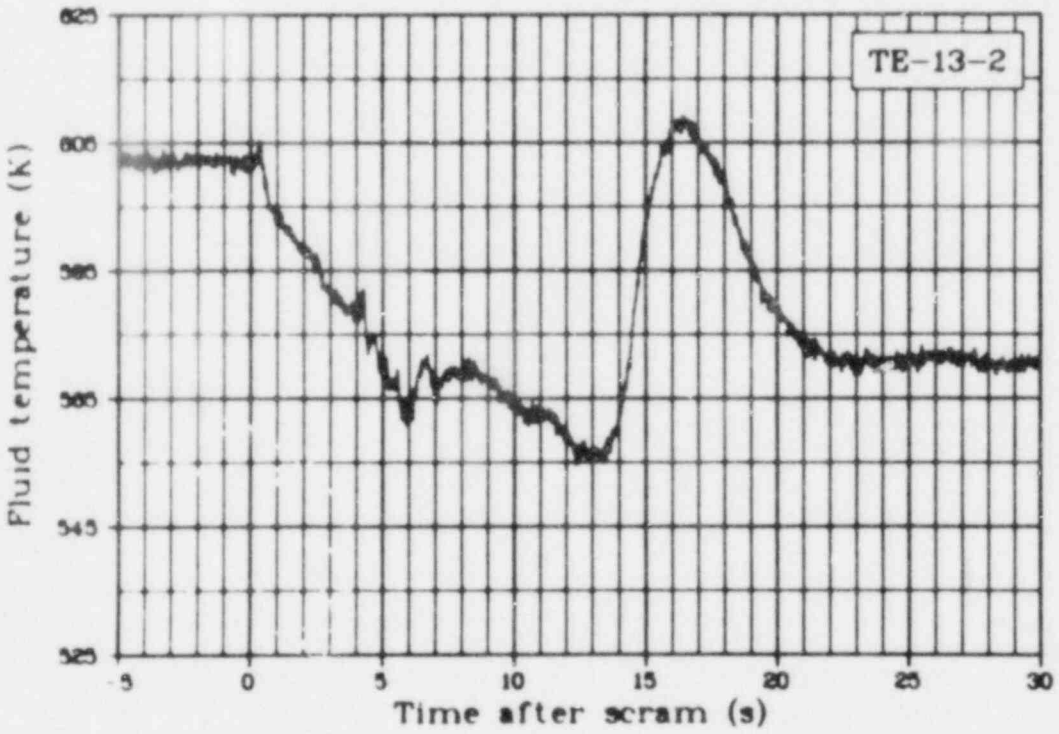

Fig. 157 Fluid temperature of Rod 2, 0.30 m above fuel stack bottom (TE-13-2), Test LOC-11C.

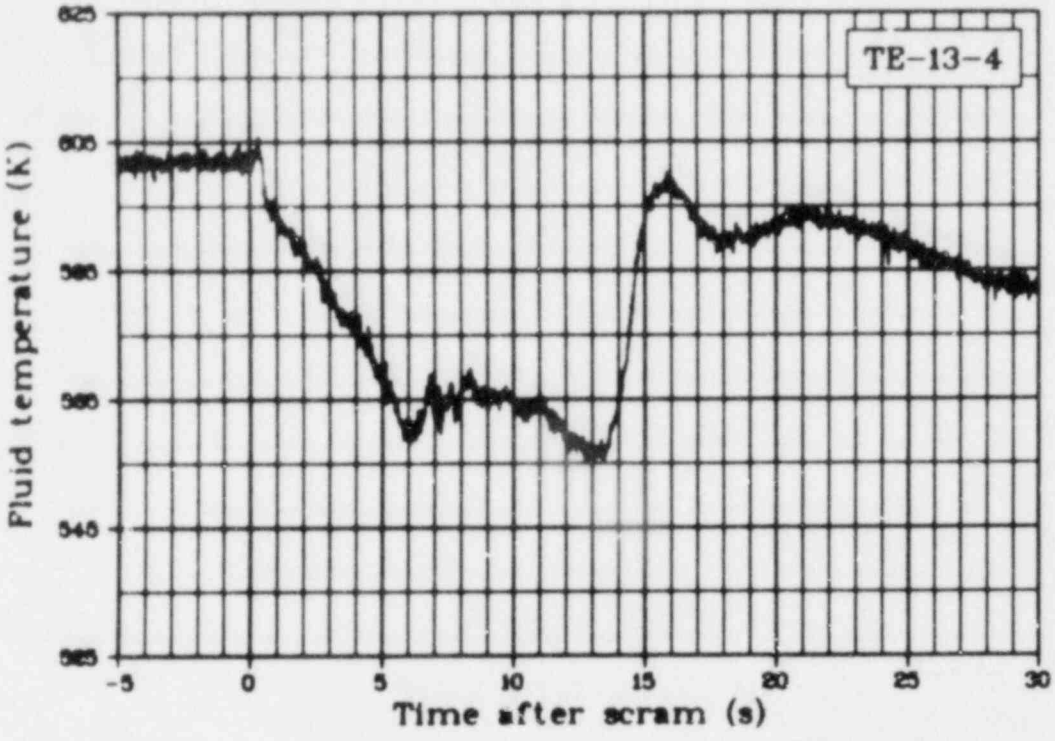

Fig. 158 Fluid temperature of Rod 4, 0.30 m above fuel stack bottom (TE-13-4), Test LOC-11C.

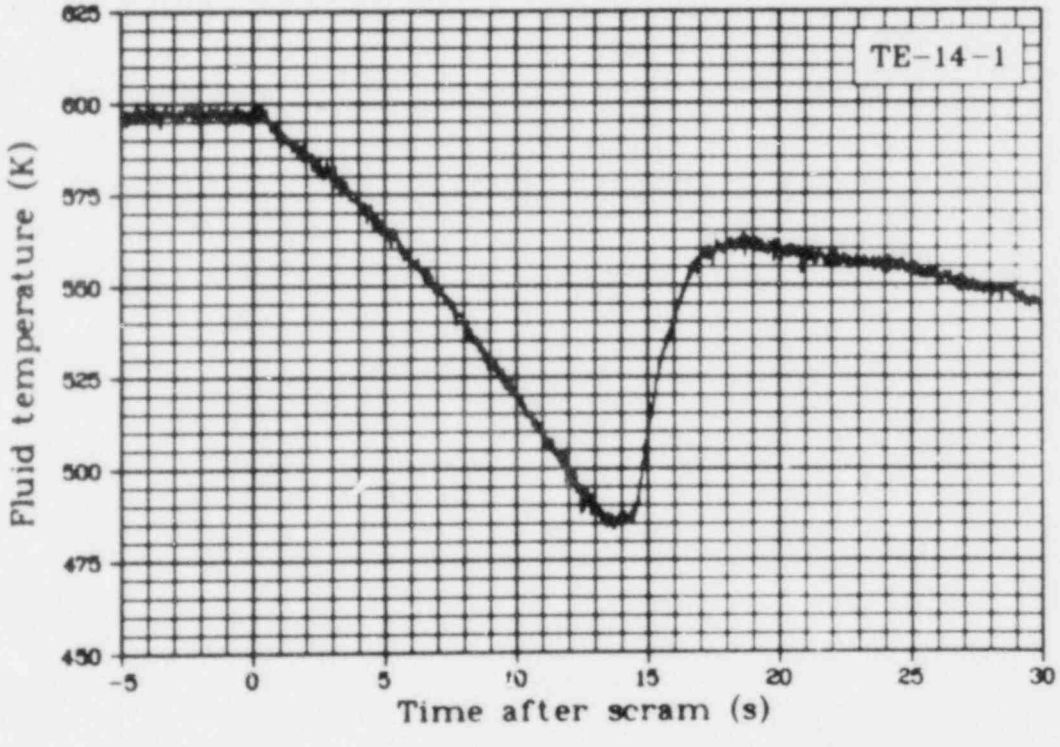

Fig. 159 Fluid temperature of Rod 1 inlet coolant (TE-14-1), Test LOC-11C.

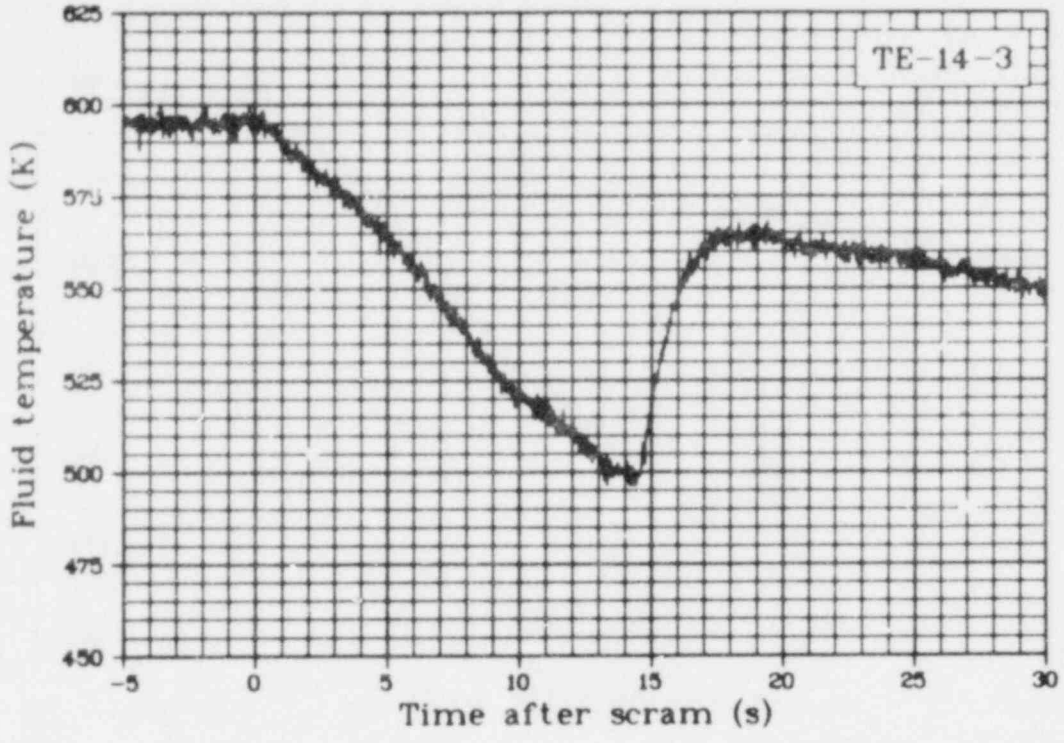

Fig. 160 Fluid temperature of Rod 3 inlet coolant (TE-14-3), Test LOC-11C.

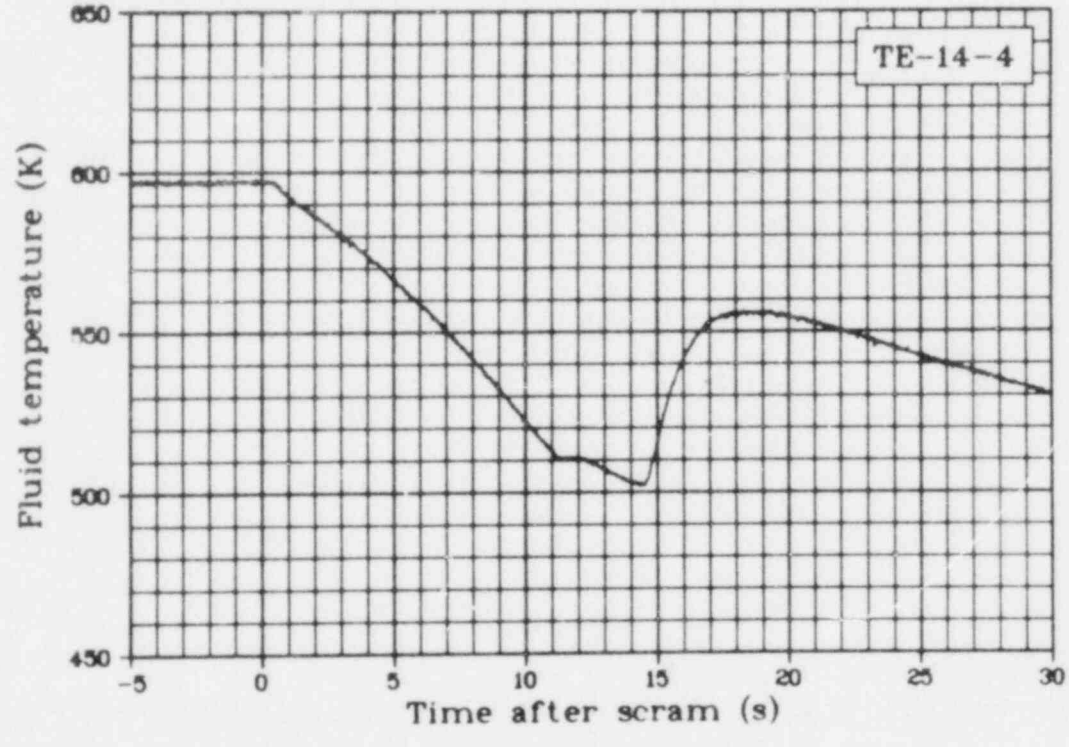

Fig. 161 Fluid temperature of Rod 4 inlet coolant (TE-14-4), Test LOC-11C.

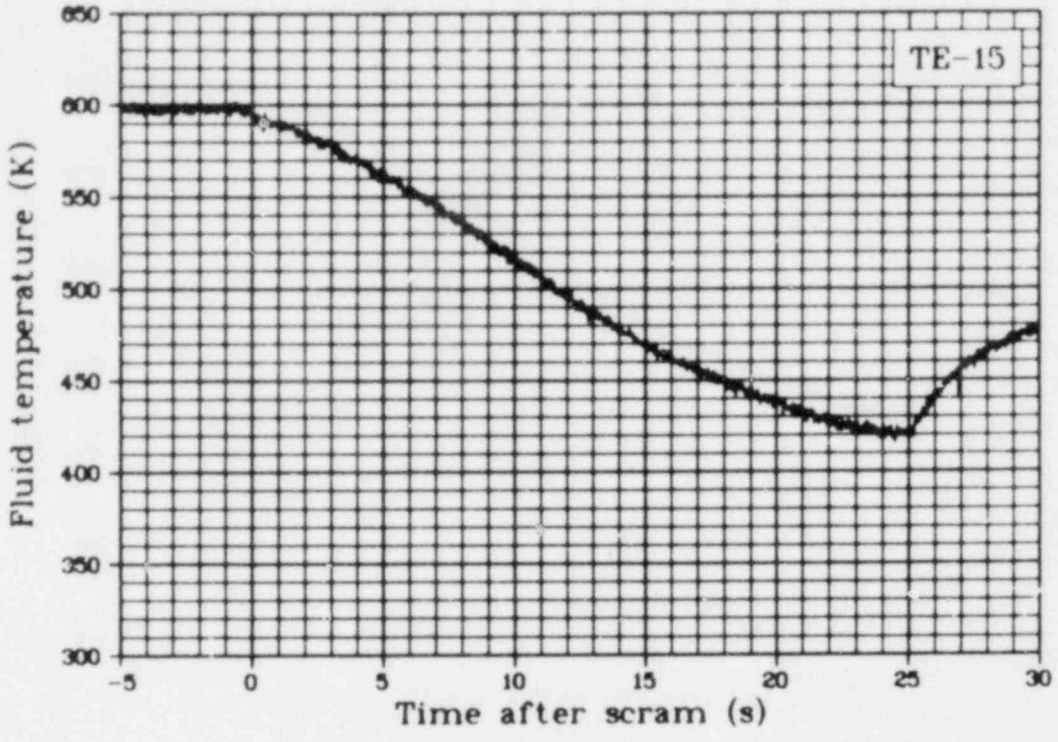

Fig. 162 Fluid temperature in test train lower particle screen (TE-15), Test LOC-11C.

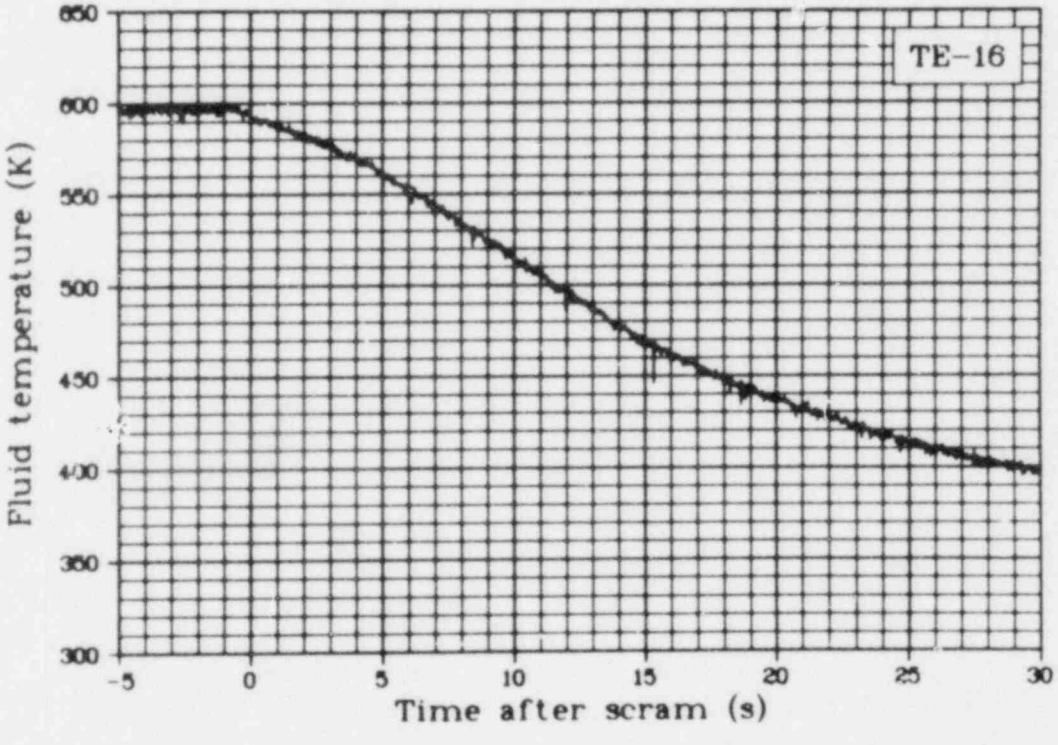

Fig. 163 Fluid temperature in test train lower particle screen (TE-16), Test LOC-11C.

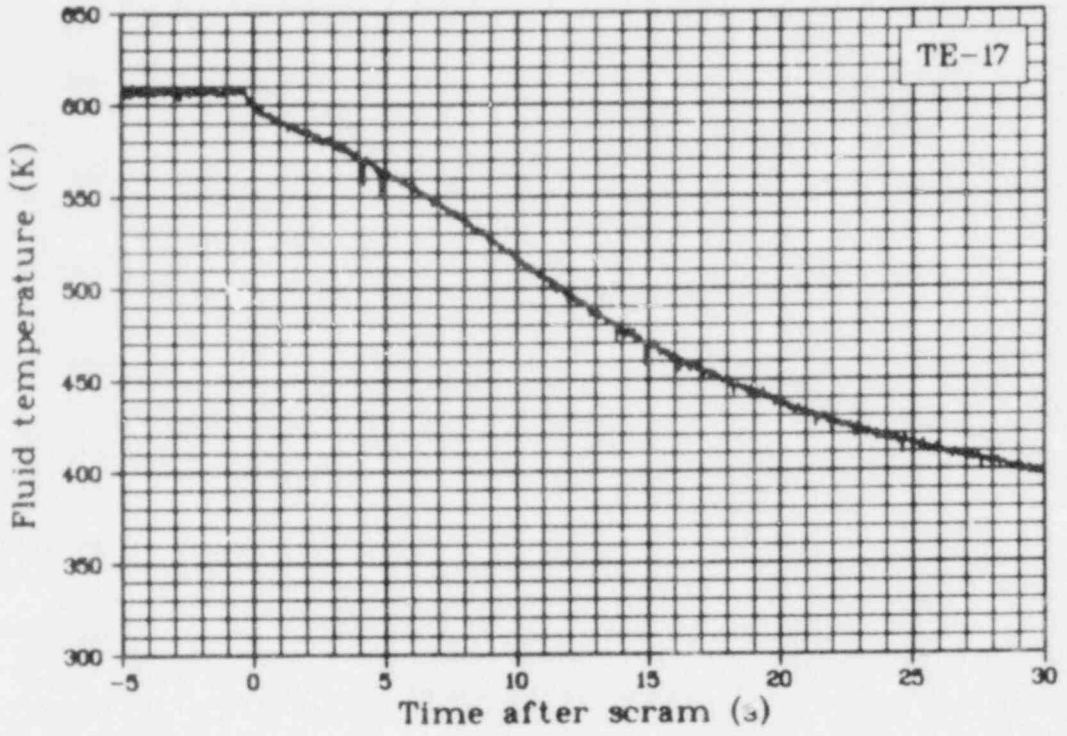

Fig. 164 Fluid temperature in test train bypass flow (TE-17), Test LOC-11C.

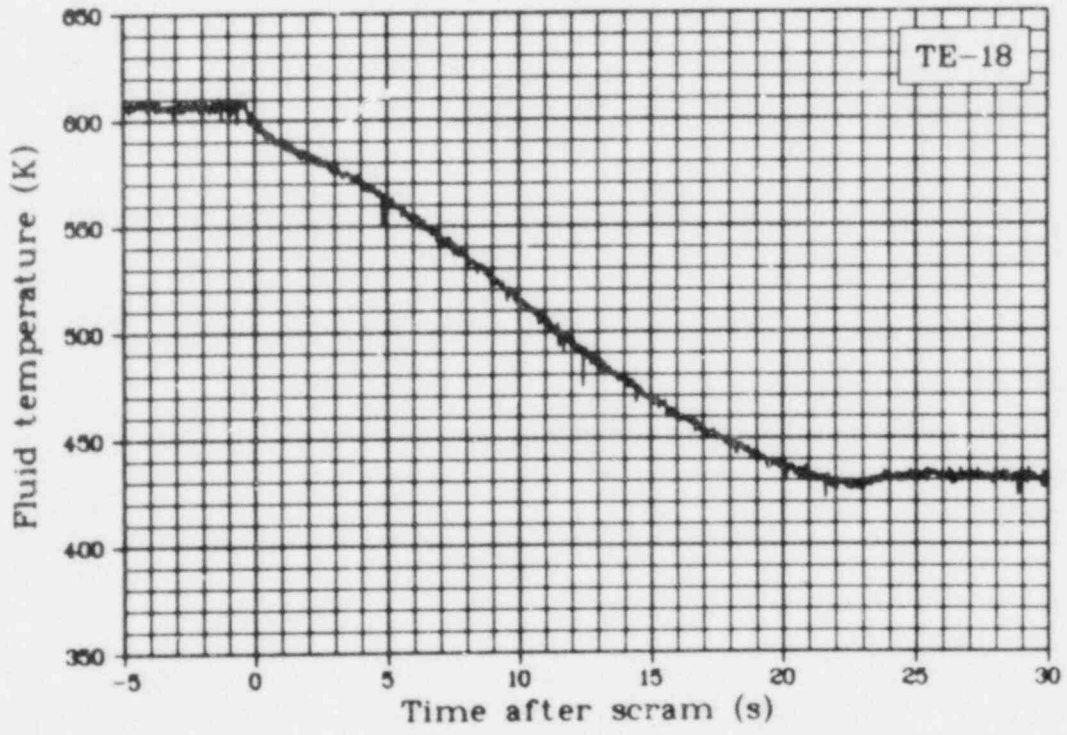

Fig. 165 Fluid temperature in upper plenum exit (TE-18), Test LOC-11C.

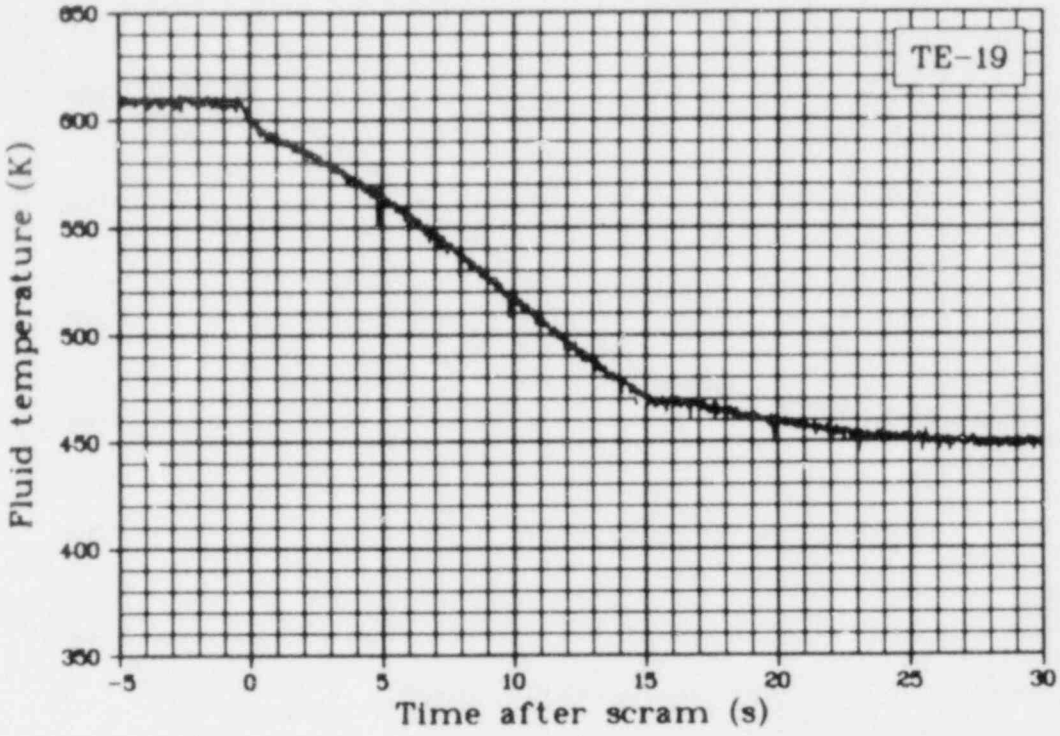

Fig. 166 Fluid temperature in upper plenum exit (TE-19), Test LOC-11C.

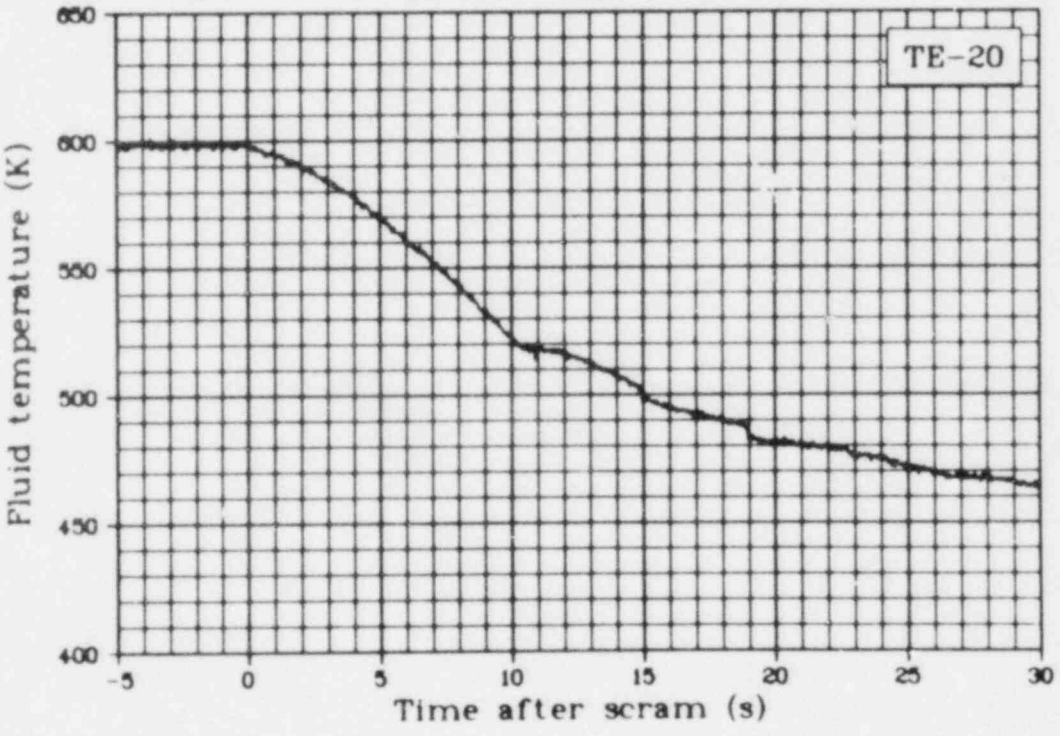

Fig. 167 Fluid temperature in inlet spool (TE-20), Test LOC-11C.

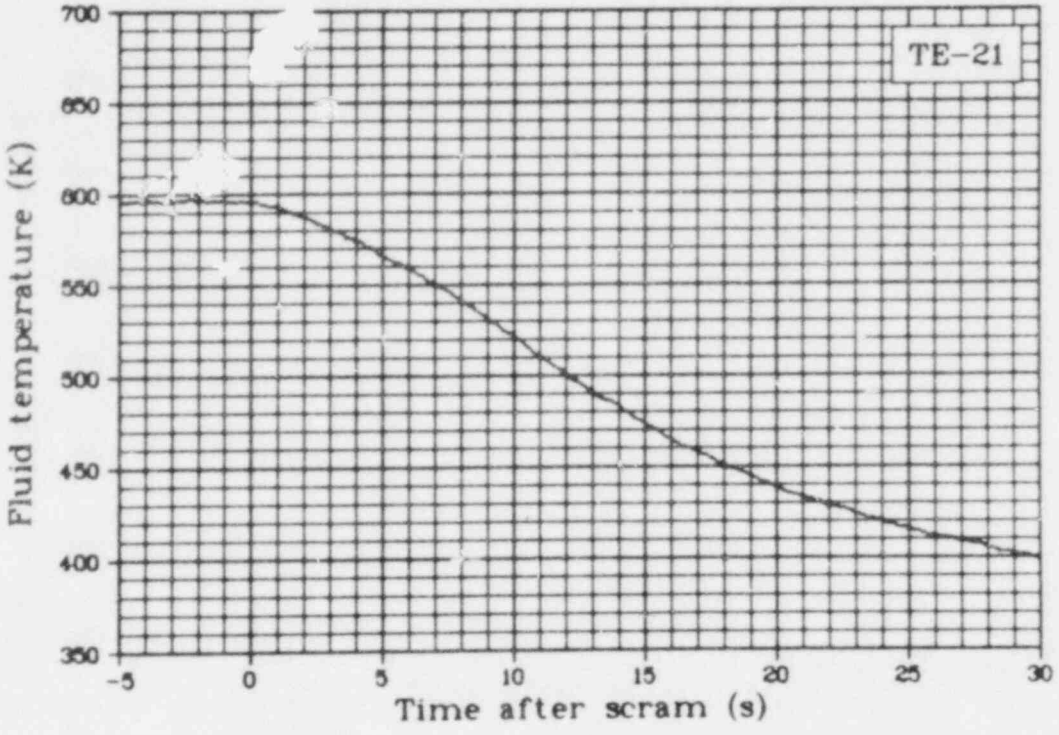

Fig. 168 Fluid temperature in inlet spool (TE-21), Test LOC-11C.

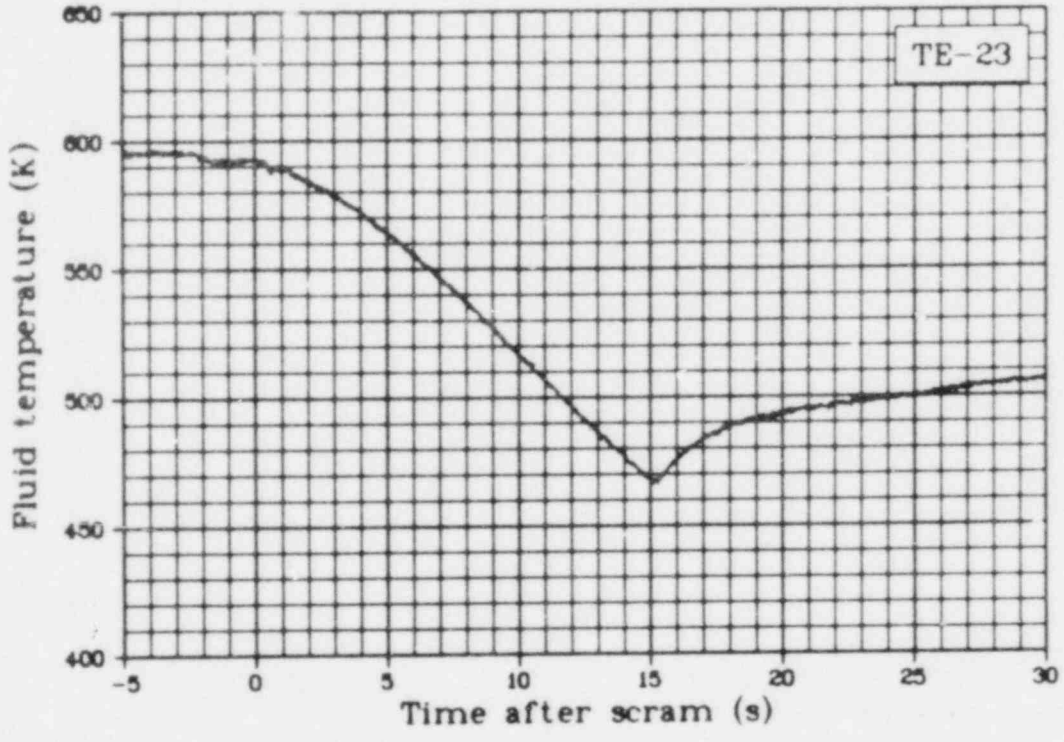

Fig. 169 Fluid temperature in cold leg blowdown spool (TE-23), Test LOC-11C.

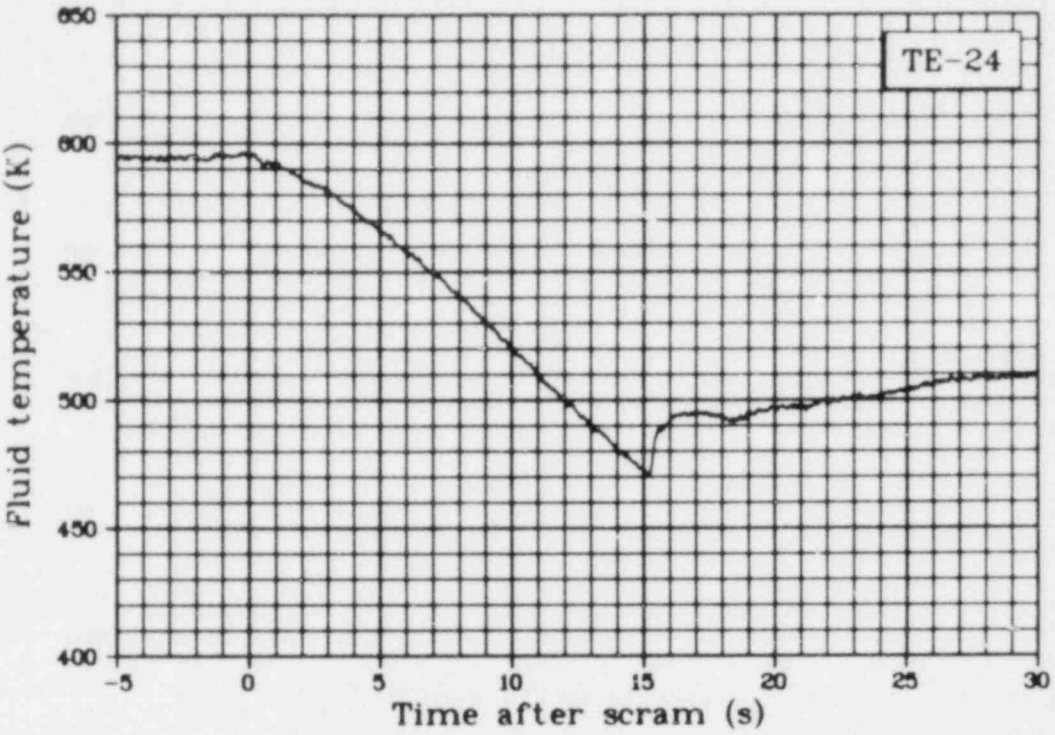

Fig. 170 Fluid temperature in cold leg blowdown spool (TE-24), Test LOC-11C.

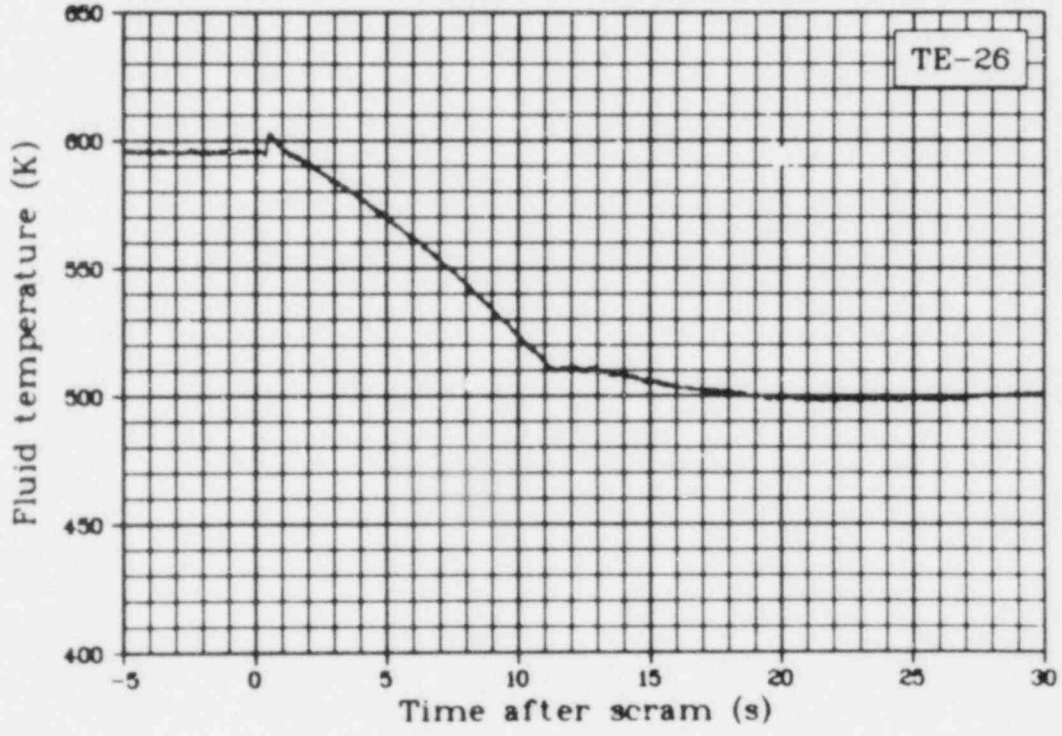

Fig. 171 Fluid temperature in hot leg blowdown spool (TE-26), Test LOC-11C.

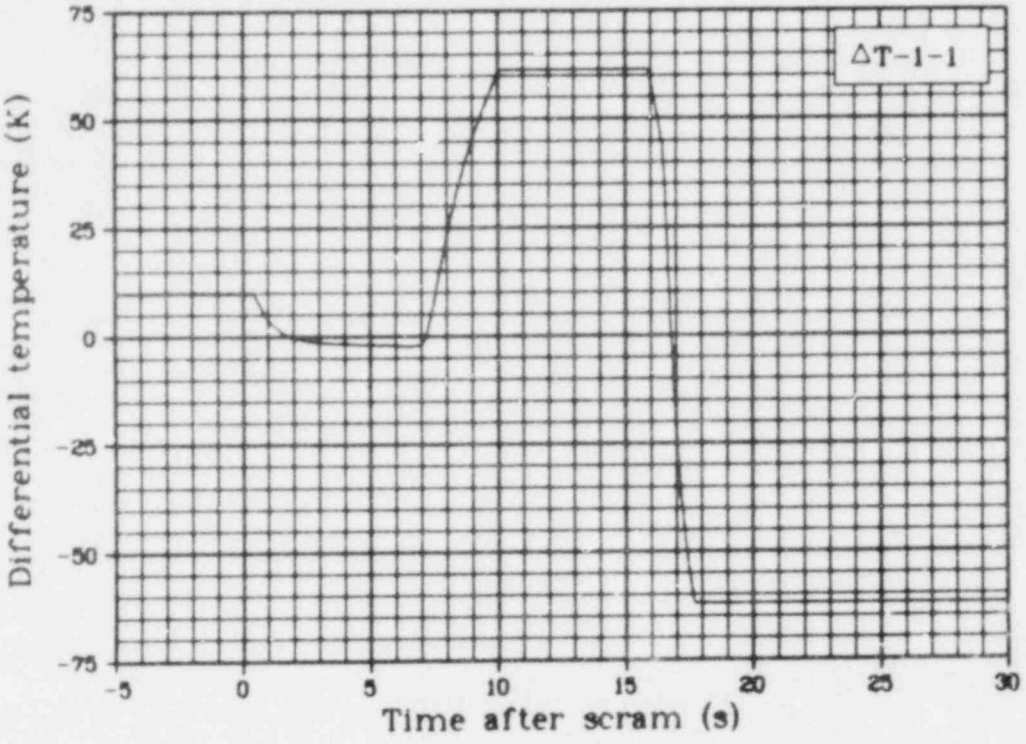

Fig. 172 Differential temperature at fuel inlet and outlet Rod 1 (ΔT-1-1), Test LOC-11C.

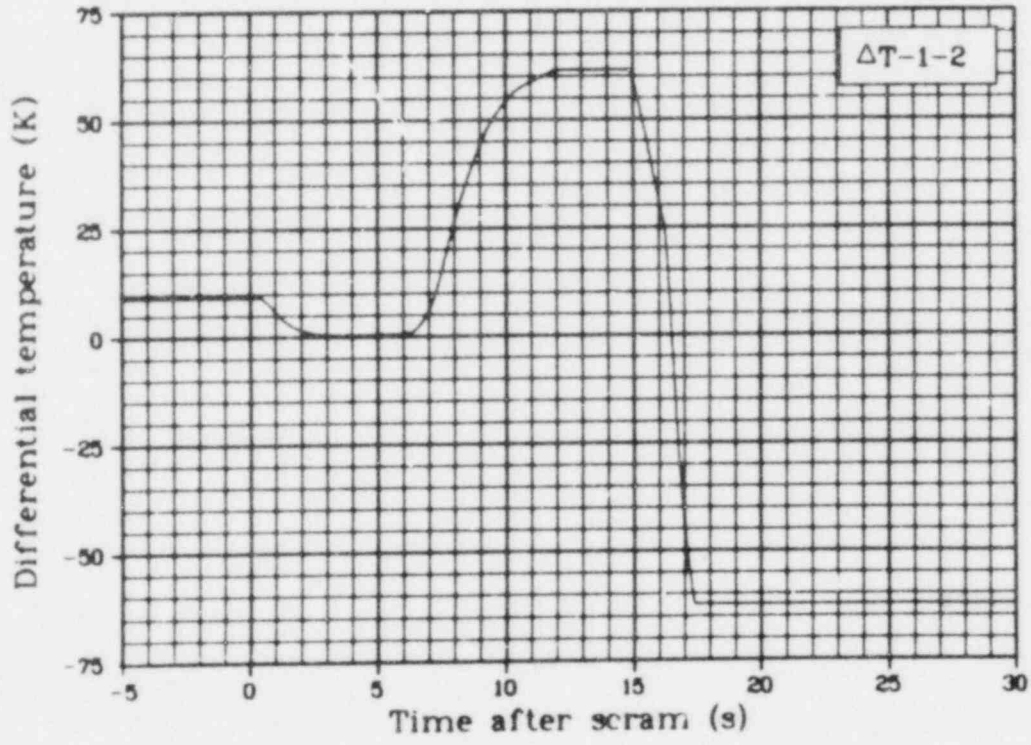

Fig. 173 Differential temperature at fuel inlet and outlet Rod 2 (ΔT-1-2), Test LOC-11C.

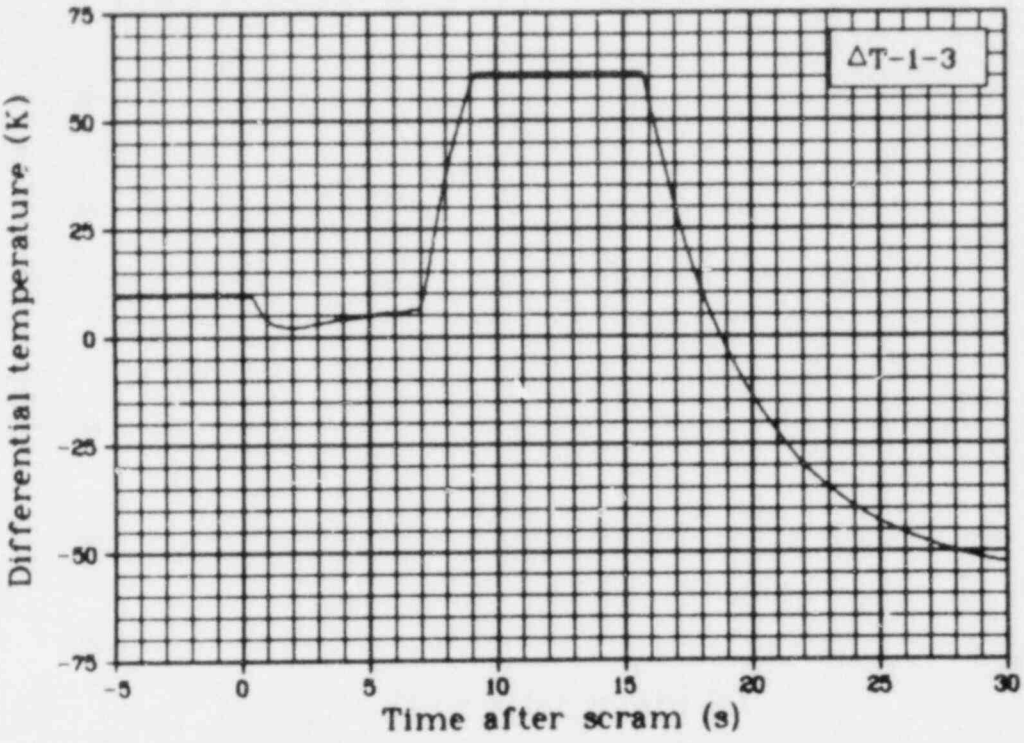

Fig. 174 Differential temperature at fuel inlet and outlet Rod 3 (ΔT-1-3), Test LOC-11C.

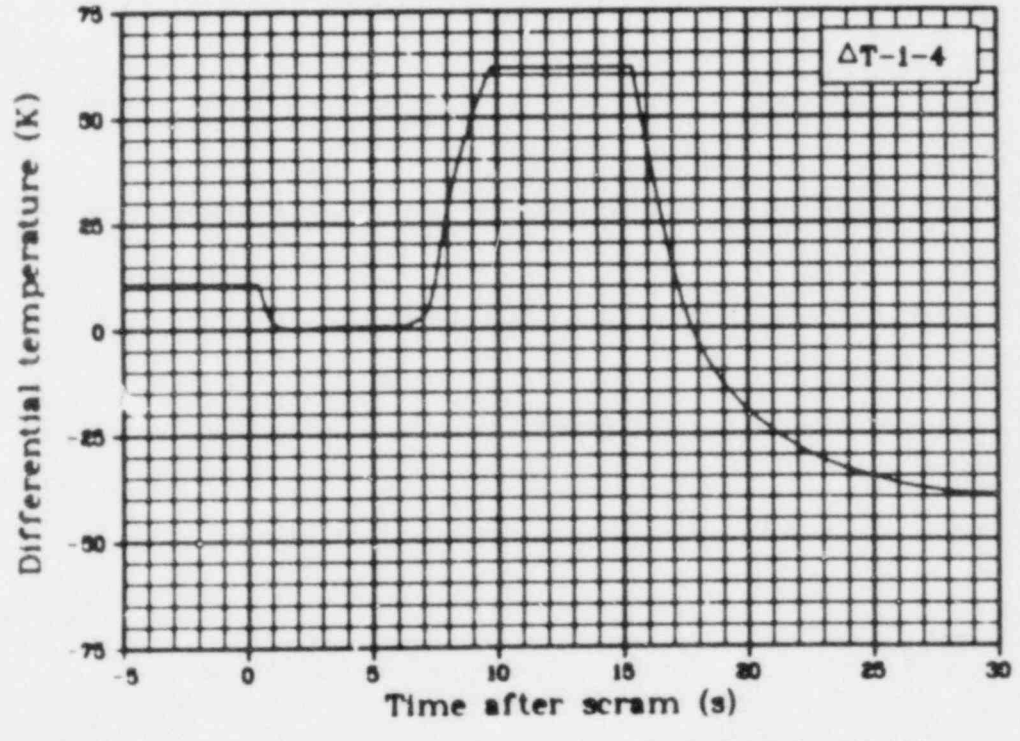

Fig. 175 Differential temperature at fuel inlet and outlet Rod 4 (ΔT-1-4), Test LOC-11C.

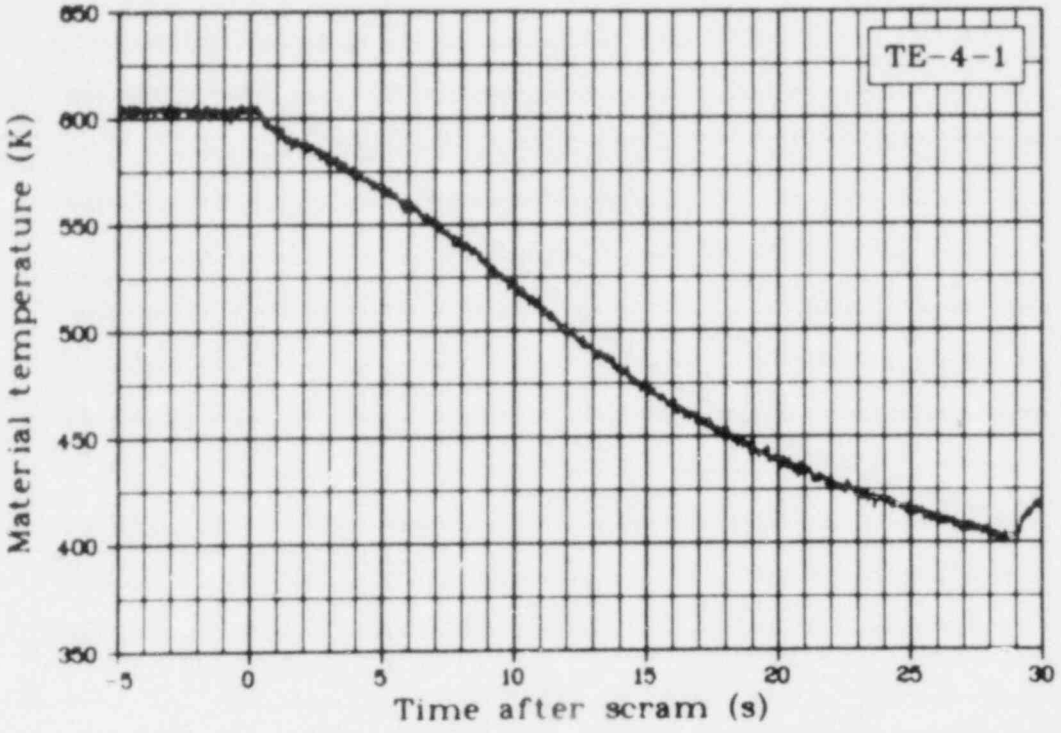

Fig. 176 Material temperature Rod 1, 0.61 m above fuel stack bottom (TE-4-1), Test LOC-11C.

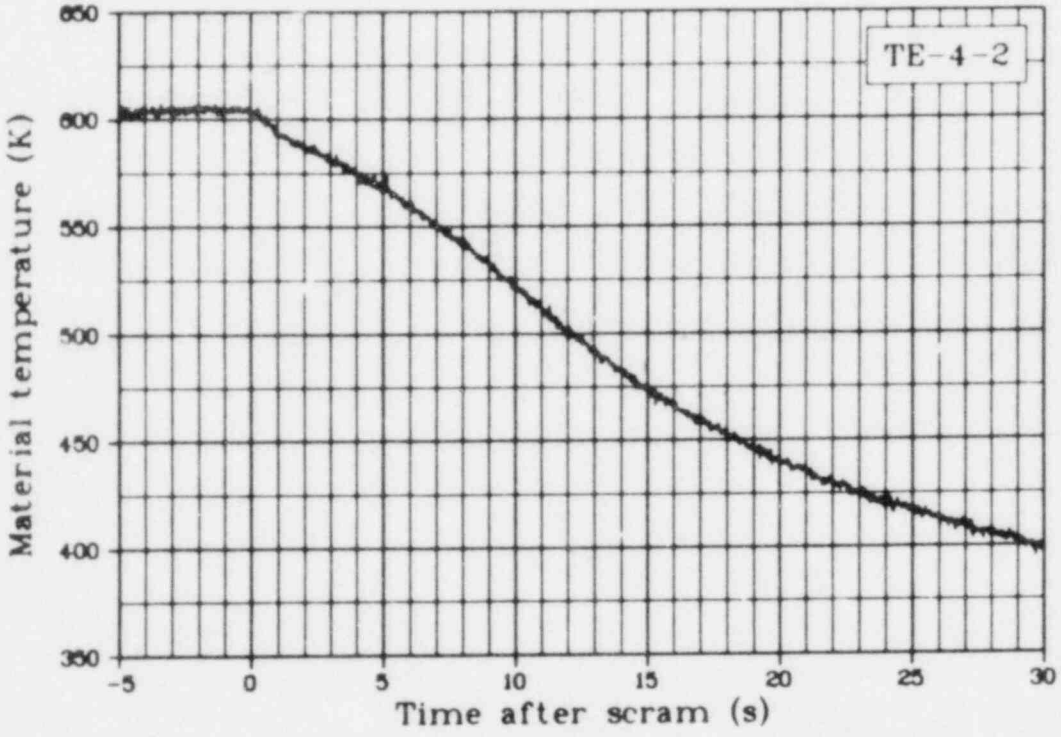

Fig. 177 Material temperature Rod 2, 0.61 m above fuel stack bottom (TE-4-2), Test LOC-11C.

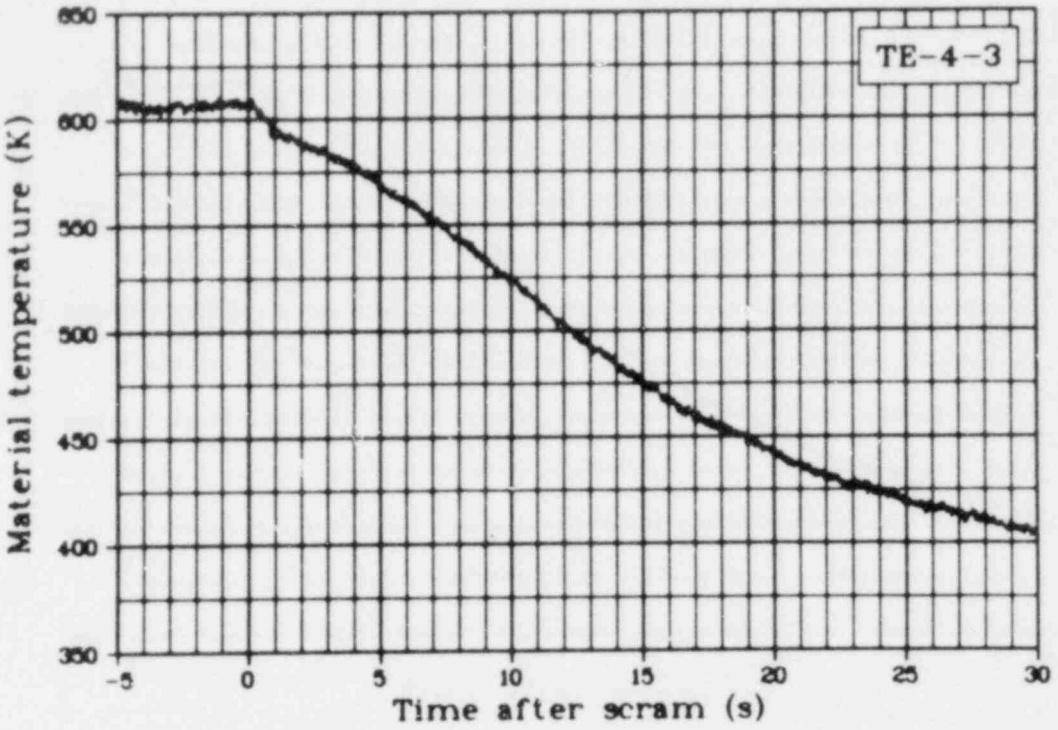

Fig. 178 Material temperature Rod 3, 0.61 m above fuel stack bottom (TE-4-3), Test LOC-11C.

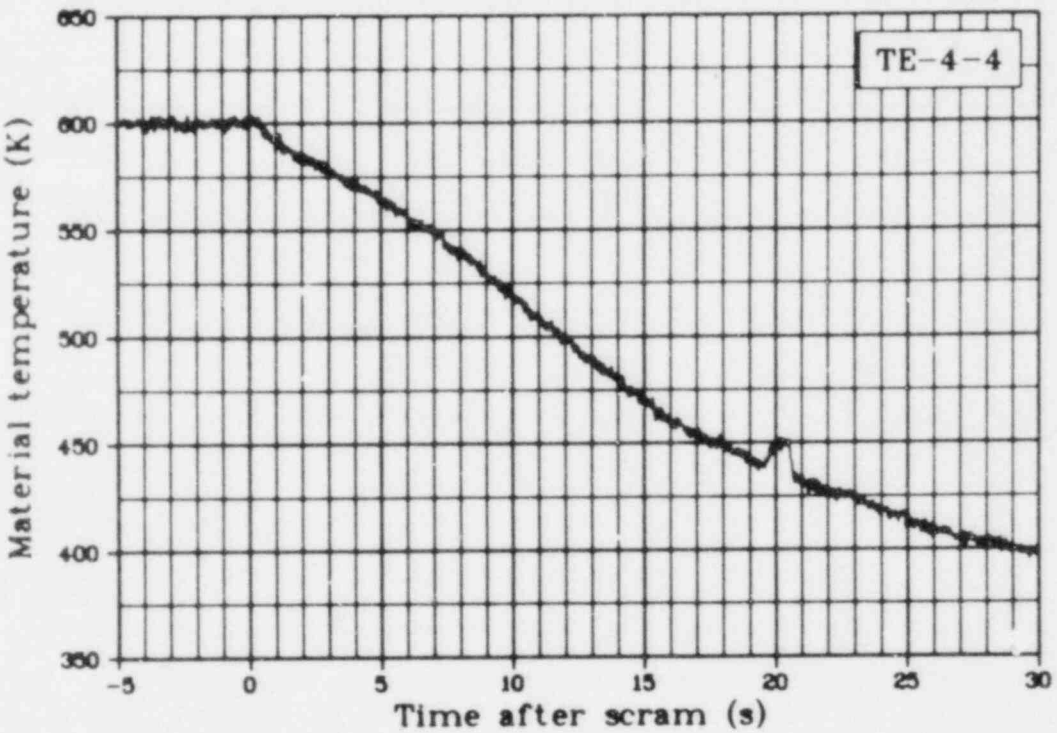

Fig. 179 Material temperature Rod 4, 0.61 m above fuel stack bottom (TE-4-4), Test LOC-11C.

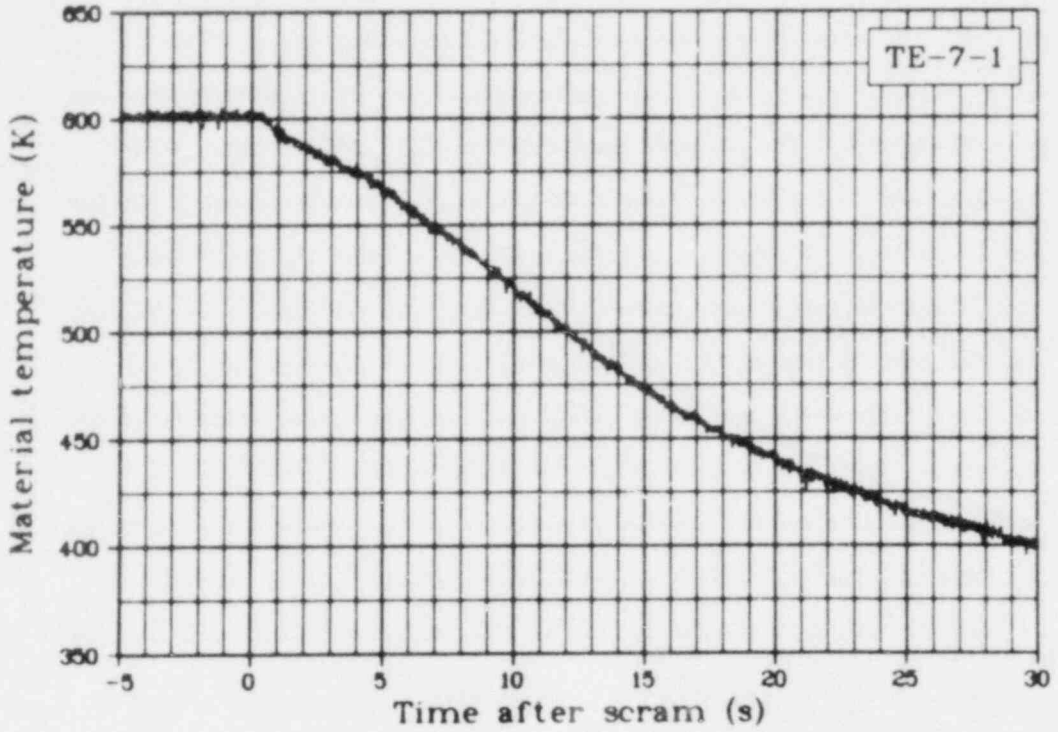

Fig. 180 Material temperature Rod 1, 0.46 m above fuel stack bottom (TE-7-1), Test LOC-11C.

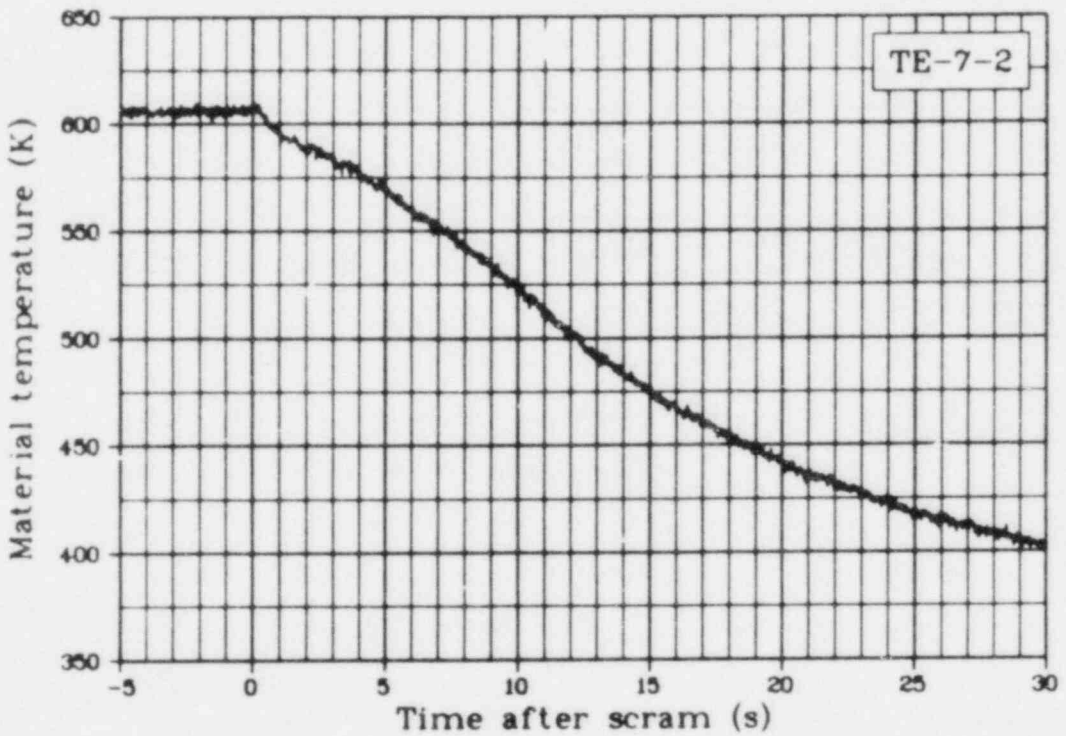

Fig. 181 Material temperature Rod 2, 0.46 m above fuel stack bottom (TE-7-2), Test LOC-11C.

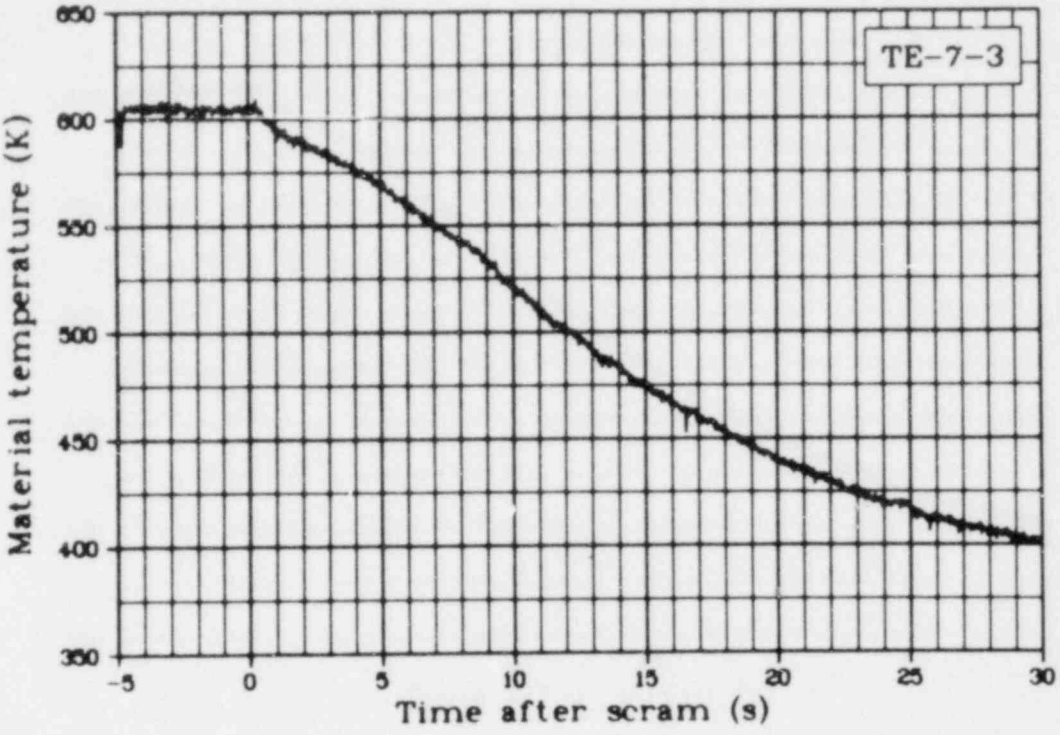

Fig. 182 Material temperature Rod 3, 0.46 m above fuel stack bottom (TE-7-3), Test LOC-11C.

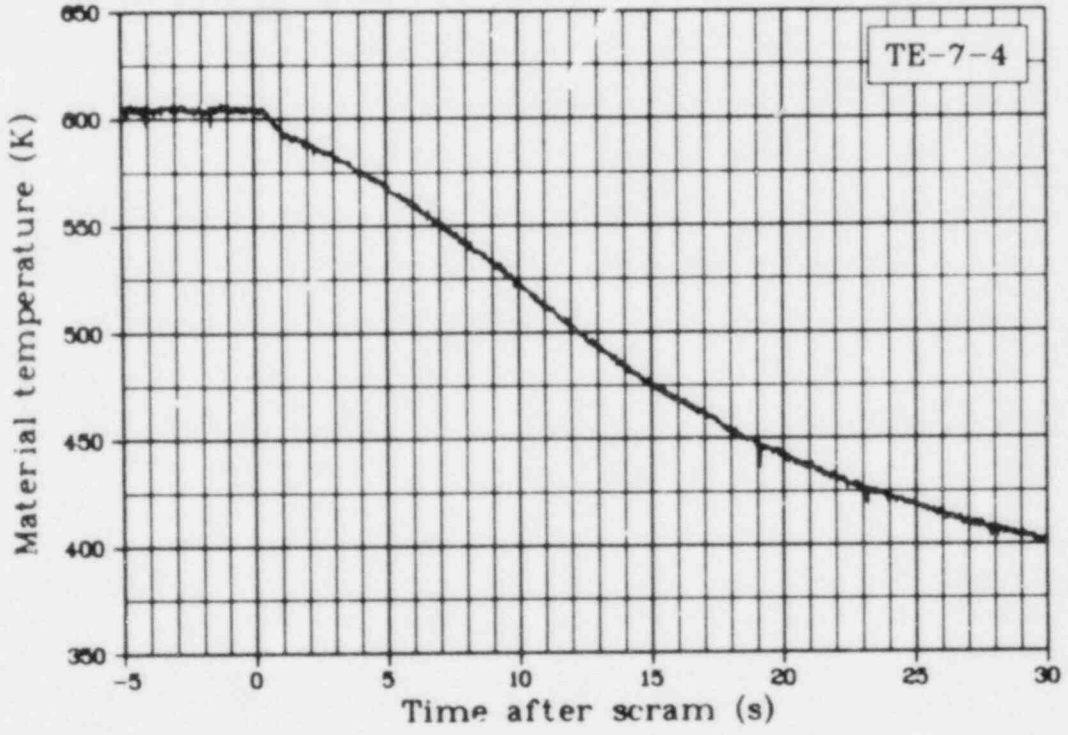

Fig. 183 Material temperature Rod 4, 0.46 m above fuel stack bottom (TE-7-4), Test LOC-11C.

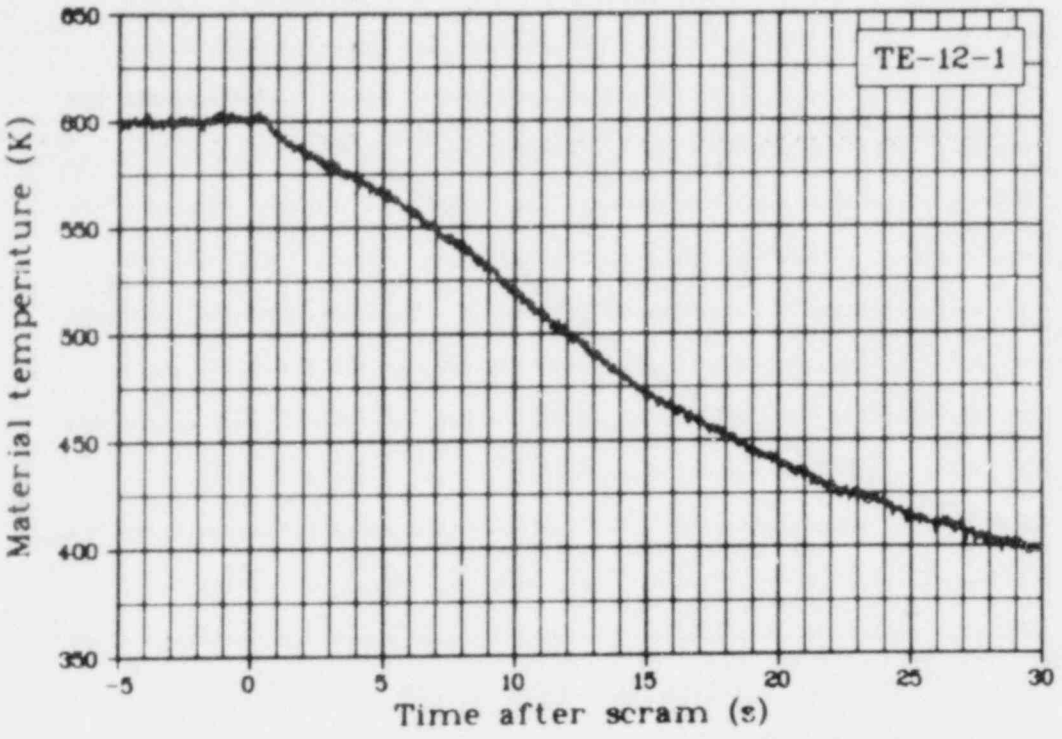

Fig. 184 Material temperature Rod 1, 0.30 m above fuel stack bottom (TE-12-1), Test LOC-11C.

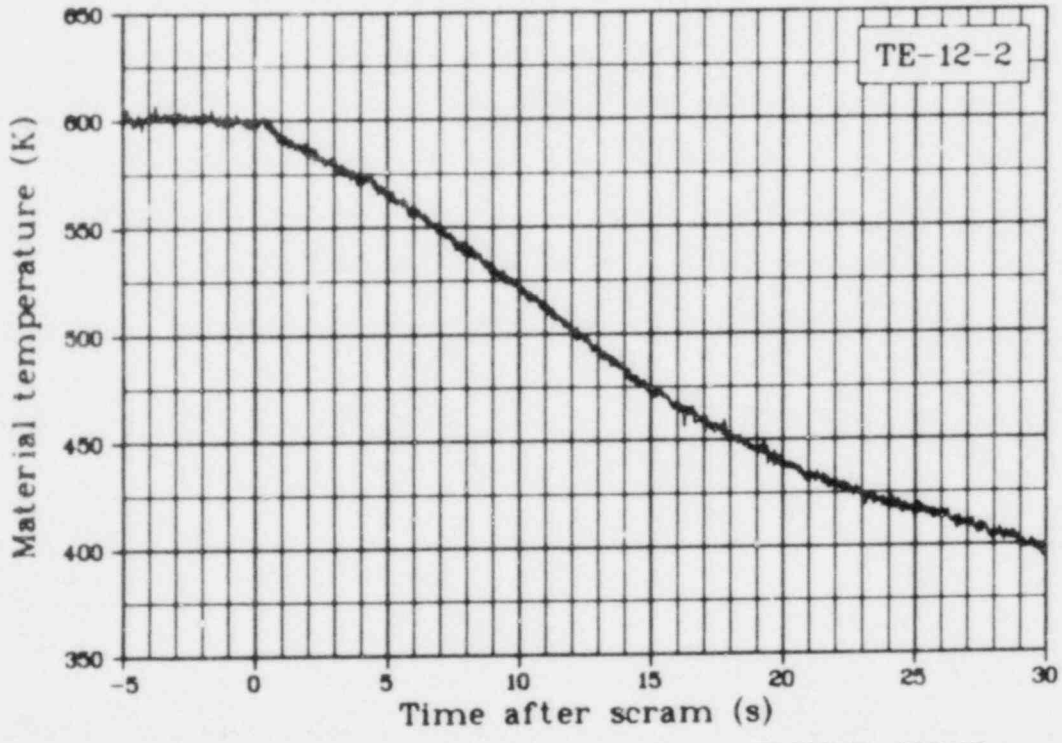

Fig. 185 Material temperature Rod 2, 0.30 m above fuel stack bottom (TE-12-2), Test LOC-11C.

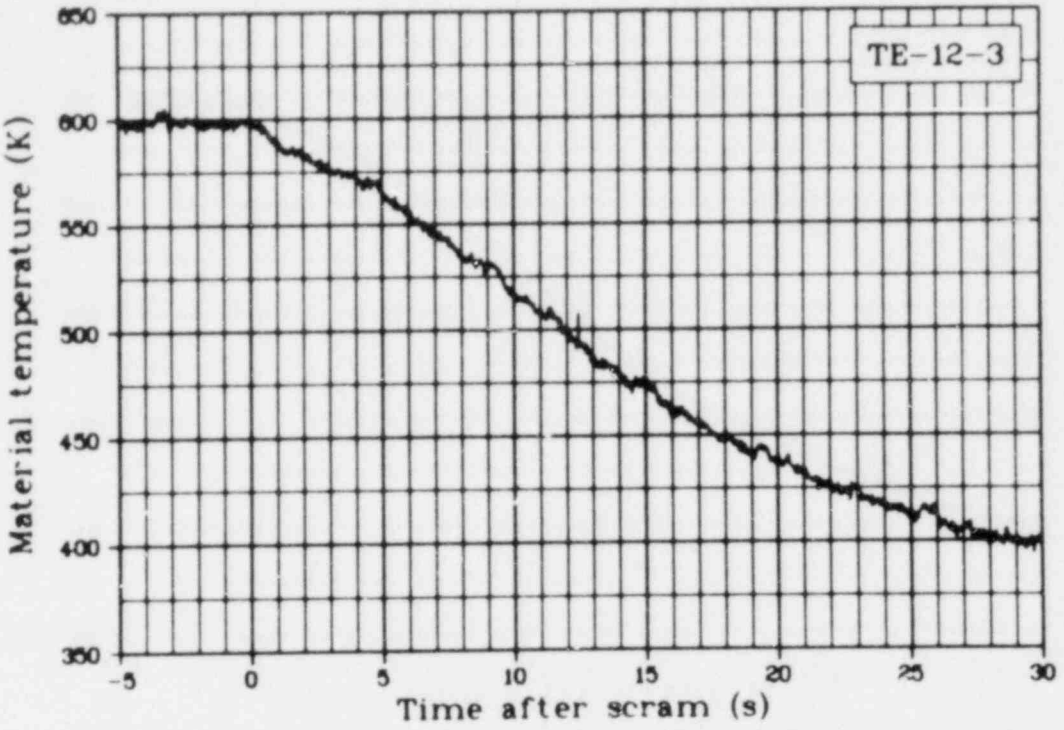

Fig. 186 Material temperature Rod 3, 0.30 m above fuel stack bottom (TE-12-3), Test LOC-11C.

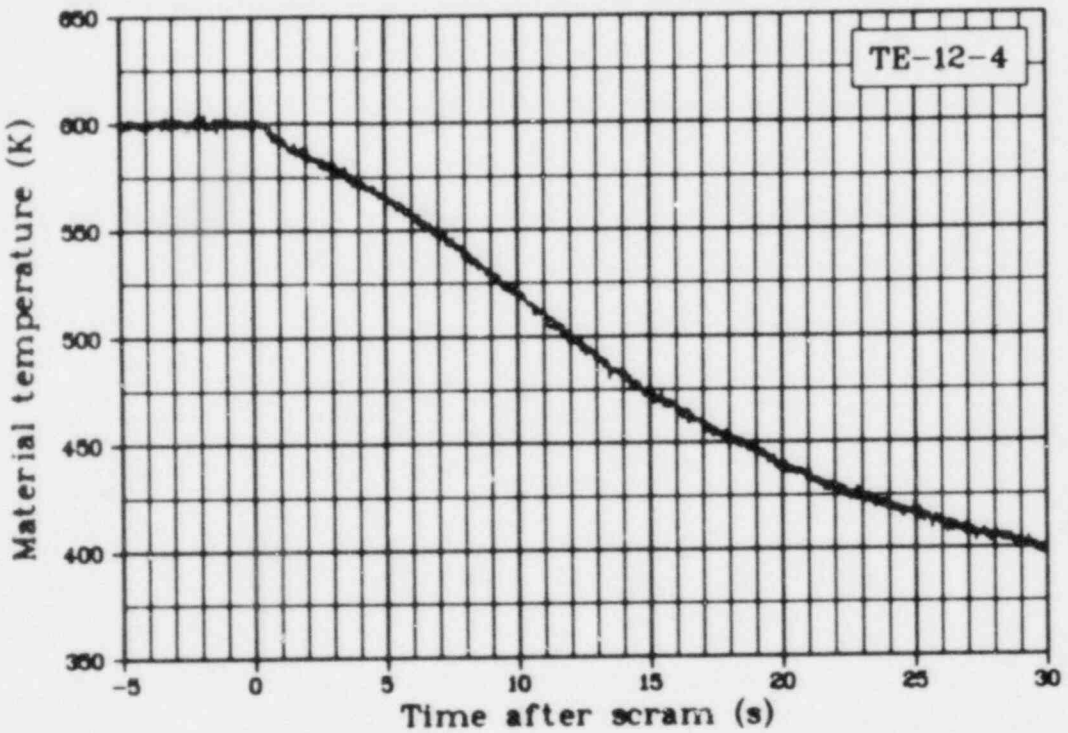

Fig. 187 Material temperature Rod 4, 0.30 m above fuel stack bottom (TE-12-4), Test LOC-11C.

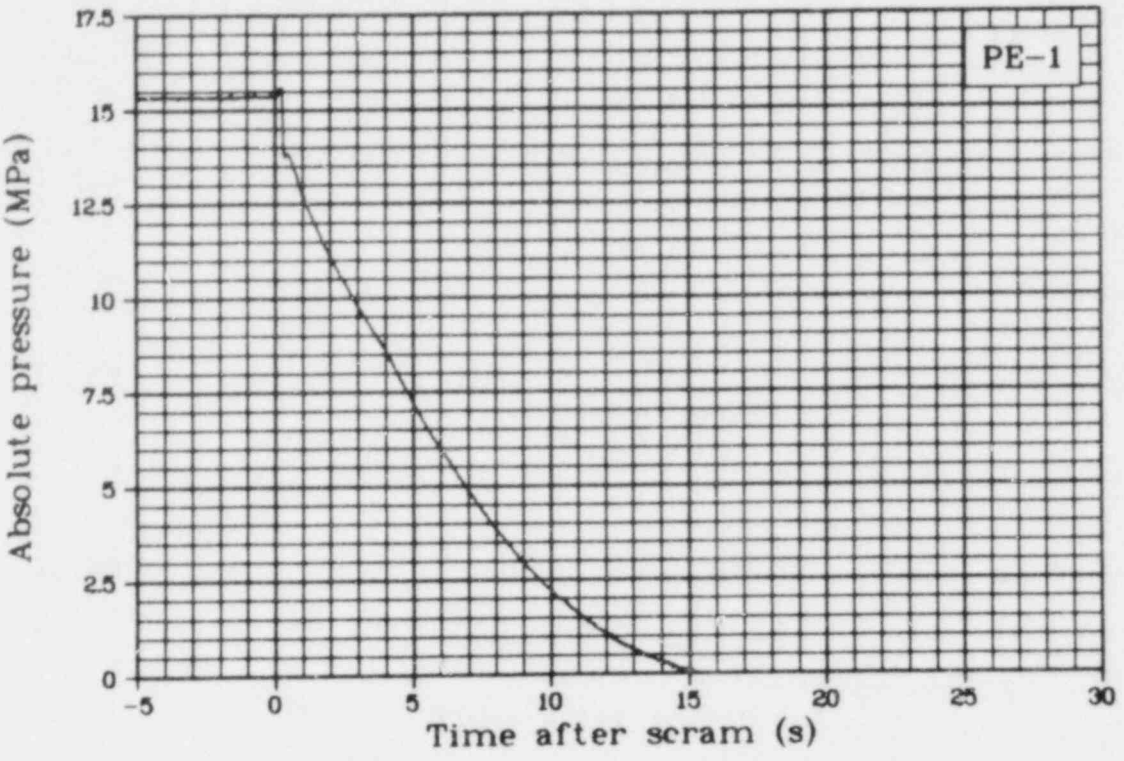

Fig. 188 Absolute pressure in upper test train (PE-1), Test LOC-11C.

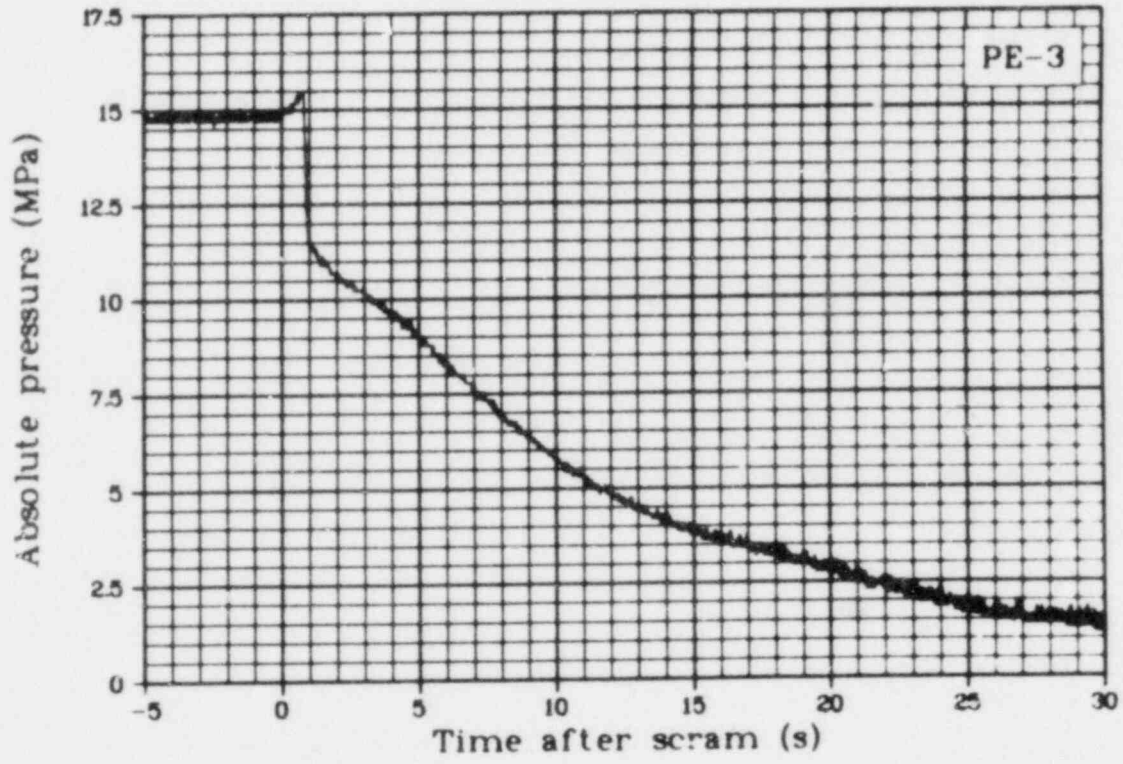

Fig. 189 Absolute pressure in upper test train (PE-3), Test LOC-11C.

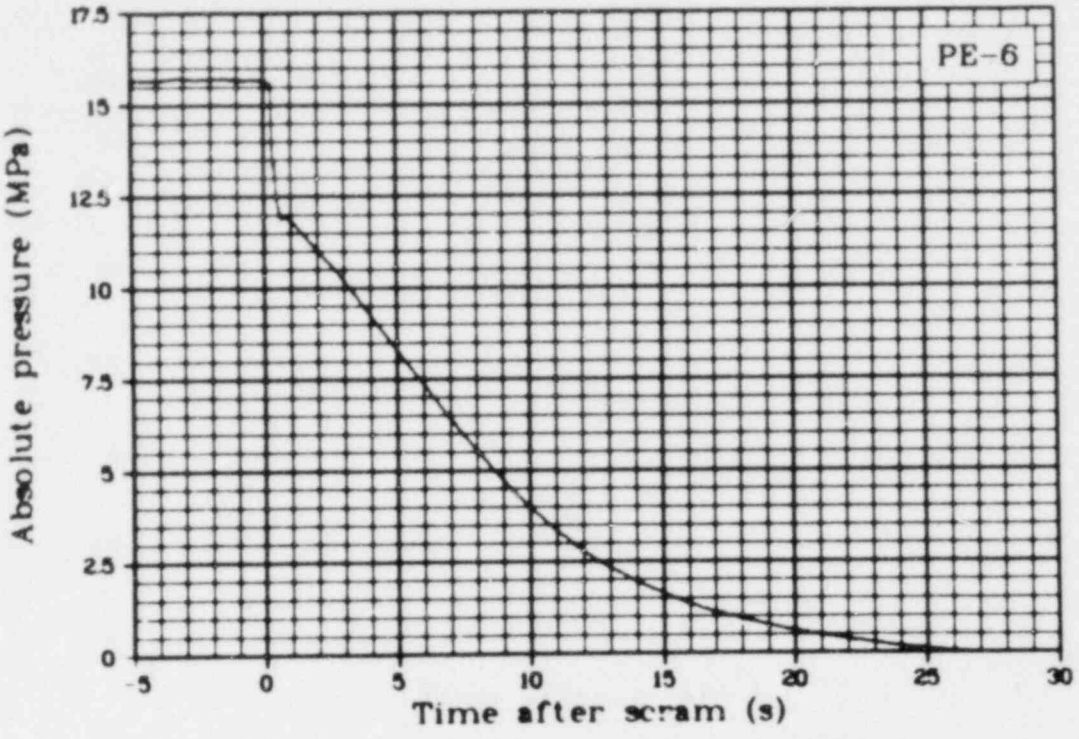

Fig. 190 Absolute pressure below test train fuel rod (PE-6), Test LOC-11C.

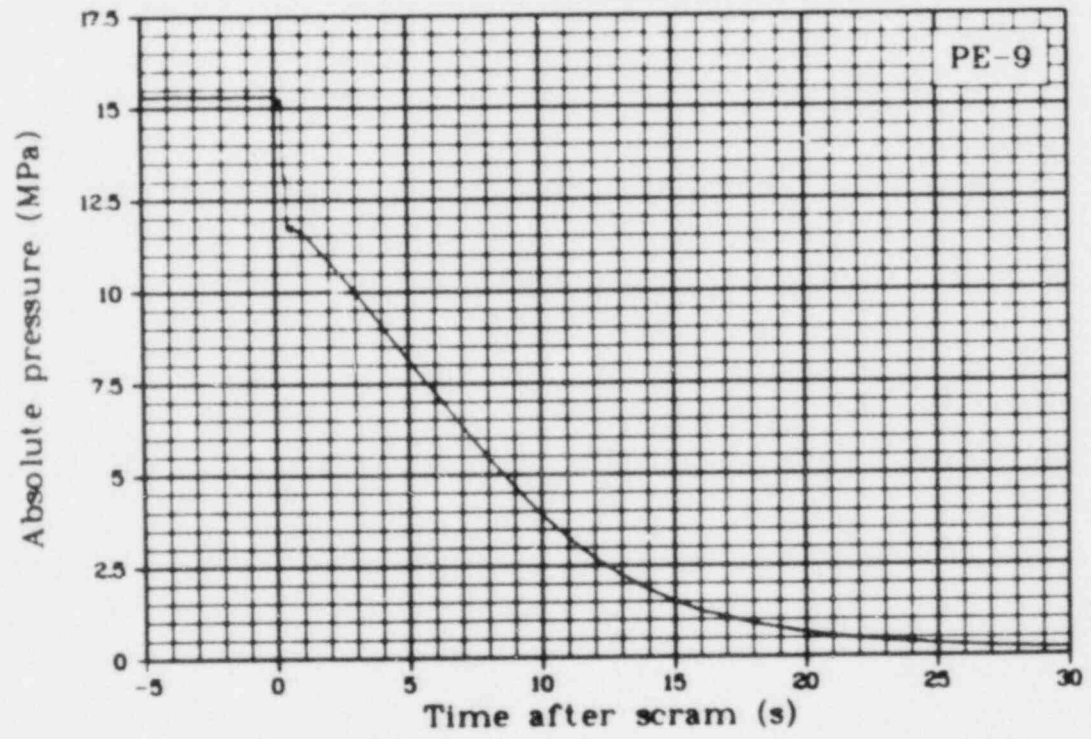

Fig. 191 Absolute pressure in inlet spool (PE-9), Test LOC-11C.

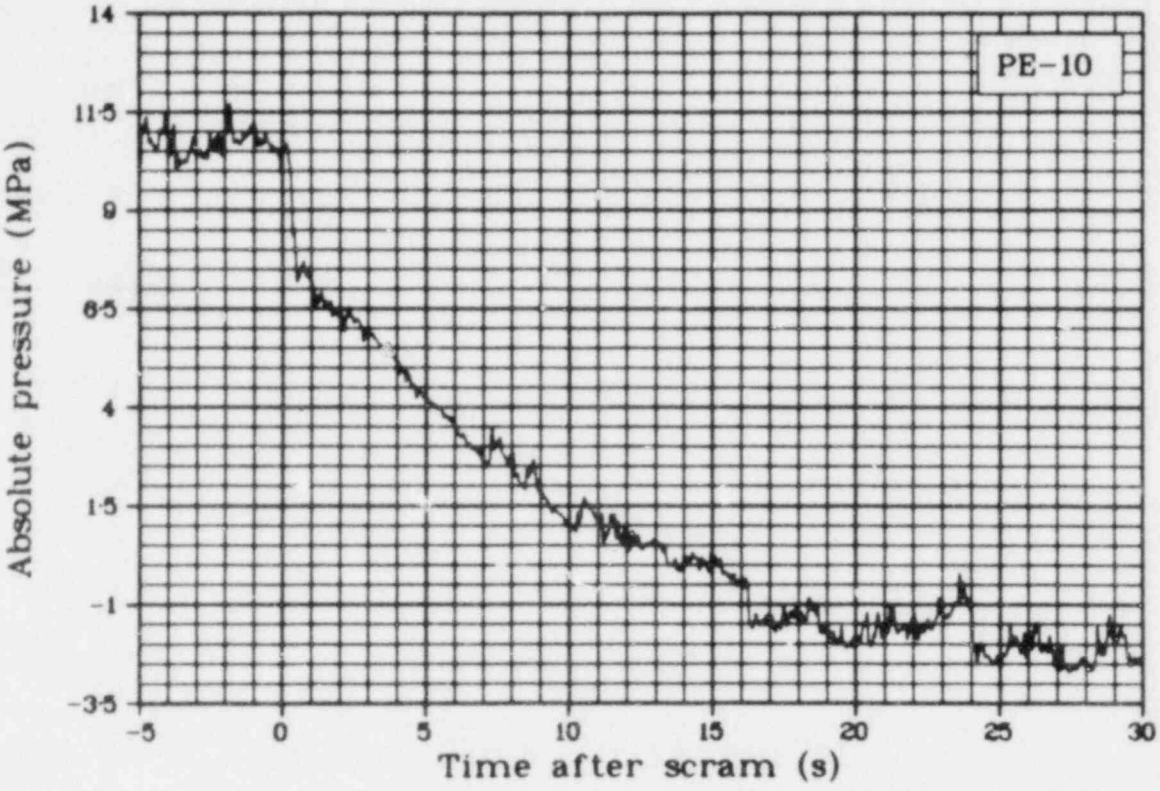

Fig. 192 Absolute pressure in cold leg blowdown spool (PE-10), Test LOC-11C.

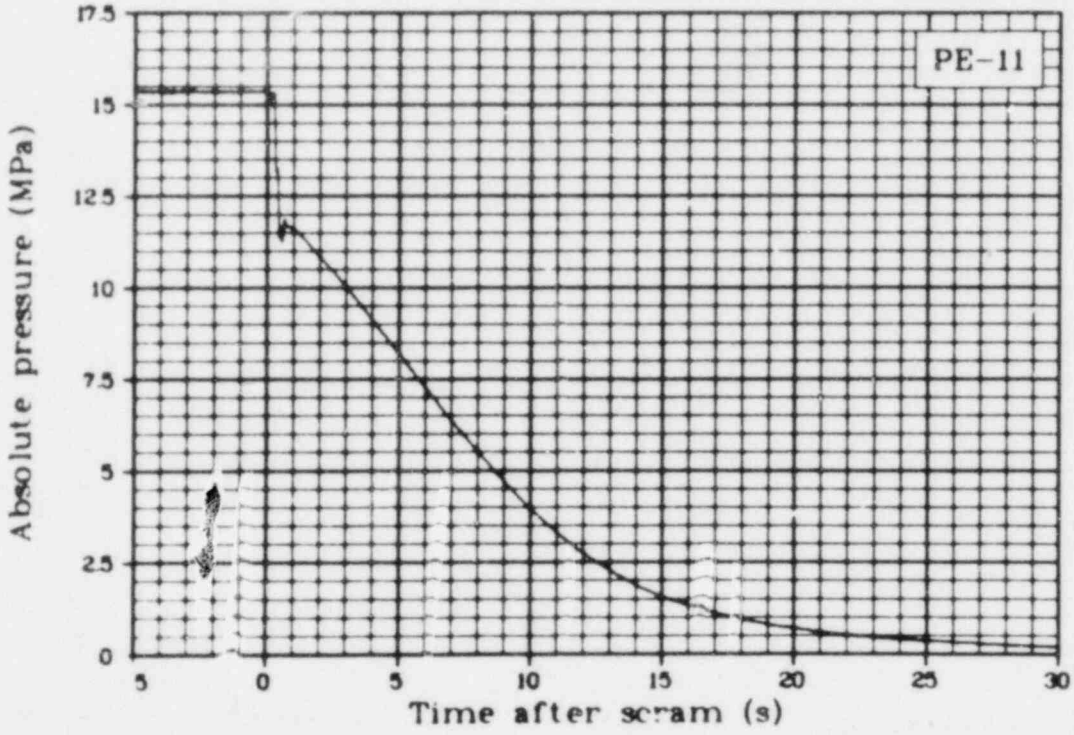

Fig. 193 Absolute pressure in cold leg blowdown spool (PE-11), Test LOC-11C.

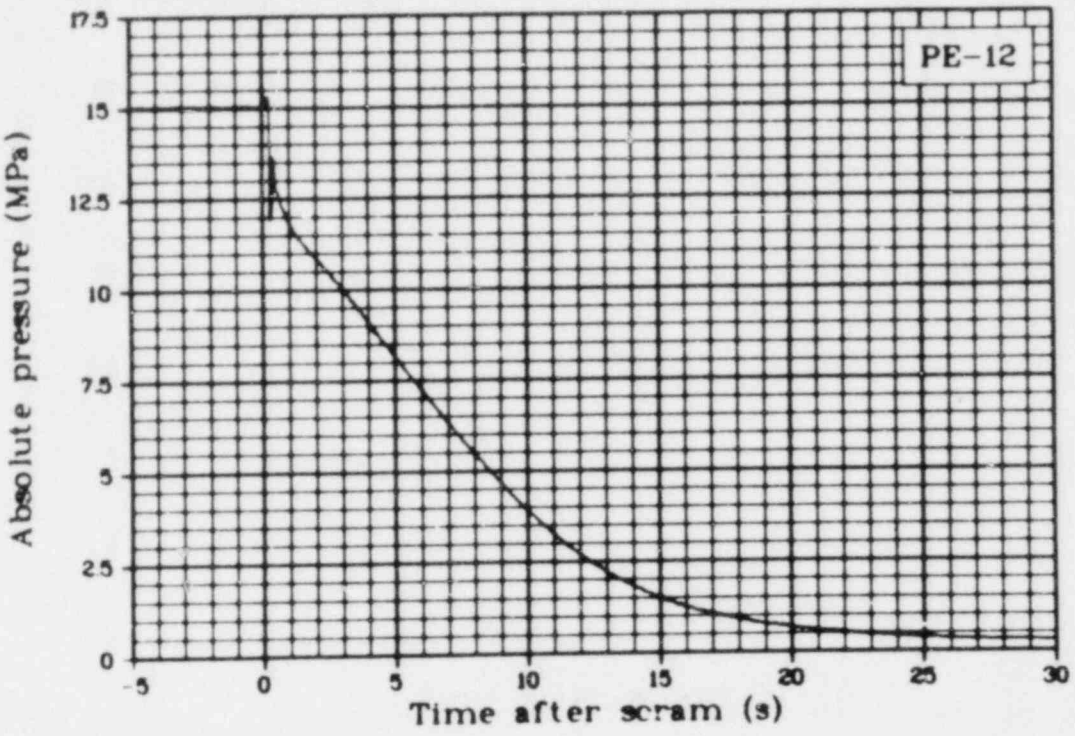

Fig. 194 Absolute pressure in hot leg blowdown spool (PE-12), Test LOC-11C.

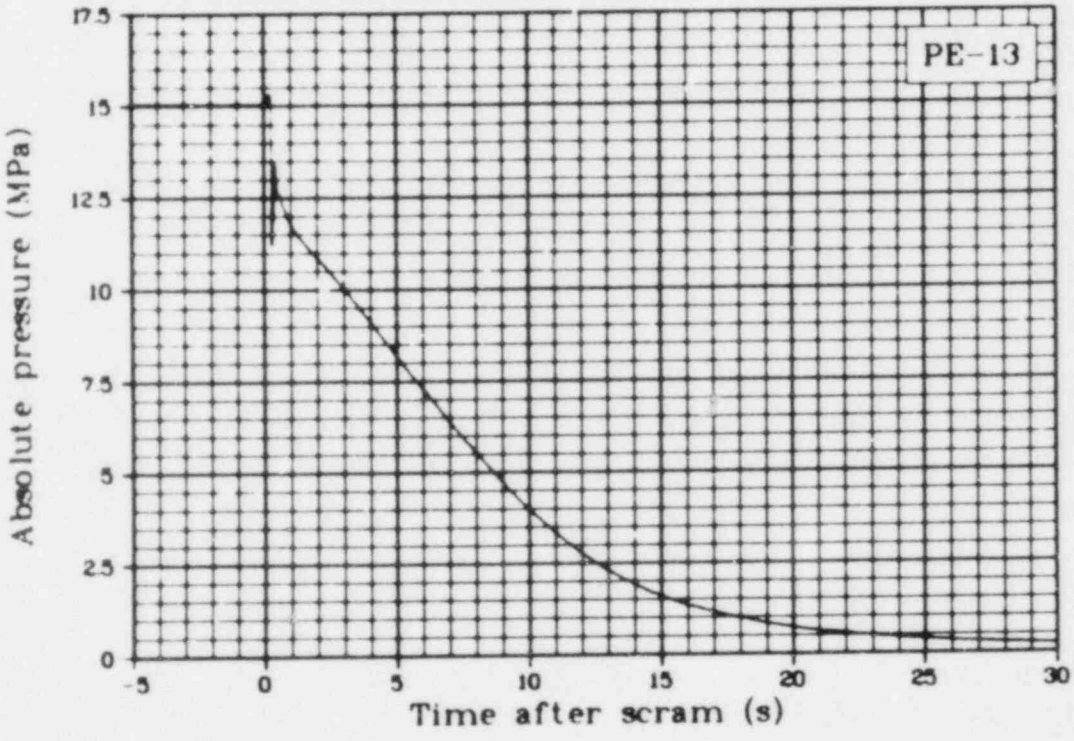

Fig. 195 Absolute pressure in hot leg blowdown spool (PE-13), Test LOC-11C.

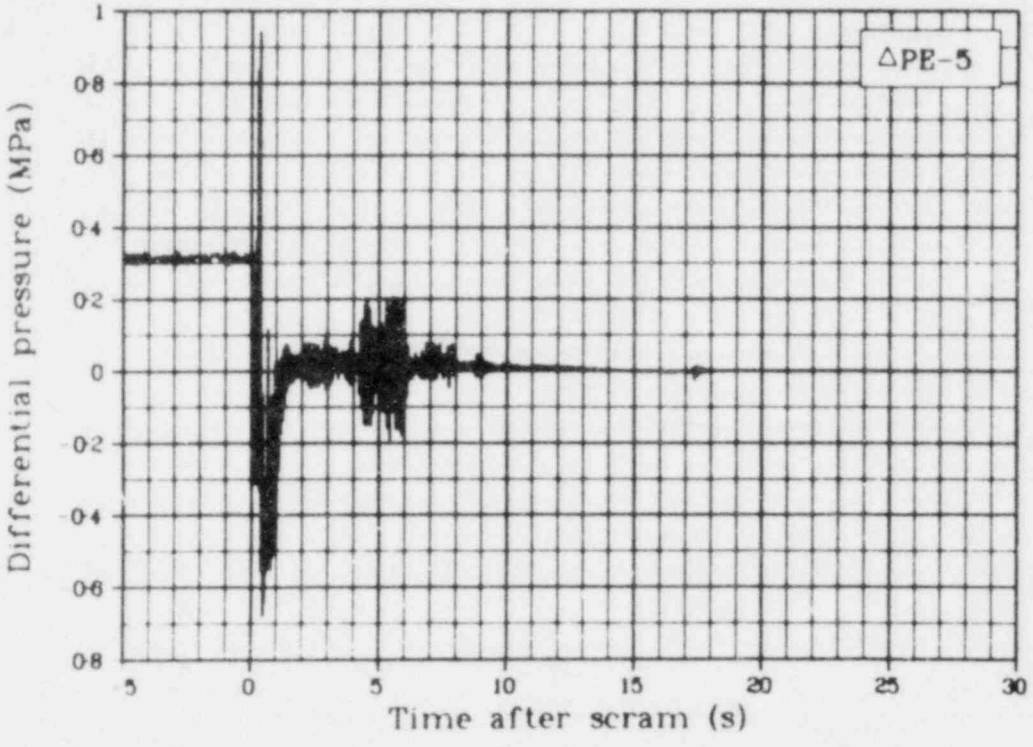

Fig. 196 Differential pressure between blowdown spools (ΔPE-5), Test LOC-11C.

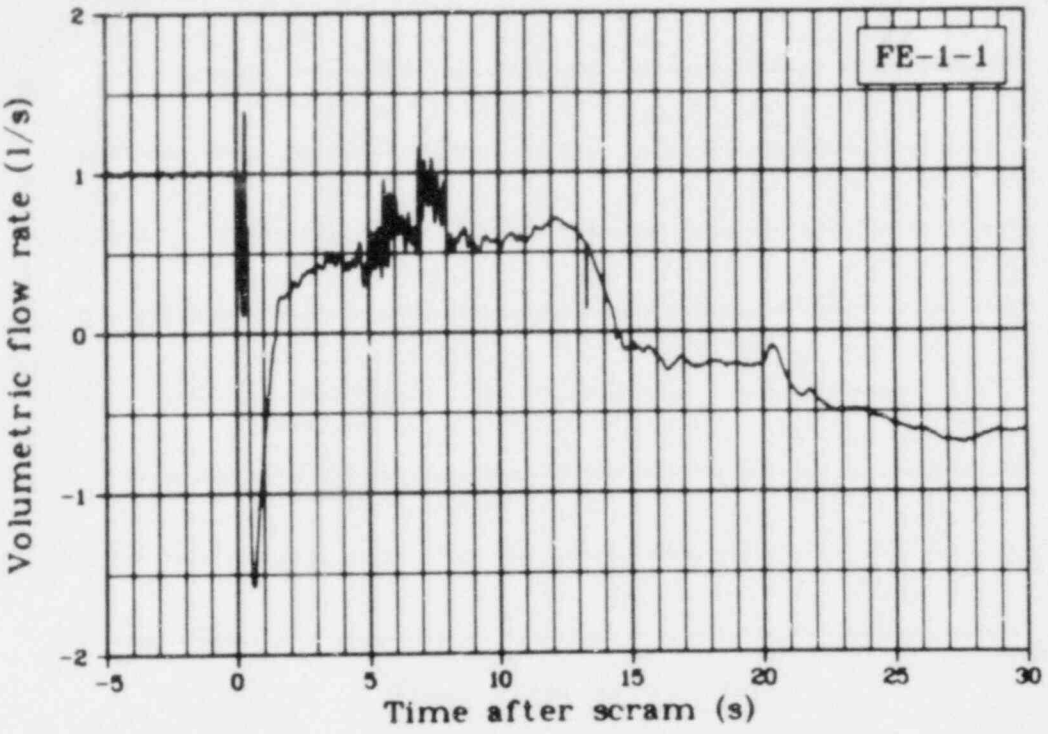

Fig. 197 Volumetric flow rate in fuel Rod 1 upper shroud (FE-1-1), Test LOC-11C.

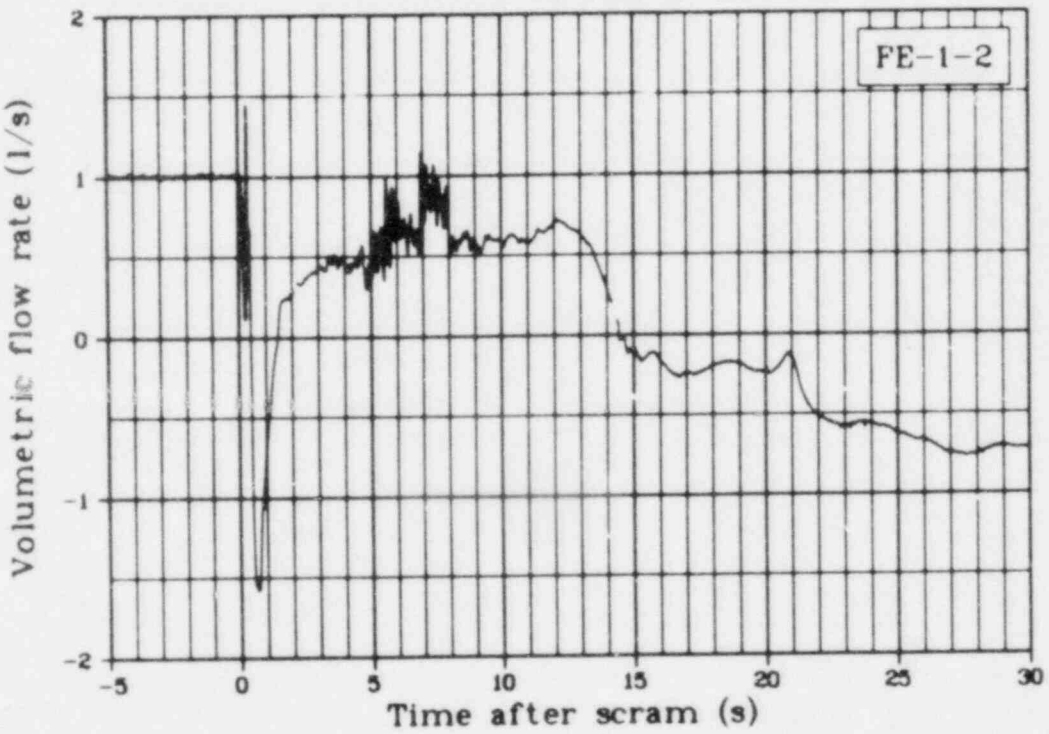

Fig. 198 Volumetric flow rate in fuel Rod 2 upper shroud (FE-1-2), Test LOC-11C.

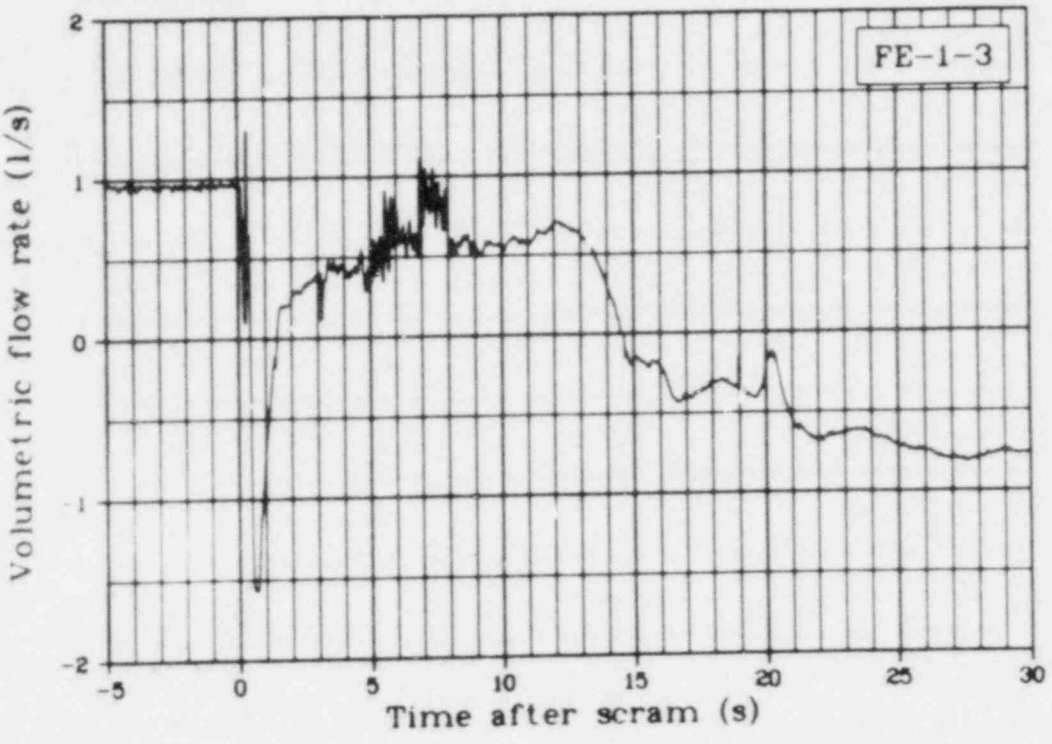

Fig. 199 Volumetric flow rate in fuel Rod 3 upper shroud (FE-1-3), Test LOC-11C.

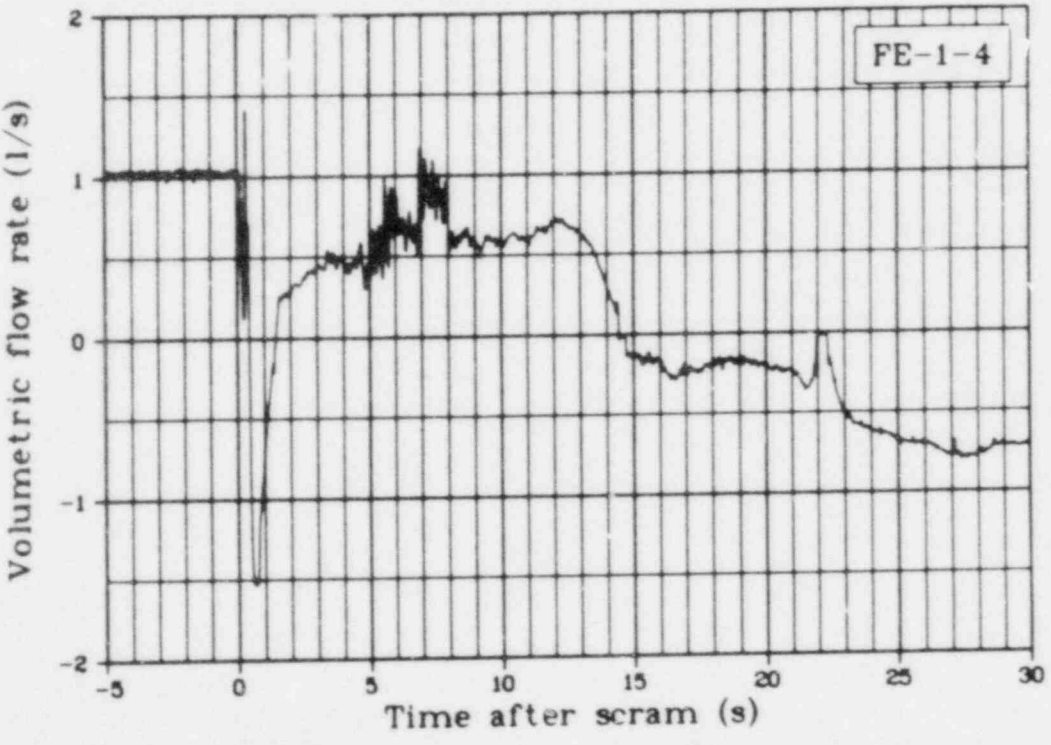

Fig. 200 Volumetric flow rate in fuel Rod 4 upper shroud (FE-1-4), Test LOC-11C.

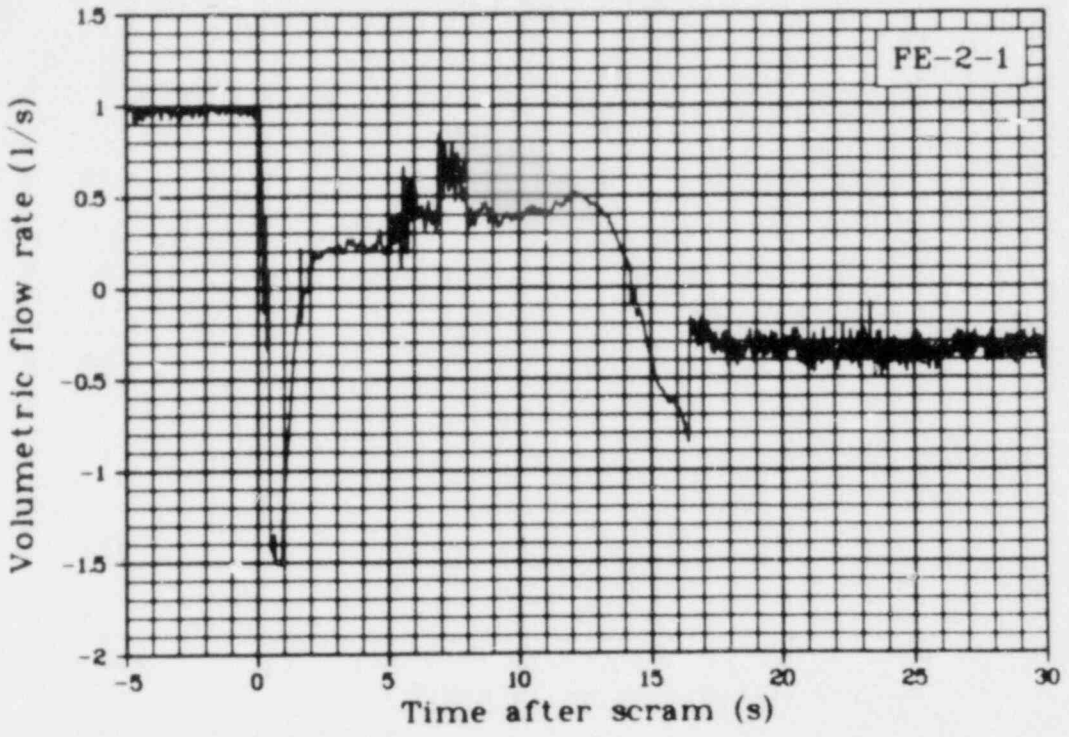

Fig. 201 Volumetric flow rate in fuel Rod 1 lower shroud (FE-2-1), Test LOC-11C.

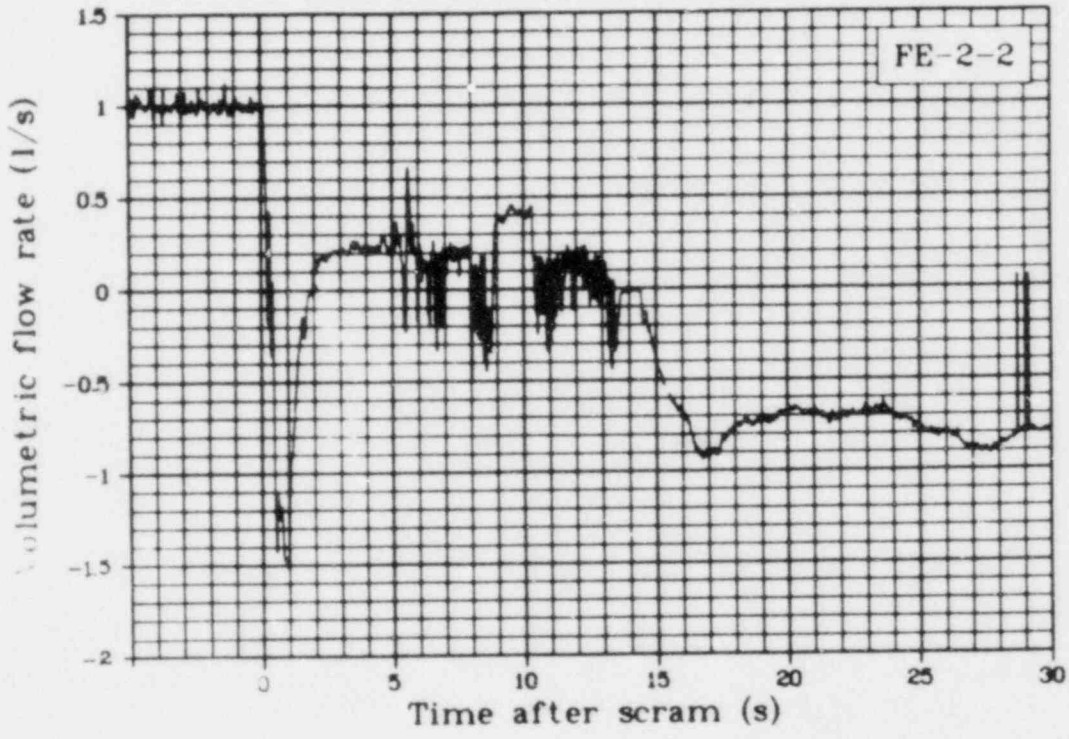

Fig. 202 Volumetric flow rate in fuel Rod 2 lower shroud (FE-2-2), Test LOC-11C.

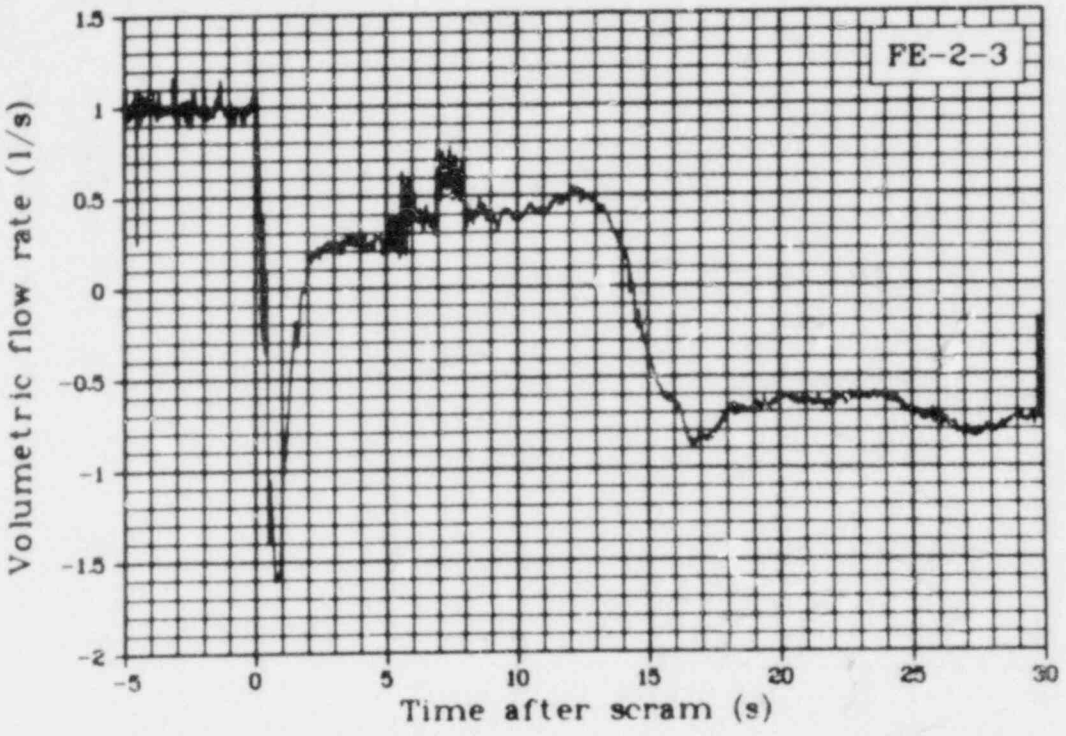

Fig. 203 Volumetric flow rate in fuel Rod 3 lower shroud (FE-2-3), Test LOC-11C.

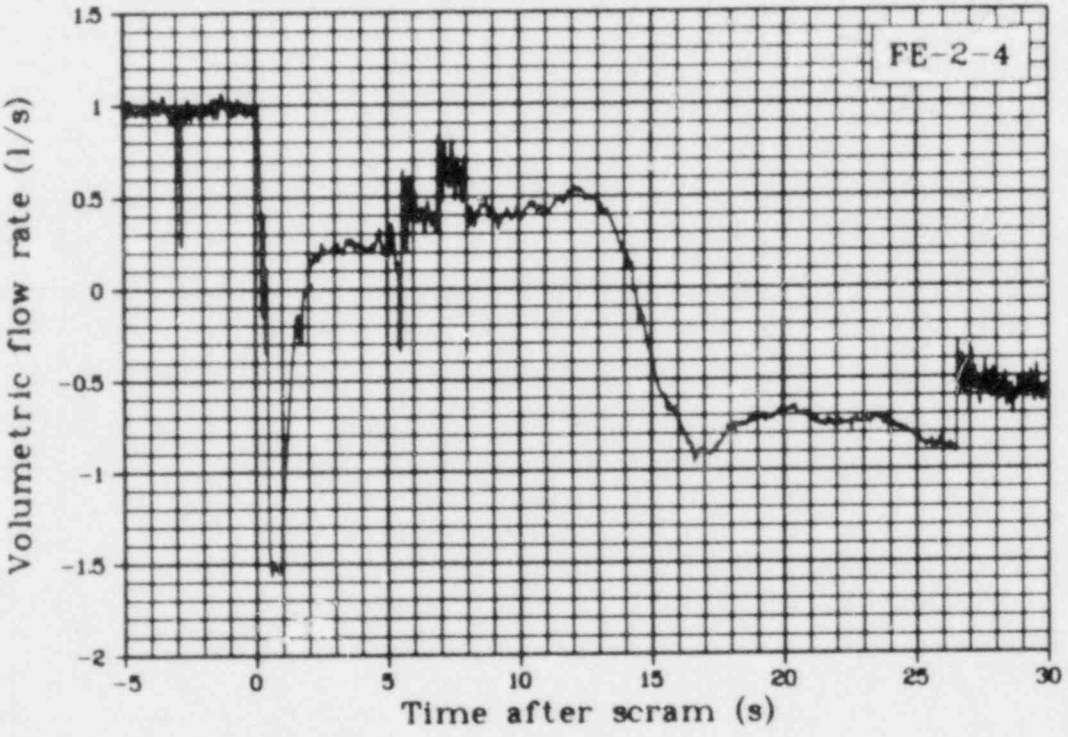

Fig. 204 Volumetric flow rate in fuel Rod 4 lower shroud (FE-2-4), Test LOC-11C.

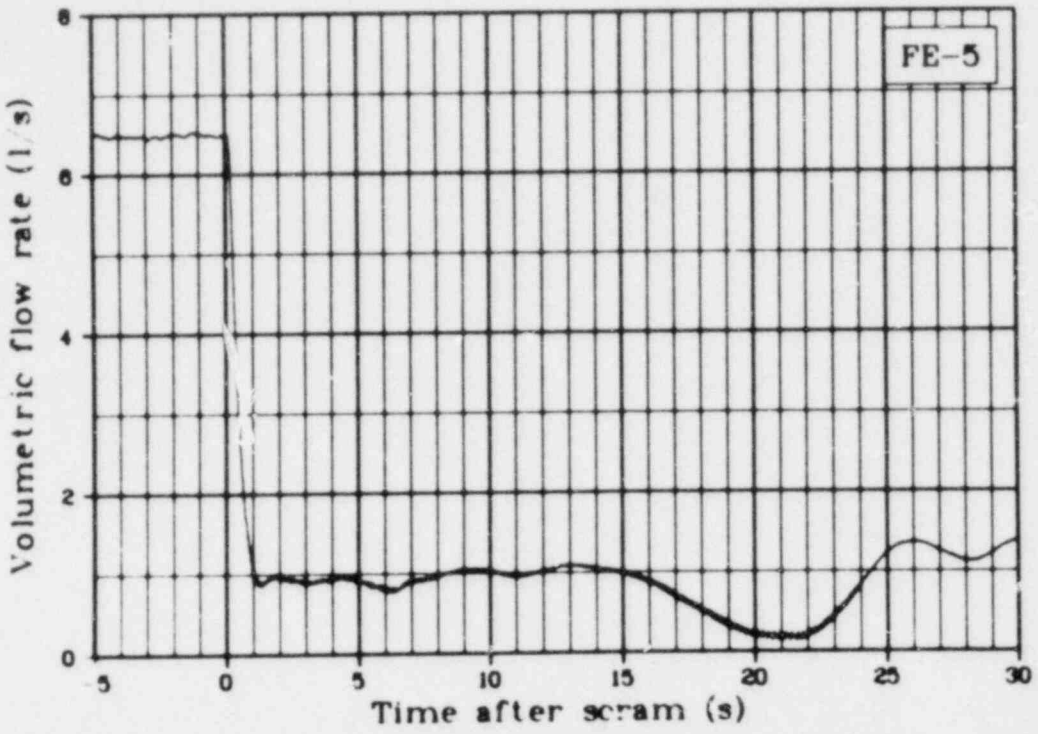

Fig. 205 Volumetric flow rate from flowmeter in inlet spool (FE-5), Test LOC-11C.

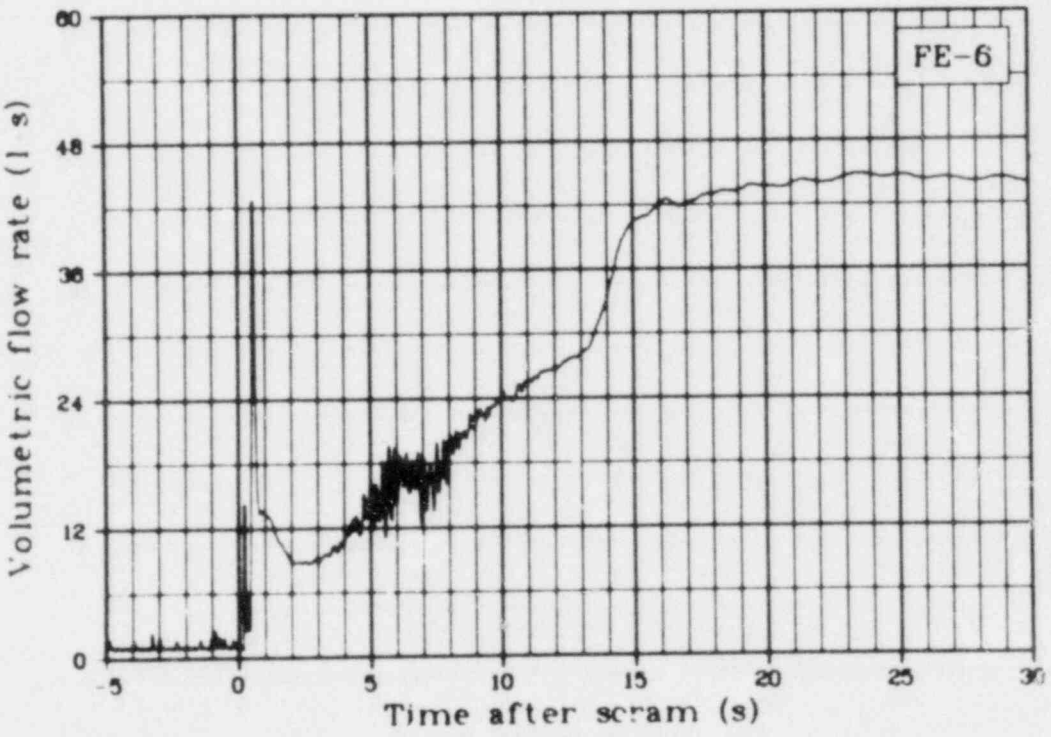

Fig. 206 Volumetric flow rate in cold leg blowdown spool (FE-6), Test LOC-11C.

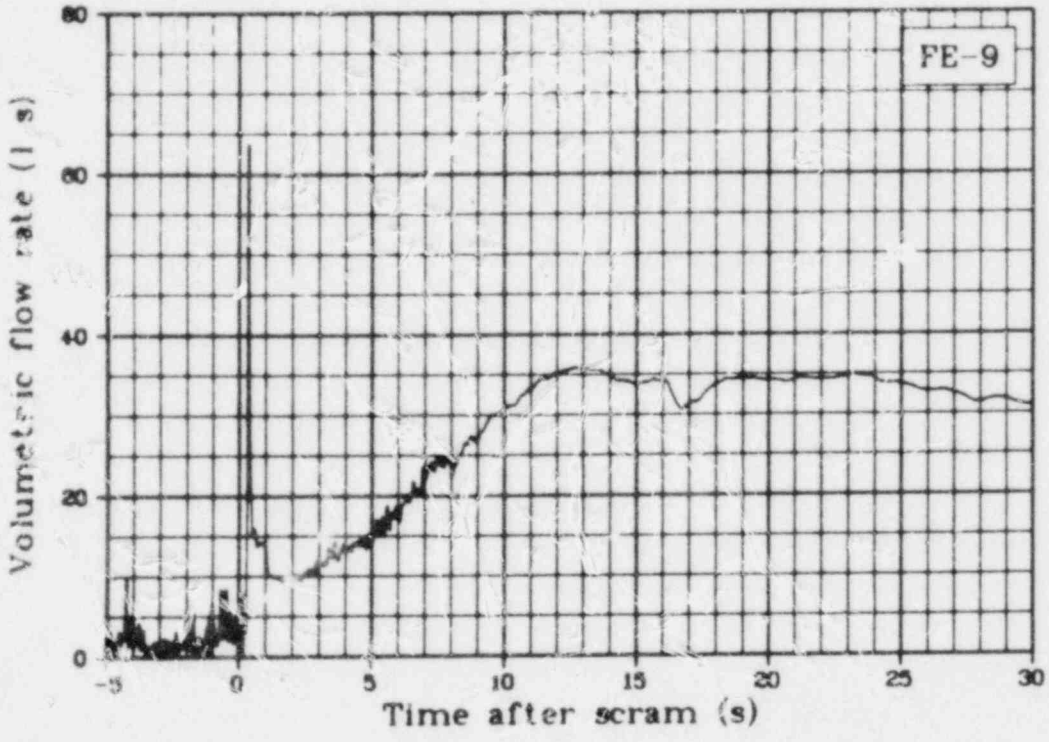

Fig. 207 Volumetric flow rate in hot leg blowdown spool (FE-9), Test LOC-11C.

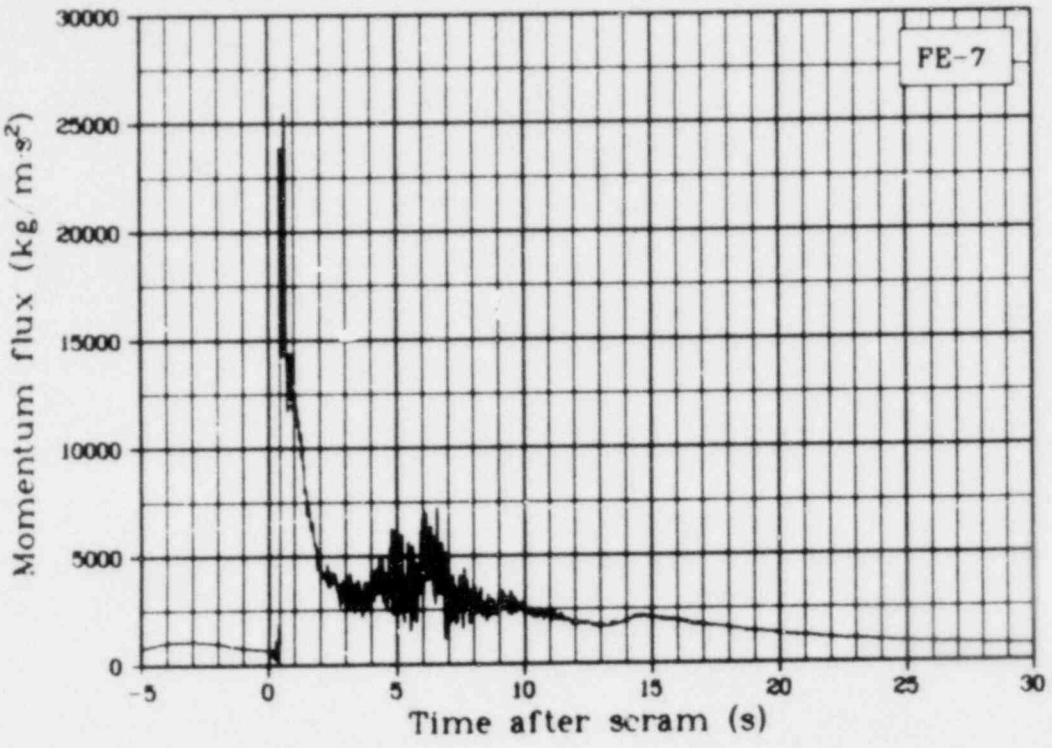

Fig. 208 Momentum flux in cold leg blowdown spool (FE-7), Test LOC-11C.

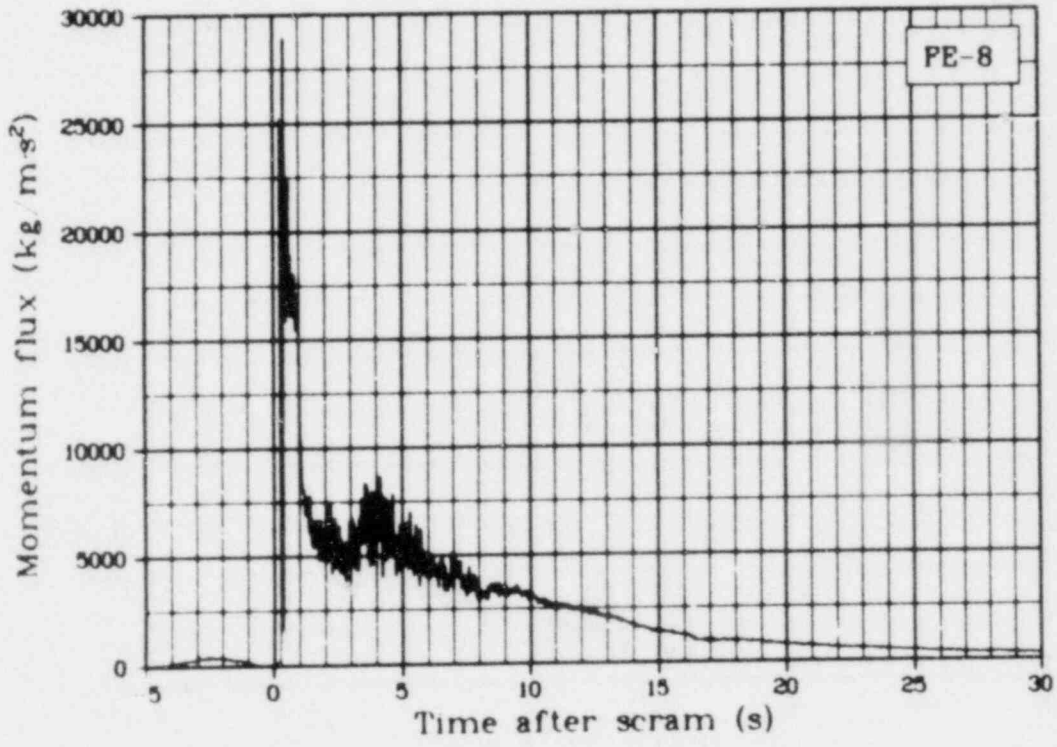

Fig. 209 Momentum flux in hot leg blowdown spool (FE-8), Test LOC-11C.

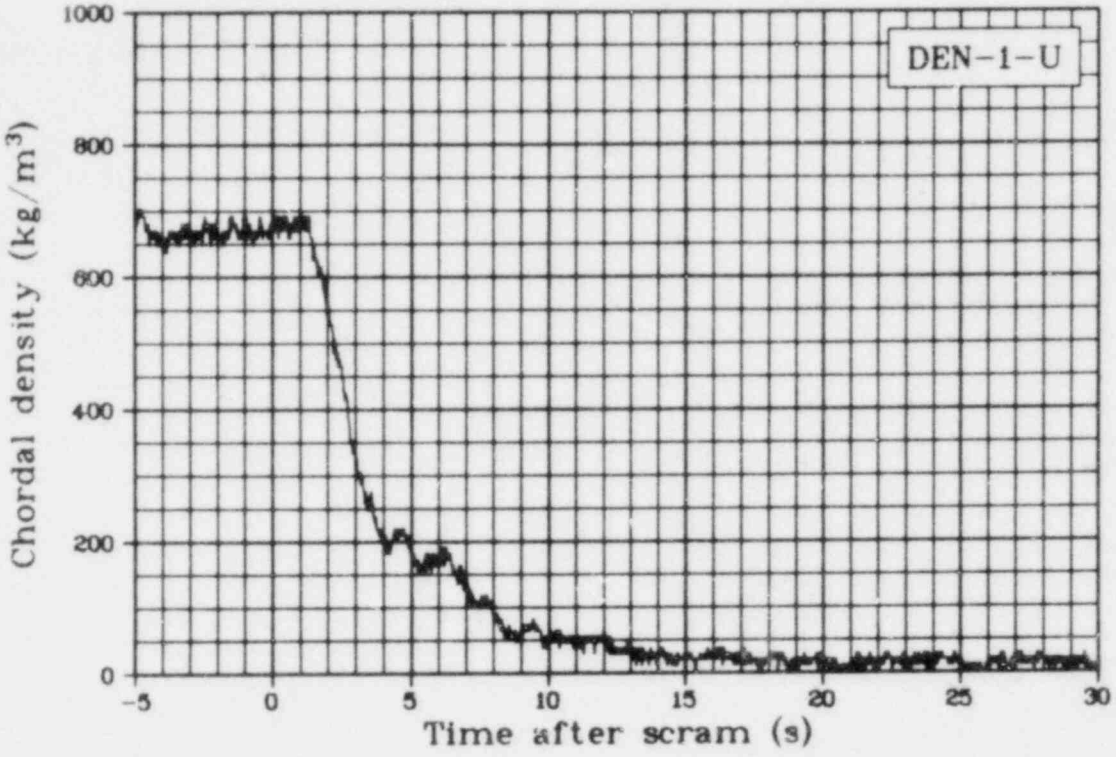

Fig. 210 Chordal density in upper gamma beam in cold leg (DEN-1-U), Test LOC-11C.

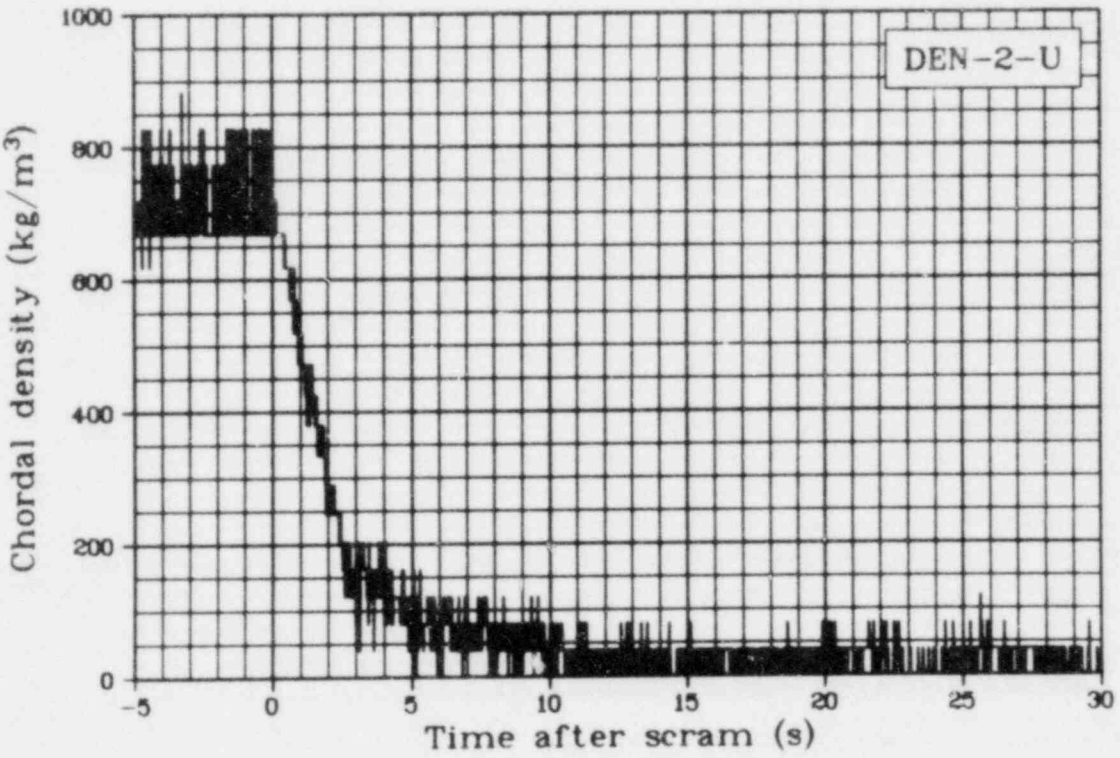

Fig. 211 Chordal density in upper gamma beam in hot leg blowdown spool (DEN-2-U), Test LOC-11C.

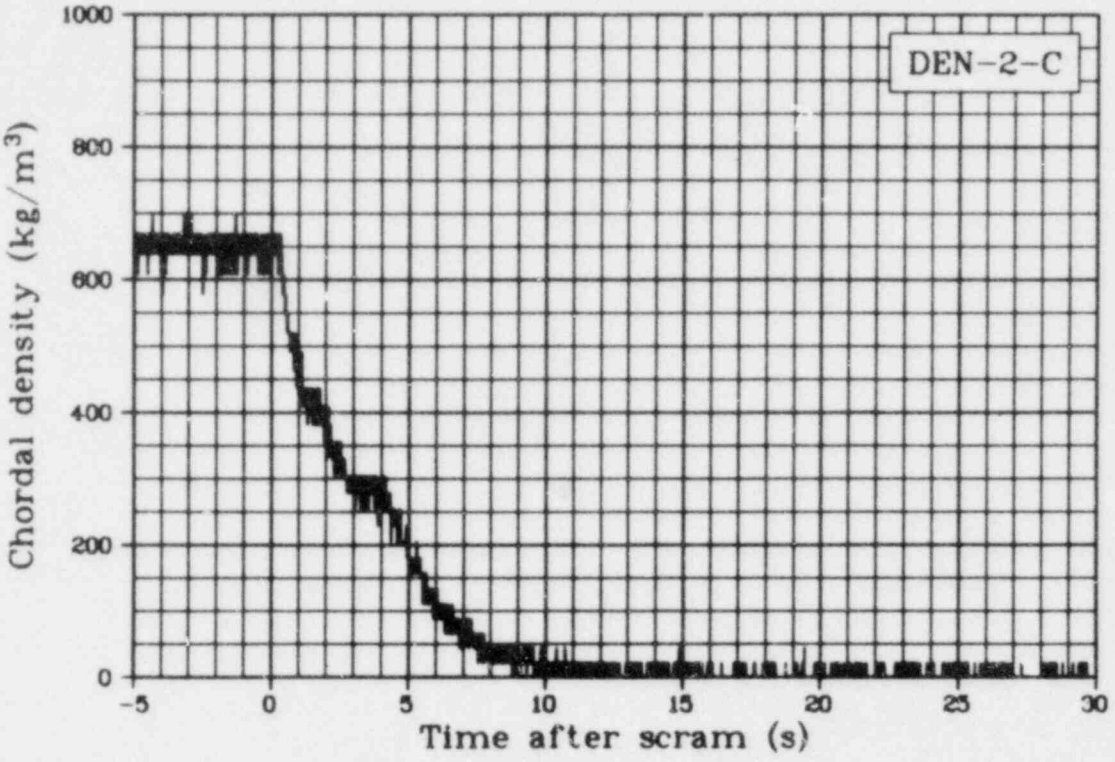

Fig. 212 Chordal density in center gamma beam in hot leg blowdown spool (DEN-2-C), Test LOC-11C.

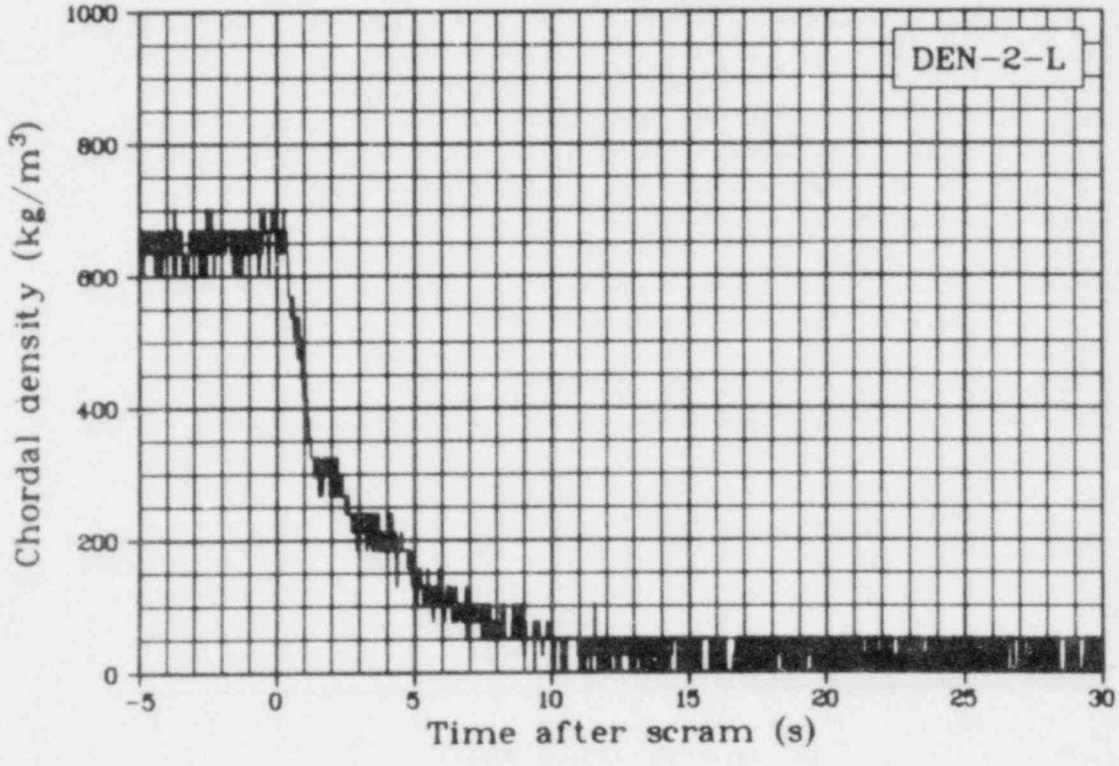

Fig. 213 Chordal density in lower gamma beam in hot leg blowdown spool (DEN-2-L), Test LOC-11C.

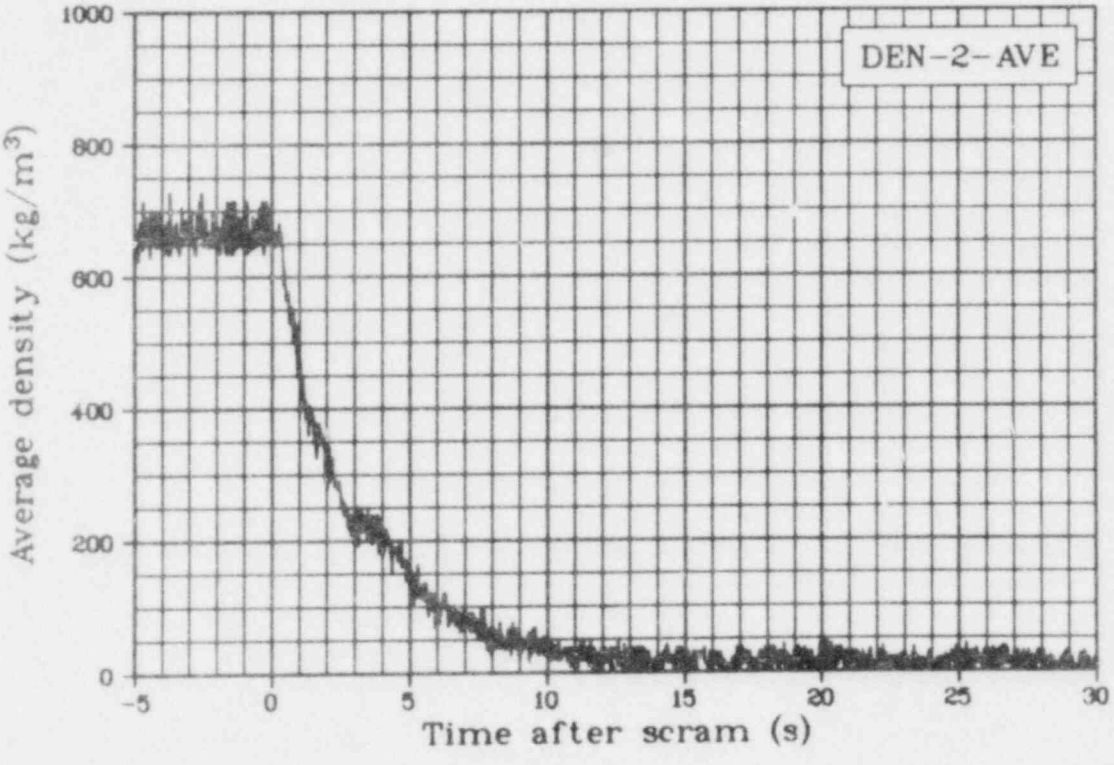

Fig. 214 Average density of hot leg blowdown spool (DEN-2-AVE), Test LOC-11C.

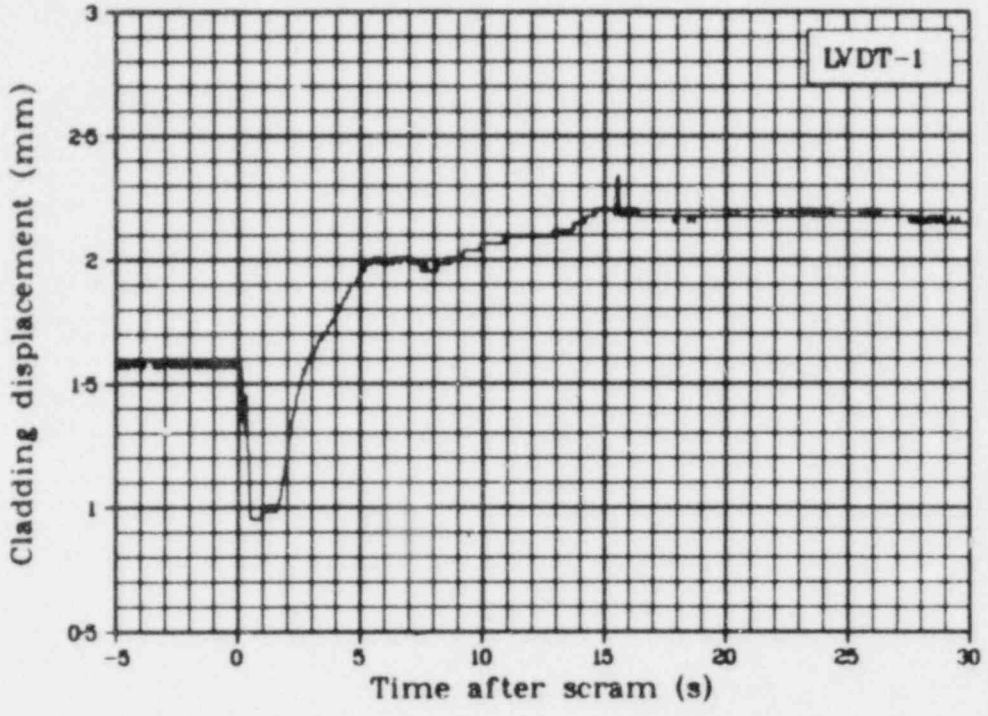

Fig. 215 Cladding displacement of Rod 1 (LVDT-1), Test LOC-11C.

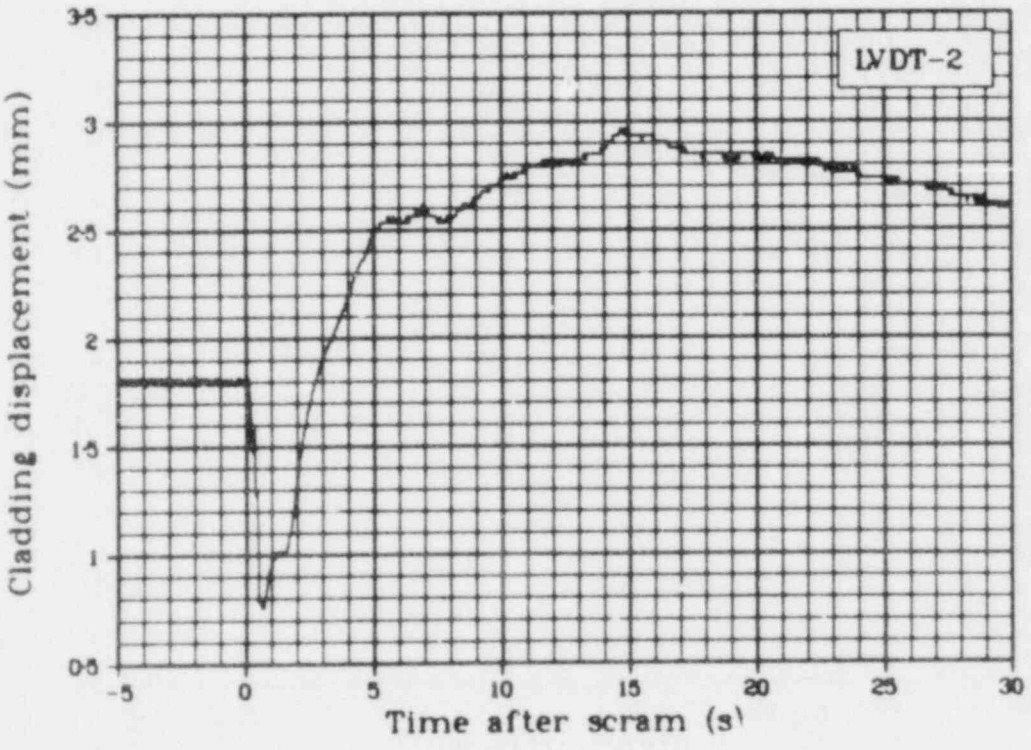

Fig. 216 Cladding displacement of Rod 2 (LVDT-2), Test LOC-11C.

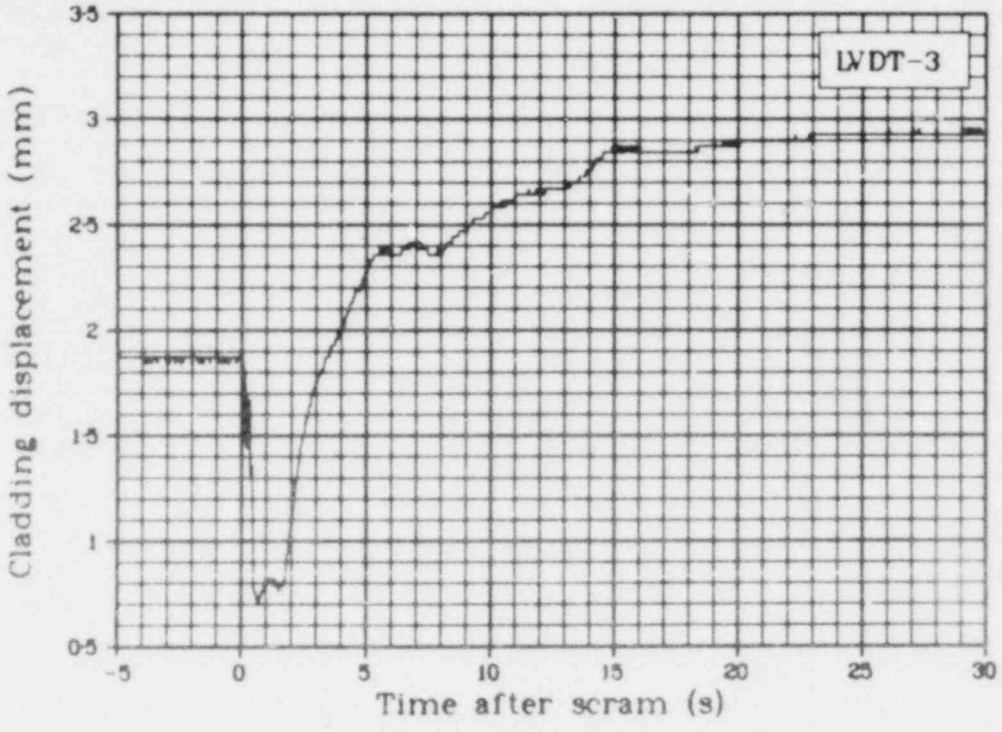

Fig. 217 Cladding displacement of Rod 3 (LVDT-3), Test LOC-11C.

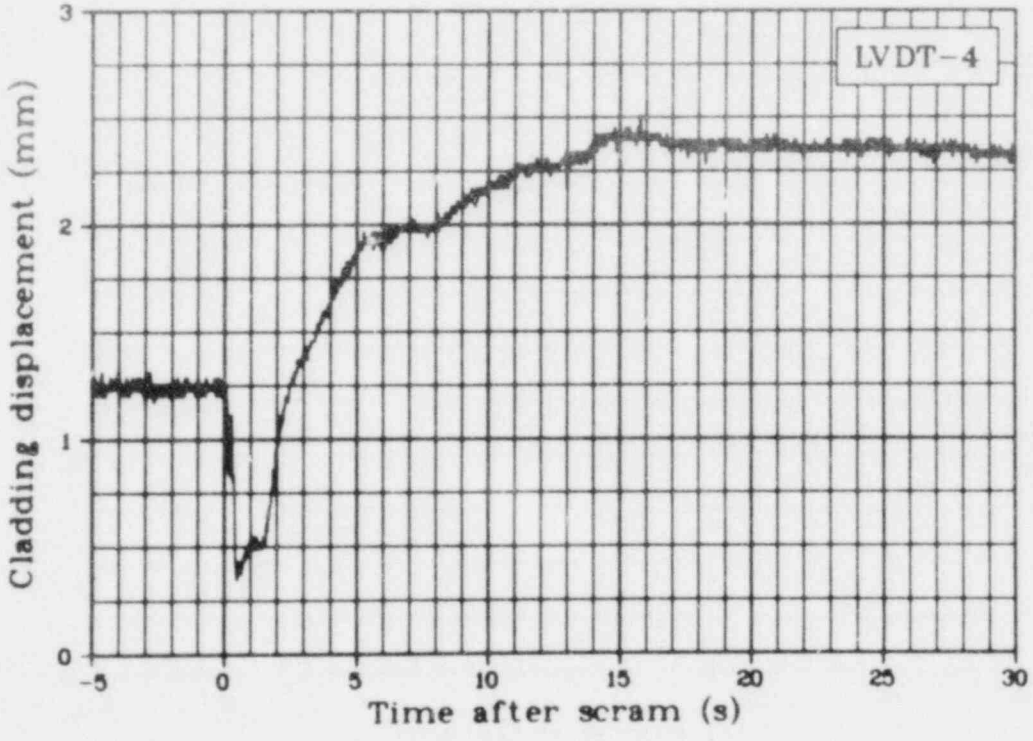

Fig. 218 Cladding displacement of Rod 4 (LVDT-4), Test LOC-11C.

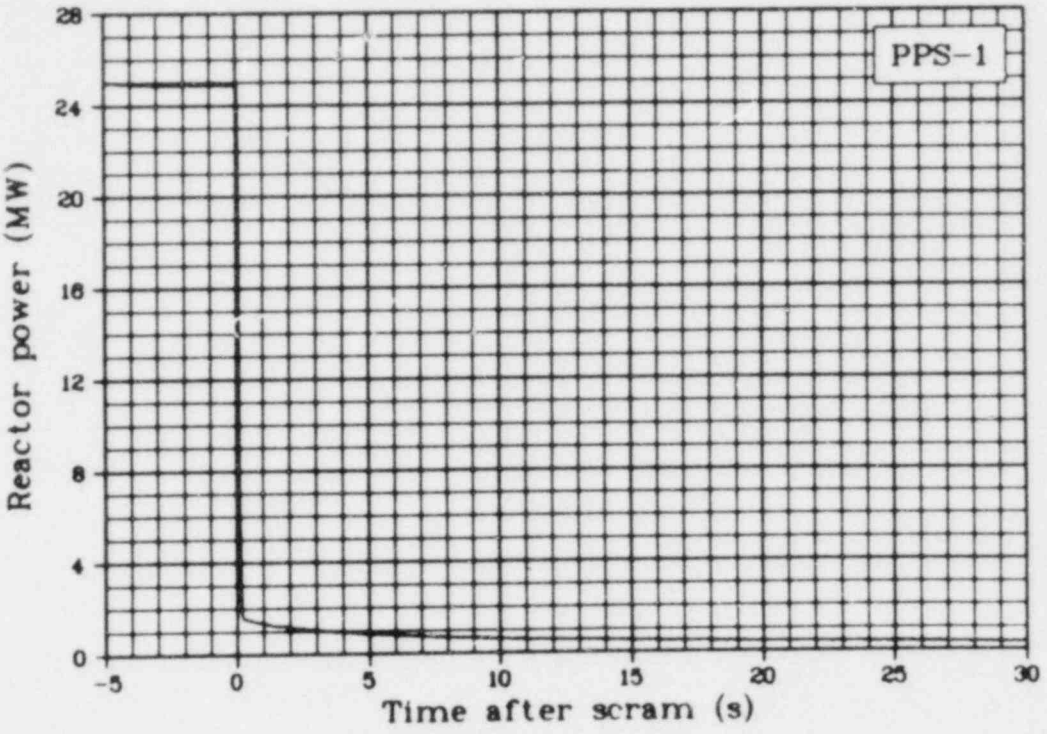

Fig. 219 Reactor power from plant protective system (PPS-1), Test LOC-11C.

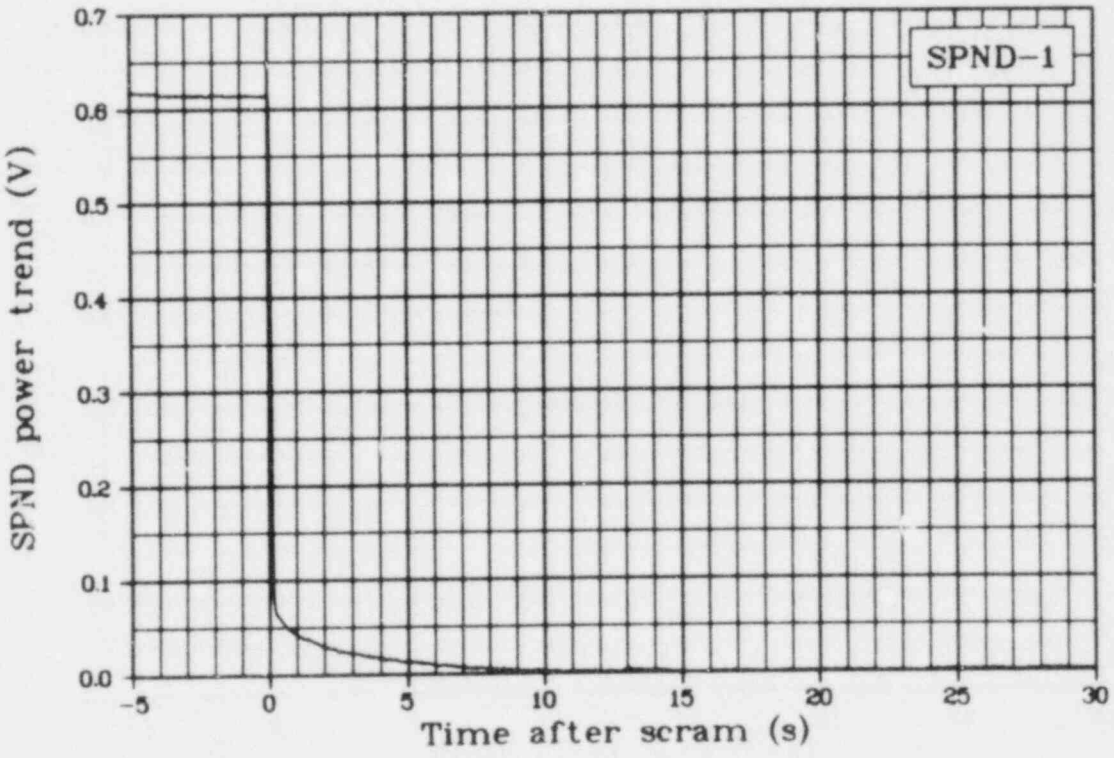

Fig. 220 SPND power trend 0.76 m above fuel stack bottom (SPND-1), Test LOC-11C.

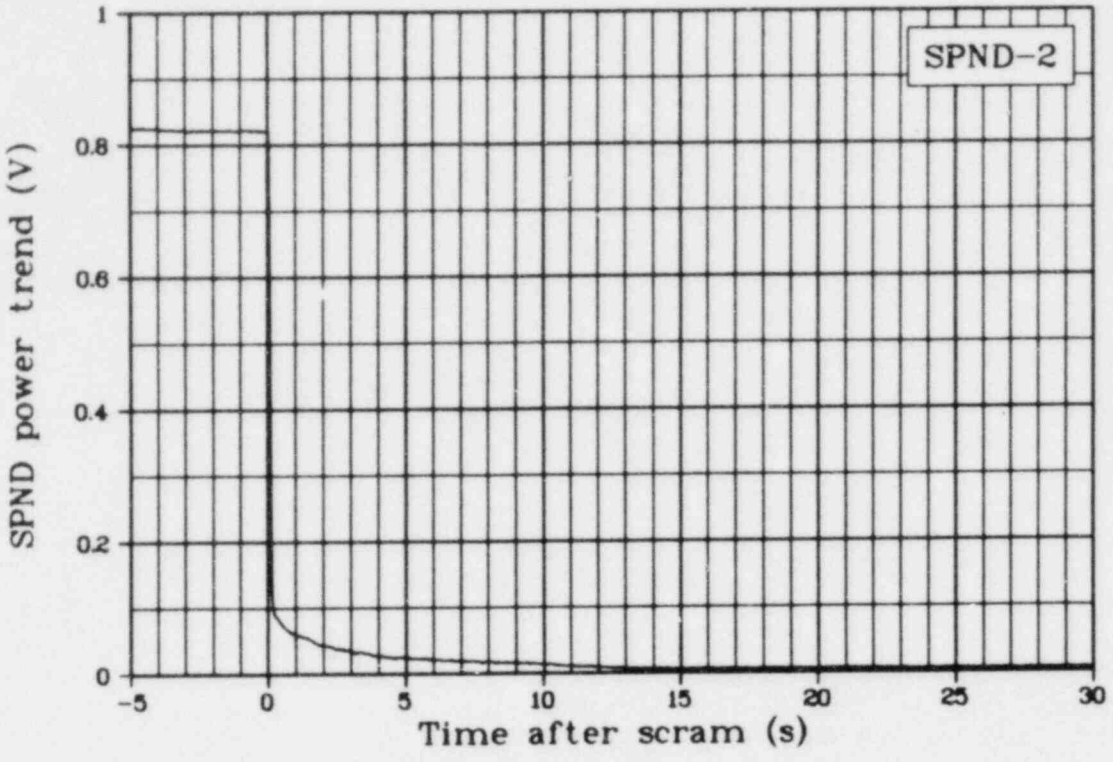

Fig. 221 SPND power trend 0.61 m above fuel stack bottom (SPND-2), Test LOC-11C.

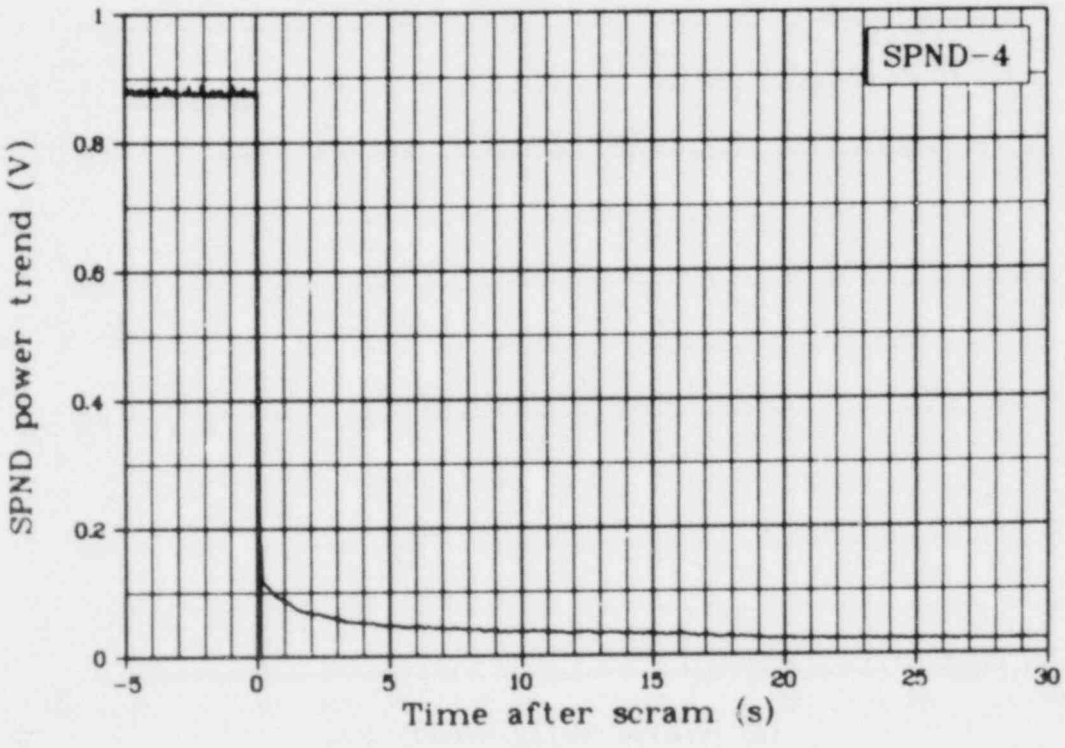

Fig. 222 SPND power trend 0.30 m above fuel stack bottom (SPND-4), Test LOC-11C.

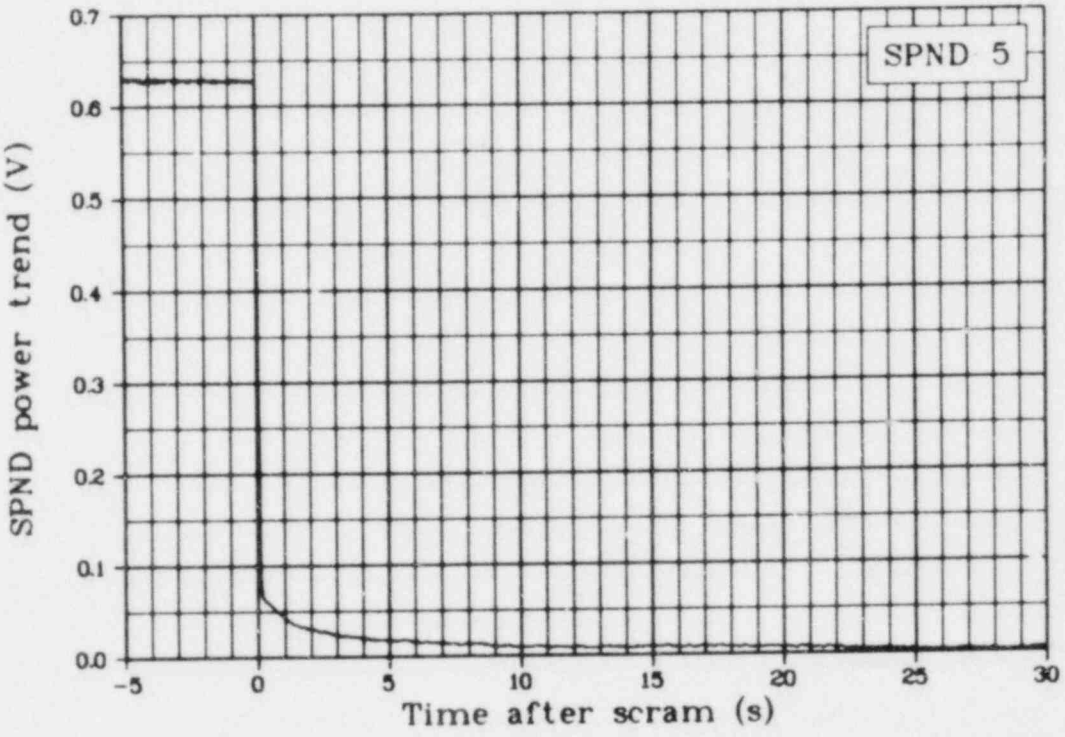

Fig. 223 SPND power trend 0.15 m above fuel stack bottom (SPND-5), Test LOC-11C.

VI. REFERENCE

1. *Quarterly Technical Report on Water Reactor Safety Programs Sponsored by the Nuclear Regulatory Commission's Division of Reactor Safety Reserach, January – March 1975*, ANCR-1254 (September 1975) pp 61-93.

APPENDIX A

TEST TRAIN HISTORY

APPENDIX A

TEST TRAIN HISTORY

The LOC-11 experiment test train was installed in the PBF-IPT on November 11, 1977. The following two month period consisted of final completion of the new PBF-loop system LOCA modification and associated system operational checks. Numerous hydrostatic tests to system operating pressure (15.2 MPa) were performed on the new loop LOCA piping which included the IPT and experiment in some cases.

Nonnuclear system blowdown tests were also performed with the loop system and test train operating at temperatures greater than 550 K.

The first nuclear blowdown performed on the system was Test LOC-11A which, because of improper blowdown valve operation, was repeated as Tests LOC-11B and 11C.

All thermal cycles performed on the LOC-11 test train are tabulated in Table A-I. Table A-II provides a complete listing of all nuclear operation experienced by the test train as taken from the reactor power log. Blowdown events and other explanatory comments are included.

TABLE A-I

TEST TRAIN THERMAL CYCLES

Event	Temperature Reached (K)	Date
System operational checkout. Partial blowdown caused by piping failure.	556	December 6, 1977
System operational checkout. Terminated by satisfactory blowdown sequence and quench.	585	December 7, 1977
System operational checkout. Terminated by unplanned blowdown valve cycling resulting in system blowdown.	592	December 14, 1977
Operating temperature for aborted Test LOC-11A. Normal cooldown of system with no blowdown.	605	December 20, 1977
Operating temperature for Test LOC-11A. Terminated by blowdown sequence and quench.	600	January 4 through January 6, 1978
System operational checkout. Terminated by satisfactory blowdown sequence and quench.	589	January 27, 1978
Operating temperature for Test LOC-11B. Terminated by blowdown sequence and quench.	591	January 31 through February 1, 1978
Operating temperature for Test LOC-11C. Terminated by blowdown sequence and quench.	598	February 15, 1978

TABLE A-II

REACTOR POWER LOG[a]

Date	Time Interval	Reactor Power (MW)	Comments
January 4, 1978	5:40 - 6:05	0.1	Test LOC-11A start-up
	6:35 - 7:05	2.0	Started power calibration
	7:07 - 10:59	0	Shutdown
	10:59 - 11:36	0.1	Test LOC-11A restart
	11:47 - 11:52	1.0	Start of power calibration
	11:57 - 12:03	2.0	
	12:11 - 12:19	4.0	
	12:27 - 12:55	6.0	
	12:59 - 13:35	6.8	
	13:41 - 13:48	5.0	
	13:53 - 14:00	3.0	
	14:13 - 14:26	0.1	
	14:26 - 20:30	0	End of power calibration
	20:30 - 20:56	0.1	
	21:12 - 21:23	8.0	Start of preconditioning
	21:32 - 22:11	12.9	
	22:20 - 22:57	16.9	
	23:01 - 23:37	16.0	
	0:16 - 0:19	0.1	
January 5, 1978	0:19 - 0:33	0	Shutdown
	0:33 - 0:34	0.1	Restart
	1:09 - 3:19	16.0	Preconditioning
	3:55 - 15:17	0	Shutdown
	15:17 - 15:19	0.1	Restart
	15:25 - 15:42	2.0	Preconditioning
	15:47 - 16:11	4.0	
	16:17 - 16:22	6.0	
	16:27 - 16:32	8.0	
	16:37 - 16:45	10.0	
	16:49 - 17:30	12.0	
	17:36 - 17:40	14.0	
	17:43 - 18:37	15.0	
	18:55 -	0	End of preconditioning
January 6, 1978	19:49 - 19:51	0.1	Restart
	20:20 - 20:45	15.1	Start of decay heat
	20:49 - 21:08	16.0	build up
January 7, 1978	21:13 - 2:08	17.0	
	2:08 -	0	Reactor scram for Test LOC-11A blowdown initiation

TABLE A-II (continued)

Date	Time Interval	Reactor Power (MW)	Comments
January 31, 1978	10:45 - 10:50	0.1	Test LOC-11B start-up
	11:01 - 11:13	2.0	Start of power calibration
	11:19 - 11:28	4.0	
	11:33 - 11:39	6.0	
	11:45 - 11:58	8.0	
	12:14 - 12:31	0	Shutdown
	12:31 - 13:02	[b]	Preconditioning
	13:02 - 13:30	0	Shutdown
	13:47 - 13:58	10.0	Start of decay heat buildup
	14:03 - 14:17	12.0	
	14:19 - 14:40	14.0	
	14:42 - 17:36	13.5	
	17:38 - 20:25	14.2	
	20:26 - 1:46	14.9	
February 1, 1978	1:46 -	0	Reactor scram for Test LOC-11B blowdown initiation
February 13, 1978	13:45 - 14:00	0.1	Test LOC-11C start-up
	14:27 - 15:39	8.3	Start of power calibration
	15:54 - 16:00	4.0	
	16:07 - 16:11	6.0	
	16:17 - 16:20	8.0	
	16:27 - 16:33	10.0	
	16:38 - 16:42	12.0	
	16:47 - 16:52	14.0	
	16:57 - 17:06	16.0	
	17:10 - 17:28	18.0	
	17:35 -	0	Shutdown
February 14, 1978	3:06 - 3:10	0.1	Restart
	3:27 - 4:04	10.0	Start of preconditioning
	4:14 - 4:53	0	Shutdown
	4:53 - 4:54	0.1	Restart
	5:07 - 6:24	10.0	Continuing preconditioning
	6:27 - 7:26	14.0	
	7:28 - 12:22	0	Shutdown
	12:22 - 12:24	0.1	Restart
	12:53 - 14:04	12.0	Start of decay heat buildup
	14:09 - 14:42	14.0	
	14:47 - 14:52	12.0	

TABLE A-II (continued)

Date	Time Interval	Reactor Power (MW)	Comments
	14:55 - 15:01	10.0	
	15:13 - 15:17	16.0	
	15:21 - 15:41	18.0	
	15:46 - 16:40	20.0	
	16:47 - 17:06	21.0	
	17:10 - 17:38	23.0	
	17:40 - 22:49	23.5	
February 15, 1978	22:56 - 0:25	25.1	
	0:25 -	0	Reactor scram for Test LOC-11C blowdown initiation

[a] The time noted between successive time intervals is the time required to change to the new power level at a constant ramp rate.

[b] Reactor power continuously ramped up to 8.0 MW then immediately ramped down to 0.

APPENDIX B

POSTTEST DATA ADJUSTMENTS AND VERIFICATION

APPENDIX B

POSTTEST DATA ADJUSTMENTS AND VERIFICATION

Measurement systems used at the PBF are affected by various systematic inputs caused by pressure, temperature, neutron flux, gamma radiation, vibration, mechanical strain, and data transmittal. Significant improvement in measurement accuracy can be achieved by identifying and removing these secondary input errors following the test.

Data acquired at the PBF during the performance of TFBP testing are subjected to appraisal by a data integrity review committee (DIRC) for quality and validity. The appraisal process determines whether each individual measurement properly responded to its physical stimulus and whether the measurement channel output represents the expected, predicted, or required response. The data review and examination process ascertains that verified calibration equations have been applied and that offsets and corrections have been applied to remove any spurious secondary effects from the data. As a result of the review and examination by the DIRC, each measurement is assigned one or more of the following verification classifications as a function of time.

(1) Verified engineering unit data (Verified):

These data must meet the following criteria:

(a) Calibration corrections applied

(b) Comparison with independent data with agreement during the period of interest within specified uncertainty limits

(c) Verified to represent the variable being measured.

(2) Restrained Data:

Restrained data are data that appear reasonable but cannot be classified verified because they fail to meet either one of the following criteria:

(a) They are not within uncertainty bands established by reference measurements or derived from redundant measurements when such are available; or

(b) Comparison against independent data for applying required calibration corrections during particular time periods.

(3) Trend Data:

These data have been verified to represent the relative changes in the phenomenon but do not necessarily represent the absolute level in the measured phenomenon. The data are suitable for illustrative purposes.

(4) Failed Data:

The data are irretrievable due to a failure in measurement channel or in the data acquisition system.

The corrections and offsets applied to the data are based on pretest and posttest calibrations of the data acquisition system, calibration coefficient checks, and independent system comparisons. The majority of the Test LOC-11B corrections are based on testing performed just prior to the LOC-11C test. The validity of applying these offsets is somewhat suspect due to changes in the data system grounding and the length of time between tests. In general, if the applied offsets resulted in reasonable data they were incorporated; if they did not improve the data they were not applied.

The following sections outline the methods used to determine the offset correction for various classes and types of instrumentation.

(1) Pressures

Three methods were used for determining offset corrections in the pressure data:

(a) Comparison with a loop system dial gage (resolution to within approximately ± 0.05 MPa)

(b) Comparison of saturation curves

(c) Comparison with an independent data acquisition system.

(2) Temperatures

The inlet spool resistance temperature detectors (RTD) electronics were given an end-to-end calibration by inserting precision resistors in place of the RTD and reading the resistance off the DARS system. The offset was found to be multiplicative and of a magnitude 0.9955 times the reading in ohms. This offset is approximately 2.5 ± 0.3 K over the range of coolant temperatures in the experiment. The inlet spool RTD was then used as a reference to determine the temperature offsets in a manner similar to that used for the pressures.

(3) Drag Discs

The calibration coefficients used with the hot leg and cold leg drag discs were incorrect. The listed offsets and multiplication factors correct the coefficients as well as take out any offsets. The offsets were determined by assuming that the drag discs had zero output at the end of the test (hot leg – 30 s after blowdown; cold leg – 75 s after blowdown).

(4) Turbine Flowmeters

The cold leg turbine indicates 1.04 ℓ/s as the preblowdown flow. This value compares favorably with the predicted warm-up flow rate. At the end of the blowdown, the turbine flowmeter indicates 1.91 ℓ/s where it should be indicating zero. This flow rate, however, corresponds to a pick-up frequency of 58 Hz so it is assumed that this is due to line frequency noise. This problem may only exist when the turbine is not turning due to an increased sensitivity of the electronics. The hot leg turbine was corrected by assuming a reverse flow of 1.04 ℓ/s during the preblowdown times.

The resultant linear offset adjustments applied to Tests LOC-11B and LOC-11C data per the review committee approval are presented in Table B-I.

TABLE B-I

OFFSET VALUES APPLIED TO TEST LOC-11B AND 11C

Measurement	Test LOC-11B Offset	Test LOC-11C Offset
Plenum Temperature (K)		
Fuel Rod		
TE-3-1	-5.7	-5.7
TE-3-2	1.4	1.4
TE-3-3	0.6	0.6
Cladding Temperature (K)		
Fuel Rod		
TE-5-1	-10.6	-10.6
TE-5-2	0	8.7
TE-5-3	0	-12.7
TE-5-4	-15.9	-15.9
TE-8-1	0	-3.4
TE-8-2	142.2	142.2
TE-8-3	0	-3.7
TE-8-4	0	-2.6
TE-10-1	0	0
TE-10-2	-4.8	-4.8
TE-10-3	0.9	0.9
TE-10-4	-5.7	-5.7
TE-22-1	0	-6.4
TE-22-2	-10.4	-10.4
TE-22-3	0	-3.8
TE-22-4	12.5	-12.5
Centerline Temperature (K)		
Fuel Rod		
TE-11-1	-8.7	-8.7
TE-11-2	-2.9	-2.9
TE-11-3	-3.7	-3.7
TE-11-4	-4.7	-4.7
Fluid Temperature (K)		
Test Train		
TE-1	-7.4	-7.4
TE-2-1	20.4	20.4
TE-2-2	-4.2	-4.2

TABLE B-I (continued)

Measurement	Test LOC-11B Offset	Test LOC-11C Offset
Test Train (continued)		
TE-2-4	0	0
TE-6-1	-4.6	0
TE-6-3	0	0
TE-6-4	0	0
TE-9-1	0	0
TE-9-2	0	0
TE-9-3	0	0
TE-9-4	0	0
TE-13-1	-3.5	-3.5
TE-13-2	-9.4	-9.4
TE-13-4	-1.1	-1.1
TE-14-1	-18.3	-18.3
TE-14-3	-14.4	-14.4
TE-14-4	-3.6	-3.6
TE-15	-18.3	-18.3
TE-16	0	-10.1
TE-17	-6.2	-6.2
TE-18	-1.8	-1.8
TE-19	-0.7	-0.7
Inlet Spool		
TE-20	-2.5	-2.5
TE-21	-13.7	-13.7
Blowdown Spool		
TE-23	-10.9	-10.9
TE-24	-18.1	-18.1
TE-25	-4.3	0
TE-26	-3.1	-3.1
Differential Temperature (K)		
Test Train		
ΔT-1-1	-0.17	-0.17
ΔT-1-2	-0.40	-0.40
ΔT-1-3	-0.09	-0.09
ΔT-1-4	0.06	0.06
Material Temperature (K)		

TABLE B-I (continued)

Measurement	Test LOC-11B Offset	Test LOC-11C Offset
Rod Shrouds		
TE-4-1	0	-9.5
TE-4-2	-17.4	-17.4
TE-4-3	0	-44.5
TE-4-4	0	-35.1
TE-7-1	-20.1	-20.1
TE-7-2	-11.9	-11.9
TE-7-3	0	-4.2
TE-7-4	-16.2	-16.2
TE-12-1	0	-60.1
TE-12-2	0	-33.6
TE-12-3	-13.0	-13.0
TE-12-4	-8.9	-8.9
Absolute Pressure (MPa)		
Test Train		
PE-1	-0.30	-0.30
PE-3	-0.95	-0.95
PE-6	-0.17	-0.54
Inlet Spool		
PE-9	0.76	0.76
Blowdown Spool		
PE-10	-0.03	0[a]
PE-11	1.29	1.29
PE-12	7.18	1.71
PE-13	1.26	1.26
ΔPE-5	0	0
Volumetric Flow (ℓ/s)		
Test Train		
FE-1-1	0	0
FE-1-2	0	0
FE-1-3	0	0
FE-1-4	0	0

TABLE B-I (continued)

Measurement	Test LOC-11B Offset	Test LOC-11C Offset
Test Train (continued)		
FE-2-1	0	0
FE-2-2	0	0
FE-2-3	0	0
FE-2-4	0	0
Inlet Spool		
FE-5	0	0
Blowdown Spool		
FE-6	0	0
FE-9	-3.37	-3.37
Momentum Flux ($kg/m \cdot s^2$)		
Blowdown Spool		
FE-7	(Reading + 151 600) x (0.0781)	(Reading + 154 000) x (0.0781)
FE-8	(Reading + 160 960) x (0.1517)	(Reading + 160 960) x (0.1517)
Cladding Displacement (mm)		
LVDT-1	0	0
LVDT-2	0	0
LVDT-3	0	0
LVDT-4	0	0
SPND Power Trend (V)		
SPND-1	0	0
SPND-2	0	0
SPND-3	0	0
SPND-4	0	0
SPND-5	0	0

[a] For Test LOC-11C an accurate offset could not be determined or applied because of noisy data.

APPENDIX C

UNCERTAINTY ANALYSIS

APPENDIX C

UNCERTAINTY ANALYSIS

The uncertainty analysis presented in this appendix has been divided into three areas of consideration. The results of each area of analysis are determinations of the standard deviation (σ) expected in each measurement system. The values listed in the following tables correspond to 1.96 σ which represents a 95% confidence level. An overall 95% confidence deviation can be determined by calculating the root mean of the sum of the three individual deviations.

The areas of consideration are:

(1) Conversion to engineering unit uncertainties

In the calibration and development of computer conversion polynomials for each measurement device a value for the standard deviation of that measurement was determined. Table C-I lists these 2-σ deviations assigned to each measurement device.

(2) Bias uncertainties due to offset applications

All data in this report were subjected to a thorough review to ensure accuracy or note discrepancies. Instrument channel outputs were compared with corresponding parameter channels, test predictions, calculated quantities, and preblowdown initial conditions to provide the basis for adjustments or offsets that were applied to the data. The bias uncertainty is the expected error in the offsets that was applied to the data. These 2-σ deviations assigned to each measurement device are listed in Table C-I.

(3) Random uncertainties

Additional analyses have been performed on selected representative Test LOC-11C data to provide a guide to uncertainties obtained from analysis of the data itself. To determine this random uncertainty the data traces under analysis were empirically fitted with a linear difference equation, which was subject to a white noise input at each sampling time point. The object of the empirical fitting procedure was to characterize the white noise, which was taken to represent the random uncertainty. The procedures for fitting the difference equation are discussed in

depth in Reference C-I. A data trace was often segmented and different equations were fitted to each segment with statistical correlations between successive observations accounted for by the fitting procedure. The white noise input was assumed to arise from a normally distributed population. The standard deviation of the white noise, as found during the fitting procedures, was taken as an estimate of the random uncertainty standard deviation and is shown in Table C-I. It should be noted that if any filtering process is applied to the original data, then the random uncertainty obtained from the original data would no longer precisely apply.

Of importance to note is the fact that this analysis assumes a homogeneous coolant. A significant additional measurement uncertainty results when the transducer systems are subjected to two-phase flow regimes and total steam environments during the course of the blowdown transient. Other uncertainties are also introduced by the physical presence of the measurement device itself in the measured medium. These uncertainties were considered and documented in the data verifying procedure discussed in Appendix B.

Certain systematic errors in these data were known to exist but could not be satisfactorily resolved. In addition, it was observed that the method used to estimate the random component of the uncertainty tended to reflect the total noise content of the data that arises from sample repeatability, electrical noise, the event being measured, and extraneous phenomena occurring during the test. It would be difficult to rigorously characterize the separate random components of the measurement, although it may be possible to filter one or more of these components from the noise which was used to determine the random uncertainty.

A more detailed and comprehensive uncertainty analysis of the PBF measurement systems is currently in progress. The results of this analysis are expected to be invaluable for determining engineering confidence limits on future data published by the Thermal Fuels Behavior Program.

TABLE C-I

GENERAL MEASUREMENT UNCERTAINTIES FOR TESTS LOC-11B AND 11C

The values listed apply to both Tests LOC-11B and 11C measurements unless otherwise noted.

Measurement	Engineering Unit Conversion (2σ)	Offset Application Bias (2σ)	Random Uncertainty (2σ)[a]
PLENUM TEMPERATURE (K)			
Fuel Rod			
TE-3-1	± 1.5	+ 3, -13 (+3, -18)[b]	TE-3-3
TE-3-2	± 1.5	± 3	± 3.3 (-5 to 0 s)
TE-3-3	± 1.5	± 3	± 3.4 (0 to 30 s)
CLADDING TEMPERATURE (K)			
Fuel Rod			
TE-5-1	± 1.5	± 3	TE-5-3
TE-5-2	± 1.5	± 3	± 5.6 (0 to 1.62 s)
TE-5-3	± 1.5	± 3	± 11.3 (1.62 to 5.1 s)
TE-5-4	± 1.5	± 3	± 8.1 (5.1 to 30 s)
TE-8-1	± 1.5	± 3	TE-8-3
TE-8-2	± 1.5	± 3	± 4.4 (0 to 1.7 s)
TE-8-3	± 1.5	± 3	± 8.4 (1.7 to 5.6 s)
TE-8-4	± 1.5	± 3	± 3.5 (5.6 to 30 s)
TE-10-1	± 1.5	± 3	TE-10-3
TE-10-2	± 1.5	± 3	± 4.7 (0 to 1.6 s)
TE-10-3	± 1.5	± 3	± 7.9 (1.6 to 5.5 s)
TE-10-4	± 1.5	± 3	± 3.1 (5.5 to 30 s)
TE-22-1	± 1.5	± 3 (+0, -1100)[b]	TE-22-3
TE-22-2	± 1.5	± 3	± 2.3 (-5 to 0 s)

TABLE C-I (continued)

Measurement	Engineering Unit Conversion (2σ)	Offset Application Bias (2σ)	Random Uncertainty (2σ)[a]
Fuel Rod (continued)			
TE-22-3	± 1.5	± 3	± 7.1 (0 to 3.8 s)
TE-22-4	± 1.5	± 3	± 6.9 (3.8 to 15.6 s)
			± 2.6 (15.6 to 30 s)
CENTERLINE TEMPERATURE (K)			
Fuel Rod			
			TE-11-3
TE-11-1	± 8.0	± 20	± 4.6 (0 to 30 s)
TE-11-2	± 8.0	± 20	
TE-11-3	± 8.0	± 20	
TE-11-4	± 8.0	± 20	
FLUID TEMPERATURE (K)			
Test Train			
			TE-1
TE-1	± 1.5	± 3 (+22, -3)[b]	± 3.0 (0 to 30 s)
			TE-2-2
TE-2-1	± 1.5	± 3	± 3.3 (0 to 7 s)
TE-2-2	± 1.5	± 3	± 4.4 (7 to 8.4 s)
TE-2-4	± 1.5	± 3	± 3.3 (8.4 to 30 s)
TE-6-1	± 1.5	± 3	
TE-6-3	± 1.5	± 3	
TE-6-4	± 1.5	± 3	
TE-9-1	± 1.5	± 3	
TE-9-2	± 1.5	± 3	

TABLE C-I (continued)

Measurement	Engineering Unit Conversion (2σ)	Offset Application Bias (2σ)	Random Uncertainty (2σ)[a]
Test Train (continued)			
TE-9-3	± 1.5	± 3	
TE-9-4	± 1.5	± 3	
TE-13-1	± 1.5	± 3	TE-13-2
TE-13-2	± 1.5	± 3	± 2.5 (0 to 13.8 s)
TE-13-4	± 1.5	± 3	± 2.2 (13.8 to 19.9 s)
			± 2.0 (19.9 to 30 s)
TE-14-1	± 1.5	± 3	TE-14-3
TE-14-3	± 1.5	± 3	± 3.7 (0 to 14.6 s)
TE-14-4	± 1.5	± 3	± 4.0 (14.6 to 17.9 s)
			± 3.5 (17.9 to 30 s)
TE-15	± 1.5	± 3	
TE-16	± 1.5	± 3 (+30, -0)[b]	
TE-17	± 1.5	± 3	
TE-18	± 1.5	± 3	
TE-19	± 1.5	± 3	
Inlet Spool			
TE-20	± 0.3	± 3	
TE-21	± 1.5	± 3	
Blowdown Spool			
TE-23	± 0.3	± 3	TE-23
			± 1.2 (0 to 30 s)
TE-24	± 1.5	± 3	TE-24
			± 1.4 (0 to 15.2 s)
			± 1.5 (15.2 to 30 s)

TABLE C-I (continued)

Measurement	Engineering Unit Conversion (2σ)	Offset Application Bias (2σ)	Random Uncertainty (2σ)[a]
Blowdown Spool (continued)			
TE-25	± 1.5	± 3	
TE-26	± 0.3	± 3	TE-26 ± 1.1 (0 to 30 s)
DIFFERENTIAL TEMPERATURE (K)			
Test Train			
ΔT-1-1	± 0.47	0	ΔT-1-3
ΔT-1-2	± 0.47	0	± 0.15 (0 to 7 s)
ΔT-1-3	± 0.41	0	± 0.22 (7 to 9.1 s)
ΔT-1-4	± 0.44	0	± 0.18 (9.1 to 15.7 s) ± 0.19 (15.7 to 30 s)
MATERIAL TEMPERATURE (K)			
Rod Shrouds			
TE-4-1	± 1.5	± 3	
TE-4-2	± 1.5	± 3	
TE-4-3	± 1.5	± 3 (0, -150)[b]	
TE-4-4	± 1.5	± 3	
TE-7-1	± 1.5	± 3	
TE-7-2	± 1.5	± 3	
TE-7-3	± 1.5	± 3 (+15, 0)[b]	
TE-7-4	± 1.5	± 3	
TE-12-1	± 1.5	± 3 (+20, -0)[b]	

TABLE C-I (continued)

Measurement	Engineering Unit Conversion (2σ)	Offset Application Bias (2σ)	Random Uncertainty (2σ)[a]
Rod Shrouds (continued)			
TE-12-2	± 1.5	± 3	
TE-12-3	± 1.5	± 3	
TE-12-4	± 1.5	± 3	
ABSOLUTE PRESSURE (MPa)			
Test Train			
PE-1	± 0.14	+ 3, -1.5 (+3, -1)[b]	
PE-3		± 0.6	
PE-6		± 0.7	PE-6 ± 0.02 (-5 to 0 s) ± 0.09 (0 to 30 s)
Inlet Spool			
PE-9	± 0.04	± 0.6	
Blowdown Spool			
PE-10	± 0.08	± 3.5, 0 (± 0.6)[b]	
PE-11	± 0.03	± 0.6	
PE-12	± 0.05	± 0.6	
PE-13	± 0.06	± 0.6	PE-13 ± 0.01 (-5 to 0 s) ± 1.52 (0 to 0.7 s) ± 0.09 (0.7 to 30 s)

TABLE C-I (continued)

Measurement		Engineering Unit Conversion (2σ)	Offset Application Bias (2σ)	Random Uncertainty (2σ)[a]
Blowdown Spool (continued)				
PE-5		± 0.0004	0	
VOLUMETRIC FLOW (l/s)				
Test Train				
FE-1-1	Forward	± 0.0005	0	FE-1-3
	Reverse	± 0.0005		± 0.0146 (-5 to 0 s)
FE-1-2	Forward	± 0.0008	0	± 0.5480 (0 to 1.6 s)
	Reverse	± 0.0011		± 0.0857 (1.6 to 5.1 s)
FE-1-3	Forward	± 0.0015	0 (+0.6, 0)[b]	± 0.1438 (5.1 to 8.0 s)
	Reverse	± 0.0014		± 0.0437 (8.0 to 12.2 s)
FE-1-4	Forward	± 0.0004	0	± 0.0325 (12.2 to 30 s)
	Reverse	± 0.0005		
FE-2-1	Forward	± 0.0004	0	FE-2-3
	Reverse	± 0.0015		± 0.0934 (-5 to 0 s)
FE-2-2	Forward	± 0.0006	0	± 0.4011 (0 to 2.2 s)
	Reverse	± 0.0005		± 0.0613 (2.2 to 5.5 s)
FE-2-3	Forward	± 0.0003	0	± 0.1274 (5.5 to 8.0 s)
	Reverse	± 0.0003		± 0.0524 (8.0 to 29.3 s)
FE-2-4	Forward	± 0.0009	0	± 0.2221 (29.3 to 30 s)
	Reverse	± 0.0004		
Inlet Spool				
FE-5		± 0.047	0	

TABLE C-I (continued)

Measurement	Engineering Unit Conversion (2σ)	Offset Application Bias (2σ)	Random Uncertainty (2σ)[a]
Blowdown Spool			
FE-6	± 0.070	0	
FE-9	± 0.028	0	FE-9 ± 25.3 (0 to 1 s) ± 0.9 (1 to 30 s)
MOMENTUM FLUX ($kg/m \cdot s^2$)			
Blowdown Spool			
FE-7		0 (0, -400)[b]	
FE-8		0	FE-8 ± 59 (-5 to 0 s) ± 11500 (0 to 0.7 s) ± 1650 (0.7 to 8.9 s) ± 119 (8.9 to 30 s)
DENSITY (kg/m^3)			
Blowdown Spool			
DEN-1-U		± 5	
DEN-1-L		± 5	
DEN-2-U		± 5	DEN-2-U ± 104.6 (-5 to 0 s) ± 58. (0 to 30 s)
DEN-2-C		± 5	DEN-2-C ± 39.3 (-5 to 0 s) ± 35.0 (0 to 30 s)

TABLE C-I (continued)

Measurement	Engineering Unit Conversion (2σ)	Offset Application Bias (2σ)	Random Uncertainty (2σ)[a]
DEN-2-L		± 5	DEN-2-L ± 50.1 (-5 to 0 s) ± 48.7 (0 to 30 s)
DEN-2-AVE		± 5	DEN-2-AVE ± 38.6 (-5 to 0 s) ± 28.7 (0 to 30 s)
FUEL ROD DISPLACEMENT (mm)			
LVDT-1	± 1.0	0	
LVDT-2	± 0.9	0	
LVDT-3	± 0.9	0	
LVDT-4	± 0.9	0	
ROD POWER (V)			
SPND-1		0	
SPND-2		0	
SPND-3		0	
SPND-4		0	SPND-4 0.0082 (0.1 to 30 s)
SPND-5		0	

[a] Analysis performed on selected Test LOC-11C data only and segmented according to parenthesis time spans.

[b] Offset bias in parenthesis applies to Test LOC-11B only.

REFERENCE

C-1. G. E. P. Box and B. M. Jenkins, *Time Series Analysis – Forecasting and Control*, San Francisco: Holden-Day, 1970.

DISTRIBUTION RECORD FOR NUREG/CR-0303 (TREE-1232)

Internal Distribution

1 - Chicago Patent Group - DOE
9800 South Cass
Argonne, IL 60439

2 - R. L. Blackledge
Idaho Operations Office - DOE
Idaho Falls, ID 83401

3 - R. J. Beers, ID

4 - P. E. Litteneker, ID

5 - R. E. Tiller, ID

6 - H. P. Pearson
Information Management - EG&G

7-12 - INEL Technical Library

13-22 - Authors

23-103 - Special Internal

External Distribution

104-105 - Saul Levine, Director
Office of Nuclear Regulatory Research, NRC
Washington, D.C. 20555

106-107 - Special External

108-134 - Technical Information Center - DOE
Box 62
Oak Ridge, TN 37830

135-427 - Distribution under R3, Water Reactor Safety Research - Fuel Behavior